

# Mechanism of Free Radical Oxygenation of Polyunsaturated Fatty Acids by Cyclooxygenases

Carol A. Rouzer and Lawrence J. Marnett\*

*A. B. Hancock Jr. Memorial Laboratory for Cancer Research, Departments of Biochemistry and Chemistry, Vanderbilt Institute of Chemical Biology, Center in Molecular Toxicology, Vanderbilt Ingram Comprehensive Cancer Center, Vanderbilt University School of Medicine, Nashville, Tennessee 37232-0146*

Received November 7, 2002

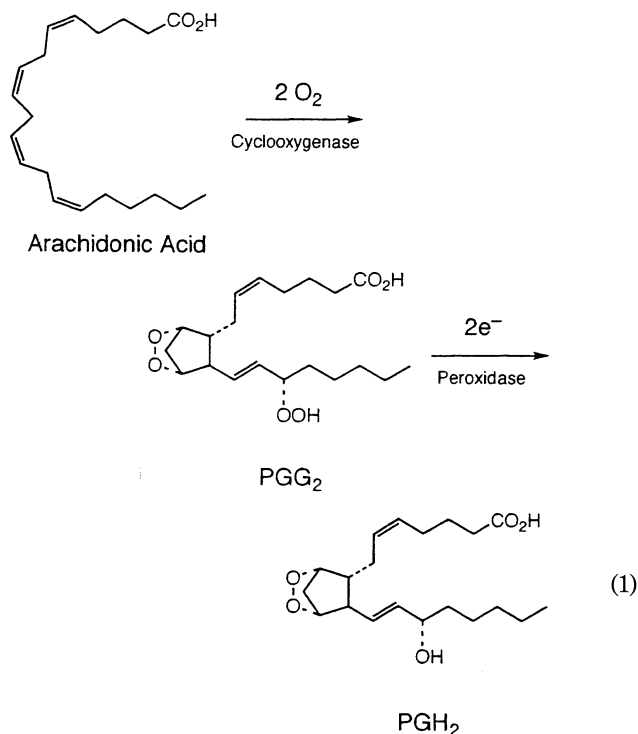
## Contents

I. Introduction	2240	A. The Three-Dimensional Structure	2270
II. Fatty Acid Autoxidation	2241	B. The Heme-Binding Site and Peroxidase Active Site	2272
A. Mechanism of Autoxidation	2241	C. The Cyclooxygenase Active Site	2272
B. PG Formation via Fatty Acid Autoxidation	2243	D. Comparison of COX-2 and COX-1	2273
III. Enzymatic Transformation of Unsaturated Fatty Acids into PG's	2243	E. Structure of COX Complexes with Substrate	2275
A. Isotope Studies	2243	F. Identification of Critical Residues	2277
B. Proposed Chemical Mechanism	2246	VIII. Differences between COX-2 and COX-1	2278
C. Minor Cyclooxygenase Products	2247	A. Effects of Aspirin	2278
IV. Relationship between the Cyclooxygenase and Peroxidase Activities of COX	2248	B. Hydroperoxide Initiator Requirement	2280
A. COX as a Hemeprotein	2249	C. Apparent Cooperativity	2281
B. The Peroxidase Activity of COX	2249	D. Hydroperoxide Oxidation by Compound I	2281
C. Assays for Peroxidase and Cyclooxygenase Activities	2250	E. Effects of His Mutations at the Heme-Binding Site	2281
D. Peroxidase-Dependent Activation of Cyclooxygenase Activity	2250	F. Substrate Specificity	2283
E. Peroxidase-Dependent Inactivation of Cyclooxygenase Activity	2251	IX. Mechanistic Studies of COX Substituted with Manganese Protoporphyrin IX	2284
V. Mechanism of Peroxidase Catalysis	2252	A. Spectral Studies of Higher Oxidation States	2284
A. Spectral Studies of Peroxidase Turnover	2252	B. Tyrosyl Radicals in Mn–COX-1	2286
1. Identification of Higher Oxidation State Intermediates	2252	C. One-Electron versus Two-Electron Reductions by Mn–COX-1	2287
2. Spectral Evidence for Peroxidase Self-Inactivation	2256	D. Inactivation of Mn–COX	2287
B. Peroxidase Reductants	2257	X. Hydroperoxide Activation under Physiological Conditions	2288
1. Role of Peroxidase Reductants in the Cyclooxygenase Reaction	2257	XI. Structural Changes Associated with Enzyme Inactivation	2289
2. Chemical Mechanisms for Peroxidase Substrate Oxidation	2257	XII. Alternative Cyclooxygenase Mechanisms and Refinements of the Branched-Chain Mechanism	2291
3. Structure–Activity Relationships for Peroxidase Reductants	2259	A. The Tightly Coupled Mechanism	2291
VI. Mechanism of Cyclooxygenase Catalysis	2262	1. Studies of Reaction Stoichiometry	2291
A. Free Radicals in COX Catalysis	2262	2. Kinetics of Intermediate I/Compound II Formation	2292
1. Substrate-Derived Radicals	2262	3. Effects of Peroxidase Reductants	2293
2. Protein-Derived Radicals	2262	B. Comparison of the Branched-Chain and Tightly Coupled Mechanisms	2294
B. The Branched-Chain Mechanism	2264	1. Reaction Stoichiometry	2294
1. Characterization of the Tyrosyl Radical	2265	2. Kinetics of Intermediate I/Compound II Formation	2294
2. Kinetics of Tyrosyl Radical Formation and Cyclooxygenase Catalysis	2266	3. Interaction between the Cyclooxygenase and Peroxidase Activities	2295
3. Identity of COX Tyrosyl Radicals	2267	4. Predictions from Mathematical Models	2295
4. Oxidation of 20:4 by COX Tyrosyl Radicals	2268	5. Remaining Questions	2297
VII. The Structural Basis of Cyclooxygenase Catalysis	2270	C. The Ferrous Iron Mechanism	2297
		XIII. COX as a Catalyst for Fatty Acid Autoxidation	2299
		XIV. Conclusion	2300
		XV. Abbreviations	2300
		XVI. Acknowledgments	2301
		XVII. Note Added in Proof	2301
		XVIII. References	2301

\* To whom correspondence should be addressed. Phone: (615) 343-7329. Fax: (615) 343-7534. E-mail: marnett@toxicology.mc.vanderbilt.edu.

## 1. Introduction

Cyclooxygenase (COX) catalyzes the bis-dioxygenation of arachidonic acid (5,8,11,14-eicosatetraenoic acid, 20:4) to the hydroperoxy endoperoxide, prostaglandin (PG)  $G_2$ , and the reduction of  $PGG_2$  to the hydroxy endoperoxide,  $PGH_2$  (eq 1).<sup>1–3</sup>  $PGH_2$  is the



substrate for five different metabolizing enzymes that convert the endoperoxide moiety to the tetra-substituted cyclopentane ring characteristic of PG's ( $PGE_2$ ,  $PGD_2$ ,  $PGF_{2\alpha}$ , or  $PGI_2$ ) or the oxane ring present in thromboxane (TX)  $A_2$  (Figure 1).<sup>4</sup> Each of these molecules binds to one or more membrane-bound, G-protein-coupled receptors through which they exert their biological effects.<sup>5</sup> Thus, cyclooxygenase sits atop a complex metabolic cascade that converts a polyunsaturated fatty acid into one or more bioactive lipids. The importance of this cascade in human health is suggested by the fact that cyclooxygenase is the molecular target for the pharmacological action of non-steroidal anti-inflammatory drugs (NSAIDs).<sup>6,7</sup>

In vertebrates, two COX genes and proteins exist that are differentially regulated.<sup>8</sup> COX-1 is the form of the protein expressed constitutively in most tissues, whereas COX-2 is inducible in response to stimulation of cells with a very broad range of agonists.<sup>9–14</sup> COX-2 appears to be the major target for the anti-inflammatory and analgesic action of NSAIDs, and COX-2-selective inhibitors exhibit these activities with reduced gastrointestinal side effects.<sup>15–17</sup> COX-1 and COX-2 from a range of organisms (fish  $\rightarrow$  humans) are approximately 60% identical in sequence and are virtually identical in overall folding.<sup>18–21</sup> Some important, albeit subtle, differences in structure between the two proteins convey differences in substrate specificity and sen-



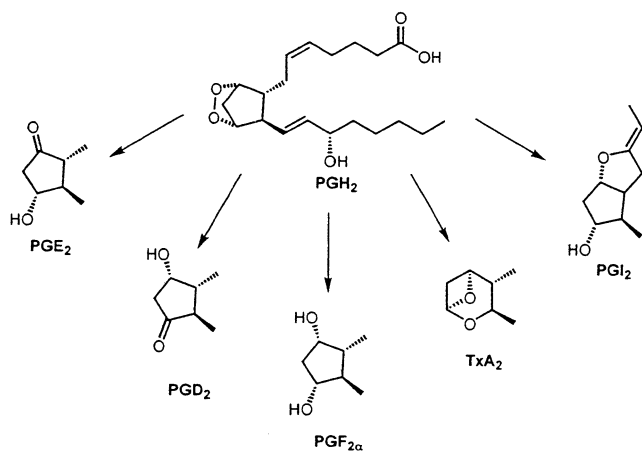
Carol A. Rouzer received her B.A. in chemistry from McDaniel College, her Ph.D. in biomedical sciences from The Rockefeller University (1982), and her M.D. from the Weill Medical College of Cornell University (1983). After postdoctoral work at the Karolinska Institute, she accepted a position as Research Fellow at the Merck Frosst Center for Therapeutic Research. She moved to McDaniel College in 1989, where she was engaged primarily in undergraduate education until 2000, when she joined the Biochemistry Faculty of Vanderbilt University as Research Professor. Her main research interests focus on the total metabolism of arachidonic acid in inflammatory and malignant cells with particular emphasis on the metabolism of neutral derivatives of arachidonic acid by COX-2. She is the author of over 50 publications.



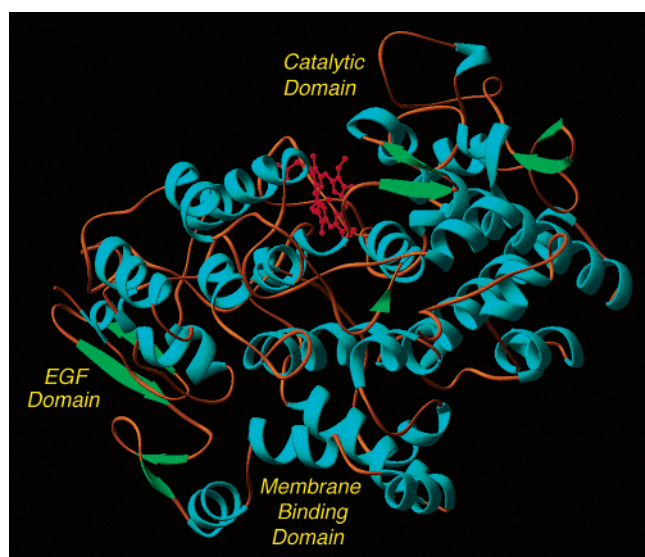
Lawrence J. Marnett received his B.S. in chemistry from Rockhurst College and his Ph.D. in chemistry from Duke University in 1973. He did postdoctoral work at the Karolinska Institute and at Wayne State University. He was hired on the faculty at Wayne in 1975 and rose through the ranks to Professor of Chemistry. In 1989, he moved to Vanderbilt University, where he is the Director of the Vanderbilt Institute of Chemical Biology, Mary Geddes Stahlman Professor of Cancer Research, Professor of Biochemistry, and Professor of Chemistry. Marnett's research program focuses on the role of the enzyme cyclooxygenase-2 in cancer and inflammation and on the contribution of normal metabolism to the generation of DNA damage and mutation. He is the author of over 300 research publications and 11 patents. He is the founding and current editor-in-chief of the American Chemical Society journal, *Chemical Research in Toxicology*.

sitivity to certain inhibitors.<sup>22–28</sup> A splice variant of COX-1 in which intron 1 is retained has recently been reported.<sup>29</sup> This enzyme, which has been designated COX-3, possesses interesting differences in pharmacologic properties from COX-1 and COX-2, but its exact physiological significance remains unknown. COX-3 is discussed in greater detail in section VII.

Both COX proteins (COX-1 and COX-2) are homodimers of 70 kDa subunits, each of which contains one molecule of  $Fe^{3+}$ -protoporphyrin IX ( $Fe^{3+}$ -PPIX,



**Figure 1.** PG metabolites formed from  $\text{PGH}_2$  by the action of specific synthases. In the absence of additional synthase enzymes,  $\text{PGH}_2$  decomposes in aqueous media to form a mixture of  $\text{PGE}_2$  and  $\text{PGD}_2$ .



**Figure 2.** Domain structure of COX proteins. The N-terminus is not visible in the crystal structure but connects to the epidermal growth factor domain. The membrane-binding domain is connected to the C-terminal end of the epidermal growth factor domain and is comprised of helices A–D. Helix D connects the membrane-binding domain to the catalytic domain.  $\alpha$ -Helices are colored blue, and  $\beta$ -sheets are colored green. The heme prosthetic group is colored red.

Figure 2).<sup>19,30,31</sup> The heme prosthetic group is noncovalently associated and can be reversibly removed and reconstituted with little loss in enzyme activity.<sup>32,33</sup> This property has been utilized to produce COX proteins substituted with different metal porphyrins for mechanistic and structural studies.<sup>33,34</sup> COX proteins are membrane-bound and localize to the lumen of the endoplasmic reticulum and the inside of the nuclear envelope.<sup>35</sup> In addition to enabling insertion into lipid bilayers, the membrane-binding domain is intimately related to substrate association and catalytic activity.<sup>36</sup>

COX proteins carry out the synthesis of  $\text{PGG}_2$  (cyclooxygenase activity) and its reduction to  $\text{PGH}_2$  (peroxidase activity).<sup>37</sup> This has led to some challenges in nomenclature. Multiple names have been given for the overall bifunctional protein, including

cyclooxygenase (COX), prostaglandin endoperoxide synthase (PES), prostaglandin H synthase (PGHS), and prostaglandin G/H synthase (PGG/HS). For the present review, we will use COX-1 or COX-2 to refer to the proteins and cyclooxygenase and peroxidase to designate the catalytic activities. Our choice of COX as an abbreviation reflects its historical roots and its widespread recognition in the lay community as a result the development and marketing of COX-2-selective inhibitors.

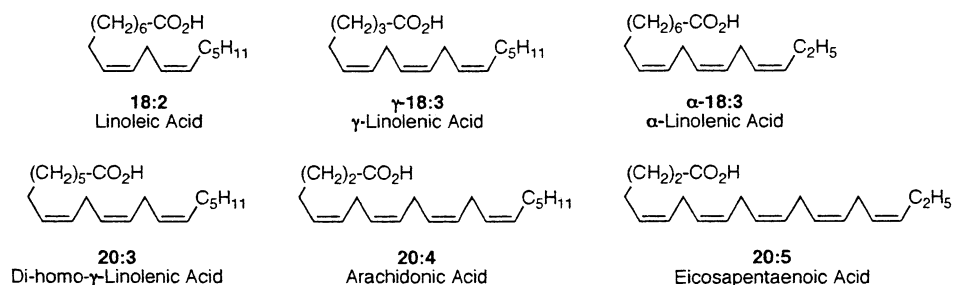
The cyclooxygenase reaction is a fascinating chemical transformation in which an achiral polyunsaturated fatty acid is oxygenated twice, one carbon–carbon and three carbon–oxygen bonds are formed, and five chiral centers are introduced. No cofactors are required, and the transformation occurs at a single active site with no covalent intermediates. The product of this reaction diffuses from the cyclooxygenase active site and binds to the peroxidase active site where its hydroperoxide group is reduced. The two active sites are located on opposite sides of the protein, and both require the presence and redox action of the heme prosthetic group.<sup>19,38</sup> The peroxidase activity of the protein is required to activate the cyclooxygenase activity.<sup>39</sup> In fact, COX proteins are members of the myeloperoxidase superfamily.<sup>40</sup> Thus, COX's appear to have evolved from peroxidase ancestors that lack any cyclooxygenase function. Perhaps most interesting, the cyclooxygenase reaction occurs by a chemically well-precedented free radical reaction that utilizes a protein-derived oxidant. Interestingly, COX has been called the first protein for which a protein radical was demonstrated to have a clear catalytic function.<sup>41</sup>

The conceptual framework for the cyclooxygenase reaction is that of a controlled free radical autoxidation. Therefore, this review will begin with a consideration of the chemistry of fatty acid autoxidation and its parallels to PG biosynthesis. It will then lay out the case for the formation of substrate- and protein-derived free radicals during catalysis. The role of the peroxidase in activating the cyclooxygenase will be defined, and then the structural basis for catalytic activity will be considered. Other features of catalysis will then be presented. A somewhat historical approach has been adopted to highlight the many contributions that have been made to the evolution in our understanding of cyclooxygenase function as well as the context in which these contributions were made. The latter is important because some controversies have existed about interpretation of experimental observations that can be confusing to the neophyte.

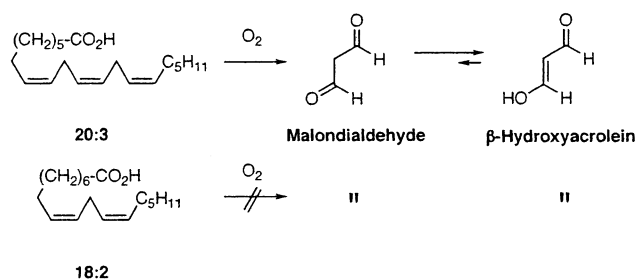
## II. Fatty Acid Autoxidation

### A. Mechanism of Autoxidation

Fatty acid autoxidation has been studied for over 60 years as part of an effort to understand and prevent the rancidification of foods.<sup>42</sup> It was quickly appreciated that such investigations offered insights into the mechanism of aerobic degradation of the unsaturated fatty acid components of biological membranes.<sup>43,44</sup> The common polyunsaturated fatty acids



**Figure 3.** Structures of common polyunsaturated fatty acids. The common names for each compound are shown below the structure, along with the abbreviation that will be used in this article.



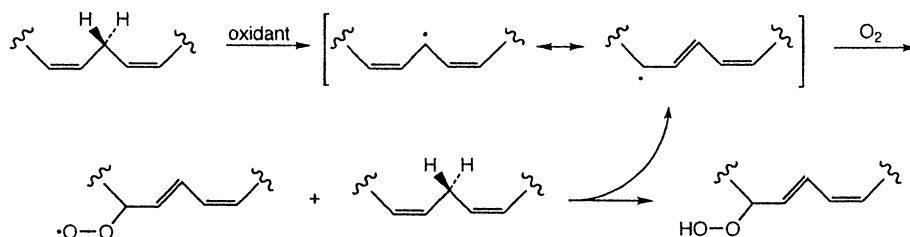
**Figure 4.** Autoxidation of polyunsaturated fatty acids to malondialdehyde. Fatty acids with three or more double bonds generate malondialdehyde as a product of autoxidation, whereas fatty acids with two double bonds do not.

are shown in Figure 3. The methylene groups between the cis double bonds are readily oxidized, and the higher the number of methylene groups, the more sensitive the fatty acid is to autoxidation [e.g., 20:4 is considerably more sensitive to autoxidation than 9,12-octadecadienoic acid (linoleic acid, 18:2)].<sup>45</sup> The latter is usually the principal polyunsaturated fatty acid in cellular membranes in mammals. Another difference in the autoxidation of various polyunsaturated fatty acids is the product profile. As the number of double bonds in the fatty acid increases, so does the complexity of products formed.<sup>46</sup> For example, fatty acids with three or more double bonds produce malondialdehyde, whereas fatty acids with two double bonds do not (Figure 4).<sup>47,48</sup>

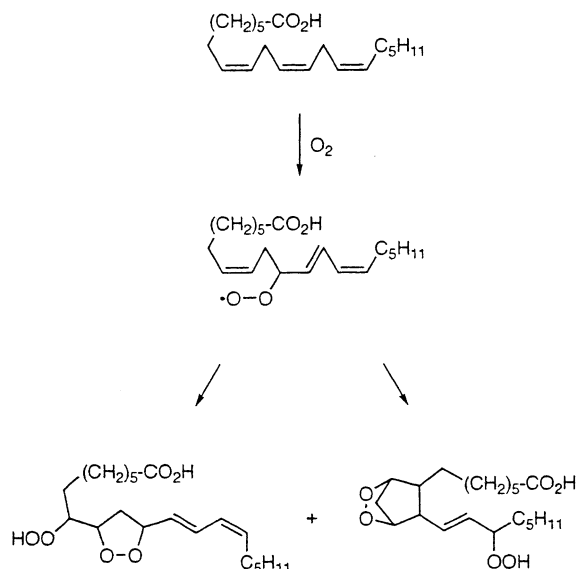
The reactions in Figure 5 represent the simplest scheme for autoxidation of a polyunsaturated fatty acid.<sup>49</sup> The initiation event is the removal of a bis-allylic hydrogen to form a carbon-centered radical with electron density at the central carbon and the two termini. Oxygen trapping of the carbon-centered radicals produces peroxy radicals, which react with another molecule of fatty acid to produce hydroperoxide products and another carbon-centered radical. This represents the propagation step, which enables

the continuation of the free radical chain reaction. The length of the chain (number of fatty acid molecules oxidized/initiation event) is a function of the rate of the propagation reaction. Fatty acids with more bis-allylic methylene groups have higher rate constants for propagation and exhibit longer radical chains. Under standard conditions, the number of molecules oxidized per initiation event is 60 for 18:2 (1-CH<sub>2</sub>) and 200 for 20:4 (3-CH<sub>2</sub>).<sup>50</sup> Termination of the chain autoxidation occurs when the peroxy radicals react to form nonradical products; this becomes significant as the fatty acids are depleted.

Oxygen trapping of the initially formed carbon-centered radical occurs at a diffusion-controlled rate and can take place at one of multiple carbons to form a bis-allylic peroxy radical or pentadienyl peroxy radicals (Figure 5). For many years, it was felt that pentadienyl peroxy radicals were the sole products of O<sub>2</sub> trapping because of the enhanced stabilization of the pentadienyl radical intermediates. Recently, though, Brash reported that bis-allylic hydroperoxides can be formed efficiently if the autoxidation is carried out in the presence of a phenolic antioxidant.<sup>51</sup> The bis-allylic peroxy radical is actually the kinetic product of O<sub>2</sub> trapping, whereas the pentadienyl peroxy radicals are the thermodynamic products. The inability to detect the kinetic product results from the well-known reversibility of peroxy radical formation, which ultimately shifts the products of O<sub>2</sub> trapping from the kinetic to the thermodynamic (Figure 5).<sup>52</sup> In the presence of increasing concentrations of antioxidant, however, the bis-allylic peroxy radical undergoes hydrogen abstraction as opposed to β-fragmentation, resulting in the formation of the corresponding hydroperoxide.<sup>53</sup> In the case of higher polyunsaturated fatty acids, a complex pattern of products results from intramolecular cyclization of the peroxy radical intermediates to form mono- and bicyclic peroxides (Figure 6).<sup>54</sup> The quan-



**Figure 5.** Basic reactions of fatty acid autoxidation. Oxidation of a bis-allylic hydrogen (initiation) generates carbon-centered radicals that couple to molecular oxygen to form peroxy radicals. The latter oxidize another molecule of fatty acid (propagation). For simplicity, only two possible pentadienyl radicals and one of the derivative peroxy radicals are shown.



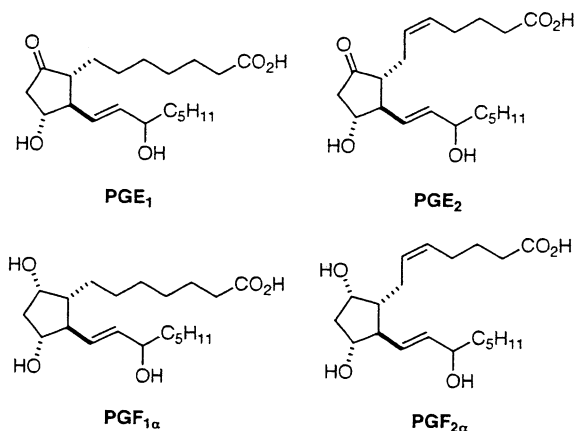
**Figure 6.** Cyclic peroxide products of fatty acid autoxidation. Two of a number of monocyclic and bicyclic peroxide products of fatty acid autoxidation are depicted.

tification of products derived from certain of these cyclic peroxides (isoprostanes) has emerged as the technique of choice for monitoring lipid autoxidation and oxidative stress in vivo.<sup>55</sup>

The kinetics of fatty acid autoxidation are typical of a free radical chain reaction in that a lag phase precedes the attainment of the maximal rate.<sup>56,57</sup> Phenolic antioxidants, such as butylated hydroxytoluene or  $\alpha$ -tocopherol (vitamin E), prolong the lag phase but do not reduce the maximal rate.<sup>58</sup> Antioxidants induce a lag phase by reducing peroxy radical intermediates, thereby preventing propagation.<sup>56,59</sup> This consumes the antioxidant, which leads to the end of the lag phase. Since there is no antioxidant remaining, the maximal rate of autoxidation is the same following the lag phase as in control autoxidations without antioxidant.

## B. PG Formation via Fatty Acid Autoxidation

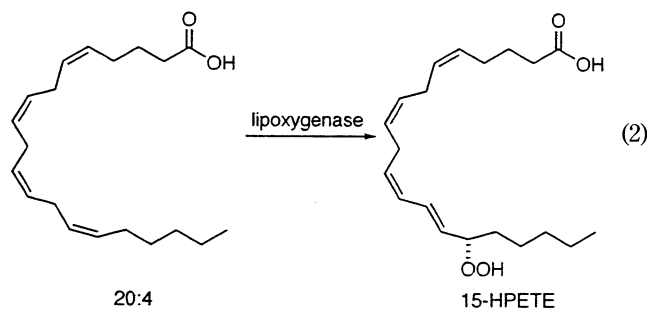
The formation of cyclic peroxides and their breakdown products generates molecules structurally analogous to PG's. PG's were characterized as smooth muscle stimulating molecules in the 1930s, but their structures were not identified until some 25 years later (Figure 7).<sup>60–63</sup> In fact, the related molecules, thromboxane and prostacyclin, were not identified until 1975 and 1976, respectively.<sup>64,65</sup> PG's are distinguished by the presence of a five-membered ring containing oxygen functionality at the 1,3-positions and trans-dialkyl substitution at the 4,5-positions. The structural similarity between fatty acid autoxidation products and PG's is not coincidental. Nugteren and co-workers reported in 1966 that autoxidation of 8,11,14-eicosatrienoic acid (20:3) produces PG's as minor products ( $\sim 1$ –2%), and model studies by Stanley and Pryor and by Funk and Porter indicated that peroxy radicals undergo serial cyclization to produce PG-like products.<sup>46,47,66</sup> Further investigation indicated that peroxy radical cyclization to bicyclic peroxides produces cis-dialkyl substitution instead of the trans substitution observed in the natural products. An early kinetic study of the



**Figure 7.** Prostaglandins E and F of the 1 and 2 series. PGE<sub>1</sub> and PGF<sub>1 $\alpha$</sub>  were the first PG's identified and were named because of their abilities to partition into ether or phosphate buffer, respectively.

enzymatic oxygenation of 20:4 to PG's revealed a lag phase prior to the attainment of the maximal rate of O<sub>2</sub> uptake, which could be prolonged by phenolic antioxidants.<sup>67</sup>

The similarities between nonenzymatic and enzymatic oxygenation of polyunsaturated fatty acids suggest that nature has adapted a facile chemical process to generate an important class of bioactive lipids. Actually, earlier evidence for such a chemomimetic strategy existed from the study of lipoxygenase enzymes, which catalyze the enzymatic oxygenation of polyunsaturated fatty acids to pentadienyl hydroperoxides (eq 2).<sup>68</sup> In the case of PG biosynthe-

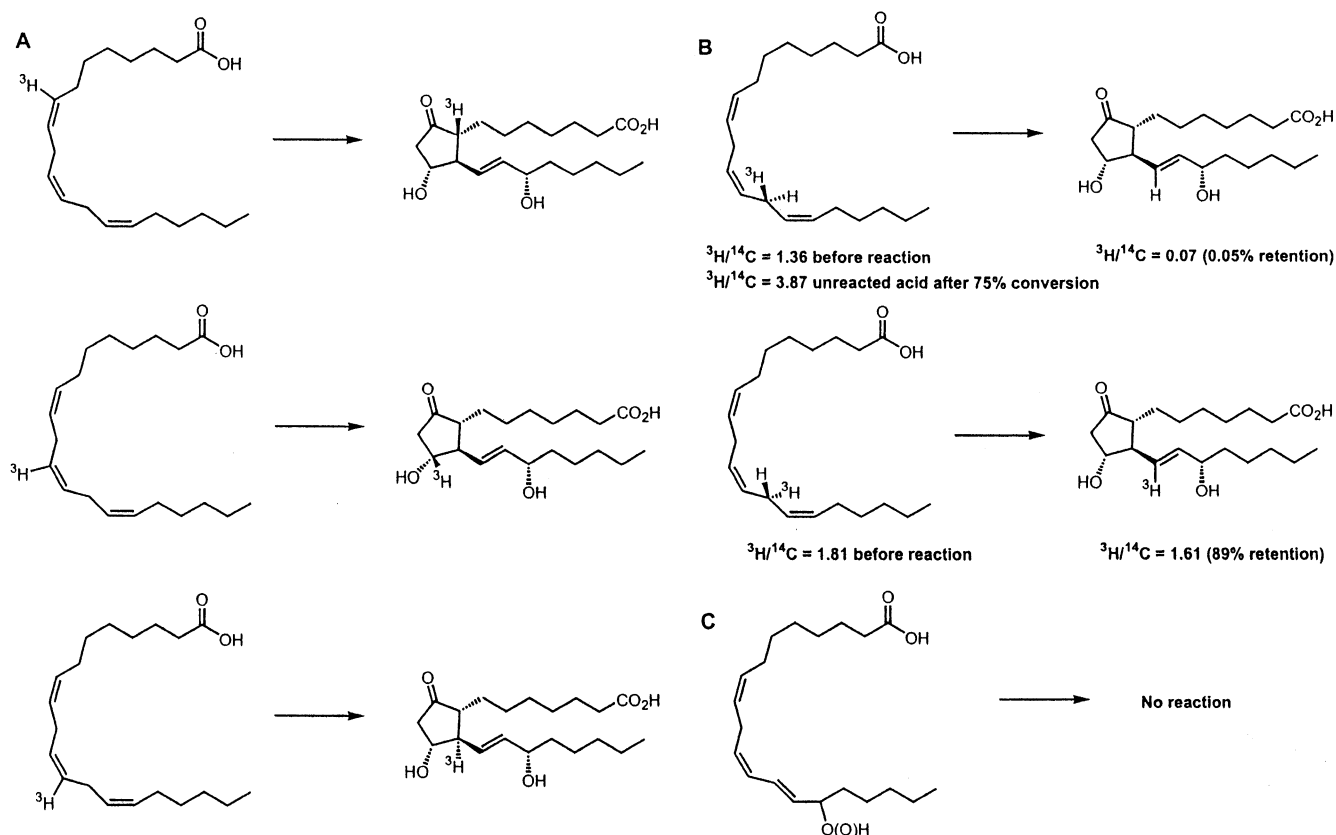


sis, there are three key questions to be answered: (1) How does the enzyme abstract the bis-allylic hydrogen? (2) How does the enzyme control the regiochemistry and stereochemistry of fatty acid oxygenation? (3) How does the enzyme catalyze what appears to be a controlled free radical autoxidation?

## III. Enzymatic Transformation of Unsaturated Fatty Acids into PG's

### A. Isotope Studies

PG's were isolated from sheep prostate glands and seminal vesicles. The latter is a particularly rich source of these bioactive lipids, so it was natural to begin studies of the enzymatic transformation of polyunsaturated fatty acids with this tissue.<sup>63</sup> This presented something of a practical problem prior to molecular cloning because ram seminal vesicles are in relatively short supply worldwide. Most male sheep are castrated early in life in many countries,



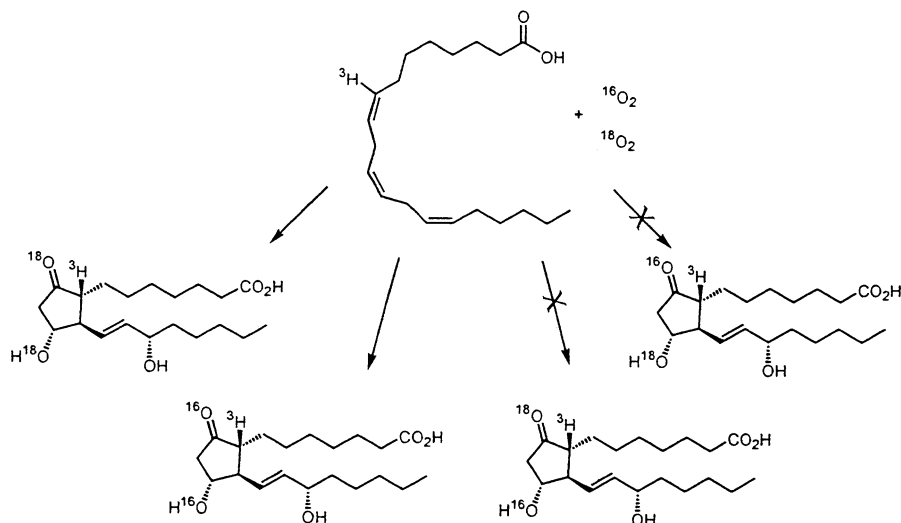
**Figure 8.** (A) Retention of tritium during the reaction of seminal vesicle microsomes with 20:3 labeled with tritium at carbon 8, 11, or 12.<sup>72</sup> (B) The 13-*pro-S* hydrogen atom is specifically removed during the reaction of seminal vesicle microsomes with 20:3. Fatty acid specifically labeled with tritium in either the 13-*pro-S* or 13-*pro-R* position was combined with fatty acid labeled with  $^{14}\text{C}$  at carbon 3. The mixture of labeled substrates was incubated with COX-1. The ratio of  $^3\text{H}/^{14}\text{C}$  was reduced almost to zero in the case of the fatty acid labeled in the 13-*pro-S* position, and unreacted substrate demonstrated an increase in the  $^3\text{H}/^{14}\text{C}$  ratio. In contrast, there was little change in the  $^3\text{H}/^{14}\text{C}$  ratio for the fatty acid labeled in the 13-*pro-R* position.<sup>259</sup> (C) 15-HPETE and 15-HETE are not converted to PG's by seminal vesicle microsomes.<sup>259</sup>

and seminal vesicles do not develop well in castrated animals. Also, the tissue from these animals does not generate PG's. PG's were isolated on an industrial scale by extraction prior to the development of efficient methods for their synthesis, which further restricted the availability of tissue to researchers. [At one point, all of the seminal vesicles from the two major sheep-farming countries in the world, Australia and New Zealand, were contracted to the Upjohn Company, which generously provided tissue and PG's free of charge to academic investigators worldwide.] Some studies were conducted with bull seminal vesicles, but the activity is lower, which made such studies more difficult. Nevertheless, the first reported purification of COX (by Hayaishi and associates) was carried out from bull seminal vesicles.<sup>32</sup> The enzyme in ram and bull seminal vesicles is predominantly COX-1, so much of the mechanistic work has been done with this protein. However, all of the key mechanistic properties exhibited by COX-1 are recapitulated by COX-2.

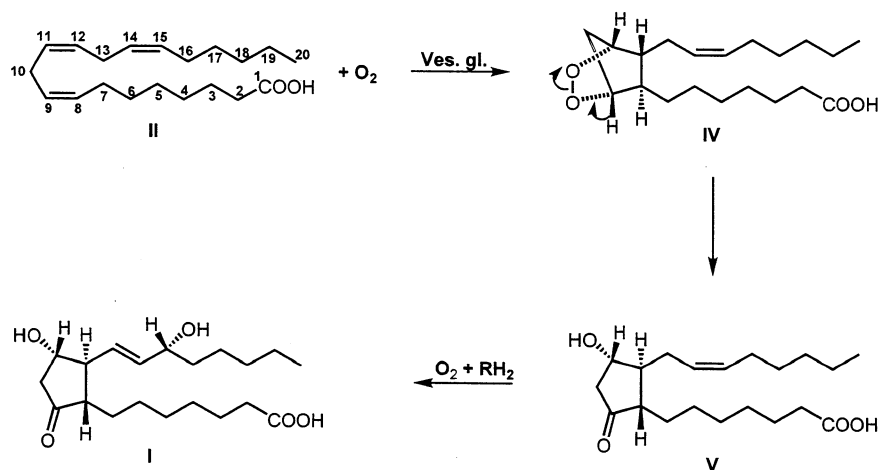
Studies by Van Dorp et al. and by Bergström et al. demonstrated that radioactively labeled 20:4 is converted into radioactively labeled PGE<sub>2</sub> on incubation with homogenates of ram seminal vesicles.<sup>69,70</sup> This verified the hypothesis that polyunsaturated fatty acids are the biosynthetic precursors of PG's, providing a possible explanation for the nutritional "es-

sentiality" of polyunsaturated fatty acids. [The introduction to the manuscript by Bergström et al. acknowledges a gift of  $^3\text{H}$ -labeled 20:4 from the laboratory of Van Dorp and the fact that the Van Dorp laboratory was testing the same hypothesis by performing the same experiments. This was an impressive material transfer, given the competitive positions of the research groups.] COX enzymes are capable of converting 20:3, 20:4, and 5,8,11,14,17-eicosapentaenoic acid (20:5) to PG's, though the relative efficiencies of the three substrates varies (20:4 > 20:3  $\gg$  20:5).<sup>71</sup> The nomenclature of the products differs with regard to the number of double bonds, as indicated by the subscript in the designation of the PG. Thus, metabolism of 20:3, 20:4, and 20:5 yields PGG<sub>1</sub>, PGG<sub>2</sub>, and PGG<sub>3</sub>, respectively.

The identification of polyunsaturated fatty acids as the substrate for PG synthesis led to further studies exploring the mechanism of the reaction. Incubation of ram seminal vesicle microsomes (predominantly COX-1) with 20:3, specifically labeled with tritium at vinylic carbons 8, 11, and 12, produced PGE<sub>1</sub> that retained all three tritium atoms (Figure 8A).<sup>72</sup> Experiments with 20:3, stereospecifically labeled with  $^3\text{H}$  at the bis-allylic carbon 13 as substrate, demonstrated that the *pro-S* hydrogen atom was selectively removed (Figure 8B).<sup>73</sup> These studies also revealed an enrichment of tritium in the unreacted 13-*pro-*



**Figure 9.** Oxygen atoms at carbons 9 and 11 of PGE<sub>1</sub> generated from the reaction of seminal vesicle microsomes with 20:3 come from the same oxygen molecule. When the fatty acid was reacted in the presence of mixtures of <sup>16</sup>O<sub>2</sub> and <sup>18</sup>O<sub>2</sub>, all product molecules contained either <sup>16</sup>O or <sup>18</sup>O at both positions. No product molecules were isolated that contained one <sup>18</sup>O atom and one <sup>16</sup>O atom in the cyclopentenone ring.<sup>76,77,78,79,128</sup>



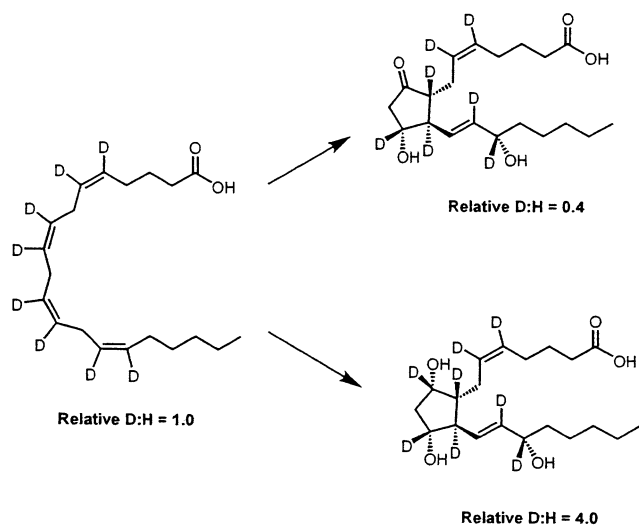
**Figure 10.** Mechanism for the COX reaction that proposes an endoperoxide intermediate. Reproduced with permission from ref 76. Copyright 1965 American Chemical Society.

(*S*) substrate but not the 13-*pro*-(*R*) substrate, allowing the authors to conclude that the tritium-containing substrate reacted more slowly than the substrate containing hydrogen. This kinetic isotope effect indicated that the hydrogen abstraction step must precede the addition of oxygen at carbons 9 and 11. Attempts to observe PG synthesis using 15-(*S*)-hydroperoxy-8,11,13-eicosatrienoic acid or 15-(*S*)-hydroxy-8,11,13-eicosatrienoic acid were unsuccessful, demonstrating that neither compound is an intermediate in PG synthesis (Figure 8C).<sup>73</sup> These results are consistent with a mechanism similar to that of nonenzymatic autoxidation, which begins with the abstraction of a bis-allylic hydrogen atom followed by oxygen addition.

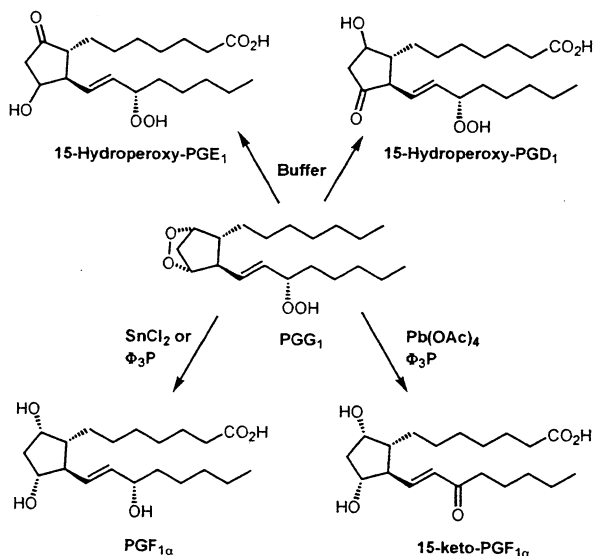
Reaction of 20:3 with seminal vesicle microsomes in the presence of <sup>18</sup>O<sub>2</sub> showed that the oxygen atoms at positions 9, 11, and 15 of the resulting PGE<sub>1</sub> all derived from molecular oxygen.<sup>74–76</sup> Further studies in which the enzyme present in bovine seminal vesicle microsomes was incubated with 20:3 in the presence of mixtures of <sup>18</sup>O<sub>2</sub> and <sup>16</sup>O<sub>2</sub> demonstrated that the oxygens on carbons 9 and 11 of PGE<sub>1</sub> and

PGF<sub>1α</sub> contained either two atoms of <sup>18</sup>O or two atoms of <sup>16</sup>O, but not one atom of <sup>18</sup>O and one atom of <sup>16</sup>O (Figure 9). This indicated that these two oxygen atoms are derived from the same molecule of O<sub>2</sub>.<sup>76–79</sup> The subsequent finding that PGE<sub>2</sub> and PGF<sub>2α</sub> were both produced by incubation of 20:4 with COX-containing guinea pig lung tissue, and that the two PG's were not interconvertible, suggested that they came from a common intermediate.<sup>80</sup> These labeling experiments led Hamberg and Samuelsson to propose the existence of a cyclic peroxide intermediate that was subsequently converted to the ultimate PG products (Figure 10).

Later, studies by Wlodawer and Samuelsson using 5,6,8,9,11,12,14,15-octadeuterio-20:4 provided further support for these conclusions. The formation of PGE<sub>2</sub> and PGD<sub>2</sub> from this substrate requires carbon-deuterium bond cleavage, whereas the formation of PGF<sub>2α</sub> does not (Figure 11).<sup>81</sup> Incubation of the octadeuterated substrate with the enzyme from sheep vesicular gland microsomes led to the formation of PGE<sub>2</sub> and PGD<sub>2</sub> in which the ratio of deuterated molecules to hydrogen-containing molecules was



**Figure 11.** Conversion of octadeuterated 20:4 to PGE<sub>2</sub> and PGF<sub>2α</sub>. Formation of PGE<sub>2</sub> requires cleavage of the carbon to deuterium bond at position 9, resulting in a kinetic isotope effect. This is not the case for PGF<sub>2α</sub>. The kinetic isotope effect leads to the selective conversion of nondeuterated PGH<sub>2</sub> to PGE<sub>2</sub>, so the ratio of deuterium to hydrogen in the PGE<sub>2</sub> product is lower than that of the starting material (relative D:H = 0.4). The remaining PGH<sub>2</sub> is enriched in deuterium, and it is converted to PGF<sub>2α</sub>. Thus, the product, PGF<sub>2α</sub>, has a higher ratio of deuterium to hydrogen than the starting material (relative D:H 4.0). The latter finding could occur only if both products are made from the same pool of endoperoxide.



**Figure 12.** Chemical conversions of PGG<sub>1</sub> used to confirm its identity in reaction mixtures of seminal vesicle microsomes with 20:3. Spontaneous decay leads to the formation of 15-hydroperoxy-PGE<sub>1</sub> and 15-hydroperoxy-PGD<sub>1</sub>. Stannous chloride or triphenylphosphine reduction yields PGF<sub>1α</sub>. Lead acetate followed by triphenylphosphine produces 15-keto-PGF<sub>1α</sub>.<sup>3</sup>

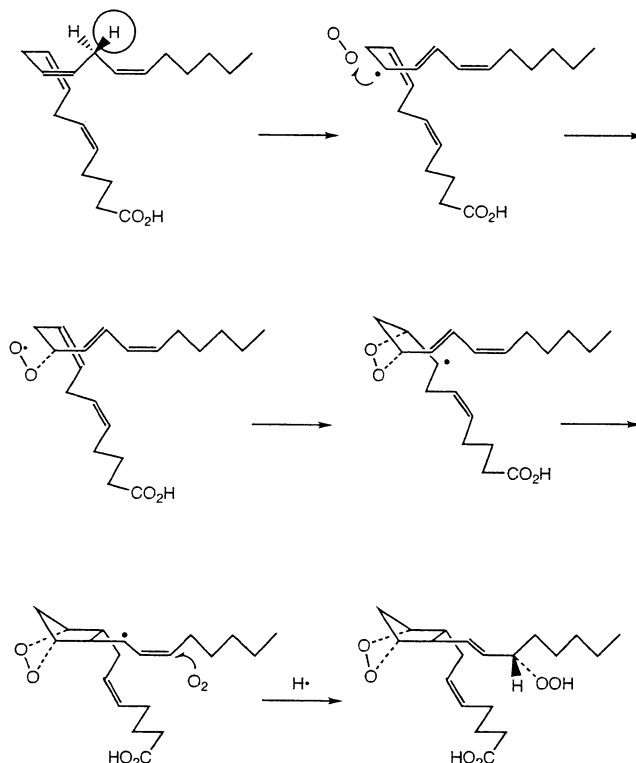
reduced relative to that of the starting material. In contrast, the deuterium-to-hydrogen ratio was higher than that of the starting material for PGF<sub>2α</sub>. The reduction in the deuterium-to-hydrogen ratio for PGE<sub>2</sub> and PGD<sub>2</sub> was explained on the basis of a kinetic isotope effect, assuming that the rate-limiting step in the formation of these PG's from PGH<sub>2</sub> is carbon–deuterium bond cleavage. The slower rate of reaction for deuterium-containing PGH<sub>2</sub> would lead

to an enrichment of deuterium in the pool of PGH<sub>2</sub> that did not react to form PGE<sub>2</sub> and PGD<sub>2</sub>. If PGF<sub>2α</sub> is synthesized from this pool, it would become enriched in deuterium-containing molecules. Such an enrichment in the relative deuterium-to-hydrogen ratio would not be seen in PGF<sub>2α</sub> if it is synthesized from an independent pool of PGH<sub>2</sub>. Thus, these results support the assertion that a common intermediate gives rise to all of the PG products and rule out the possibility that separate COX enzymes give rise to individual PG's.

The proposed endoperoxide intermediates, PGG<sub>1</sub> and PGH<sub>1</sub>, were isolated and shown to be produced prior to PGE<sub>1</sub> during the reaction of COX with 20:3. [Similarly, PGG<sub>2</sub> and PGH<sub>2</sub> were shown to be synthesized from 20:4.] The identities of the endoperoxides were confirmed by spontaneous rearrangement of PGH<sub>1</sub> and PGG<sub>1</sub> to form PGE<sub>1</sub> plus PGD<sub>1</sub> or the 15-hydroperoxy derivatives of PGE<sub>1</sub> plus PGD<sub>1</sub>, respectively. Stannous chloride reduction converted both endoperoxides to PGF<sub>1α</sub>, and treatment with lead acetate plus triphenylphosphine converted PGG<sub>1</sub> to 15-keto-PGF<sub>1α</sub> (Figure 12). These results confirmed the role of endoperoxides as intermediates in PG synthesis.<sup>1–3</sup>

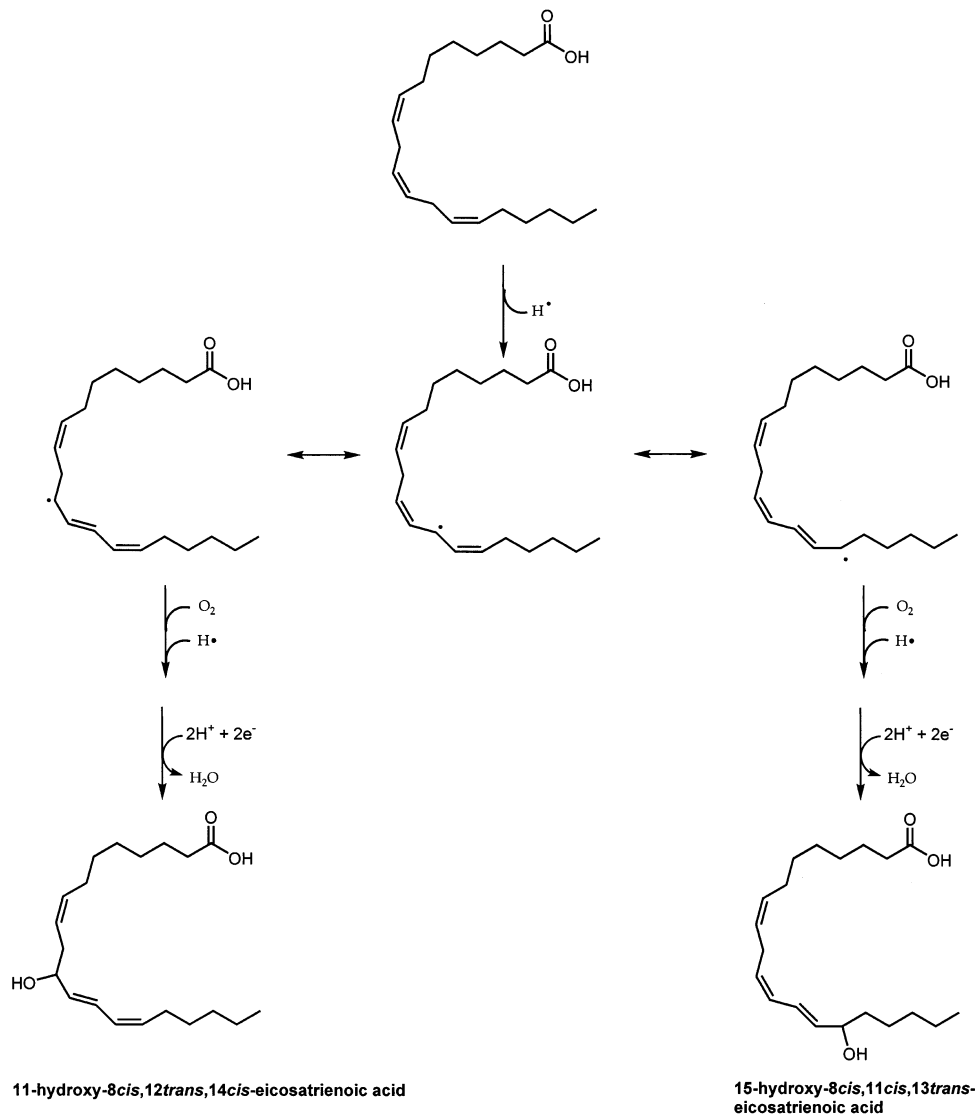
## B. Proposed Chemical Mechanism

Consideration of the mechanistic information on the enzymatic and nonenzymatic oxygenation of polyunsaturated fatty acids led Hamberg and Samuelsson to propose a free radical mechanism for the oxygenation catalyzed by COX.<sup>73,76,82</sup> The sequence of reactions outlined in Figure 13 is an adaptation



**Figure 13.** Detailed proposed mechanism for the COX reaction. Abstraction of the 13-*pro*(*S*) hydrogen atom of 20:4, followed by addition of two oxygen molecules and the formation of the cyclic peroxide ring system, leads to the formation of PGG<sub>2</sub>. PGH<sub>2</sub> is formed from PGG<sub>2</sub> by the peroxidase activity of the enzyme.



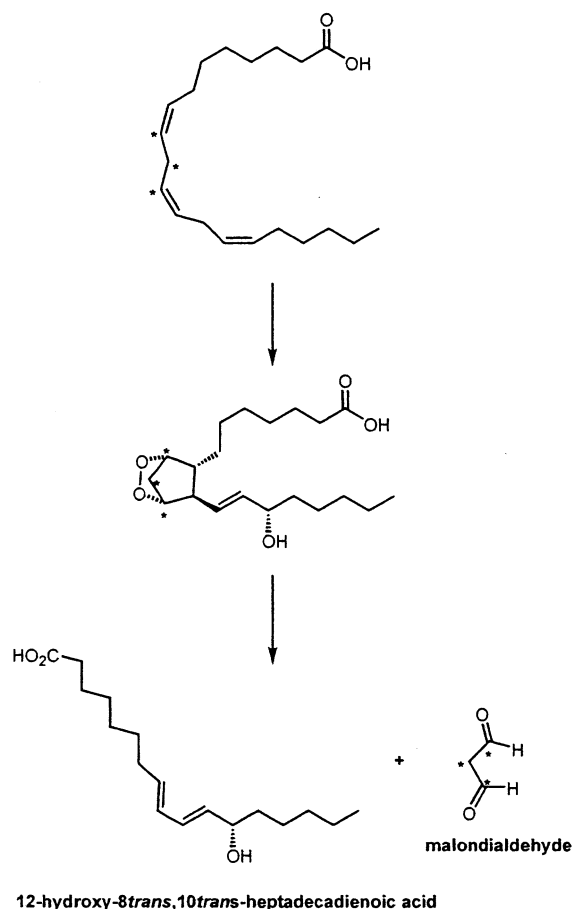


**Figure 14.** Formation of hydroxyeicosatrienoic acids from the reaction of 20:3 with seminal vesicle microsomes. After abstraction of the 13-*pro*(*S*) hydrogen atom, two resonance forms place the radical at either carbon 11 or carbon 15. Addition of oxygen at these positions, followed by peroxidase reduction, results in the corresponding hydroxyeicosatrienoic acids.<sup>77,82</sup>

of the original mechanism that explains the production of five chiral centers from a symmetric substrate with minimal motion of the intermediates during catalysis. A key prediction is that the polyunsaturated fatty acid is bound in an L-shaped conformation in order to generate a cyclopentane ring with trans-dialkyl substitution.<sup>83</sup> Removal of the 13-*pro*(*S*) hydrogen produces a pentadienyl radical that is trapped by  $\text{O}_2$  at carbon 11 to form an 11-(*R*)-peroxyl radical. This peroxyl radical undergoes a 5-*exo* cyclization to form a cyclic peroxide with a carbon-centered radical at carbon 8. The latter undergoes another 5-*exo* cyclization to generate the bicyclic peroxide and an allylic radical with electron density at carbons 13 and 15. Trapping of the allylic radical at carbon 15 with a second molecule of  $\text{O}_2$ , followed by reduction of the incipient peroxyl radical to a hydroperoxide, produces  $\text{PGG}_2$ , the product of the cyclooxygenase reaction. This mechanism is consistent with the results of all the isotopic labeling experiments.

### C. Minor Cyclooxygenase Products

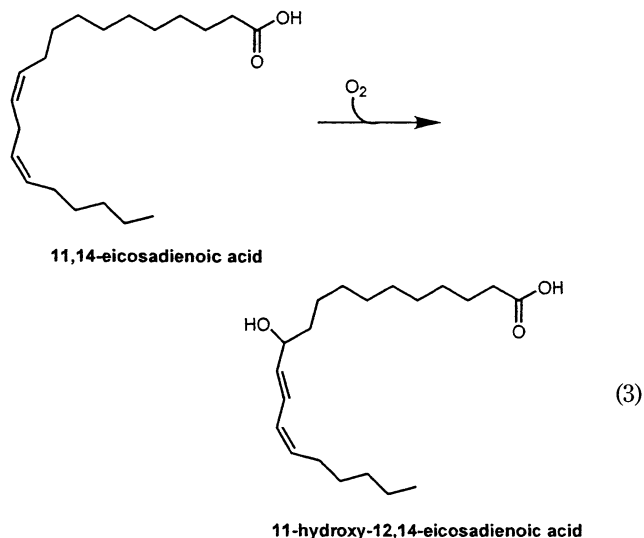
COX produces small amounts of compounds other than PG's. This phenomenon was noted by Nugteren et al., who identified 11-hydroxy-8-*cis*,12-*trans*,14-*cis*-eicosatrienoic acid and 12-hydroxy-8-*trans*,10-*trans*-heptadecadienoic acid as minor products of the reaction of 20:3 with ram seminal vesicle microsomes.<sup>77</sup> This finding was confirmed by Hamberg and Samuelsson, who also identified 15-hydroxy-8-*cis*,11-*cis*,13-*trans*-eicosatrienoic acid and malondialdehyde as minor products.<sup>82</sup> Hamberg and Samuelsson proposed that these byproducts could all be explained on the basis of the proposed mechanism of PG biosynthesis. Following abstraction of the 13-*pro*(*S*) hydrogen atom, addition of oxygen at carbon 11 would yield 11-hydroperoxy-8-*cis*,12-*trans*,14-*cis*-eicosatrienoic acid if the peroxyl radical did not cyclize to form the endoperoxide ring at carbon 9. Alternatively, trapping of the initial pentadienyl radical at carbon 15 instead of carbon 11 would result in the formation of 15-hydroperoxy-8-*cis*,11-*cis*,13-*trans*-eicosatrienoic acid (Figure 14). Finally, break-



**Figure 15.** Formation of malondialdehyde and 12-hydroxy-8,10-heptadecadienoic acid from the reaction of 20:3 with seminal vesicle microsomes. Following formation of the endoperoxide, spontaneous decomposition yields the two products. Asterisks indicate the locations of tritium-labeled carbon atoms.<sup>82</sup>

down of the endoperoxide intermediate with loss of carbons 9, 10, and 11 would yield 12-hydroxy-8-*trans*,10-*trans*-heptadecadienoic acid and malondialdehyde. Using 20:3, specifically labeled with tritium at positions 9, 10, and 11, Hamberg and Samuelsson confirmed that these hydrogens were present in the malondialdehyde product but not in the 12-hydroxy-8-*trans*,10-*trans*-heptadecadienoic acid, a finding consistent with the proposed mechanism (Figure 15).

Although the reports of hydroxy fatty acids as minor products of the COX reaction were convincing, these studies were all performed with impure enzyme preparations, so the possibility existed that a separate enzyme was responsible for these compounds. This concern was eliminated by the work of Hemler et al., who showed that purified COX-1 exhibits lipoxygenase activity if 8,11-eicosadienoic acid (20:2) is used as substrate (eq 3).<sup>84</sup> Furthermore, Hecker et al. confirmed the formation of 11-(*R*)-hydroperoxy-5-*cis*,8-*cis*,12-*trans*,14-*cis*-eicosatetraenoic acid, 12-(*S*)-hydroperoxy-5-*cis*,8-*trans*,10-*trans*-heptadecatrienoic acid, 12-(*S*)-hydroxy-5-*cis*,8-*trans*,10-*trans*-heptadecatrienoic acid, 15-(*RS*)-hydroperoxy-5-*cis*,8-*cis*,12-*cis*,13-*trans*-eicosatetraenoic acid, and 15-(*RS*)-hydroxy-5-*cis*,8-*cis*,12-*cis*,13-*trans*-eicosatetraenoic acid by purified COX-1 in its reaction with 20:4.<sup>85</sup> These investigators also identified 13-hydroxy-5-*cis*,14-*cis*-



PGH<sub>2</sub> (13-hydroxy-PGH<sub>2</sub>), 15(*S*)-hydroxy-8-*iso*-5-*cis*,13-*trans*-PGH<sub>2</sub> (8-*iso*-PGH<sub>2</sub>), and 15-*oxo*-PGH<sub>2</sub> as minor reaction products. On the basis of the proposed mechanism for PG synthesis shown in Figure 13, Hecker et al. explained 13-hydroxy-PGH<sub>2</sub> formation by trapping of the allylic radical product of the second 5-*exo* cyclization at carbon 13 rather than at carbon 15. Subsequent reduction of the resulting hydroperoxide by the enzyme's peroxidase activity yields the alcohol at carbon 13. Hecker et al. also suggested that 15-*oxo*-PGH<sub>2</sub> formation can occur via the iron- or enzyme-catalyzed loss of water from PGG<sub>2</sub>. Thus, the formation of minor products of the COX reaction provides support for the mechanism outlined in Figure 13. The fact that oxygen addition can occur at a number of different sites suggests facile access of O<sub>2</sub> to radical intermediates in the enzyme active site or diffusion of radical intermediates from the active site to encounter O<sub>2</sub> in solution. The latter possibility may explain the formation of minor products with randomized stereochemistry.

The mechanism outlined in Figure 13 provides a suitable explanation for the chemical steps in the oxygenation of polyunsaturated fatty acids to PG endoperoxides. It also suggests that the COX protein controls the stereochemistry of the individual reactions by binding the substrate in an L-shaped conformation. The key tenets of this mechanism have been verified in studies that will be outlined in more detail later. But the questions that will consume most of our attention in this review will be concerned with how the enzyme removes the 13-*pro*(*S*) hydrogen and how it reduces the final peroxy radical to the hydroperoxide. An additional question that any proposed mechanism must answer is how the enzymatic oxidant is regenerated at the end of each catalytic cycle.

#### IV. Relationship between the Cyclooxygenase and Peroxidase Activities of COX

Several discoveries in the early to mid-1970s provided critical insights into the generation of oxidants by the COX protein. The first was the identification of heme as the heat-stable stimulatory

factor for COX in seminal vesicle extracts. The second was the nearly simultaneous discovery by several groups that ram seminal vesicles contain a peroxidase activity that is apparently related to the action of the cyclooxygenase. The third was that the ability of COX to oxygenate polyunsaturated fatty acids is somehow dependent on the functioning of the peroxidase.

### A. COX as a Hemeprotein

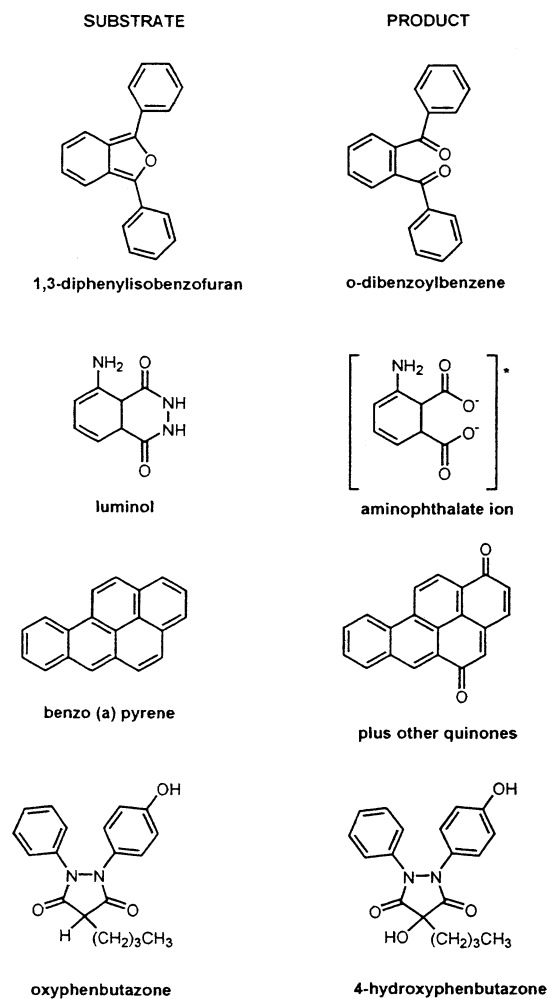
Samuelsson first reported that cytoplasmic extracts of seminal vesicle homogenates contained a heat-stable factor that stimulated PG formation by seminal vesicle microsomes.<sup>86</sup> Partial purification of this factor from bovine seminal vesicles by Yoshimoto et al. revealed that it exhibited spectral characteristics analogous to those of hemoglobin.<sup>87</sup> Addition of hemoglobin, methemoglobin, or heme alone dramatically stimulated the cyclooxygenase activity of bovine seminal vesicle microsomes. When 20:4 was added to suspensions of bovine seminal vesicle microsomes, spectral changes occurred consistent with the loss of absorbance from a hemeprotein. This led Yoshimoto et al. to propose that the 20:4 oxygenating activity was due to a heme-containing protein.

These observations not only provided the first hint that COX was a hemeprotein but also offered a practical insight that was important in the eventual purification of the COX protein. Since COX is a membrane protein, the first step in its purification is solubilization with nonionic detergents. The solubilization procedure releases heme from the protein, so the isolated enzyme appears to be inactive. This was interpreted to indicate extreme lability. Actually, the solubilized protein is quite stable in the absence of heme but lacks oxygenase activity. When heme is added, cyclooxygenase activity is nearly completely reconstituted. Since the heme donor can be free heme or one of several hemeproteins, Yoshimoto et al. proposed that reconstitution from a hemeprotein results from exchange of the heme from the donor protein.

### B. The Peroxidase Activity of COX

Initial evidence for the existence of a peroxidase activity associated with COX came from early studies of Marnett et al., who demonstrated that the reaction of ram seminal vesicle microsomes with 20:4 led to the co-oxygenation of aromatic compounds such as 1,3-diphenylisobenzofuran, luminol, oxyphenbutazone, and benzopyrene (Figure 16).<sup>88</sup> The co-oxygenation reactions required the presence of 20:4 and active enzyme and were inhibited by cyclooxygenase inhibitors. Similar results were obtained when 20:4 was replaced by either PGG<sub>2</sub> or 15-hydroperoxy-5,8,11,13-eicosatetraenoic acid (15-HPETE), but not PGH<sub>2</sub>. However, the hydroperoxide-dependent oxidations were not inhibited by cyclooxygenase inhibitors. The authors concluded that the co-oxygenation reactions were the result of the interaction of an enzyme system in the microsomes with a hydroperoxide intermediate of PG biosynthesis.

Soon thereafter, O'Brien and Rahimtula demonstrated that sheep seminal vesicle microsomes pos-



**Figure 16.** Co-oxygenation of various organic compounds during the reaction of vesicular gland microsomes with 20:4. Structures of the co-oxygenated substrates and identified products are shown.<sup>88</sup> The identification of the products of benzo[a]pyrene co-oxygenation was reported later.<sup>260</sup>

sess a strong peroxidase activity with broad hydroperoxide and reducing substrate specificity.<sup>89</sup> Since the peroxidase activity displayed subcellular localization, activation by heme, inhibition by heme ligands, and inactivation by hydroperoxides similar to those observed for the cyclooxygenase activity of COX, O'Brien and Rahimtula concluded that the peroxidase activity was an integral part of the cyclooxygenase enzyme complex. This conclusion was verified by co-purification of the cyclooxygenase and peroxidase activities of ram seminal vesicle microsomes and by co-immunoprecipitation of the peroxidase activity with monoclonal antibodies raised against the cyclooxygenase protein.<sup>30,32,90</sup> The interdependence of the two activities was suggested by the findings that both required heme<sup>30,32,33,37</sup> and that addition of peroxidase reducing substrates accelerated hydroperoxide reduction and helped to stabilize both the peroxidase and the cyclooxygenase reactions.<sup>30,32,33,91,92</sup> Finally, as will be discussed in detail below (section IV.D), intact peroxidase activity has been shown to be required for the activation of the cyclooxygenase catalytic activity.

Although the cyclooxygenase and peroxidase activities appeared to be related, several studies sug-

gested that their active sites are separate: (1) aspirin and other non-steroidal anti-inflammatory drugs inhibit the cyclooxygenase, but not the peroxidase activity;<sup>30,93</sup> (2) reconstitution of apoprotein with  $Mn^{3+}$ -PPIX produces an enzyme ( $Mn$ -COX) with cyclooxygenase activity but low peroxidase activity (discussed in section IX); (3) certain site-directed mutants of COX-1 and COX-2 selectively alter either the cyclooxygenase or the peroxidase activity (discussed in section VIII.E); (4) docosahexenoic acid is a competitive inhibitor for the cyclooxygenase, but not the peroxidase activity;<sup>93</sup> and (5) although both the cyclooxygenase and peroxidase activities are inactivated during the conversion of 20:4 to  $PGH_2$  (see section IV.E), inactivation of the cyclooxygenase activity occurs more rapidly than inactivation of the peroxidase activity.<sup>94,95</sup>

### C. Assays for Peroxidase and Cyclooxygenase Activities

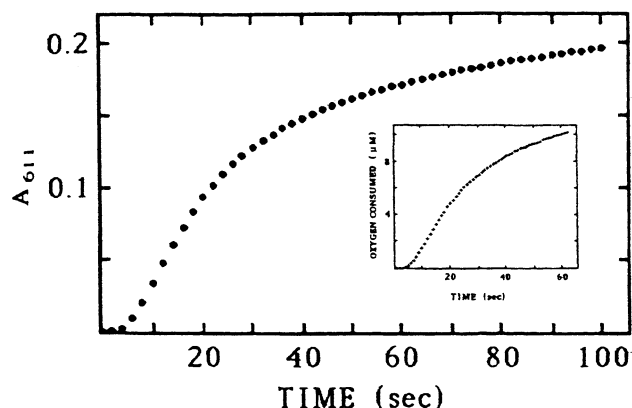
The cyclooxygenase and peroxidase reactions may be monitored separately or in tandem. The cyclooxygenase reaction is most conveniently monitored by the decrease in oxygen concentration that occurs during fatty acid oxygenation, assuming that two molecules of oxygen are consumed per molecule of fatty acid. In the absence of peroxidase reductant, only the cyclooxygenase reaction occurs. In the presence of peroxidase reductant, the peroxidase reaction also occurs though, theoretically, it should not contribute directly to the rate or extent of oxygen consumption. A disadvantage of the use of the oxygen electrode is the fact that the rate of oxygen diffusion across the electrode membrane may be slower than the rate of the cyclooxygenase reaction under some circumstances, leading to an underestimation of the reaction rate.<sup>96</sup> Furthermore, since the COX reaction generates minor quantities of hydroxy fatty acids, the 2:1 reaction stoichiometry is not absolutely correct.<sup>77,82,97,98,85</sup> The latter concern is usually only problematic in studies of enzyme inhibition or site-directed mutagenesis, in which the ratio of hydroxy fatty acid to PG is significantly increased. An alternative method for monitoring cyclooxygenase activity is to use radiolabeled fatty acid as substrate and chromatographically separate and quantify each of the reaction products. This method avoids the problems associated with the use of the oxygen electrode, but since it is a radiochemical assay, it is discontinuous and, therefore, not well-suited to extensive kinetic studies.

The peroxidase reaction is most easily monitored spectrophotometrically using hydroperoxide substrates or peroxidase reductants that exhibit a change in absorbance upon reduction or oxidation, respectively. The hydroperoxides can be added exogenously or generated in situ via the cyclooxygenase reaction. For example, *N,N,N,N*-tetramethylphenylenediamine (TMPD) exhibits an absorbance increase at 611 nm upon oxidation, and this is used in a coupled assay for cyclooxygenase activity.<sup>94</sup> The assay is commonly employed for the identification of cyclooxygenase inhibitors, with the caveat that easily oxidized compounds can appear to be cyclooxygenase inhibi-

tors by preventing the oxidation of TMPD. A direct assay for hydroperoxide reduction has been developed using the synthetic compound, 5-phenyl-4-pentenyl hydroperoxide (PPHP). PPHP substrate and product alcohol (PPA) are extracted from the incubation mixture and separated by HPLC with UV detection. PPHP is an efficient substrate for several other peroxidases, so this has been developed into a general assay.<sup>99</sup>

### D. Peroxidase-Dependent Activation of Cyclooxygenase Activity

The interdependence of the cyclooxygenase and peroxidase activities of COX directly impacts the kinetics of the two reactions. The consequences are illustrated Figure 17, which shows the time course



**Figure 17.** Time course of the COX-1 reaction. The reaction mixture contained 20 nM enzyme monomer, 40  $\mu$ M 20:4, and 84  $\mu$ M TMPD in 0.1 M Tris-HCl buffer, pH 8.5. Oxidation of TMPD was monitored by change in absorbance at 611 nm, and oxygen consumption was measured by polarographic oxygen electrode (inset). Reproduced with permission from ref 94. Copyright 1987 Elsevier Science.

of the COX reaction in a mixture containing 20 nM enzyme monomer (COX-1), 40  $\mu$ M 20:4, and 84  $\mu$ M TMPD as peroxidase reductant.<sup>94</sup> The reaction was monitored by the change in absorbance at 611 nm resulting from the oxidation of TMPD, and by oxygen consumption as measured by an oxygen electrode. The progress of the reaction is characterized by a lag phase, a period of rapid reaction, and then a gradual decrease in rate until the reaction ceases. The lag phase is attributed to the requirement of the enzyme for activation of the oxygenase activity by product hydroperoxide, and the cessation of reaction, which occurs prior to complete consumption of substrate, is the result of enzyme inactivation. Both of these characteristics of the cyclooxygenase reaction are dependent on the peroxidase activity, as will be discussed below. The impact of the activation and inactivation of COX is that the enzyme does not actually achieve a steady state during the cyclooxygenase reaction, or if it does, it is for only a brief period. Consequently, other parameters are often used to express enzyme activity, including maximal rate achieved, total substrate consumed, and length of time required to achieve maximal activity.

Lands et al. proposed a role for peroxide activation of COX in 1971, when they reported that the combi-

nation of glutathione (GSH) plus GSH peroxidase markedly inhibited the cyclooxygenase reaction.<sup>100</sup> GSH peroxidase catalyzes the efficient reduction of a range of hydroperoxides, including fatty acid hydroperoxides and PGG<sub>2</sub>, so its inhibition of cyclooxygenase activity implied a role for hydroperoxides in stimulating and supporting the latter. Further evidence for peroxide-dependent activation was provided by Cook and Lands, who showed that COX activity in an acetone powder of sheep vesicular glands demonstrated both a lag phase and enzyme inactivation.<sup>101</sup> If the enzyme was allowed to react until all activity ceased, fresh enzyme added to the reaction mixture exhibited no lag phase, indicating that an activating factor had been produced during the course of the first reaction. Hemler et al. later demonstrated that addition of PGG<sub>2</sub> and other lipid hydroperoxides to preparations of COX eliminated the lag phase, whereas the hydroxy fatty acid, PGH<sub>2</sub>, did not.<sup>102,103</sup> Also consistent with a role for hydroperoxides in enzyme activation was the observation that antioxidants, such as diethyldithiocarbamate (DDC) or phenol, produced exaggerated lag phases.<sup>102–104</sup> Since any possible direct reaction between DDC or phenol with hydroperoxides would be slow relative to the rate of the COX reaction, the effect of these compounds on the lag phase must be due to their interaction with the enzyme itself.

The requirement for hydroperoxides in the activation of COX appears to be paradoxical, since the peroxidase activity of COX would be expected to destroy the required activating hydroperoxide. This seeming contradiction was emphasized in studies of enzyme inhibition by GSH and GSH peroxidase, which demonstrated that the requirement for peroxide persisted throughout the cyclooxygenase reaction.<sup>104</sup> Kulmacz and Lands resolved this issue through experiments in which varying levels of GSH and GSH peroxidase were used to regulate the "peroxide tone" in reaction mixtures containing purified COX-1.<sup>105</sup> These studies allowed the determination of the concentration of peroxide required for activation and indicated that the apparent  $K_M$  for this process (20 nM) was much lower than the  $K_M$  for the peroxidase reaction (2.5  $\mu$ M). Thus, the peroxidase activity of COX-1 is not capable of lowering the peroxide concentration to levels below those necessary to maintain enzyme activation under normal circumstances. However, in later studies, Kulmacz et al. demonstrated that the addition of aspirin-treated COX-1 (which exhibits normal peroxidase activity in the absence of cyclooxygenase activity) to untreated COX-1 results in suppression of the cyclooxygenase reaction.<sup>92</sup> Thus, the peroxidase activity of COX-1 was shown to be capable of acting like GSH peroxidase, although a ratio of aspirin-treated to untreated enzyme of 10:1 was required for complete suppression of cyclooxygenase activity.

Spectrophotometric data demonstrated that CN<sup>-</sup>, but not CO, could form a complex with the heme of ovine vesicular gland COX (COX-1) and inhibit the peroxidase activity of the enzyme.<sup>37,92,101,104,106</sup> CN<sup>-</sup>, but not CO, treatment extended the cyclooxygenase reaction lag phase and increased the enzyme's sen-

sitivity to GSH peroxidase inhibition.<sup>101,104,107</sup> Spectrophotometric studies also demonstrated that CN<sup>-</sup> bound to heme with a  $K_D$  of 0.19 mM, a value close to the  $K_I$  (0.23 mM) for peroxidase inhibition and for suppression of peroxidase activation of the cyclooxygenase activity.<sup>106</sup> Finally, replacement of the heme prosthetic group of COX-1 with Mn<sup>3+</sup>-PPIX, an alteration resulting in an enzyme with markedly reduced peroxidase activity, resulted in retention of cyclooxygenase activity, but with exaggerated lag phases and increased sensitivity to GSH peroxidase inhibition.<sup>102,108,109</sup> These data clearly indicate that the peroxidase active site, and specifically the heme moiety, are involved in the hydroperoxide-dependent activation of the cyclooxygenase activity.

### E. Peroxidase-Dependent Inactivation of Cyclooxygenase Activity

The self-inactivation of COX in sheep vesicular gland microsomes (COX-1) was described by Smith and Lands, who noted an apparent first-order decrease in cyclooxygenase activity in the presence of fatty acid substrate.<sup>110</sup> Significant inactivation was also observed after exposure of the enzyme preparation to hydroperoxides. Supporting evidence for the possible involvement of hydroperoxides in the self-inactivation of COX-1 was provided by Egan et al., who observed a rapid decrease in the peroxidase activity of the enzyme in the presence of lipid hydroperoxide substrates.<sup>111</sup> The generation of free radicals on addition of hydroperoxides to the peroxidase was detected by electron paramagnetic resonance (EPR). Since the radical signal and the rate of inactivation both decreased in the presence of peroxidase reductants, Egan et al. concluded that oxidants generated during the course of the peroxidase reaction inactivate critical residues on the enzyme protein and that the presence of peroxidase reductants reduces the concentration of these oxidants.

Markey et al. further explored the role of hydroperoxides in COX inactivation.<sup>112</sup> They showed that a 2-min incubation of COX-1 (352 nM) with 15-HPETE inactivated both the cyclooxygenase and peroxidase activities with IC<sub>50</sub> values of 4.0 and 2.5  $\mu$ M, respectively. These values were determined in the presence of a 4  $\mu$ M concentration of the peroxidase reductant, DDC. In the absence of DDC, IC<sub>50</sub> values for the inactivation of the cyclooxygenase activity of COX-1 were 2.8, 0.3, and 0.6  $\mu$ M for 15-HPETE, H<sub>2</sub>O<sub>2</sub>, and 20:4, respectively. Inactivation of the enzyme required the presence of the heme prosthetic group. When 20:4 was added to a preparation of COX-1 that contained only 37% holoenzyme, complete inactivation of the cyclooxygenase activity occurred. However, reconstitution of the inactivated enzyme with heme resulted in recovery of 60% of the activity of an identical preparation that had been fully reconstituted with heme but not pretreated with 20:4. Thus, only the holoenzyme was inactivated by 20:4 pretreatment, suggesting that inactivation by peroxides required the presence of an intact peroxidase activity. These experiments also argued against a role for a diffusible oxidant in the inactivation.

In kinetic studies of the COX-1 peroxidase reaction, Kulmacz observed that increasing peroxide concen-

**Table 1. Summary of COX Intermediates in the Cyclooxygenase and Peroxidase Reaction Mechanisms<sup>a</sup>**

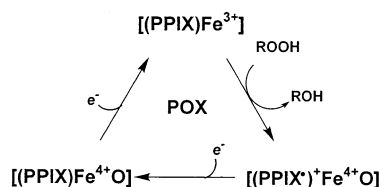
name	description	symbol	other designations
compound I	two-electron oxidized state with iron as Fe <sup>4+</sup> and porphyrin as cation radical	[(PPIX) <sup>+</sup> Fe <sup>4+</sup> O]	intermediate I
compound II	one-electron oxidized state with iron as Fe <sup>4+</sup>	[(PPIX)Fe <sup>4+</sup> O]	
intermediate I	two-electron oxidized state with iron as Fe <sup>4+</sup> and protein tyrosyl radical	[(PPIX)Fe <sup>4+</sup> O]tyr <sup>•</sup>	intermediate II
intermediate II	two-electron oxidized state with iron as Fe <sup>4+</sup> and unknown protein radical	[(PPIX) <sup>4+</sup> O]X <sup>•+</sup>	intermediate III
native	iron as Fe <sup>3+</sup> ; no heme or protein radicals	[(PPIX)Fe <sup>3+</sup> ]	

<sup>a</sup> The nomenclature of intermediates in the cyclooxygenase and peroxidase reactions is not totally consistent in the literature and is confusing. In this review, we have chosen to designate compound I and compound II of COX to correspond to the two-electron and one-electron oxidized species of horseradish peroxidase, respectively, which bear those same designations. We have reserved the term "intermediate" to refer to species that contain a protein radical. Intermediate I contains the catalytically active tyrosyl radical and is a two-electron-oxidized species. Intermediate II is believed to derive from intermediate I through transfer of the radical to a different (and unknown) protein residue.

trations resulted in a decreased extent of the peroxidase reaction.<sup>113</sup> From this observation, he concluded that the rate of inactivation of the peroxidase was directly related to the substrate hydroperoxide concentration. However, more detailed kinetic studies were later performed in which COX-1 was reacted with selected peroxides for varying times and the remaining peroxidase activity was measured using guaiacol and hydrogen peroxide. The results demonstrated that the inactivation was first-order with respect to enzyme and independent of hydroperoxide structure and concentration. The first-order rate constant for peroxidase inactivation was 0.2–0.5 s<sup>-1</sup> at 24 °C.<sup>114,115</sup>

## V. Mechanism of Peroxidase Catalysis

The discovery that the *activation and inactivation* of the cyclooxygenase reaction of COX were both dependent upon the peroxidase reaction suggested that an understanding of the peroxidase reaction mechanism should yield insights into the cyclooxygenase reaction as well. The preponderance of evidence indicates that the peroxidase reaction of COX occurs via a mechanism that is similar to those of other heme peroxidases, such as horseradish peroxidase or cytochrome *c* peroxidase. The basic mechanism for the COX peroxidase is outlined in Figure 18. It begins with native COX in the [(protoporphyrin



**Figure 18.** Basic mechanism for the COX peroxidase reaction. Native enzyme ([PPIX)Fe<sup>3+</sup>]) reacts with substrate peroxide (ROOH), reducing it to the corresponding alcohol (ROH) and converting the enzyme to compound I [(PPIX)<sup>+</sup>Fe<sup>4+</sup>O]). Two sequential one-electron reductions using peroxidase reductant as the electron source convert compound I to compound II [(PPIX)Fe<sup>4+</sup>O]) and then back to native enzyme. Identification of symbols for all intermediates is given in Table 1.

IX)Fe<sup>3+</sup>] state, which is indicated as [(PPIX)Fe<sup>3+</sup>] in this and all subsequent figures. [See Table 1 for a summary and definition of intermediate symbols and nomenclature.] The first step involves a two-electron

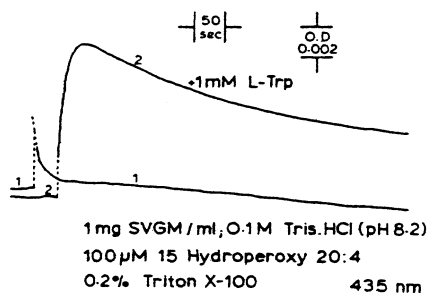
reduction of the hydroperoxide substrate to the alcohol product, which is supported by the two-electron oxidation of the resting heme to the oxoferryl form, designated compound I. Analogous to compound I of horseradish peroxidase, COX compound I contains Fe<sup>4+</sup> and a porphyrin radical cation [(PPIX)<sup>+</sup>Fe<sup>4+</sup>O]. One-electron reduction of the porphyrin cation radical produces compound II [(PPIX)Fe<sup>4+</sup>O], and a second one-electron reduction regenerates the resting enzyme. The source of electrons (designated e<sup>-</sup> in all figures) is the peroxidase reductant. Support for this mechanism comes largely from studies of spectral changes that occur during the interaction of COX with hydroperoxides, the kinetics of those changes, and the chemistry of hydroperoxide reduction.

## A. Spectral Studies of Peroxidase Turnover

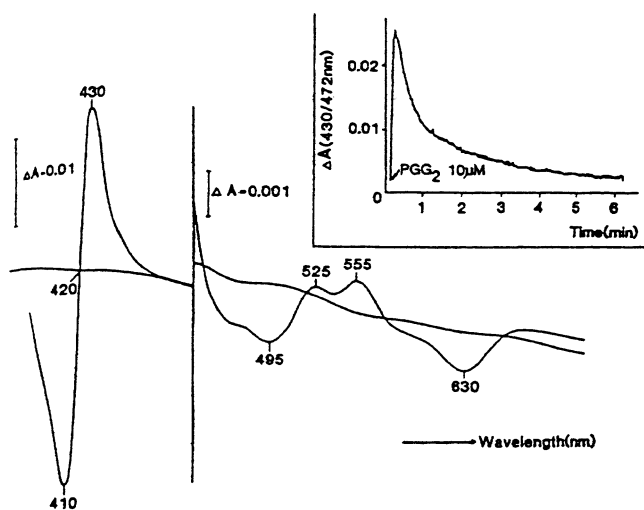
### 1. Identification of Higher Oxidation State Intermediates

Resonance Raman spectroscopy has shown that the ferric heme in resting, native COX-1 is in the high-spin, hexacoordinate state at room temperature.<sup>116,117</sup> The preponderance of spectral data shows that the proximal ligand to the iron is histidine (consistent with X-ray crystallographic data, as discussed in section VII.B) and that the sixth ligand is water. EPR studies demonstrated the presence of both high- and low-spin ferric heme in native COX-1. At room temperature, 80% of the heme was characterized as high-spin, and that percentage decreased with decreasing temperature.<sup>118</sup>

Early observations performed by O'Brien demonstrated that the addition of 20:4, PGG<sub>2</sub>, or 15-HPETE to ram seminal vesicle microsomes at 5 °C produced a rapidly decaying difference spectrum, with a band at 435 nm and a trough at 411 nm (Figure 19).<sup>119</sup> Similar results were obtained by Nastainczyk et al., who added 20:4 or PGG<sub>2</sub> to purified COX-1 at -15 °C and reported a difference spectrum with maxima at 430, 525, and 555 nm, a trough at 410 nm, and an isosbestic point at 421 nm (Figure 20).<sup>120</sup> The maximum at 430 nm decayed with a half-life of 1 min and shifted to 438 nm with a 3-fold increase in the trough at 410 nm. If high concentrations of 20:4 were used, a second addition did not result in a new difference spectrum, indicating a loss of enzyme activity. Both O'Brien and Nastainczyk et al. demonstrated that



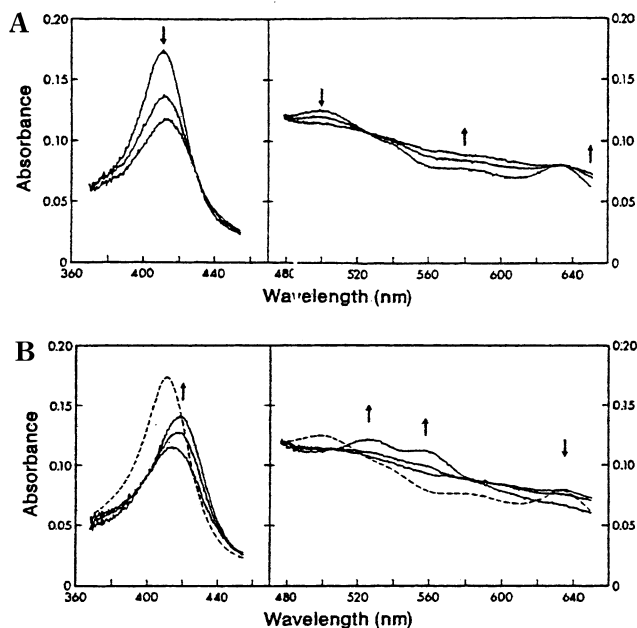
**Figure 19.** Spectral changes observed at 435 nm after mixing ovine seminal vesicle microsomes (1 mg/mL protein) with 100  $\mu$ M 15-HPETE in 0.1 M Tris-HCl buffer, pH 8.2, at 5  $^{\circ}$ C. Trace 1: Reaction was run in the absence of L-tryptophan. Trace 2: Addition of L-tryptophan delayed the spectral changes but resulted in greater and more prolonged increases in the absorbance at 435 nm. Reproduced with permission from ref 119. Copyright 1981 Elsevier.



**Figure 20.** Difference spectrum obtained by mixing 2.5  $\mu$ M COX-1 plus 2.5  $\mu$ M hematin, with 30  $\mu$ M PGG<sub>2</sub> in 0.1 M Tris-HCl buffer, pH 8.1 (40% glycerol), at -15  $^{\circ}$ C. Reproduced with permission from ref 120. Copyright 1984 Blackwell Publishing.

formation of the difference spectrum was inhibited by CN<sup>-</sup> or N<sub>3</sub><sup>-</sup> at concentrations that agreed with those required for inhibition of the peroxidase reaction. Spectral changes were reduced in the presence of peroxidase reductants but not cyclooxygenase inhibitors. Nastainczyk et al. further showed that the oxene donor, iodosobenzene, produced a similar difference spectrum upon addition to COX-1 reaction mixtures, suggesting that the spectral changes reflected the formation of an oxo-ferryl complex similar to that observed in the reaction of horseradish peroxidase with peroxides.

Lambeir et al. used rapid-scan spectroscopy techniques to monitor changes in the absolute spectrum of purified COX-1 after addition of PPHP at 5  $^{\circ}$ C.<sup>121</sup> They observed the formation of a species with a maximum absorbance at 412 nm similar to compound I of horseradish peroxidase (Figure 21A). The estimated second-order rate constant for formation of this species (which is designated compound I in this review) was  $1.3 \times 10^7 \text{ M}^{-1} \text{ s}^{-1}$ . [See Table 2 for reported rate constant values for the conversion of native enzyme to compound I.] Within 170 ms, this



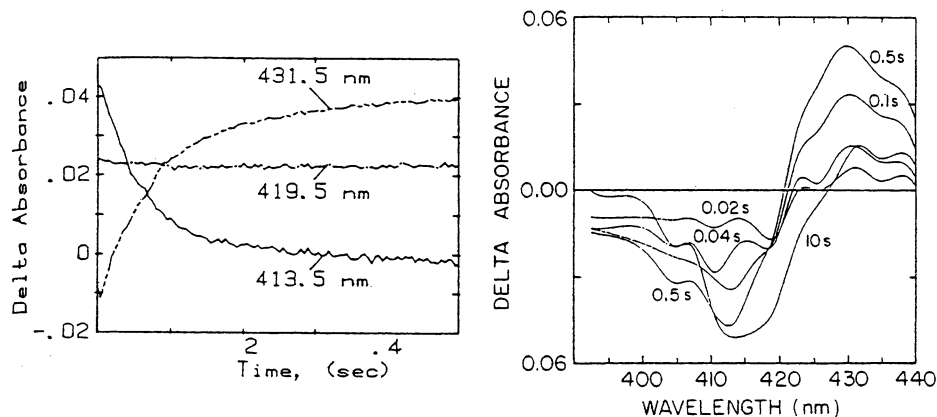
**Figure 21.** (A) Spectral changes observed after mixing COX-1 with 17  $\mu$ M PPHP at 5  $^{\circ}$ C. Concentrations of enzyme were 1.5  $\mu$ M for the Soret region and 12.1  $\mu$ M for the visible region. Spectra were taken at 0, 1, and 3 ms after mixing in the Soret region and 0, 2, and 16 ms after mixing in the visible region. Arrows indicate the change in direction of absorbance with time. (B) Spectral changes observed after mixing COX-1 with PPHP. Experimental conditions are the same as those for (A). Spectra in the Soret region are given for 11, 22, and 132 ms after mixing, and spectra in the visible region are given for 16, 34, and 166 ms after mixing. Reproduced with permission from ref 121. Copyright 1985 American Society for Biochemistry and Molecular Biology.

**Table 2. Reported Rate Constants for the Conversion Native Enzyme + Hydroperoxide  $\rightarrow$  Compound I + Alcohol**

COX isoform	peroxide substrate	temp ( $^{\circ}$ C)	rate constant ( $\text{M}^{-1} \text{s}^{-1}$ )	ref
COX-1	PPHP	5	$1.3 \times 10^7$	121
COX-1	15-HPETE	5	$1.5 \times 10^6$	121
COX-1	15-HPETE	rt <sup>a</sup>	$7.1 \times 10^7$	94
COX-1	H <sub>2</sub> O <sub>2</sub>	rt	$9.1 \times 10^4$	94
COX-1	PGG <sub>2</sub>	1	$1.4 \times 10^7$	39
COX-1	PPHP	4	$1.7 \times 10^7$	258
COX-1	H <sub>2</sub> O <sub>2</sub>	0.5	$(1.3 \pm 0.1) \times 10^6$	245
COX-1	<i>t</i> -butylOOH	6.7	$(5.9 \pm 0.1) \times 10^4$	248
COX-1	EtOOH	6.7	$(2.5 \pm 0.1) \times 10^6$	248
COX-1	<i>m</i> -Cl PBA	6.7	$(5.1 \pm 0.6) \times 10^7$	248
COX-1	PPHP	1	$9.0 \times 10^6$	123
COX-1	15-HPETE	1	$1.8 \times 10^7$	123
COX-1	EtOOH	1	$2.7 \times 10^6$	123
COX-1	H <sub>2</sub> O <sub>2</sub>	1	$1 \times 10^4$	123
COX-1	15-HPETE	4	$2.3 \times 10^7$	211
COX-2	15-HPETE	4	$2.5 \times 10^7$	211
COX-1	15-HPETE	20	$1.0 \times 10^8$	123
COX-1	EtOOH	20	$1.7 \times 10^7$	123
Mn-COX-1	15-HPETE	20	$1.0 \times 10^6$	123
Mn-COX-1	EtOOH	20	$6.8 \times 10^2$	123

<sup>a</sup> rt, room temperature.

species was converted to one having an absorbance maximum at 420 nm, similar to compound II of horseradish peroxidase (Figure 21B). Because the rate of formation of the second species was dependent on hydroperoxide concentration, a second-order rate



**Figure 22.** Spectral changes observed after mixing COX-1 (12  $\mu\text{M}$  heme) with 2 equiv of  $\text{H}_2\text{O}_2$  at 22  $^\circ\text{C}$ . Left: Stopped-flow traces of absorbance changes at 431, 419, and 413 nm. Right: Difference spectra obtained from absorbance measurements at 16 wavelengths measured at the five times indicated. Reproduced with permission from ref 118. Copyright 1987 American Society for Biochemistry and Molecular Biology.

constant for this transformation was reported to be  $1.2 \times 10^6 \text{ M}^{-1} \text{ s}^{-1}$  (from experiments with 16.8  $\mu\text{M}$  PPHP as substrate). [The exact identity of the second species, and the molecularity of the conversion of compound I to that species, will be discussed in greater detail in sections VI.A.2, VI.B, and XII.B.5.] Spontaneous decay of the second species to resting enzyme followed (first-order rate constant  $k < 0.1 \text{ s}^{-1}$ ), with a slight decrease in final absorbance, consistent with partial enzyme inactivation.

This cycle could be repeated multiple times with a small reduction in final absorbance each time. Similar results were obtained using 15-HPETE, but conversion to compound I occurred at a slower rate ( $k = 1.5 \times 10^6 \text{ M}^{-1} \text{ s}^{-1}$ ). During the reaction of COX-1 with 20:4, only the compound II-like spectrum was observed. This was attributed to the slow rate of formation of peroxide ( $\text{PGG}_2$ ) from 20:4, resulting in a correspondingly slow rate of formation of compound I, so that its conversion to the second species occurred as quickly as its formation. These experiments were the first to demonstrate the formation of higher oxidation states of COX-1 that are characteristic of heme peroxidase reactions and to record full spectra of these states. They also demonstrated that the difference spectra observed by O'Brien and Nastainczyk et al. were due to the formation of a species resembling compound II.<sup>119,120</sup>

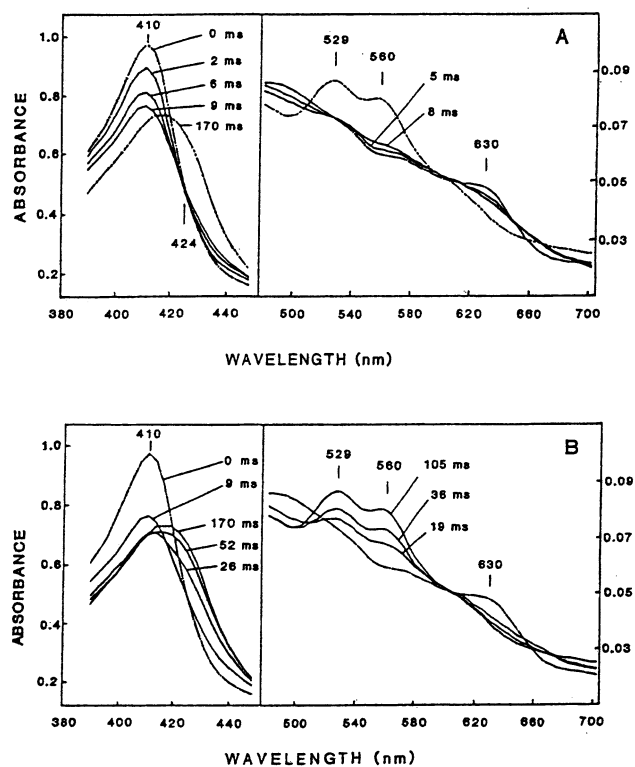
Kulmacz et al. reported spectral changes that occurred more slowly when COX-1 was reacted with hydrogen peroxide in lieu of lipid hydroperoxide.<sup>118</sup> Using 2 equiv of the peroxide at an enzyme concentration of 12  $\mu\text{M}$ , difference spectra showed a maximum at 430 nm, a zero crossing at 420 nm, and a minimum at 414 nm within the first 500 ms (Figure 22). Subsequently, the peak decreased sharply, shifting to 433 nm, and the zero crossing shifted to 427 nm, while the trough remained unchanged. Differences between these results and those of Lambeir et al. were attributed to the slower reaction with hydrogen peroxide, such that conversion from compound I to the second species occurred before full conversion of the enzyme to compound I had been completed.<sup>121</sup> Furthermore, Kulmacz et al. reported that the spectral changes they observed were more

similar to those seen in the formation of compound ES of cytochrome *c* peroxidase than to those seen in the formation of compound I of horseradish peroxidase. Compound ES contains oxo-ferryl heme but a tryptophan radical cation ( $\text{Trp}^{\bullet+}$ ) rather than a porphyrin radical cation.<sup>122</sup>

Rapid kinetic studies of the reaction of COX-1 with  $\text{PGG}_2$  at 1  $^\circ\text{C}$  allowed a more detailed study of the spectral intermediates and their rates of formation.<sup>39</sup> Analysis of the native enzyme displayed the typical spectrum of ferric high-spin heme, with maxima at 410 and 630 nm. Within the first 20 ms of reaction with  $\text{PGG}_2$ , this spectrum demonstrated a marked decrease at 410 nm, to yield a new spectrum having a maximum at 410 nm with lower absorbance and no features in the visible region. The isosbestic point for this change was 424 nm (Figure 23). As noted previously by Lambeir et al., these changes were consistent with the formation of a species similar to compound I of horseradish peroxidase, and the structure was proposed to be  $[(\text{PPIX}^{\bullet+})\text{Fe}^{4+}\text{O}]$ .<sup>121</sup> Kinetic studies indicated that this species was formed in a bimolecular reaction with peroxide, having a rate constant ( $k_1$ ) of  $1.4 \times 10^7 \text{ M}^{-1} \text{ s}^{-1}$ , similar to the value reported by Lambeir et al. for the reaction of COX-1 with PPHP (Table 2).<sup>121</sup> After the formation of compound I, a second spectral change was observed, leading to the formation of a species having absorbance maxima at 420, 529, and 560 nm. The isosbestic point for this transition was 410 nm (Figure 23). The spectral properties of the second intermediate were most similar to those of compound ES of cytochrome *c* peroxidase, a two-electron oxidized state,  $[(\text{PPIX})\text{Fe}^{4+}\text{O}]\text{Trp}^{\bullet+}$ . Thus, an intramolecular electron transfer from a protein amino acid to the porphyrin was proposed to occur in COX, forming an intermediate which will be named intermediate I in this review.

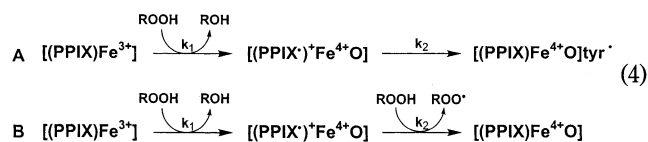
The rate of conversion of compound I to intermediate I exhibited pseudo-first-order behavior. However, the observed rate constants were dependent on hydroperoxide concentration, showing a linear increase at low concentrations and saturation at high concentrations. Using mathematical modeling, Dietz et al. showed that the data were consistent with a





**Figure 23.** Spectra obtained during the reaction of COX-1 (5  $\mu\text{M}$ ) with 0.16  $\mu\text{M}$  PGG<sub>2</sub> at 1 °C. (A) Spectra were obtained during the first 10 ms of reaction at the times indicated. (B) Spectra were obtained from 10 to 170 ms at the times indicated. Native enzyme spectra (labeled 0 ms) were obtained after the addition of PGG<sub>2</sub> vehicle (propanol) in the absence of PGG<sub>2</sub>. Reproduced with permission from ref 39. Copyright 1988 Blackwell Publishing.

mechanism in which enzyme and hydroperoxide react in a bimolecular process to form compound I, which then undergoes a unimolecular process to form intermediate I (eq 4A).<sup>39</sup> [Note that intermediate I

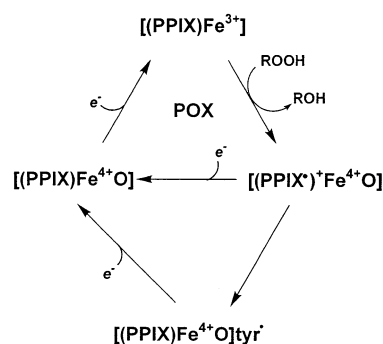


is designated [(PPIX)Fe<sup>4+</sup>O]tyr\* in this equation and all figures. The identification of the tyrosine residue as the site of the radical in intermediate I will be discussed in detail in sections VI.A.2 and VI.B.] According to eq 4A, the formation of compound I is rate-limiting at low hydroperoxide concentrations, so that the rate of formation of intermediate I appears to be linearly dependent on hydroperoxide. At high hydroperoxide concentrations, the formation of intermediate I is rate-limiting, and its rate of formation is then independent of hydroperoxide. An alternative model, in which the formation of the second intermediate is the result of a bimolecular reaction with hydroperoxide, leading to the formation of peroxy radical and reduction of compound I to compound II, was tested and did not fit the data (eq 4B). Dietz et al. concluded that the kinetic data were consistent with the conclusion that the second species was the two-electron-oxidized state designated intermediate I, and they reported a unimolecular rate constant (*k*<sub>2</sub>)

**Table 3. Reported Rate Constants for the Conversion Compound I → Intermediate I**

COX isoform	peroxide substrate	temp (°C)	rate constant (s <sup>-1</sup> )	ref
COX-1	PGG <sub>2</sub>	1	65	39
COX-1	PPHP	1	280	123
COX-1	15-HPETE	1	250	123
COX-1	EtOOH	1	68	123
COX-1	15-HPETE	4	100–1000	211
COX-2	15-HPETE	4	≥1000	211
Mn-COX-1	15-HPETE	20	400	123

of 65 s<sup>-1</sup> for its formation. [See Table 3 for a listing of reported rate constant values for the conversion of compound I to intermediate I.] This concept has provided an important key to understanding the link between the peroxidase and cyclooxygenase activities of the enzyme, which will be discussed in greater detail below (section VI.B).



**Figure 24.** Expanded mechanism for the COX peroxidase reaction. All steps shown in Figure 18 are included, along with the conversion of compound I to intermediate I [(PPIX)Fe<sup>4+</sup>O]tyr\* and the subsequent conversion of intermediate I to compound II by peroxidase reductant. Identification of symbols for all intermediates is given in Table 1.

Figure 24 shows an expanded mechanism for the peroxidase reaction. It indicates the formation of intermediate I [(PPIX)Fe<sup>4+</sup>O]tyr\* from compound I and the reduction of intermediate I to compound II. Note that reduction of intermediate I requires the donation of an electron from a peroxidase reductant. This step was not observed in the work of Dietz et al. since no peroxidase reductant was present in the incubation mixtures. It should be noted that intermediate I and compound II have identical heme structures and therefore indistinguishable optical spectra. Thus, it is likely that the second species observed by Lambeir et al. was intermediate I, as opposed to compound II. Similarly, the finding of Lambeir et al. that the rate of formation of this second species from compound I was hydroperoxide-dependent can probably be explained by the kinetic mechanism used by Dietz et al.<sup>39,121</sup>

Tsai et al. expanded on the work of Dietz et al. by monitoring the changes in absorbance during the reaction of COX-1 with various hydroperoxides.<sup>123</sup> Decreases in absorbance at 410 nm (the absorbance maximum for native enzyme) and increases in absorbance at 424 nm (the isosbestic point between native enzyme and compound I) were used to observe the formation of compound I and intermediate I,

respectively. Values of  $k_1$  and  $k_2$  were reported for 15-HPETE, ethyl hydroperoxide (EtOOH), and hydrogen peroxide at 1 °C (Tables 2 and 3). Tsai et al. also observed that the rate of formation of intermediate I was dependent on hydroperoxide concentration, and they used a method similar to that employed by Dietz et al. to derive first-order rate constants for the compound I-to-intermediate I transition. Interestingly, they found that values for both  $k_1$  and  $k_2$  varied with hydroperoxide structure. This result would not be expected for the simple intramolecular electron transfer believed to convert compound I to intermediate I and will be discussed in greater detail in section XII.B.5.

The spectral changes described above were observed in the absence of peroxidase reductant. As shown in Figure 18, an appropriate peroxidase reductant should effect a one-electron reduction of compound I, yielding a species similar to horseradish peroxidase compound II ( $[(\text{PPIX})\text{Fe}^{4+}\text{O}]$ ). A second one-electron reduction then returns the enzyme to its native state. Kinetic studies reported by Kulmacz indicated that, in the presence of peroxidase reductants, the peroxidase exhibits behavior consistent with an ordered bi-substrate reaction mechanism in which the hydroperoxide substrate reacts with the enzyme prior to the rate-determining step.<sup>113</sup> Thus, the rate-determining step must be one of the reduction reactions shown in Figure 18. Using this model, Kulmacz estimated the second-order rate constant for the formation of compound I to be  $7.1 \times 10^7 \text{ M}^{-1} \text{ s}^{-1}$  for lipid peroxide and  $9.1 \times 10^4 \text{ M}^{-1} \text{ s}^{-1}$  for hydrogen peroxide at room temperature using TMPD as peroxidase reductant. The rate constant for regeneration of native enzyme was estimated to be  $9.2 \times 10^6 \text{ M}^{-1} \text{ s}^{-1}$  in the presence of lipid hydroperoxide and  $3.5 \times 10^6 \text{ M}^{-1} \text{ s}^{-1}$  in the presence of hydrogen peroxide (both in the presence of TMPD). No attempt was made to determine which of the reduction steps in Figure 18 is rate-determining.

The observation of the conversion of COX compound I to compound II and native enzyme is complicated by the fact that the spectral properties of intermediate I are indistinguishable from those of compound II.<sup>39,124</sup> The conversion of compound I to intermediate I is an intramolecular electron transfer and would be expected to be the most likely fate of compound I in the absence of peroxidase reductant. However, addition of peroxidase reductant allows reduction of compound I to compound II and native enzyme. Thus, in the presence of peroxidase reductant, competing processes influence the fate of compound I, and these processes cannot be distinguished by electronic spectral studies alone.<sup>124</sup> Nevertheless, attempts have been made to study the conversion of compound II/intermediate I to native enzyme in the presence of phenol and hydroquinone as peroxidase reductants by monitoring the rate of increase in absorbance at 410 nm after a minimum at this wavelength was reached.<sup>124</sup> From these experiments, the second-order rate constant for this process was determined to be  $4.3 \times 10^5 \text{ M}^{-1} \text{ s}^{-1}$  for phenol and  $2.1 \times 10^6 \text{ M}^{-1} \text{ s}^{-1}$  for hydroquinone at 4 °C using PPHP as hydroperoxide substrate. Since these values

were of the same order of magnitude as those reported by Kulmacz for the rate-determining step of the peroxidase reaction, it is reasonable to conclude that the conversion of compound II/intermediate I to native enzyme is the rate-limiting step of the peroxidase reaction.<sup>113</sup> This is similar to the rate-limiting step of other heme peroxidases.<sup>125</sup>

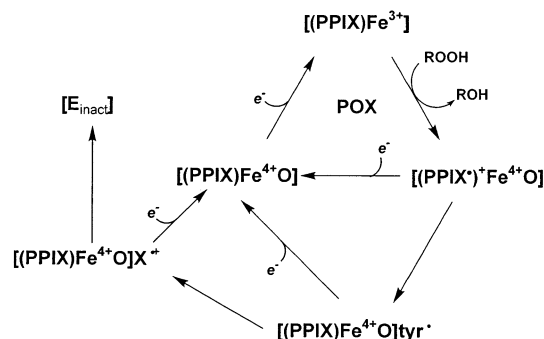
## 2. Spectral Evidence for Peroxidase Self-Inactivation

Spectral studies also have been used to investigate the self-inactivation of COX-1. On the basis of kinetic studies of the peroxidase reaction, Kulmacz proposed that inactivation occurred as a result of a reaction involving compound I or compound II.<sup>113</sup> On the basis of the protective effect of peroxidase reductants, Kulmacz argued that involvement of compound I would appear to be most likely.

Detailed studies of spectral changes during the reaction of COX-1 with EtOOH in the absence of peroxidase reductant allowed Wu et al. to identify a species formed from intermediate I that exhibits an absorbance maximum at 403–404 nm.<sup>114</sup> This new species, designated here as intermediate II, was converted to an additional species, with an absorbance maximum at 412–413 nm, which Wu et al. designated the terminal species. The conversion of intermediate I to intermediate II followed first-order kinetics, with a rate constant of  $1.98 \text{ s}^{-1}$  at 24 °C, which agreed reasonably well with the rate constant for inactivation of the peroxidase activity of the enzyme ( $k = 0.4 \text{ s}^{-1}$ ). In contrast, the conversion of intermediate II to the terminal species occurred much more slowly ( $k = 0.02 \text{ s}^{-1}$ ). Thus, it appeared that inactivation of the peroxidase activity correlated with a reaction that converted intermediate I to intermediate II, a derivative of unknown heme or protein structure.

Additional studies demonstrated that the presence of the non-steroidal anti-inflammatory drugs indomethacin and flurbiprofen had little effect on either the rate of peroxidase inactivation or the rate of conversion of intermediate I to intermediate II or from intermediate II to the terminal species.<sup>115</sup> This result was not totally unexpected, since these compounds inhibit the cyclooxygenase activity but have little to no effect on the peroxidase activity of COX.<sup>30</sup>

The combined results of the above studies led Wu et al. to propose the modified mechanism for the peroxidase reaction that is outlined in Figure 25.<sup>114</sup> In addition to the steps outlined in Figure 24, this mechanism adds the conversion of intermediate I to intermediate II (designated  $[(\text{PPIX})\text{Fe}^{4+}\text{O}]\text{X}^+$ ) to indicate a presumed transfer of the radical to some unknown moiety of the enzyme as well as the subsequent conversion of intermediate II to the terminal species (designated  $\text{E}_{\text{inact}}$ ). Alternatively, reduction of intermediate II to compound II, as proposed in a later mechanism by Bambai et al., would prevent inactivation (see section V.B.1 for a discussion of the role of peroxidase reductants in self-inactivation).<sup>126</sup> Thus, despite important similarities, considerably greater complexity is noted in the peroxidase reaction of COX than in many other, classic peroxidases.



**Figure 25.** Expanded mechanism for the COX peroxidase reaction. All steps shown in Figure 24 are included, in addition to the conversion of intermediate I to intermediate II ( $[(\text{PPIX})\text{Fe}^{4+}\text{O}]\text{X}^{+}$ ), leading to enzyme inactivation. Identification of symbols for all intermediates is given in Table 1.

## B. Peroxidase Reductants

### 1. Role of Peroxidase Reductants in the Cyclooxygenase Reaction

It has been well-established that a source of reducing equivalents is needed for the peroxidase activity of COX. However, the effects of organic compounds that can play this role on the cyclooxygenase activity are not simple and include increases in the rate and/or extent of the reaction, protection from self-inactivation, and even enzyme inhibition. In early studies of PG formation by the COX activity in sheep vesicular gland, Nugteren et al. reported that the reaction required GSH and was facilitated by hydroquinone or propylgallate.<sup>77</sup> They proposed that the role for the latter two compounds was to serve as an antioxidant, although high concentrations of antioxidants were found to be inhibitory. Nugteren's observations were confirmed by Yoshimoto et al. and Takeguchi et al., who observed a stimulation of COX activity in bovine seminal vesicle microsomes by GSH and hydroquinone.<sup>87,127</sup> Because both groups of investigators were specifically measuring  $\text{PGE}_2$  formation, the effects of GSH can be explained on the basis of its role as a cofactor in the conversion of  $\text{PGH}_2$  to  $\text{PGE}_2$  by PGE isomerase. This conclusion is consistent with the finding that other sulfhydryl reagents could not replace GSH in the assay and that omission of GSH completely inhibited product formation. In contrast, in the absence of hydroquinone, about 30% of COX activity remained, and this compound could be replaced with *p*-benzoquinone, ascorbate, pyrogallol, ubiquinone, *p*-aminophenol, L-norepinephrine, serotonin, or 5-hydroxyindoleacetic acid.

In their search for the natural cellular counterpart for hydroquinone, Sih et al. showed that epinephrine, norepinephrine, serotonin, and 5-hydroxyindole-3-acetic acid were significantly more effective than dopamine or L-3,4-dihydroxyphenylalanine in supporting total PG synthesis by bovine seminal vesicle microsomes.<sup>128</sup> They discovered that the product ratio was influenced by the exact reductant used. Furthermore, in studies using 5-hydroxyindole-3-acetic acid, they demonstrated that 2 mol of this compound were consumed per mole of PG produced, indicating that it served as a source of reducing equivalents for the

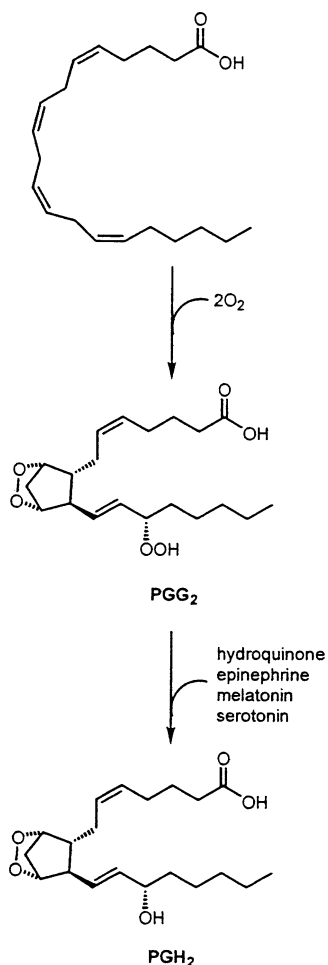
reaction. If GSH was also included, consumption of the indoleacetic acid dropped to 0.2 mol per mole of PG. Sih et al. concluded that the GSH converted the oxidized indoleacetic acid back to its reduced form. Although the data do not exclude the possibility that GSH had replaced the 5-hydroxyindole-3-acetic acid as the primary reductant in the enzymatic reaction, this is unlikely since GSH is a poor substrate for the peroxidase of COX.<sup>112</sup>

Because the stimulatory effects of compounds such as hydroquinone had been attributed to their antioxidant properties, Vanderhoek and Lands tested the ability of a variety of antioxidant compounds to increase COX activity in sheep vesicular gland microsomes.<sup>129</sup> Their results showed that all of the compounds were inhibitory under their assay conditions, and none had a stimulatory effect. Kinetic analysis indicated that some compounds were competitive and others were noncompetitive inhibitors. Inhibitory potency exhibited no correlation with antioxidant activity.

Miyamoto et al. were among the first to use purified COX-1 (from bovine seminal vesicles) to better define the role of the peroxidase reductant.<sup>32</sup> They demonstrated that, in the absence of any reductant, the enzyme produced predominantly  $\text{PGG}_2$ . Addition of tryptophan or any of a variety of other aromatic compounds (including hydroquinone, epinephrine, melatonin, and serotonin) facilitated the conversion of  $\text{PGG}_2$  to  $\text{PGH}_2$  (Figure 26). Thus, the role of the peroxidase reductant as the source of reducing equivalents for the peroxidase reaction was clarified. Further clarification came from the work of Van Der Ouderdaa et al. using their preparation of purified enzyme from ovine vesicular glands.<sup>30</sup> They found that enzyme activity required the presence of hydroquinone, phenol, tryptophan, serotonin, or epinephrine in stoichiometric quantities. They also found that the reducing substrate must be present prior to addition of the fatty acid substrate in order to prevent rapid enzyme inactivation. They concluded that hydroperoxides generated during the cyclooxygenase reaction cause enzyme inactivation and that the presence of the reducing substrates promotes the rapid reduction of the hydroperoxides. A protective effect of tryptophan was also observed by Ogino et al. in their studies of purified enzyme from bovine vesicular gland microsomes.<sup>33</sup> Interestingly, they found that rapid inactivation of the enzyme occurred upon reconstitution of apoenzyme with heme and that this inactivation was prevented by inclusion of tryptophan in the incubation mixture.

### 2. Chemical Mechanisms for Peroxidase Substrate Oxidation

Specific studies of the peroxidase activity of purified COX-1 led to further insights into the role of reducing substrates. Ohki et al. showed that the reduction of  $\text{PGG}_1$  to  $\text{PGH}_1$  by purified bovine seminal vesicle COX-1 was stimulated by guaiacol, epinephrine, and tryptophan but not by GSH.<sup>37</sup> Testing of a wide variety of other compounds demonstrated peroxidase reductant activity in the case of those that were known to be hydrogen donors in other well-



**Figure 26.** Effect of peroxidase reductants on products formed from the reaction of COX-1 with 20:4. In the absence of reductants, PGG<sub>2</sub> was the predominant product. Inclusion of reductants such as hydroquinone, epinephrine, melatonin, and serotonin led to the conversion of PGG<sub>2</sub> to PGH<sub>2</sub>.<sup>32</sup>

described peroxidase reactions such as that of horseradish peroxidase. In contrast, compounds reported to be oxygenated during microsomal PGE<sub>2</sub> synthesis, compounds known to accept oxygen from peroxides during the reaction of pea seed peroxygenase, and compounds known to be oxygenated during the reaction of cytochrome P450 with peroxides were generally poor reductants. These results suggested that the peroxidase reaction of COX-1 involved a peroxidic dehydrogenation similar to that seen with other well-characterized heme peroxidases. Spectrophotometric studies demonstrated dehydrogenation of 1.3 mol of epinephrine and 0.9 mol of guaiacol per mole of PGG<sub>1</sub>. However, stoichiometric dehydrogenation of tryptophan could not be demonstrated, leading the investigators to conclude that the stimulatory effect of tryptophan must be due to some mechanism other than its serving as a peroxidase reductant. Alternatively, it is possible that tryptophan was oxidized to a product that was not detected by the methods used.

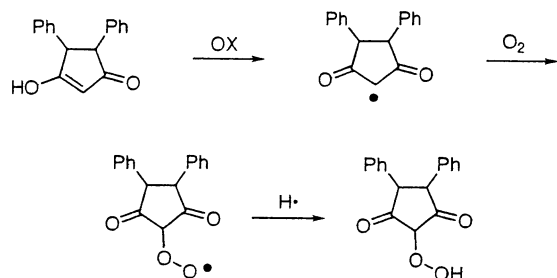
Egan et al. investigated the effects of peroxidase reductants on the peroxidase activity of ram seminal vesicle microsomes using 15-hydroperoxy-PGE<sub>1</sub> as substrate.<sup>130</sup> They found that the addition of either

phenol or sulindac sulfide (*cis*-5-fluoro-2-methyl-1-[*p*-(methylthio)benzylidene]indene-3-acetic acid) in the presence of seminal vesicle microsomes reduced the hydroperoxide. The product of phenol oxidation could not be identified or quantified because of polymerization. However, the product of sulindac sulfide oxidation was identified as sulindac sulfoxide (known generically as sulindac). Under conditions of low microsomal protein or high sulindac sulfide concentration, the molar ratio of hydroperoxide reduction to sulindac sulfide oxidation was approximately 1:1.

The conversion of sulindac sulfide to the sulfoxide led Egan et al. to investigate the source of the sulfoxide oxygen.<sup>131</sup> They oxidized sulindac sulfide with seminal vesicle microsomes using 15-hydroperoxy-PGE<sub>2</sub> that was labeled with <sup>18</sup>O in both oxygen atoms of the hydroperoxide moiety. The resulting sulfoxide product contained exclusively <sup>18</sup>O, indicating that the sulfoxide oxygen originated directly from the hydroperoxide substrate. Similar results were obtained for the oxidation of methylphenyl sulfide using preparations of purified COX-1.<sup>132</sup>

These results indicate that direct oxygen transfer from the hydroperoxide substrate to the peroxidase reductant is possible. It should be noted that other examples of peroxidase reductant oxygenation have been reported. For example, as noted in section IV.B, Marnett et al. reported the co-oxygenation of 1,3-diphenylisobenzofuran, luminol, oxyphenbutazone, and benzopyrene during the metabolism of 20:4 with vesicular gland microsomes (Figure 16).<sup>88</sup> The incorporation of oxygen into these molecules suggests the possibility that they also may represent oxygen-transfer reactions. However, in subsequent studies, using 15-HPETE labeled with <sup>18</sup>O in the hydroperoxy moiety, Marnett et al. showed that no direct transfer of oxygen occurred in the oxidation of 1,3-diphenylisobenzofuran by purified COX-1. Instead, <sup>18</sup>O was incorporated from <sup>18</sup>O<sub>2</sub>, but not from H<sub>2</sub><sup>18</sup>O.<sup>133</sup> Furthermore, studies using PGG<sub>2</sub> as the peroxide substrate indicated that the stoichiometry of diphenylisobenzofuran oxidized to PGG<sub>2</sub> reduced was much greater than 1:1. Together these results indicated that the oxidation of diphenylisobenzofuran by COX-1 involved a one-electron transfer followed by a free radical chain reaction in solution.

The hydroperoxide-dependent oxygenation of phenylbutazone also proceeds with the incorporation of O<sub>2</sub> into the oxidized product (in this case, 4-hydroxyphenylbutazone), but the stoichiometry of hydroperoxide reduced to phenylbutazone oxidized is approximately 1:1.<sup>134,135</sup> Figure 27 outlines a mechanism of oxygenation in which a peroxy radical intermediate is formed that does not oxidize another molecule of phenylbutazone to propagate a radical chain. The phenylbutazone peroxy radical is able to oxygenate double bonds such as the 9,10-double bond of 7,8-dihydroxy-7,8-dihydrobenzo[*a*]pyrene.<sup>263</sup> The immediate product of phenylbutazone oxidation is 4-hydroperoxyphenylbutazone, which is reduced to the alcohol by the peroxidase activity of COX [P. Siedlik and L. J. Marnett, unpublished observations]. The source of electrons to reduce the peroxy radical



**Figure 27.** Mechanism of peroxidase-dependent oxygenation of phenylbutazone to 4-hydroperoxyphenylbutazone.

to the hydroperoxide was obviously contained in the microsomal preparations used as the enzyme source in these studies. However, the exact identity of this electron source is not known.

COX-1 also has been shown to catalyze the oxidative N-dealkylation of amines, leading to aldehyde formation.<sup>132,136</sup> Once again, the source of the oxygen atom in the aldehyde product is of interest. Using EPR, Egan et al. demonstrated the generation of a free radical signal during the oxidation of aminopyrine by COX-1.<sup>132</sup> The EPR signal persisted after cessation of the cyclooxygenase reaction and was accompanied by the formation of a blue color that faded to tan as the EPR signal disappeared. Egan et al. concluded that oxidation of aminopyrene occurred via a one-electron transfer. These findings were confirmed by Lasker et al., who showed a close correlation between the formation of the aminopyrene free radical and formaldehyde production.<sup>137</sup> Lasker et al. concluded that the EPR signal was produced by a one-electron-oxidized cation radical of aminopyrine. They proposed that the metabolism of aminopyrine occurred via two sequential one-electron oxidations to generate an iminium cation. Subsequent hydrolysis would yield formaldehyde and the demethylated amine. On the basis of this mechanism, the oxygen in formaldehyde would come from water. They concluded that, as suggested by Ohki et al., most peroxidase reductants react with COX via a one-electron-transfer process.<sup>37</sup> However, the resultant radical cations are subject to a variety of subsequent reactions that may or may not involve oxygenation.

### 3. Structure–Activity Relationships for Peroxidase Reductants

Markey et al. performed kinetic studies of the peroxidase activity of purified COX-1 from ram seminal vesicles using PPHP as substrate and a variety of peroxidase reductants.<sup>112</sup> Their results indicated that the enzyme behaves as a classical heme peroxidase having a catalytic efficiency similar to that of horseradish peroxidase. They investigated a large number of phenols, aromatic amines,  $\beta$ -dicarbonyls, naturally occurring compounds, and non-steroidal anti-inflammatory agents as reducing substrates (Table 4). Reducing substrate efficiency was measured by comparing the total amount of PPHP reduced by a 200  $\mu$ M concentration of the test compound under conditions resulting in the reduction of 50% of the PPHP by 200  $\mu$ M phenol. In the absence

**Table 4. Selected Compounds Tested for Efficiency as Peroxidase Reductants<sup>112,a</sup>**


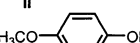
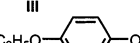
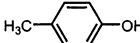

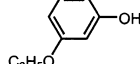
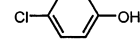
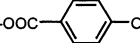
compound	index
<i>n</i> -propyl gallate	1.00 $\pm$ 0.00
butylated hydroxyanisole	1.00 $\pm$ 0.01
hydroquinone	0.99 $\pm$ 0.01
sulindac sulfide	0.96 $\pm$ 0.05
L-epinephrine	0.92 $\pm$ 0.01
acetaminophen	0.86 $\pm$ 0.04
guaiacol	0.64 $\pm$ 0.05
methylphenyl sulfide	0.62 $\pm$ 0.01
lipoic acid	0.59 $\pm$ 0.07
L-etodolac	0.55 $\pm$ 0.03
luminol	0.53 $\pm$ 0.02
phenol	0.50 $\pm$ 0.07
D-etodolac	0.46 $\pm$ 0.01
indoleacetic acid	0.45 $\pm$ 0.03
ascorbic acid	0.43 $\pm$ 0.01
L-tryptophan	0.27 $\pm$ 0.00
(-)-MK-410	0.27 $\pm$ 0.01
(+)-MK-410	0.26 $\pm$ 0.01
phenylbutazone	0.23 $\pm$ 0.00
gutathione (reduced)	0.21 $\pm$ 0.09
no reducing substrate	0.13 $\pm$ 0.03
1,3-diphenylisobenzofuran	0.12 $\pm$ 0.09
salicylic acid	0.06 $\pm$ 0.06
aspirin	0.04 $\pm$ 0.01

<sup>a</sup> The peroxidase assay was performed using PPHP as substrate. Conditions of PPHP and enzyme concentration were established so that reduction of 50% of the PPHP occurred in the presence of 200  $\mu$ M phenol (index of 0.50). Therefore, the index value represents the fraction of PPHP reduced by each compound under those same conditions.

of reducing substrate, no PPHP reduction occurred. The various compounds that were tested displayed considerable differences in their efficiency as reducing substrates for COX-1 versus horseradish peroxidase. Furthermore, although some non-steroidal anti-inflammatory compounds were effective as peroxidase reductants, there was no correlation between their activity in this regard and their potency as inhibitors of the cyclooxygenase activity of the enzyme. In fact, in the case of the resolved enantiomers of MK-410 and etodolac, opposite enantioselectivity was noted for their efficacy as peroxidase reductant or as cyclooxygenase inhibitors. Thus, the investigators concluded that a significant difference must exist in the geometry of the cyclooxygenase versus the peroxidase active sites.

Markey et al. also studied the effects of peroxidase reductants on the peroxide-induced inactivation of COX-1.<sup>112</sup> The addition of 500  $\mu$ M phenol to a reaction mixture containing 352 nM COX-1 raised the IC<sub>50</sub> for inactivation of the cyclooxygenase activity by 15-HPETE from 2.8 to 92  $\mu$ M, and no inactivation of the peroxidase activity by 15-HPETE was noted for concentrations up to 10  $\mu$ M. When 20:4 was used as the inactivating agent, the IC<sub>50</sub> value for cyclooxygenase inactivation was 8.7  $\mu$ M in the presence of 500  $\mu$ M phenol, as compared to 0.6  $\mu$ M in its absence. Markey et al. compared the ability of hydroquinone, phenol, and tryptophan to protect the enzyme from inactivation by 15-HPETE. They found a direct correlation between the efficacy of each compound as a peroxidase reductant and its ability to protect the enzyme against peroxide-induced inactivation. For both activities, the rank order of potency was hyd-

**Table 5. Selected Peroxidase Reductants Evaluated by Hsuanyu and Dunford<sup>138,a</sup>**

Substituted Phenol	$\sigma$	$\pi$	$A_{50}(\mu\text{M})$	$I_{50}(\text{mM})$
I 	-0.37	-0.67	$20 \pm 1$	$1.65 \pm 0.07$
II 	-0.27	-0.02	$14 \pm 1$	$0.41 \pm 0.01$
III 	-0.24	0.38	$5.5 \pm 0.5$	$0.28 \pm 0.01$
IV 	-0.076	0.56	$23 \pm 1$	$0.81 \pm 0.02$
V 	0	0	$65 \pm 4$	$5.9 \pm 0.4$
VI 	0.10	0.38	$50 \pm 2$	$1.6 \pm 0.1$
VII 	0.23	0.71	$35 \pm 1$	$1.33 \pm 0.05$
VIII 	0.35	-4.36	$1,120 \pm 50$	

<sup>a</sup> Varying concentrations of all compounds were assayed with 53 nM COX-1 and 30  $\mu\text{M}$  20:4. Concentrations required to give half-maximal stimulation ( $A_{50}$ ) or inhibition ( $I_{50}$ ) of cyclooxygenase reaction velocity are shown, along with the Hammett  $\sigma$  and Hantsch  $\pi$  values for each substituent.

roquinone > phenol > tryptophan. These results emphasized the importance of peroxidase reductant in protecting COX against inactivation and were consistent with kinetic studies reported by Kulmacz, who showed that the rate of inactivation of the peroxidase activity decreased with increasing peroxidase reductant concentration.<sup>113</sup>

The availability of a model for the peroxidase reaction has allowed more detailed studies of the effects of various peroxidase reductants on COX reaction kinetics. As described above (section V. B.2), most peroxidase reductants undergo dehydrogenation reactions, resulting from single electron transfers to compound I, compound II, or intermediate I. Phenol is an excellent example of this kind of peroxidase reductant. Hsuanyu and Dunford investigated the effects of a series of meta- and para-substituted phenols on the cyclooxygenase reaction of purified COX-1 from ram seminal vesicles using 20:4 as substrate.<sup>138</sup> They found that at low concentrations phenols stimulate the cyclooxygenase reaction rate, whereas at high concentrations they become inhibitory. Both enhancement and inhibition are increased by substituents that are electron-donating (as measured by Hammett  $\sigma$  constants) and/or hydrophobic (as measured by Hantsch  $\pi$  constants) (Table 5). Furthermore, they found that the identity of the phenol does not affect the  $K_m$  or  $k_{cat}$  values for the

cyclooxygenase reaction, although these values were not compared to those for the reaction in the absence of phenol. Hsuanyu and Dunford next evaluated the effects of the various substituents on the ability of phenol to reduce compound II. In this case, they found that electron-donating substituents increase reactivity, but very little effect was observed for changes in hydrophobicity. From these results, Hsuanyu and Dunford concluded that efficiency for compound II reduction is dictated largely by electronic effects but that efficiency for cyclooxygenase stimulation and inhibition is due to a combination of hydrophobic and electronic effects. They explained the stimulatory effect of phenols on the cyclooxygenase reaction on the basis of reduction of compound II and scavenging of  $\text{PGG}_2^*$ , processes that prevent enzyme inactivation. The inhibitory effect of phenol was explained on the basis of a proposed competition of phenol with 20:4 for the enzyme active site.

Although most peroxidase reductants interact with COX via one-electron transfers, reduction of compound I via oxygen transfer also has been demonstrated for alkyl sulfides and alkylaryl sulfides, as described above (section V.B.2). Hypothetically, reduction of compound I by oxygen transfer is different from one-electron transfer in a number of ways. In the case of oxygen transfer, the reduction of compound I to native enzyme occurs in a single step with one molecule of peroxidase reductant, rather than in a series of two steps requiring two molecules of peroxidase reductant. Thus, it is reasonable to assume that oxygen transfer should be the more efficient process, maximizing hydroperoxide reduction with minimal enzyme inactivation. Furthermore, since the oxygen atom is directly transferred to the peroxidase reductant from compound I, the peroxidase reductant molecule must bind effectively at the peroxidase active site and remain there until the oxygen transfer is complete.

Plé and Marnett investigated the structure–activity relationships for a series of alkylaryl sulfides serving as peroxidase reductants in the reaction of purified COX-1.<sup>139</sup> Using a series of para-substituted thioanisoles, with PPHP as the peroxide substrate, they found that the efficiency of reduction increased with increasing electron-donating ability of the substituent (Table 6, compounds I–VII). An exception to this rule was found with amine-containing substituents, which were far more reactive than predicted on the basis of their Hammett  $\sigma$  value. Plé and Marnett demonstrated that these compounds were oxidized by electron transfer from nitrogen rather than oxygen transfer to sulfur. Thus, the presence of an amine functional group altered the mechanism of the reaction, a finding that is not surprising since the amino group is more readily oxidized than the sulfide group. Interestingly, the compounds bearing amino functional groups exhibited the lowest apparent  $K_m$  values of all compounds tested, suggesting that a positive charge may facilitate binding at the peroxidase active site (Table 6, compounds I and II).

**Table 6. Selected Peroxidase Coreductants Evaluated by Plé et al.<sup>139,a</sup>**

Sulfide	PPA (%)	$K_m^*$ (M x 10 <sup>6</sup> )	MT* (M <sup>-1</sup> x 10 <sup>6</sup> )	MT*/ $K_m^*$ (M <sup>-1</sup> x 10 <sup>6</sup> )
<b>I</b> 	37 ± 2	20	800	40
<b>II</b> 	15 ± 1	40	400	10
<b>III</b> 	57 ± 2	440	4600	10.4
<b>IV</b> 	42 ± 1	580	4400	7.6
<b>V</b> 	16 ± 1	1150	2900	2.6
<b>VI</b> 	23 ± 1	320	2300	7.2
<b>VII</b> 	7 ± 1	350	300	0.8
<b>VIII</b> 	50 ± 1	300	2500	10.4
<b>IX</b> 	7 ± 1	170	260	1.6
<b>X</b> 	20 ± 2	65	700	10.8
<b>XI</b> 	10 ± 1	360	300	0.8
<b>XII</b> 	16 ± 2	50	600	12.0
<b>XIII</b> 	(+) 30 ± 2 (±) 25 ± 2 (-) 15 ± 1	660 690 520	2500 3000 1200	3.8 4.4 2.4

<sup>a</sup> All compounds were assayed at 200  $\mu$ M concentration using PPHP as peroxide substrate under conditions yielding 15% reduction of PPHP with 200  $\mu$ M phenol. The percent of PPHP reduced under these conditions is given for all compounds. Compounds were also assayed at varying concentrations (50  $\mu$ M to 4 mM) using enzyme and PPHP concentrations such that less than 100% PPHP reduction would occur at the highest compound concentration tested. These data were used to estimate values for apparent  $K_m$  and maximal turnover (MT).

Plé and Marnett next studied the effects of steric hindrance on sulfide oxygenation (Table 6 compounds I, VIII, and IX).<sup>139</sup> They discovered that substitution of an ethyl group for the methyl group of *p*-methoxyphenylmethyl sulfide had little effect on the compound's ability to serve as a peroxidase reductant,

but when the methyl group was replaced with an isopropyl group, reactivity was reduced approximately 10-fold. Incorporation of the sulfide into a five-membered ring had little additional effect on reactivity (Table 6, compound X). In contrast, addition of a carboxyl group anywhere on the molecule reduced reactivity significantly, and this reduction in activity could be partially or completely eliminated by conversion of the carboxyl group to an ester (Table 6, compounds X–XIII). Finally, Plé and Marnett demonstrated that chiral molecules show some stereoselectivity in their reactivity as reductants (Table 6, compound XIII).

Plé and Marnett pointed out that the apparent oxygen-transfer reaction of the sulfides with COX compound I could actually occur via an electron-transfer mechanism.<sup>139</sup> Following the electron-transfer step, the resulting radical cation intermediate would couple to the ferryl-oxo ligand, allowing the subsequent oxygen transfer. In this case, the major difference between oxygen-transfer substrates, such as sulfides, and other peroxidase reductants is the fate of the radical cation. Molecules that do not undergo oxygen transfer do not bind to the ferryl-oxo ligand but rather diffuse away from the active site. Either mechanism is consistent with the positive effects of electron-donating groups on reducing substrate reactivity.

Whether the mechanism involves an initial electron transfer or direct oxygen insertion, the sulfide peroxidase reductants must interact at the peroxidase active site of COX. Thus, it is significant that large substituents on the sulfur atom led to significant steric hindrance and that some stereoselectivity was observed. These findings suggest that the active-site region is small enough to display a degree of compound specificity. Also interesting was the finding that the presence of a carboxyl group seriously reduced reactivity. Plé and Marnett proposed the hypothesis that the peroxidase active site contains a positively charged region at some distance from the active site for the interaction of the carboxylate group of PGG<sub>2</sub>. Introduction of a carboxyl group on the sulfide peroxidase reductant would lead to interaction of the molecule at that site, which might place the sulfur atom too far from the ferryl-oxo ligand for effective oxygen transfer.<sup>139</sup>

In conclusion, early studies showed a requirement for a readily oxidized compound (usually aromatic) in order to obtain maximal PG synthesis by COX. The finding that COX has a peroxidase activity that reduces PGG<sub>2</sub> to PGH<sub>2</sub> mandates that a source of electrons is required to carry out this reaction. The enzyme has broad specificity with regard to the structure of the peroxidase reductant, and the identity of the physiological peroxidase reductant is still not known. However, it is now well-accepted that, in addition to facilitating the PGG<sub>2</sub>-to-PGH<sub>2</sub> conversion, the peroxidase reductant protects COX from self-inactivation, thereby increasing the total amount of product formation. The effects of peroxidase reductant on reaction rate are more complex, however, and will be discussed in greater detail below in the

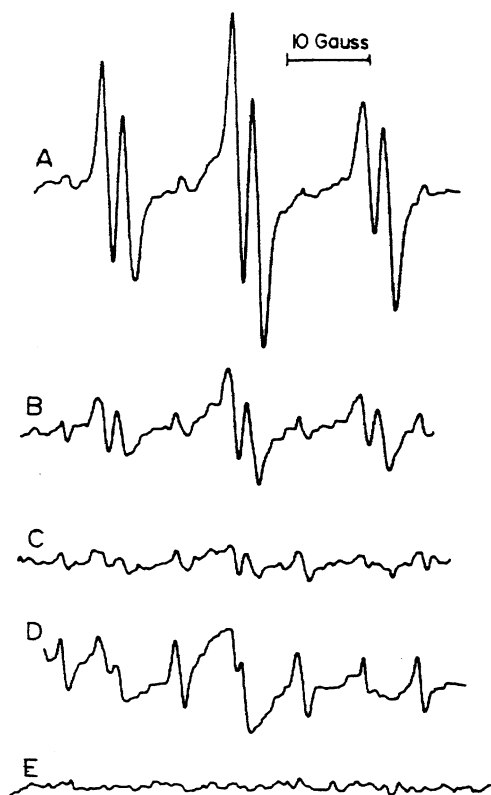
context of the mechanism of the cyclooxygenase reaction.

## VI. Mechanism of Cyclooxygenase Catalysis

### A. Free Radicals in COX Catalysis

#### 1. Substrate-Derived Radicals

The mechanism of PG synthesis described in section III.B predicts the formation of free radicals derived from the substrate fatty acid. Mason et al. incubated ram seminal vesicle microsomes with 20:4 in the presence of the spin-trap 2-methyl-2-nitrosopropane and used EPR spectroscopy to study the resulting trapped radical(s).<sup>140</sup> The EPR characteristics of the radical species (Figure 28) were similar



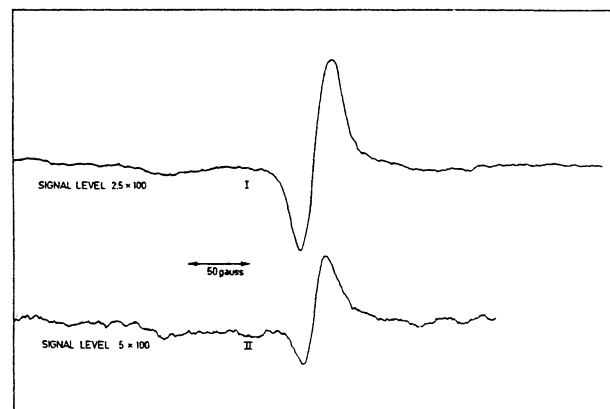
**Figure 28.** EPR spectra obtained from the incubation of ovine seminal vesicle microsomes (2.0 mg/mL protein) with 400  $\mu$ M 20:4 in the presence of 1 mg/mL 2-methyl-2-nitrosopropane. Trace A: All components of the reaction mixture were present. Trace B: Same as trace A, but the enzyme had been pretreated for 2 min with 100  $\mu$ M indomethacin. Trace C: Same as trace A, but the enzyme had been pretreated for 2 min with 400  $\mu$ M indomethacin. Trace D: Same as trace A with the omission of 20:4. Trace E: Same as trace A with the omission of the seminal vesicle microsomes. Reproduced with permission from ref 140. Copyright 1980 American Society for Biochemistry and Molecular Biology.

to those of a previously reported 18:2 radical adduct to 2-methyl-2-nitrosopropane produced by soybean lipoxygenase. The spectra of these radical adducts were distinctly different from those of oxygen-centered radicals. The formation of the spin-trapped radical was inhibited by indomethacin but not by phenol, and its rate of formation coincided with the

kinetics of the cyclooxygenase reaction. Prolonged incubation of 20:4 with 2-methyl-2-nitrosopropane resulted in the formation of a species with characteristics very similar to those of the radical generated by the cyclooxygenase reaction. Finally, the fact that 2-methyl-2-nitrosopropane inhibited oxygen uptake during the cyclooxygenase reaction provided strong evidence that the reagent had trapped an important intermediate in the enzymatic reaction. These results were later confirmed by Schreiber et al., who expanded their observations to include the use of octadeuterated 20:4 as substrate.<sup>141</sup> These experiments confirmed that the spin-trapped adduct was bound to one of the deuterated positions (carbons 5, 6, 8, 9, 11, 12, 14, or 15), as predicted by the proposed mechanism for PG synthesis.

#### 2. Protein-Derived Radicals

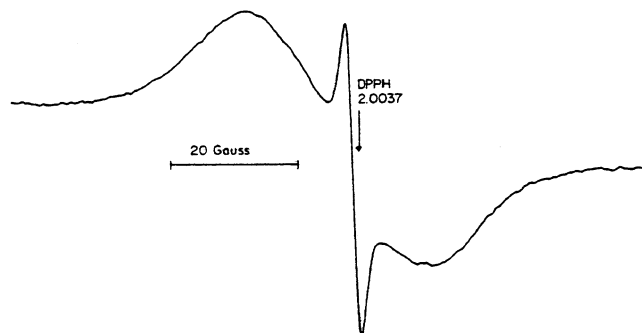
Mechanistic studies of the peroxidase activity of COX demonstrated the existence of higher oxidation states of the protein, and the work of Dietz et al. (section V.A.1) suggested the possibility of a protein-derived free radical generated during the reaction of COX with hydroperoxides. However the exact mechanism by which COX catalyzed the oxidation of 20:4 to form PG's remained a mystery. Key to understanding this process was identifying the protein-derived free radical and clarifying its role in the cyclooxygenase mechanism. As early as 1966, Nugteren et al. used EPR to show the development of a radical signal centered at  $g = 2$  during the reaction of ram seminal vesicle microsomes with 20:3 (Figure 29).<sup>77</sup> Later,



**Figure 29.** EPR spectrum of ovine vesicular gland microsomes (21 mg/mL protein) before (trace II) and after (trace I) addition of 20:3 (1.7 mg/mL) in 0.2 M Tris-HCl, pH 8.0. Following fatty acid addition, samples were rapidly frozen at  $-196^{\circ}\text{C}$  for spectral study. Reproduced with permission from ref 77. Copyright 1966 Wiley-VCH.

more detailed studies demonstrated the generation of radical species upon the addition of either lipid hydroperoxides or 20:4 to the enzyme in seminal vesicle microsomes.<sup>111,130</sup> Formation of the radical with 20:4 required the presence of oxygen and was inhibited by indomethacin, but this was not true when lipid hydroperoxides were used. Addition of phenol inhibited radical generation with all substrates. The EPR signal was described as having a line width of about 25 G, with no detectable hyperfine structure. Accurate  $g$  values could not be ascertained,



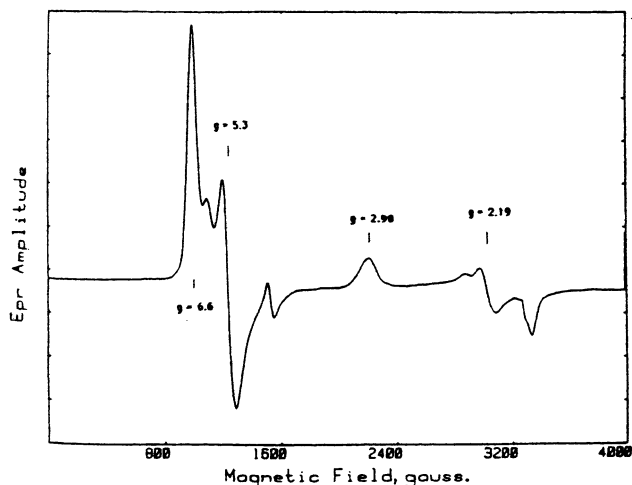


**Figure 30.** EPR spectrum of ovine vesicular gland microsomes (30 mg/mL protein) after the addition of 400  $\mu$ M 20:4 (1.7 mg/mL) in Tris-HCl, pH 7.5. Following fatty acid addition, samples were rapidly frozen at  $-196$  °C for spectral study. Reproduced with permission from ref 142. Copyright 1982 American Society for Biochemistry and Molecular Biology.

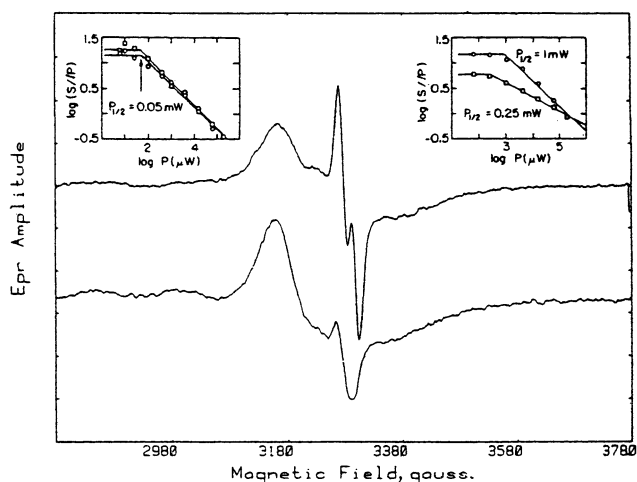
so the structure of the radical could not be determined; however, the requirement for oxygen in the case of 20:4, and the presence of oxygen in the hydroperoxides, led the investigators to conclude that the radicals were likely oxygen-centered.

Subsequent work by Kalyanaraman et al. allowed a more exact description of the free radical formed upon incubation of seminal vesicle microsomes with 20:4 (Figure 30).<sup>142</sup> They reported the  $g$  value of the radical to be 2.005, which did not correspond to any oxygen-centered free radicals that would likely be generated during the cyclooxygenase reaction. Instead, the signal was more consistent with an aromatic organic free radical. Comparison of the EPR signal to that obtained from the reaction of methemoglobin with hydrogen peroxide led the investigators to conclude that the free radical was hemoprotein-derived and was likely to be formed by the oxidation of an amino acid residue located near the heme.

The availability of purified COX-1 allowed Kulmacz et al. and Ruf et al. to perform detailed studies of the EPR signals of resting enzyme and the enzyme after reaction with hydroperoxides.<sup>118,143</sup> Depending on the conditions, the EPR signal of resting COX-1 exhibited characteristics of high-spin or low-spin ferric heme. The high-spin heme EPR signal was detected at  $g = 6.6$ – $6.7$  and  $5.3$ , with an intense component of rhombic symmetry (Figure 31). A second component at  $g = 6.0$  exhibited axial symmetry and was attributed to nonspecifically bound heme<sup>143</sup> or preparations having lower specific activity.<sup>118</sup> The low-spin heme signal was observed as a symmetric peak at  $g = 2.98$ . Integration of peak intensities for high-spin versus low-spin signals indicated that approximately 52% of the heme was in the high-spin state at 12 K. Addition of hydrogen peroxide to purified COX-1 at 12 K resulted in a decrease in the EPR signals for both the high-spin and the low-spin heme states.<sup>118</sup> Concomitantly, a new signal appeared in the  $g = 2$  region. The signal appeared to be a composite of a narrow doublet at  $g = 2.003$  that was split by 22 G (peak-to-trough width of 40 G) and a broader component characterized by a peak at  $g = 2.085$  and a trough at  $g = 1.95$  (Figure 32). When COX-1 was reacted with 15-HPETE, a similar new EPR signal was observed, consisting of



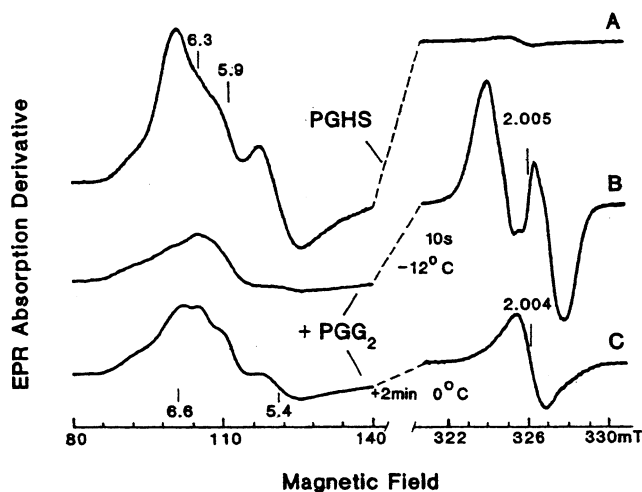
**Figure 31.** EPR spectrum of purified COX-1 (90  $\mu$ M heme) obtained at 12 K. Reproduced with permission from ref 118. Copyright 1987 American Society for Biochemistry and Molecular Biology.



**Figure 32.** EPR spectra obtained in the region of 2980–3780 G after the reaction of purified COX-1 with hydroperoxides. Upper trace: COX-1 (30  $\mu$ M heme) was treated with 2 equiv of  $H_2O_2$  in 70% glycerol and then trapped by freezing to 12 K within 1 s. Lower trace: COX-1 (86  $\mu$ M heme) was treated with 2 equiv of 15-HPETE and then trapped by freezing to 12 K within 2 s. Left inset: Power saturation of the broad ( $\square$ ) and narrow ( $\circ$ ) components of the lower trace. Right inset: Power saturation of the broad ( $\square$ ) and narrow ( $\circ$ ) components of the upper trace. Reproduced with permission from ref 118. Copyright 1987 American Society for Biochemistry and Molecular Biology.

a narrow, unresolved singlet at  $g = 2.005$ , with a line width of 25 G, superimposed on a broad background signal. Comparison of these signals to those of other heme-containing peroxidases led Kulmacz et al. to conclude that the signals were derived from a species in which the heme was present in the ferryl state complexed with a free radical derived from the hydroperoxide or a component of the hydroperoxide.<sup>118</sup>

A significant advance in understanding the structure of the radicals generated during the COX reaction with hydroperoxides came from the work of Karthein et al. combined with that of Dietz et al.<sup>39,144</sup> Karthein et al. demonstrated that reaction of purified COX-1 with PGG<sub>2</sub>, hydrogen peroxide, or 20:4 plus



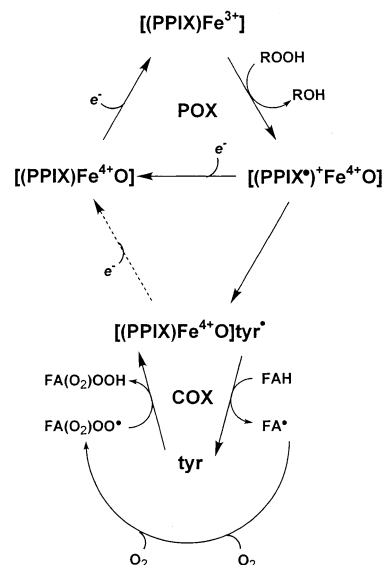
**Figure 33.** EPR spectra obtained from the reaction of COX-1 with PGG<sub>2</sub>. (A) Spectrum of COX-1 (98 μM) plus 126 μM hemin. (B) Spectrum of the enzyme after addition of 300 μM PGG<sub>2</sub> under aerobic conditions. The sample was frozen to -12 °C within 10 s. (C) The sample in (B) was thawed and incubated at 0 °C for 2 min. Reproduced with permission from ref 144. Copyright 1988 Blackwell Publishing.

oxygen resulted in the generation of a new EPR doublet radical signal at  $g = 2.005$ , as reported earlier (Figure 33).<sup>144</sup> In the reaction with PGG<sub>2</sub>, the doublet was strongest at 10 s (the earliest time observed), and with increasing incubation time, the doublet signal was replaced by a singlet at  $g = 2.004$ , concomitant with partial recovery of the ferric heme signal of the native enzyme. Formation of the doublet signal was suppressed by the inclusion of peroxidase reductants. Thus, it was reasonable to conclude that the doublet represented an intermediate in the peroxidase reaction.

Detailed characterization of the doublet signal (based on the  $g$  value) indicated that it was likely due to an organic free radical.<sup>144</sup> Since the doublet signal was not altered by a change in microwave frequency from 9.2 to 34 GHz, it appeared that the splitting resulted from a hyperfine interaction of the free electron having a nuclear spin of  $I = 1/2$ . Addition of D<sub>2</sub>O to the reaction mixture had no effect on the signal, indicating that exchangeable protons were not involved. The observations of an additional triplet structure under optimal conditions allowed numerical simulations of the  $g$  tensor and hyperfine tensors of the radical. The results indicated strong similarities to the tyrosyl radical of ribonucleotide reductase. This work, done concomitantly with the spectral studies of the Soret region of COX-1 by Dietz et al., suggested that the radical signal may be due to intermediate I, formed from compound I as described earlier (section V.A.1). The data suggested that this species results from the transfer of an electron from a protein tyrosine residue to the porphyrin cation radical of the compound I form of COX-1.

## B. The Branched-Chain Mechanism

The discovery of the intermediate I tyrosyl radical, coupled with results obtained from kinetic studies of the peroxidase reaction, allowed Dietz et al. to



**Figure 34.** Branched-chain mechanism for the cyclooxygenase reaction. All steps shown in Figure 24 are included. The enzyme is activated through the reaction with hydroperoxide to generate compound I. Following conversion of compound I to intermediate I, intermediate I abstracts a hydrogen atom from 20:4 or other suitable fatty acid substrate (FAH), reducing the tyrosyl radical and forming the fatty acid radical (FA•). Addition of two molecules of oxygen results in the formation of the peroxyl radical of the fatty acid endoperoxide (FA(O<sub>2</sub>)OO•). Reduction of this radical regenerates intermediate I and forms the hydroperoxide of the fatty acid endoperoxide (FAO<sub>2</sub>OOH, or PGG<sub>2</sub> if the substrate is 20:4). The product hydroperoxide may then be reduced to the corresponding alcohol via the peroxidase mechanism. Identification of symbols for all intermediates is given in Table 1.

propose a mechanism for the cyclooxygenase reaction, shown in Figure 34.<sup>39</sup> The mechanism proposes that the peroxidase reaction occurs through a cycling of the enzyme from the native form to compound I, and then to compound II, and finally back to native enzyme, as discussed above (section V). However, compound I may also give rise to intermediate I via an intramolecular electron transfer. Dietz et al. proposed that the tyrosyl radical of intermediate I is the proximal oxidant that effects the hydrogen abstraction from 20:4 in the cyclooxygenase reaction.<sup>39</sup> Subsequent addition of two molecules of oxygen yields the 15-peroxyl radical of PGG<sub>2</sub>, which then abstracts a hydrogen atom from the tyrosine residue to regenerate intermediate I. This branched-chain mechanism predicts that the cyclooxygenase activity is dependent on the peroxidase activity for product activation but largely independent of the peroxidase once activation has occurred.

The linkage of the peroxidase-catalyzed formation of a protein tyrosyl radical with the activation of cyclooxygenase activity represented the critical intellectual insight into the mechanism of the cyclooxygenase reaction. Its simplicity integrated a considerable body of disparate phenomenology and created a conceptual framework amenable to direct, albeit challenging, experimental tests. In addition, the proposed sequence of oxo-ferryl oxidation of tyrosine followed by tyrosyl radical oxidation of fatty acid is in excellent agreement with the redox potentials for

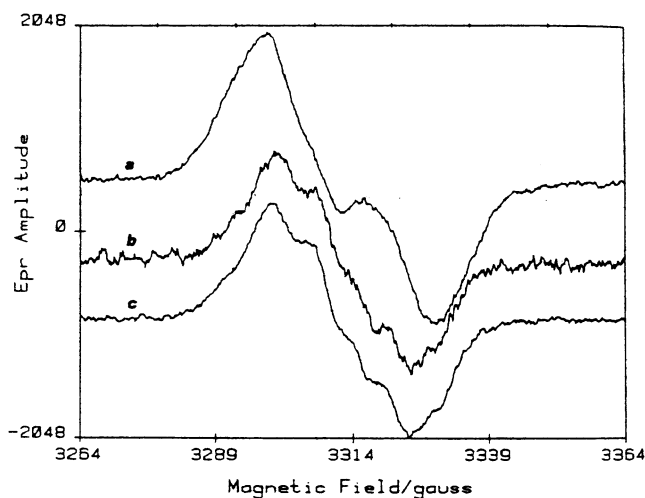
the individual half-reactions for reduction of oxoferryl heme, tyrosyl radical, and fatty acid radical (+1.0 V  $\rightarrow$  +0.9 V  $\rightarrow$  +0.6 V, respectively).<sup>145–147</sup> Such a downhill thermodynamic scheme is impossible for the resting enzyme because of the low potential for reduction of the Fe<sup>3+</sup> enzyme ( $\sim -0.15$  V for both COX proteins).<sup>148,149</sup> Thus, the branched-chain hypothesis for cyclooxygenase activation and catalysis is attractive thermodynamically as well as kinetically.

### 1. Characterization of the Tyrosyl Radical

Early efforts to test the branched-chain hypothesis centered on characterization of the tyrosyl radical and the determination of its catalytic competence for oxidation of 20:4. Kulmacz et al. studied the rate of radical formation upon addition of EtOOH or 15-HPETE to COX-1 at  $-14$  °C.<sup>150</sup> Within 5 s, both substrates led to the formation of a radical species characterized by a wide doublet EPR signal at  $g = 2.005$ , with a splitting of 16 G and a peak-to-trough width of 35 G. Over the ensuing 20–60 s, the doublet was replaced with a singlet having the same peak-to-trough width, and then the radical intensity declined. Reaction of COX-1 with EtOOH in the presence of indomethacin gave rise to a radical exhibiting an EPR signal characterized by a narrow singlet (peak-to-trough width of 24 G). No doublet signal was observed prior to or after the singlet. Reaction of the enzyme with tetranitromethane led to inactivation of the cyclooxygenase and the peroxidase activities, but the inactivation of the cyclooxygenase activity was more rapid and more complete. Reaction of tetranitromethane-treated enzyme with EtOOH yielded a radical with EPR characteristics very similar to those observed with indomethacin-treated enzyme (Figure 35). These results suggested the presence of distinct radical species associated with active versus inactive COX-1.

Similar observations were made by Lassmann et al. upon incubation of COX-1 with either PPHP or 20:4.<sup>151</sup> Formation of a radical species exhibiting an EPR spectrum characterized by a doublet centered at  $g = 2.004$ , with a splitting of 21 G and a peak-to-trough width of 33 G, was observed. This signal was replaced over time with a singlet also centered at  $g = 2.004$ , with a peak-to-trough width of 30 G. Simulation of the EPR spectrum of the doublet signal suggested that its source was a tyrosyl radical in which the dihedral angle between the strongly coupled methylene hydrogen and the  $\pi$ -orbital axis was  $34.7^\circ$ . However, these investigators noted that, under the conditions of their incubations (50  $\mu$ M COX-1, 5 mM 20:4 at 5 °C), PG synthesis occurred much more rapidly than formation of the radical species. This suggested that the detected radicals were not catalytically competent for PG formation.

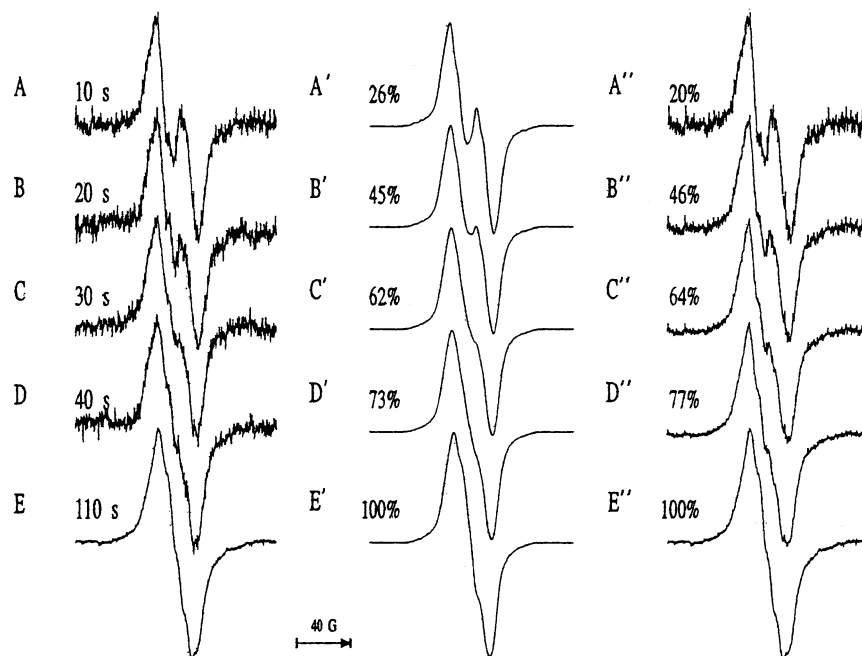
DeGray et al. noted the formation of three radical species upon incubation of COX-1 with either PPHP or 20:4.<sup>152</sup> The wide doublet and wide singlet EPR spectra similar to those described above were identified but were ultimately replaced by a narrow singlet spectrum (peak-to-trough width of 26.5 G). Detailed simulation studies indicated that the wide singlet did not represent a distinct radical species but was



**Figure 35.** EPR spectra obtained from the reaction of COX, indomethacin-treated COX, and tetranitromethane-treated COX-1 with ethyl hydroperoxide. Trace a: COX-1 (18.8  $\mu$ M heme) was treated with 20 equiv of ethyl hydroperoxide at  $-15$  °C, and the mixture was rapidly frozen to 10.6 K. Trace b: COX-1 (43  $\mu$ M subunit and 18.8  $\mu$ M heme) was treated with 43  $\mu$ M indomethacin. Ethyl hydroperoxide (190  $\mu$ M) was then added, and the sample was rapidly frozen to 11.1 K. Trace c: COX-1 (13.6  $\mu$ M subunit and 7.4  $\mu$ M heme) was treated with 1 mM tetranitromethane for 47 min. Ethyl hydroperoxide (73  $\mu$ M) was then added, and the sample was rapidly frozen to 10.6 K. Reproduced with permission from ref 150. Copyright 1990 American Chemical Society.

actually a composite of the wide doublet and narrow singlet signals (Figure 36). This implied that there were only two tyrosyl radicals actually formed. Furthermore, the finding that all three radical signals exhibited identical power saturation curves suggested that both tyrosyl radicals were located on the same tyrosine residue and that the conversion from doublet to singlet reflected a rotation of the phenyl ring relative to the methylene carbon. However, the results could not rule out the possibility that the conversion from doublet to singlet reflected an intramolecular electron transfer between two different tyrosine residues, both of which were located about the same distance from the heme.

Electron nuclear double-resonance spectroscopy was used to obtain further information on the tyrosyl radical structure of COX-1 after reaction with EtOOH.<sup>153</sup> These results agreed with those of DeGray et al., indicating that the wide singlet radical signal was a composite of the wide doublet and narrow singlet signals.<sup>152</sup> Shi et al. further concluded that the narrow singlet signal observed late in the COX-1 reaction with peroxides or 20:4 was distinct from the singlet signal observed in the case of indomethacin-treated enzyme. The investigators agreed with DeGray et al. that the conversion of wide doublet to narrow singlet reflected either a conformational change of a single tyrosine residue or migration of the radical center to a different residue.<sup>152</sup> The signal observed in the indomethacin-treated enzyme was proposed to result from either a completely different tyrosine residue or a marked change in the environment of the tyrosine consequent to indomethacin binding. Finally, the spectral characteristics of the wide doublet signal led to the conclusion that the



**Figure 36.** Time course of the changes in the EPR spectrum of COX-1 after reaction with 20:4 and comparison to simulated spectra. (A–E) COX-1 (67–133  $\mu\text{M}$ ) was incubated with 5 mM 20:4 for the indicated time periods at  $-12\text{ }^\circ\text{C}$ . Samples were then frozen, and spectra were recorded at  $-196\text{ }^\circ\text{C}$ . (A'–E') Results of computer simulations in which the simulated spectrum for the wide doublet was combined with the simulated spectrum for the narrow singlet. Percent values show the contribution of narrow singlet to each composite. (A''–E'') Results of composite spectra in which the experimental wide doublet spectrum was combined with the experimental narrow singlet spectrum. Percent values show the contribution of narrow singlet to each composite. Reproduced with permission from ref 152. Copyright 1992 American Society for Biochemistry and Molecular Biology.

tyrosine residue that gives rise to this signal is not hydrogen-bonded.

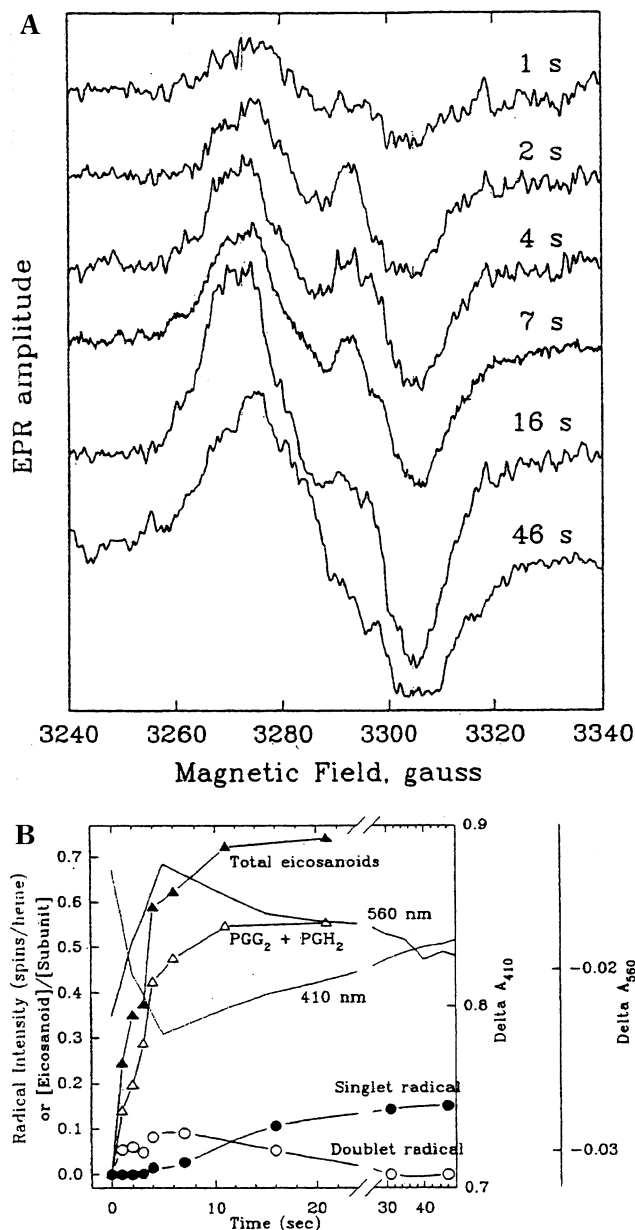
High-field EPR studies yielded conclusions similar to those of Shi et al. with regard to the likely sources and possible mechanisms of conversion of the various tyrosyl radical species.<sup>153,154</sup> However, these investigators determined that all three tyrosyl radicals formed during the reaction of COX-1 with EtOOH were hydrogen-bonded, in contrast to the conclusions of Shi et al.<sup>153</sup> The findings of Dorlet et al. indicated that the conversion of wide doublet to narrow singlet likely resulted from a rotation of the tyrosine ring with respect to the protein backbone and the hydrogen bond donor.<sup>154</sup> On the basis of their pulsed EPR measurements, they also concluded that the interaction between the radical and the oxo-ferryl heme species was weak.

## 2. Kinetics of Tyrosyl Radical Formation and Cyclooxygenase Catalysis

Studies by Lassmann et al. described above (section VI.B.1) had raised significant questions regarding the catalytic competence of the tyrosyl radical.<sup>151</sup> This prompted further kinetic studies by Tsai et al.<sup>155,156</sup> Using manual mixing techniques, the EPR signals generated after combining equimolar quantities of 20:4 and COX-1 were monitored. The progression from the wide doublet to the wide singlet signal was observed, and the rate of formation of the wide doublet signal correlated well with the rate of PG synthesis. The wide singlet signal was noted only after cessation of cyclooxygenase activity (Figure 37). Further studies using a 25 molar excess of 20:4

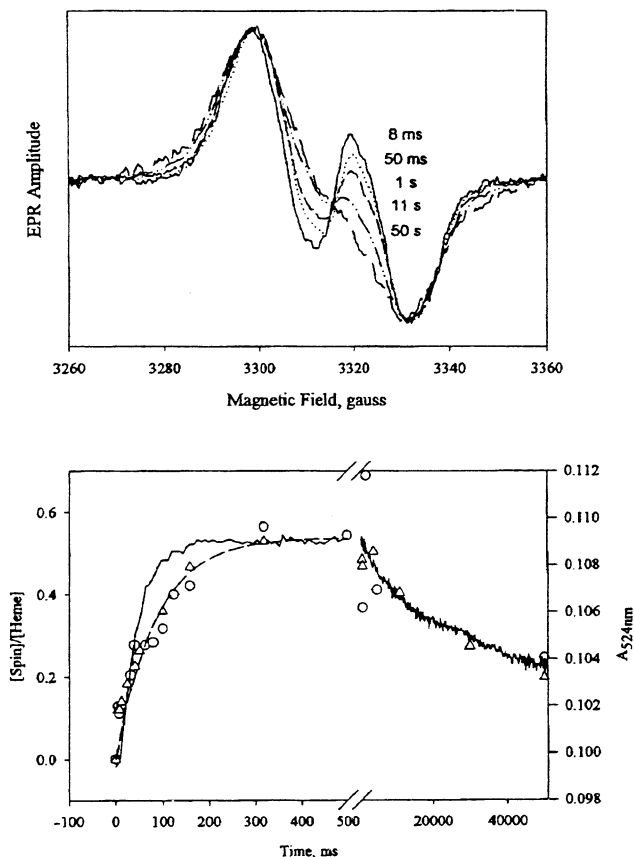
resulted in the generation of lower total amounts of product and observation of the narrow singlet species only.<sup>155</sup> Stopped-flow techniques combined with freeze-trapping were used to monitor radical signals after the addition of 5 equiv of EtOOH to COX-1 at room temperature. Results indicated the formation of the wide doublet signal within 4 ms, followed by changes to the wide singlet within 5 s. Total radical intensity correlated with the formation of intermediate I/compound II, as monitored by absorbance at 524 nm (Figure 38).<sup>156</sup> These results suggested that the wide doublet radical signal arises from intermediate I and that this intermediate contains a catalytically competent tyrosyl radical. Furthermore, the conversion from the wide doublet to the narrow singlet via the wide singlet is associated with enzyme inactivation, as suggested earlier by Lassmann et al. Tsai et al. pointed out that the reaction conditions used by Lassmann et al. led to very rapid enzyme inactivation and that this probably accounted for their inability to correlate the formation of the wide doublet signal to cyclooxygenase activity.<sup>151,155</sup>

Tsai et al. expanded their rapid-freeze EPR and stopped-flow studies of the kinetics of tyrosyl radical formation to include purified recombinant human COX-2.<sup>156</sup> Previously, Hsi et al. had demonstrated the formation of a wide singlet radical signal ( $g = 2.004$ , with a line width of 28–29 G) upon EtOOH treatment of microsomal preparations from COS-1 cells expressing the cDNA for COX-2.<sup>157</sup> Xiao et al. also observed a wide singlet signal in their studies of the reaction of EtOOH with purified recombinant COX-2.<sup>158</sup> In their kinetic studies, Tsai et al. demonstrated



**Figure 37.** (A) Time course of the changes in the EPR spectrum of COX-1 (30  $\mu\text{M}$  subunit, 15  $\mu\text{M}$  heme) after addition of 20:4 (30  $\mu\text{M}$ ). The reaction mixture was incubated at 0 °C for the indicated times, and EPR spectra were then obtained at 88 K. (B) Time course of the changes in the EPR and absorbance spectra of COX-1 as compared to the rate of eicosanoid formation. The reaction conditions are the same as described for (A). Conversion of 20:4 to PGG<sub>2</sub> plus PGH<sub>2</sub> or total products was monitored by chromatographic analysis of products from radiolabeled substrate. Absorbance changes were obtained at 410 and 560 nm using a reaction mixture containing 9.1  $\mu\text{M}$  COX-1 (6.2  $\mu\text{M}$  heme) and 6.2  $\mu\text{M}$  20:4. Reproduced with permission from ref 155. Copyright 1992 American Society for Biochemistry and Molecular Biology.

that a wide doublet radical signal could be detected very early in the reaction of COX-2 with EtOOH but that conversion to the wide singlet was complete within 50 ms for COX-2, whereas the conversion for COX-1 required 50 s.<sup>156</sup> As was observed for COX-1, the COX-2 isoform showed a strong correlation between the rate of tyrosyl radical formation and the rate of formation of intermediate I/compound II, as



**Figure 38.** Time course of the formation of the tyrosyl radical as compared to heme spectral changes. COX-1 (8.5  $\mu\text{M}$ ) was reacted with 42  $\mu\text{M}$  ethyl hydroperoxide at 24 °C. Top: EPR spectra were obtained for samples freeze-trapped at the indicated times after initiation of the reaction. Bottom: The time course of the formation of the tyrosyl radical, as determined from double integration of EPR spectral intensities, is compared to the formation of ferryl heme (intermediate I/compound II), as determined from absorbance changes at 524 nm. EPR data are represented by open triangles and circles (indicating the combination of results from two separate experiments), and the dashed line indicates the results of nonlinear regression analysis of those data to a single-exponential equation. Absorbance data are shown by the solid line. Reproduced with permission from ref 156. Copyright 1999 American Society for Biochemistry and Molecular Biology.

detected by absorbance at 524 nm. These results demonstrated the generation of a tyrosyl radical species in COX-2 that is very similar to that of COX-1 and confirmed that the tyrosyl radical and intermediate I are temporally related. Interestingly, whereas the rate of decay of oxo-ferryl heme was similar to that of the tyrosyl radical signal for COX-1, this was not the case for COX-2. Rather, the oxo-ferryl heme species was found to decay much more rapidly than the tyrosyl radical signal. Thus, the cyclooxygenase activity of COX-2 demonstrated greater independence from the heme redox state than was observed in COX-1, suggesting prolonged function of the catalytic tyrosyl radical in the absence of ongoing peroxide activation.

### 3. Identity of COX Tyrosyl Radicals

While EPR and kinetic studies provided much evidence concerning the nature of the tyrosyl radical

and its kinetic competence for PG synthesis, chemical and molecular biology techniques were used to identify the tyrosine residue(s) involved. Shimokawa et al. incubated purified COX-1 with tetranitromethane in the presence and absence of indomethacin.<sup>159</sup> Tetranitromethane treatment eliminated cyclooxygenase activity, but the activity was protected if ibuprofen or indomethacin was present during the incubation. Peptide analysis demonstrated that three tyrosine residues (Tyr-355, Tyr-385, and Tyr-417) were nitrated in the absence but not in the presence of indomethacin, suggesting that one or more of these residues might be critical for cyclooxygenase activity. Subsequent site-directed mutagenesis studies were performed in which each of the three tyrosines, plus two additional ones (Tyr-254 and Tyr-262), were mutated to phenylalanine. All mutant COX-1 enzymes were expressed in COS-1 cells, and all exhibited cyclooxygenase and peroxidase activity at or near wild-type levels with the exception of the Y385F mutant. This mutant exhibited peroxidase activity but no cyclooxygenase activity, suggesting that the Tyr-385 residue is critical for the cyclooxygenase reaction.

Tsai et al. studied the production of tyrosyl radicals formed from the reaction of EtOOH with detergent extracts of COS-1 cells expressing wild-type COX-1.<sup>160</sup> The typical wide doublet and wide singlet EPR signals were observed. When the COS-1 cells were grown in medium containing tyrosine-*d*<sub>8</sub> and phenylalanine-*d*<sub>8</sub>, resulting in isotope replacement in the expressed enzyme, no change was observed in cyclooxygenase activity or the ability to generate a tyrosyl radical signal, but the signal was now observed to be an isotropic singlet rather than a doublet. This result provided further confirmation that the source of the radical signal was a tyrosine residue. When the same experiment was carried out in cells expressing COX-1 carrying a site-directed Y385F mutation, the enzyme lacked cyclooxygenase activity, and the tyrosyl radical signal formed in response to EtOOH was a narrow singlet, similar to that seen with indomethacin-treated enzyme. Isotope replacement in the mutant enzyme resulted in further narrowing of the radical signal. These results were interpreted to mean that Tyr-385 is required for cyclooxygenase activity and is the residue that gives rise to the wide doublet radical signal. The signal observed in the mutant enzyme is also derived from a tyrosine residue but one that is distinct from Tyr-385. It is notable that the crystal structure of COX-1 has shown that there are eight tyrosine residues within 12 Å of the heme iron atom. Thus, the oxidation of an alternative residue is certainly feasible.

In an attempt to discover the source of the radical signal in the Y385F mutant enzyme, Hsi et al. compared the EPR signals generated from the reaction of EtOOH with COX-1 and three mutants, Y385F, Y348F, and Y348F/Y385F.<sup>161</sup> Tyr-348 was chosen for study because of its proximity to the heme prosthetic group, as indicated by X-ray crystallography. Results showed that Y348F has cyclooxygenase and peroxidase activities and generates ty-

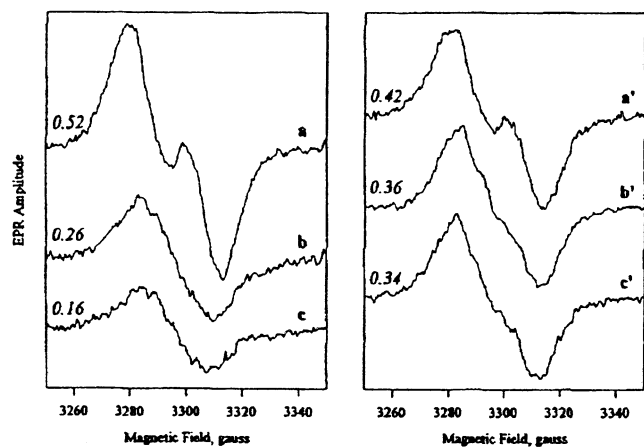
rosyl radical signals similar to those of the wild-type enzyme. The Y348F/Y385F mutant behaved very similarly to the Y385F mutant in terms of both enzyme activity and radical signal. These results indicated that Tyr-348 is not required for cyclooxygenase or peroxidase activity and that the radical signal observed in the Y385F mutant does not arise from Tyr-348, despite its proximity to the heme.

Further evidence for the involvement of Tyr-385 in the cyclooxygenase reaction was obtained by Goodwin et al., who treated COX-1 with nitric oxide (NO, generated in situ from diethylamine NONOate) in the presence of 20:4.<sup>162</sup> NO is expected to react with any tyrosyl radicals generated to form nitroso-cyclohexadienone, which would subsequently be oxidized to form nitrotyrosine. As expected, addition of NO to COX-1 during its reaction with 20:4 quenched all tyrosyl radical signals. Western blotting of the COX-1 protein using anti-nitrotyrosine antibodies indicated the presence of nitrotyrosine residues in the protein. Subsequent peptide mapping experiments indicated that only Tyr-385 had been converted to nitrotyrosine. These results confirmed that Tyr-385 had been oxidized to a tyrosyl radical during the reaction of COX-1 with 20:4. However, since the initial reaction of NO with tyrosyl radicals is reversible, the investigators could not rule out the possibility that other tyrosyl radicals had been produced and reacted with NO but failed to progress to form nitrotyrosine. Thus, these results supported but did not absolutely prove the hypothesis that Tyr-385 was the residue involved in the cyclooxygenase reaction.

#### 4. Oxidation of 20:4 by COX Tyrosyl Radicals

The studies described above demonstrated that the tyrosyl radical formed during the COX reaction is kinetically competent to serve as the primary oxidant of 20:4. The chemical competence of the radical remained to be determined. This question was first directly addressed by Tsai et al. in experiments in which 20:4 was added to preparations of purified COX-1 under anaerobic conditions following activation of the enzyme with EtOOH to generate the tyrosyl radical species.<sup>163</sup> On addition of 20:4, the tyrosyl radical signal was replaced by a featureless isotropic singlet centered at  $g = 2.004$ , with a line width of 23.5 G (Figure 39). Formation of this radical was inhibited by indomethacin, and the radical signal disappeared on addition of oxygen. The use of 5,6,8,9,11,12,14,15-octadeuterated 20:4 resulted in significant alterations in the observed EPR spectrum, verifying that the radical was formed from 20:4. These results provided strong evidence that the tyrosyl radical was chemically competent to abstract a hydrogen atom from 20:4, as proposed in the branched-chain mechanism.

Similar studies using COX-2 instead of COX-1 were performed by Tsai et al.<sup>164</sup> Once again, the enzyme was first incubated with EtOOH to generate the wide singlet radical signal. Addition of 1 equiv of 20:4 under anaerobic conditions then resulted in the disappearance of the tyrosyl radical signal and its replacement with a seven-line EPR signal. That this signal originated from a 20:4 radical was confirmed

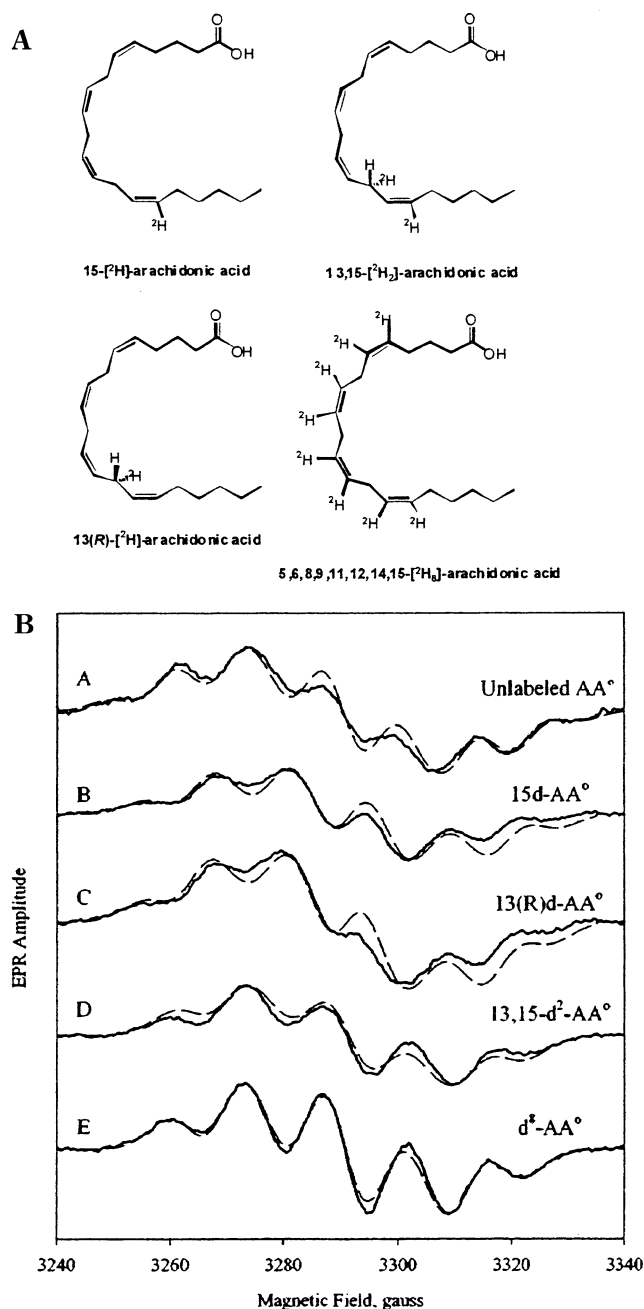


**Figure 39.** EPR spectra obtained from the incubation of COX-1 with 20:4 after activation with ethyl hydroperoxide. (Left) Trace a: COX-1 (10  $\mu$ M heme) was incubated for 12 s with 1.5 equiv of ethyl hydroperoxide under anaerobic conditions before rapid freezing and EPR spectroscopy. Trace b: A sample identical to the one described in trace a was incubated for 20 s after addition of ethyl hydroperoxide, and then 1.5 equiv of 20:4 was added. After 12 s, the sample was frozen for EPR spectroscopy. Trace c: Same as trace b, but the sample was incubated 60 s after 20:4 addition. (Right) Each sample from the left panel was thawed and incubated aerobically for 20 s, and then a second spectrum was obtained. The numbers at the left side of each trace are the signal intensities (spins/heme) obtained by double integration of the spectrum. Reproduced with permission from ref 163. Copyright 1995 American Society for Biochemistry and Molecular Biology.

using octadeuterated 20:4. Addition of oxygen led to the disappearance of the 20:4 radical signal and regeneration of the tyrosyl radical signal. When a COX-2 protein bearing a site-directed mutation homologous to Y385F of COX-1 was used, no 20:4 radical signal was generated. This was true despite the fact that a narrow singlet tyrosyl radical signal appeared upon reaction of this protein with EtOOH. These data confirmed the ability of the tyrosyl radical of COX-2 to oxidize 20:4 and strongly suggested that the site of radical formation was homologous to that in COX-1.

Peng et al. performed further studies to characterize the 20:4-derived radical formed during the anaerobic reaction of 20:4 with intermediate I of COX-2.<sup>165,166</sup> These investigators compared the EPR spectrum obtained using 20:4 versus 20:4 selectively labeled with deuterium at carbon 13 (R position) or carbon 15, or both (Figure 40A). Their results showed that the 20:4-derived radical yielded a seven-line spectrum, which was converted to a six-line multiplet upon substitution with deuterium at carbon 15 (Figure 40B). Substitution with deuterium at carbon 13 yielded a six-line signal, and double substitution yielded a five-line signal. Finally, octadeuterated 20:4 also yielded a five-line spectrum. These results are consistent with the structure of a pentadienyl radical spanning carbons 11–15 and support the mechanism for the cyclooxygenase reaction that would generate such a radical following abstraction of the 13-*pro*-(S) hydrogen atom.

The body of data summarized above provides overwhelming evidence that a tyrosyl radical is



**Figure 40.** (A) Structures of deuterated substrates used for EPR studies of the arachidonyl radical formed during the COX-1 reaction. (B) EPR spectra obtained by anaerobic incubation of COX-1 (11–14  $\mu$ M) with (A) 20:4, (B) 15- $^{2}\text{H}$ -20:4, (C) 13-(R)- $^{2}\text{H}$ -20:4, (D) 13,15- $^{2}\text{H}_2$ -20:4, and (E) 5,6,8,9,11,12,14,15- $^{2}\text{H}_8$ -20:4. Spectra were obtained on samples that had been frozen 60 s after addition of the fatty acid at 4  $^{\circ}\text{C}$ . Dashed lines indicate the results of simulations. Reproduced with permission from ref 165. Copyright 2001 American Chemical Society.

critical to the cyclooxygenase reaction and that Tyr-385 is the residue most likely involved. Therefore, it was gratifying when the X-ray crystal structure of ovine COX-1 was solved and revealed that Tyr-385 is positioned at the top of the cyclooxygenase active site, placing it 10  $\text{\AA}$  from the heme and close to the supposed location of the *pro*-(S) hydrogen at carbon 13.<sup>19</sup> Thus, strong structural evidence corroborates the role of this critical residue in the COX mechanism.

## VII. The Structural Basis of Cyclooxygenase Catalysis

The gene that codes for COX-1 is located on human chromosome 9, is 22 kb in length, and contains 11 exons and 10 introns.<sup>167</sup> It is transcribed into a 2.8-kb mRNA. The COX-2 gene is present on human chromosome 1, is 8 kb in length, and contains 10 exons and 9 introns.<sup>12</sup> It is transcribed into 2.8- and 4.6-kb mRNA's, depending on the polyadenylation site used in the 3'-untranslated region.<sup>9-13</sup> The initially translated COX-1 protein contains 599 amino acids, including a 23-amino-acid signal sequence that is removed in processing to the mature protein. The mature protein also contains several high mannose oligosaccharides, one of which appears to be important for proper folding.<sup>19,168</sup> COX-2 also contains a membrane signal sequence that is removed in processing and multiple high mannose oligosaccharides.<sup>169</sup> The absence of exon 2 in the COX-2 gene results in the deletion of 14 amino acids near the N-terminus. This deletion is compensated for by the addition of 18 amino acids near the C-terminus. Thus, the numbers of most of the amino acid residues of COX-2 are 14 units lower than the corresponding residues of COX-1 up to the point of the C-terminal insertion. By convention, the residues of both proteins are referred to by the residue numbers of the initial COX-1 translation product. That convention will be followed here. The mature proteins are approximately 60% identical in sequence.

Recently, Chandrasekharan et al. reported the cloning and characterization of a 2.6-kb cDNA from a canine cerebral cortex library.<sup>29</sup> This cDNA, which the investigators designated COX-3, represents a splice variant of COX-1, encoding the full COX-1 sequence with retention of intron 1. RT-PCR and northern blot analysis using probes based on the intron 1 sequence indicated that the COX-3 mRNA comprised about 5% of the total COX-1 mRNA in canine cerebral cortex samples. Expression of the cloned COX-3 cDNA in Sf9 cells yielded a protein that included the COX-1 sequence plus the intron 1 sequence located within the signal peptide. The presence of intron 1 apparently prevented processing of the signal peptide; however, membrane localization and glycosylation of the protein appeared to occur normally. The specific activity of the expressed protein was approximately 20% of the activity of COX-1, which in turn was approximately 20% of the activity of COX-2 expressed under the same conditions. The most interesting characteristic of the expressed protein was its sensitivity to various NSAIDs. In particular, COX-3 was more sensitive to inhibition by acetaminophen, phenacetin, and dipyron than either COX-1 or COX-2. Northern blot analysis of multiple human tissues using a probe based on the sequence of human intron 1 revealed a 5.2-kb mRNA transcript that displayed tissue-specific distribution. Expression of this mRNA was greatest in cerebral cortex and heart. Immunoblot analysis of a protein extract of human aorta revealed a 65-kDa protein that was visualized with both a monoclonal antibody directed against COX-1 and a polyclonal antibody directed against an intron 1 peptide. The

65-kDa protein exhibited faster mobility on polyacrylamide gel electrophoresis than either native COX-1 or an unglycosylated canine COX-3 standard, a finding inconsistent with the expected behavior of a fully glycosylated protein that contains the complete COX-1 sequence plus the signal peptide and intron 1.

The findings of Chandrasekharan et al. suggest the intriguing possibility that variants in mRNA processing may yield multiple isoforms of COX-1 having unique physiological and pharmacological properties. Specifically, Chandrasekharan et al. note that the analgesic and antipyretic effects of acetaminophen are poorly explained on the basis of COX-1 or COX-2 inhibition. If COX-3 plays a critical role in the pathogenesis of fever and pain, then its discovery may provide insights into the clinical efficacy of acetaminophen. However, the evidence that COX-2<sup>-/-</sup> mice show little to no pyrexia in response to LPS, and that COX-2-selective inhibitors demonstrate considerable antipyretic and analgesic activity, is inconsistent with a singular role for COX-3 in the pathogenesis of fever or pain.<sup>170-175</sup> Clearly, a complete understanding of the significance of COX-3 awaits the demonstration of active native protein under relevant physiologic or pathologic conditions. (See Note Added in Proof.)

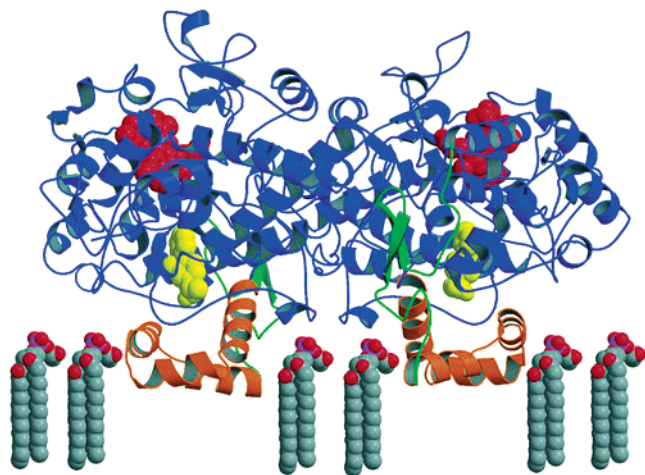
### A. The Three-Dimensional Structure

The solution of the structure of sheep seminal vesicle COX-1 by Garavito and colleagues in 1994 was a landmark accomplishment because it was only the third membrane protein to be crystallized and solved, it displayed a unique mechanism of membrane insertion, and it provided a beautiful depiction of the structural basis of the protein's function.<sup>19</sup> The structure was solved at 3.5-Å resolution and revealed an ellipsoid of dimensions 99 × 65 × 55 Å. Residues 33-586 were visible in the structure (out of 25-600 in the mature protein). The protein exists as a homodimer, which is consistent with previous gel filtration studies.<sup>30</sup> The two subunits of the dimer are related to each other by a C<sub>2</sub> axis of symmetry (Figure 41).

Approximately 40% of the protein is  $\alpha$ -helix, but only a small amount exists as  $\beta$ -sheet. Five disulfide bonds are apparent, which is consistent with previous biochemical experiments.<sup>176</sup> Three structural domains exist: an epidermal growth factor (EGF) domain (residues 34-72), a membrane-binding domain (residues 73-116), and a catalytic domain (residues 117-586) (Figures 2 and 41). The function of the EGF domain remains unclear. EGF domains in other proteins play roles in protein-protein association, and although this is an attractive possibility for COX enzymes, which provide the substrate for PGH<sub>2</sub>-metabolizing enzymes, no partners have been identified. In fact, the EGF domain in COX is close to the dimer interface.

The membrane-binding domain of each subunit comprises four  $\alpha$ -helices (A-D) that are approximately orthogonal to each other (Figure 41). Each helix projects hydrophobic residues toward the membrane, which provides the mechanism for attachment to one leaflet of the bilayer. The residues on the other





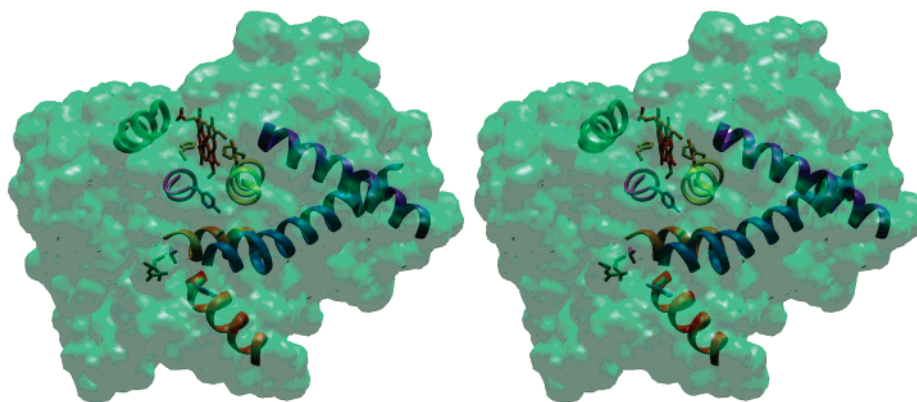
**Figure 41.** Structure of the COX-1 dimer. A  $C_2$  axis of symmetry relates the two subunits. The two membrane-binding domains are modeled into one leaflet of a membrane bilayer. Reproduced with permission from ref 8. Copyright 2000 Annual Reviews (<http://www.AnnualReviews.org>).

faces of the helices are polar and may play a role in binding phospholipid headgroups. COX proteins are termed monotopic membrane proteins, but they behave functionally like integral membrane proteins in that they require treatment with detergents to dissociate them from the membrane. The unexpected structure of the membrane-binding domain of sheep COX-1 explains the curious observation that COX proteins exhibit hydrophathy plots analogous to those of cytosolic proteins. Topological studies suggest both COX proteins (COX-1 and COX-2) are located on the luminal side of the endoplasmic reticulum and on the inside of the nuclear envelope.<sup>35</sup> This provides the basis for a functionally attractive model in which the substrate, 20:4, is released following agonist stimulation by the action of phospholipase  $A_2$ . Since phospholipase  $A_2$  attaches to the cytosolic face of intracellular membranes following activation, 20:4 released in response to cell stimulation need only diffuse across the bilayer to be acted upon by COX enzymes. Physical studies suggest that fatty acid migration across lipid bilayers is rapid.<sup>177</sup>

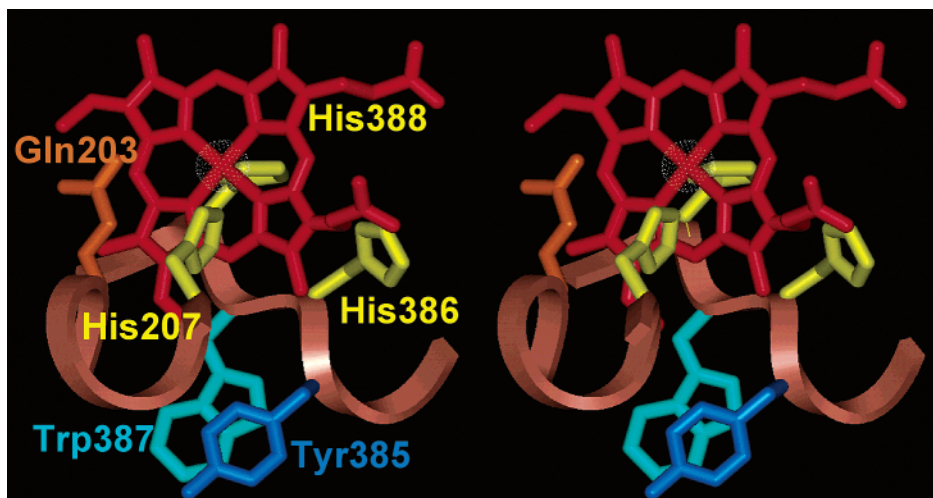
Helix D of the membrane-binding domain extends up from the membrane into the third and principal

domain of the protein, the catalytic domain. This domain contains the cyclooxygenase active site, the peroxidase active site, and the heme-binding site. The catalytic domain exhibits two lobes: the larger lobe comprises most of the heme-binding residues, whereas the smaller lobe provides an edge of the heme-binding site. The dominant structural feature of the catalytic domain is a helix bundle that constitutes the heme-binding motif and peroxidase active site (Figure 42). Two large helices (5 and 6), resembling the arms of tweezers, appear to pinch helix 2, which is positioned on the distal face of the heme. Helices 8 and 12 are located beneath the heme, and helix 8 provides the proximal heme ligand. Helices 16 and 17 complete this heme-binding bundle, and helix 17 provides other residues in the cyclooxygenase active site (e.g., the aspirin acetylation site, Ser-530). The overall structure of this helix bundle is conserved in other peroxidases; in fact, the overall helical structure of the catalytic domain is very similar to that of myeloperoxidase. COX enzymes are missing two helices (4 and 7) that are present in myeloperoxidase, but overall the folding pattern between the two proteins is very similar.<sup>178</sup>

COX is a member of the myeloperoxidase superfamily, a protein family with members from bacteria to humans.<sup>40</sup> Two distinct COX genes have been detected in a wide range of vertebrates from mammals to fish. Recently, a COX protein has been identified in coral that generates PG's with inverted stereochemistry at position 15.<sup>179</sup> The sequence homology between mammalian COX proteins and other myeloperoxidase family members is extremely low, only 14% between COX and myeloperoxidase. Interestingly, the most highly conserved region is a 10-residue peptide that is exactly reproduced in COX and myeloperoxidase.<sup>180</sup> The 10-residue peptide is present in the middle of helix H5, approximately 25 Å from the heme. Mutations in this conserved peptide have dramatic effects on both the cyclooxygenase and peroxidase activities of COX. Particularly impressive is the observation that mutation of Cys-313 to Ser (substitution of a single O for S) reduces cyclooxygenase and peroxidase activities by 90%.<sup>181</sup>



**Figure 42.** Stereo drawing of the helix bundle that comprises the cyclooxygenase and peroxidase active sites. Helix D (red) stretches from the membrane-binding domain to the catalytic domain and provides the carboxylate-binding residue, Arg-120. Helix 2 (lime) provides the residues on the distal side of the heme, whereas the extension off helix 12 (dark blue) provides the proximal heme ligand, His-388, and the catalytic residue, Tyr-385. Helices 6 (blue) and 17 (brown) constitute the walls of the cyclooxygenase active site. Helices 5 (blue) and 8 (green) provide support for the heme binding region.



**Figure 43.** Residues in the heme-binding region. The view is from the distal face of the heme.

### B. The Heme-Binding Site and Peroxidase Active Site

The residues in the heme-binding site are typical of those of heme peroxidases (Figure 43). The ligand proximal to the heme is a histidine residue (His-388), which is positioned three residues carboxyl to the end of helix 8. His-388 is one of only two residues conserved in a nine-residue region that provides the C-terminal region of helix 8 and the proximal His in COX and myeloperoxidase. Interestingly, this sequence is highly conserved between myeloperoxidase and three other mammalian peroxidases, lactoperoxidase, eosinophil peroxidase, and thyroid peroxidase.<sup>40</sup> His-388 of COX is H-bonded to the peptide carbonyl oxygen of His-386. Mutation of His-386 to alanine dramatically reduces peroxidase activity.<sup>182</sup> The proximal His of myeloperoxidase, which is also present near the end of helix 8, is H-bonded to the amide oxygen of an Asn residue located on the adjacent helix 12.

As with other peroxidases, there is no protein ligand distal to the heme in COX. His-207 and Gln-203 are located approximately 5 Å above the heme iron (Figure 43). Mutation of either residue significantly inhibits peroxidase activity. Gln-203 is superimposable on Gln-91 in the crystal structure of myeloperoxidase.<sup>178</sup> This Gln residue is conserved among all members of the myeloperoxidase family that have a His residue four residues C-terminal on helix 2. The other residues on helix 2 are highly conserved in myeloperoxidase, lactoperoxidase, and thyroid peroxidase, but not in COX-1 or COX-2.

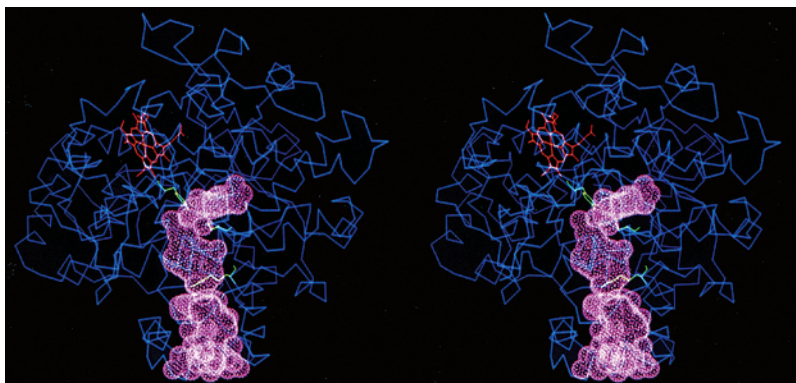
The peroxidase active site sits at the bottom of a shallow cleft in COX, with a considerable portion of the heme exposed to solvent. This contrasts with myeloperoxidase, in which the peroxidase active site is buried at the bottom of a deep channel. The difference in active-site accessibility undoubtedly contributes to the significant differences in substrate specificity of the two enzymes. The peroxidase activity of COX utilizes a range of organic hydroperoxides including primary and secondary hydroperoxides and, to a lesser extent, tertiary hydroperoxides, whereas myeloperoxidase appears to be more restricted to H<sub>2</sub>O<sub>2</sub>.<sup>183</sup> H<sub>2</sub>O<sub>2</sub> is actually a relatively poor

substrate for COX enzymes (Table 2), although its inorganic analogue, peroxyxynitrous acid, is an excellent substrate.<sup>184</sup>

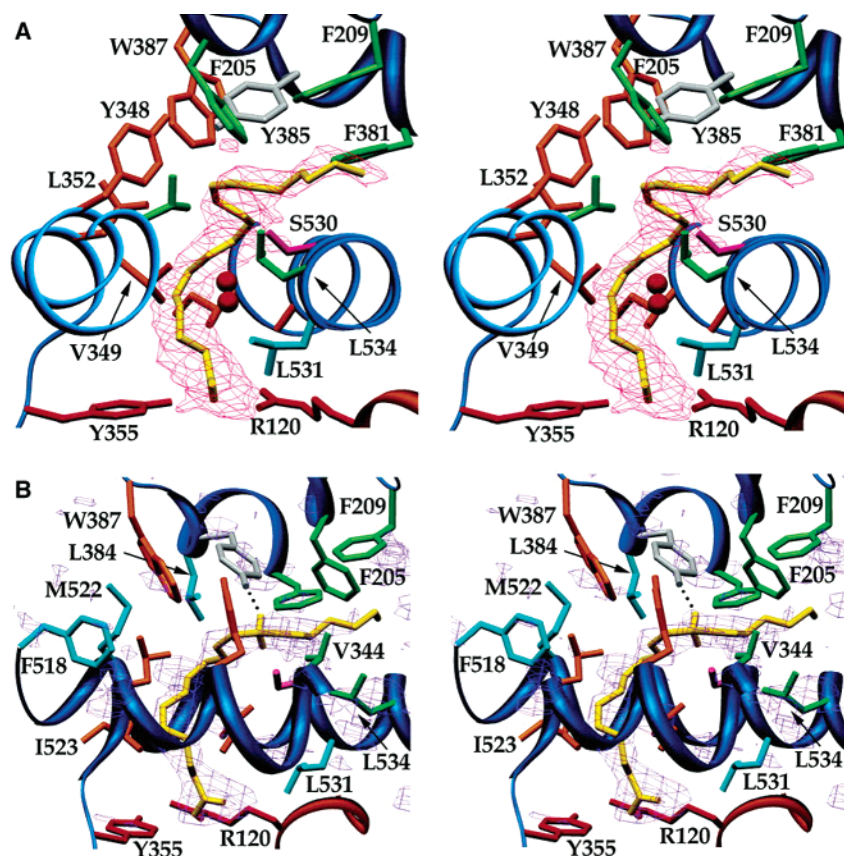
### C. The Cyclooxygenase Active Site

The cyclooxygenase active site is located at the top of a deep channel that runs from the membrane-binding domain into the catalytic domain (Figure 44). The entrance to this channel is circumscribed by the four amphipathic helices of the membrane-binding domain (A–D). The initial portion of the channel has a large volume, and we have it termed the lobby. The walls of the lobby are composed primarily of the side chains on the interior of helices A–D. A molecule of the detergent used for crystallization is visible in the lobby in the crystal structures of both COX-1 and COX-2. The channel narrows at the top of the lobby into a constriction comprised of Arg-120, Tyr-355, and Glu-524. Arg-120 is donated by the membrane-binding helix D, whereas Tyr-355 is in a loop two residues past the C-terminal end of helix 6 and Glu-524 is four residues into helix 17. The constriction at the top of the lobby must open and close in order for substrates and inhibitors to pass into or out of the cyclooxygenase active site, which is located above it. This region appears to have considerable mobility in the available COX structures, so the motion of helix D may destabilize H-bonding among the constriction residues and facilitate opening and closing. Arg-120 and Glu-524 are the only charged residues in the entire active-site channel and play an important role in binding carboxylic acid-containing substrates and inhibitors.

The actual cyclooxygenase active site lies above the Arg-120/Tyr-355/Glu-524 constriction and is demarcated by residues provided by helices 6 and 17 near the bottom and helices 2 and 8 at the top. Crystal structures of complexes of substrate fatty acids bound to Co<sup>3+</sup>-COX-1 (catalytically inactive) reveal that the fatty acid carboxylates ion-pair and H-bond to Arg-120 and Tyr-355 and the alkyl chains project upward and between helices 6 and 17, which run parallel to each other across the active site (Figure 45).<sup>34</sup> The fatty acids continue upward toward Tyr-385 and then bend sharply into a hydrophobic alcove. The residues in the alcove are provided by helix 2 (Phe-205 and



**Figure 44.** Stereo drawing of the hydrophobic channel of COX-1. The large opening in the membrane binding domain is termed the lobby. The constriction at the top of the lobby comprises Arg-120, Tyr-355, and Glu-524; this is the carboxylate-binding region. Opening of the constriction provides access to the cyclooxygenase active site, which projects up toward the catalytic Tyr-385 and then bends parallel to helix 17 and projects toward Gly-533. The heme prosthetic group is colored red, and Arg-120, Tyr-385, and Ser-530 are colored green. Figure kindly provided by R. M. Garavito.



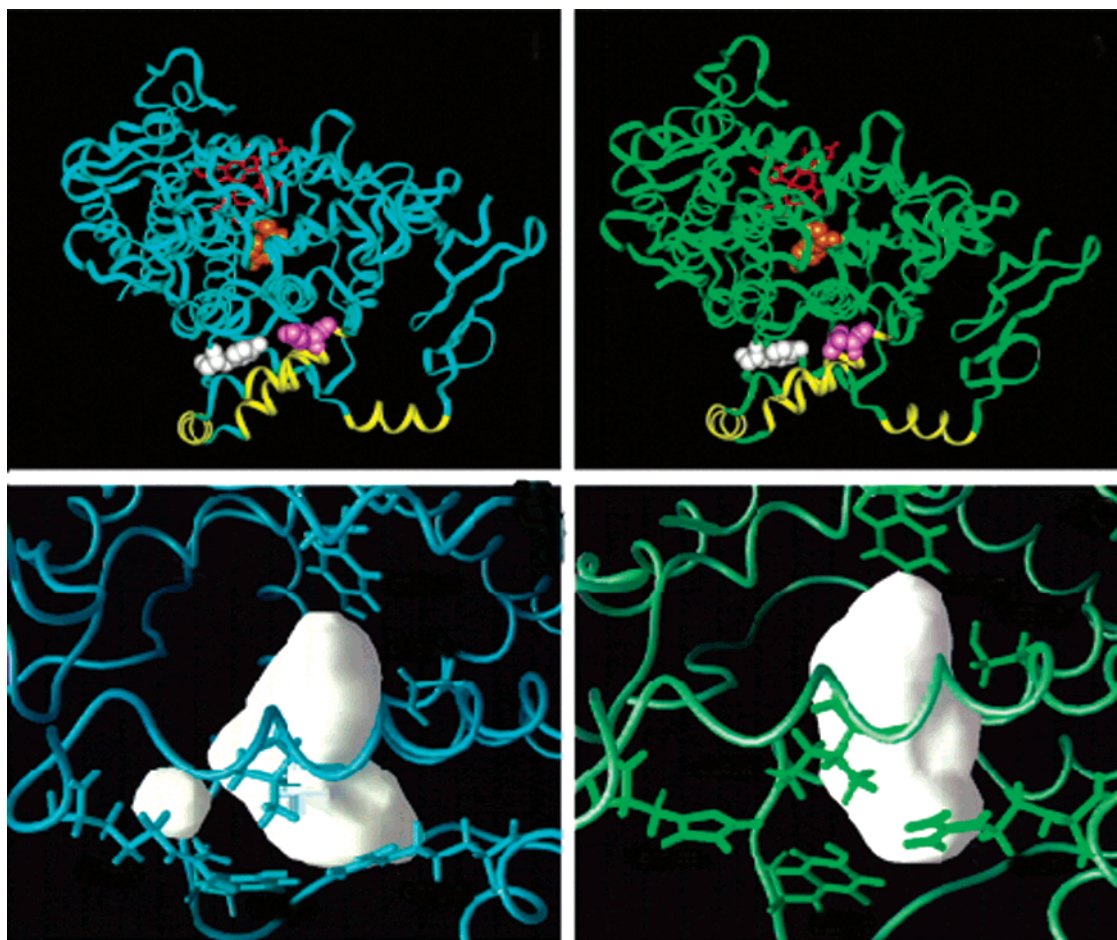
**Figure 45.** Stereoview of 20:4 bound to COX-1. (A) View down helices 6 and 17; (B) view perpendicular to helices 6 and 17. Reproduced with permission from ref 186. Copyright 2001 American Society for Biochemistry and Molecular Biology.

Phe-209), helix 8 (Phe-381), and helix 17 (Leu-534). As discussed earlier (section VI.B.4), Tyr-385 is located at the end of helix 8. Trp-387 sits next to Tyr-385 in the active site and plays an important role in PGG<sub>2</sub> formation (see below). The residues that comprise the remainder of the walls of the active site are provided by helix 6 and helix 17. The hydrophobic alcove connects to a narrow channel that ultimately exits the protein into a reservoir formed by the dimer interface.<sup>21</sup> The narrow channel emanating from the alcove has been speculated to comprise a PGG<sub>2</sub> exit channel, but it appears to be too narrow to accommodate this large product. Mutations in the alcove that are anticipated to block access to the putative

exit channel do not block oxygenase activity against certain substrates [e.g., 9,12,15-octadecatrienoic acid ( $\alpha$ -linolenic acid,  $\alpha$ -18:3) and 6,9,12,15-octadecatetraenoic acid (stearidonic acids, 18:4)], which would be anticipated to be the case if the top channel represented an exit port.<sup>185</sup> It seems more likely that this top channel provides a route for water molecules to be displaced as the substrate moves up into the active site.

#### D. Comparison of COX-2 and COX-1

Structures of human COX-2 and murine COX-2 are very similar to the structure of ovine COX-1, as revealed by a series of protein–inhibitor complexes

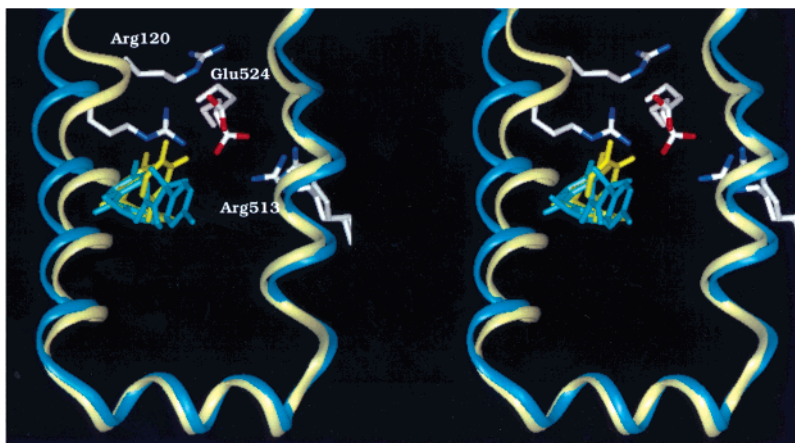


**Figure 46.** Comparison of solvent-accessible space in the cyclooxygenase active sites of COX-1 and COX-2. The upper frames provide a comparison of the backbone structures of COX-2 (blue) and COX-1 (green). The lower frames compare solvent-accessible space (white) above Arg-120 and below Tyr-385.

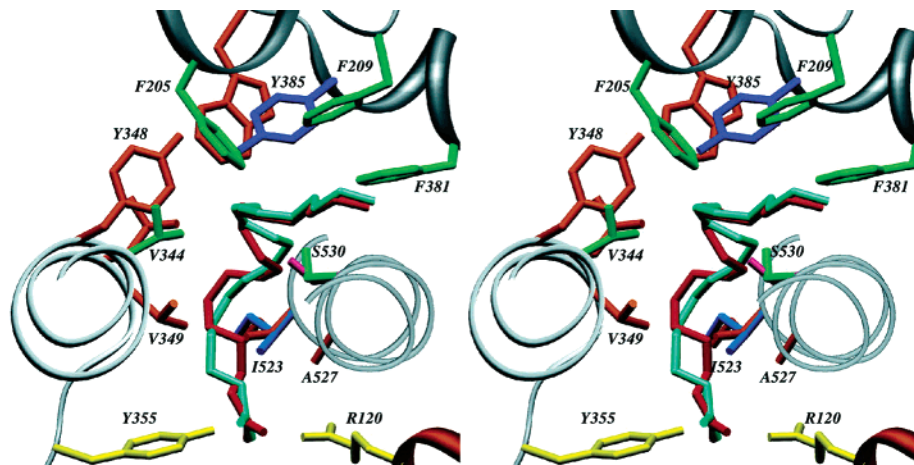
determined at 2.9–3.3- and 2.5–3.0-Å resolution, respectively.<sup>20,21</sup> The three-domain structure seen in COX-1 is also evident in COX-2. The polypeptide backbones of the three proteins are virtually superimposable and display root-mean-square (rms) deviations of 0.9 Å for all the backbone carbons. The rms deviation between ovine COX-1 and human COX-2 is 0.4 Å for the backbones of the core catalytic residues. The subunit interface is also conserved between the two proteins, although there are conserved differences in sequence between the two interfaces. There is no evidence from either crystallographic or biochemical studies for the existence of heterodimers between individual subunits of COX-1 and COX-2. The cyclooxygenase active site of COX-2 is significantly larger than that of COX-1 (Figure 46).<sup>20</sup> This is mainly due to a conserved substitution of Val for Ile at position 523 of COX-2. This opens up access to a side pocket in COX-2 which is inaccessible in COX-1. The volume of the human COX-2 active site, including the side pocket, is calculated to be 394 Å<sup>3</sup> whereas the active-site volume of COX-1 is calculated to be 316 Å<sup>3</sup>.<sup>20</sup> Additional conserved differences relating to this side pocket (COX-2 → COX-1) are R513H and V434I. The latter substitution allows Phe-518 more flexibility, which further opens up the side pocket. The presence of the side pocket in COX-2 may account for the broader range of substrates that it oxidizes (section VIII.F)

and definitely accounts for the COX-2 selectivity of the diarylheterocycles class of inhibitors.<sup>21</sup>

A structure of inhibitor-free holo murine COX-2 has been solved at 3.0-Å resolution. Contrary to expectations, this structure does not appear significantly different from those of COX-2- or COX-1-inhibitor complexes (rms deviation = 0.4 Å for C<sub>α</sub>'s of liganded and unliganded enzymes).<sup>21</sup> However, although Arg-120 remains H-bonded to Glu-524 in the unliganded enzyme, the D helix is more disordered than observed in the inhibitor complexes, as is evident from poorer resolution and higher *B* factors. This implies that movements of helix D may play a role in opening the channel between the lobby and the active site. Indeed, a complex of a selective inhibitor (a zomepirac-pyridazine) bound to COX-2 reveals a dramatic inhibitor-induced movement of Arg-120 of helix D away from its normal H-bond to Glu-524, to form H-bonds with the backbone carbonyl oxygens of Glu-524 and Phe-470 (Figure 47).<sup>20</sup> This movement interrupts helix D at this position. The carboxylate of Glu-524 moves into the side pocket to H-bond to Arg-513. The constriction normally comprised of Arg-120, Tyr-355, and Glu-524 is completely disrupted. Although this open conformation has been seen only in an inhibitor complex, it may serve as a model for the dynamic changes that result in opening and closing of the constriction between the lobby and the cyclooxygenase active site.



**Figure 47.** Effect of a binding a COX-2 inhibitor that breaches the Arg-120/Tyr-355/Glu-524 constriction on the structure of helix D. Comparison of the membrane-binding domains of COX-2 bound by two compounds, one of which breaches the constriction. The yellow helices display the interruption of helix D induced by the inhibitor as it forces Arg-120 away from its normal position at the constriction site. Reproduced with permission from ref 20. Copyright 1996 Nature Publishing Group (<http://www.nature.com>).

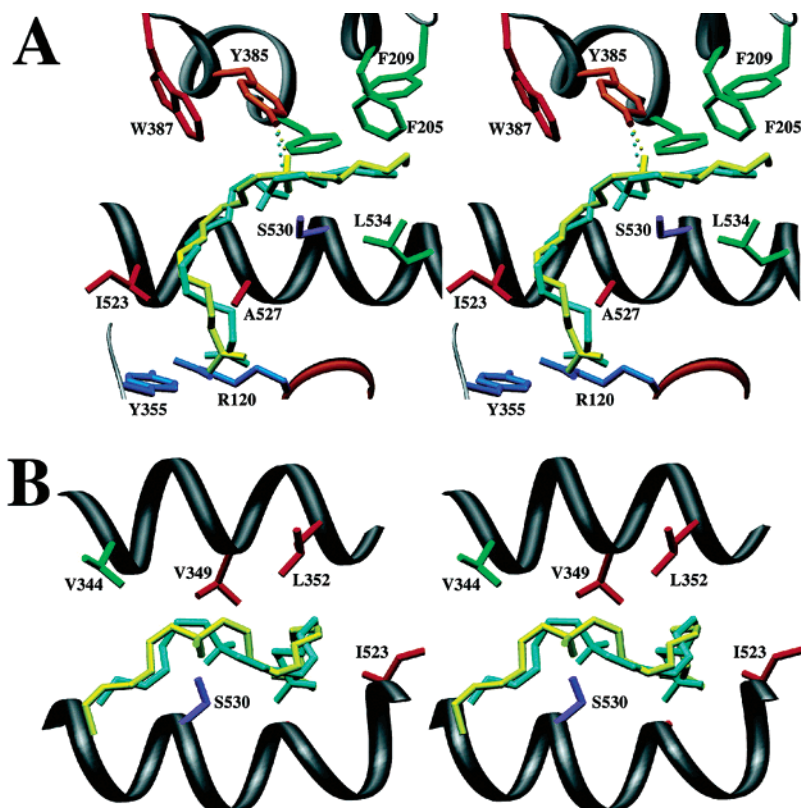


**Figure 48.** Overlay of bound fatty acids in the cocystal structures of 20:4 (light blue) and 20:3 (red) bound to COX-1. The view is parallel to the axes of helices 6 and 17. Reproduced with permission from ref 186. Copyright 2001 American Society for Biochemistry and Molecular Biology.

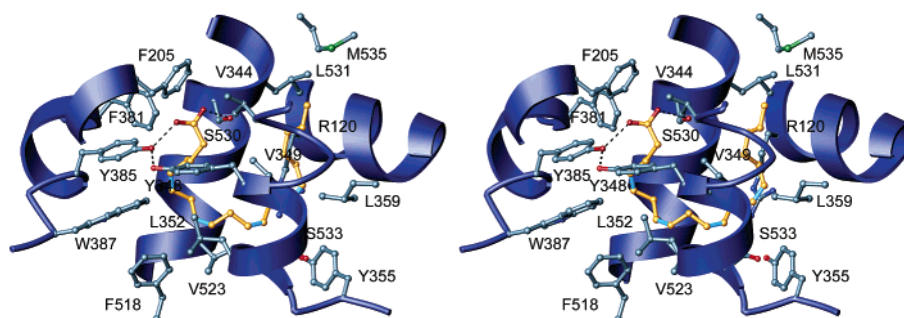
### E. Structure of COX Complexes with Substrate

Figure 48 displays an overlay of the structures of 20:4 and 20:3 bound to the  $\text{Co}^{3+}$ -PPIX derivative of ovine COX-1, determined by Thuresson et al.<sup>186</sup> The alkyl chains are virtually superimposable from carbons 11–20 but diverge from carbons 2–10 in order to accommodate the more flexible chain of 20:3. Both fatty acids make extensive contacts with active-site residues. Nineteen active-site residues make a total of 48 contacts with 20:4 in the  $\text{Co}^{3+}$ -COX-1 complex, whereas 19 residues make 62 contacts with 20:3. Most of the contacts are within van der Waals distances (3.5–4.0 Å), but a few are shorter and result from H-bonding or ionic interactions. Figure 49 displays the corresponding structures for 20:4 and 20:5.<sup>187</sup> Superposition of the structures indicates that the alkyl chains follow a very similar course through the active site. In contrast, the double bond at position 17 of 20:5 distorts the conformation of the  $\omega$ -end of the fatty acid in the alcove, which drives the abstractable hydrogen at carbon 13 away from the catalytically crucial Tyr-385. This accounts for its low activity as a COX substrate.

Determination of the structure at 2.4 Å of 20:4 bound to the apo form (heme-free) of the mouse COX-2 mutant, H207A, reveals the fatty acid bound in an upside-down orientation with the carboxyl group chelated to Tyr-385 and Ser-530 (Figure 50).<sup>188</sup> H207A is a peroxidase-deficient mutant that does not activate efficiently and has greatly reduced cyclooxygenase activity.<sup>189</sup> It was used to minimize oxygenation of 20:4 during crystallization. In the structure, 20:4 projects downward toward the Arg-120/Tyr-355/Glu-524 constriction but does not breach it. Rather, it turns and bends sharply upward so that its  $\omega$ -methyl group is positioned next to Leu-531. Leu-531 rotates away from the cyclooxygenase active site to accommodate the methyl group. Kiefer et al. speculated that conserved differences between COX-2 and COX-1 in the adjacent D helix at residues 115–125 permit COX-2 to form this unusual complex. The structure clearly represents a nonproductive 20:4-COX-2 complex because the 13-*pro*-(S)-hydrogen is located 10.5 Å from Tyr-385, which is itself coordinated to the 20:4 carboxyl group. A similar “upside-down” fatty acid conformation was reported in the structure of a complex of 20:5 with



**Figure 49.** Overlay of bound fatty acids in the cocrystal structures of 20:4 (yellow) and 20:5 (light blue) bound to COX-1. View A is perpendicular to the axes of helix17, which is shown behind the fatty acids. View B is from above helices 6 and 17. Reproduced with permission from ref 187. Copyright 2001 American Society for Biochemistry and Molecular Biology.



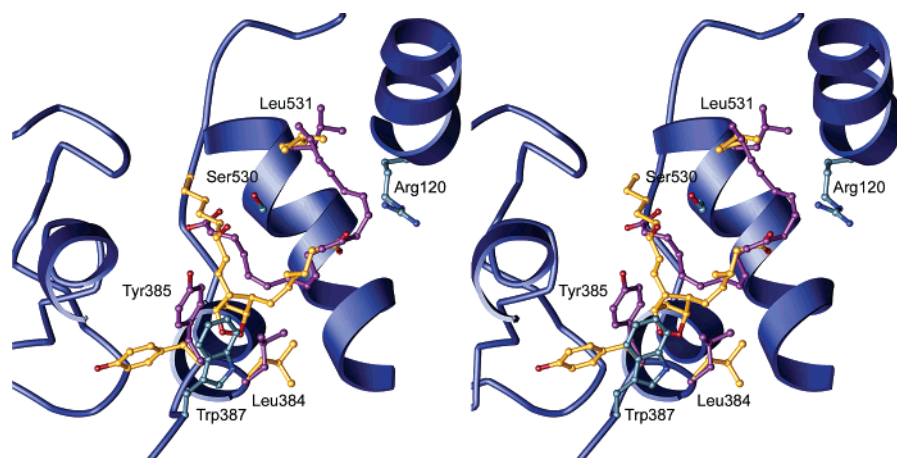
**Figure 50.** Stereoview of 20:4 bound in a nonproductive conformation to the apo form of the H207A mutant of COX-2. The 20:4 molecule is colored yellow, and its carboxyl is bound to Tyr-385 and Ser-530. Figure kindly provided by J. Kiefer.

the  $\text{Co}^{3+}$  derivative of wild-type mouse COX-2.<sup>188</sup>

In the same report, a second structure was described that was determined from a complex of wild-type apo murine COX-2 with 20:4. Electron density was observed that was consistent with the inverted 20:4 orientation superimposed on electron density from  $\text{PGG}_2$  or  $\text{PGH}_2$  bound in the "correct" orientation (Figure 51). [The presence of  $\text{PGG}_2$  or  $\text{PGH}_2$  in crystals of apoCOX-2 seems curious. Most apoCOX-1 or apoCOX-2 preparations contain small amounts of residual heme (1–5%). This gives rise to a small percentage of active enzyme in the crystallization mixture. The half-life of the endoperoxide ring of  $\text{PGG}_2$  or  $\text{PGH}_2$  in buffer at 4 °C is ~45 min to spontaneous decomposition to  $\text{PGE}_2$  and  $\text{PGD}_2$ . However,  $\text{PGG}_2$  or  $\text{PGH}_2$  bound in the hydrophobic active site of COX-2 would be anticipated to have substantially longer half-lives.] The carboxyl group of  $\text{PGG}_2/\text{PGH}_2$  was complexed with Arg-120 and Tyr-355, and the carbon chain projected upward past Tyr-385 and

Ser-530 and into the hydrophobic alcove. The  $\omega$ -methyl group sits adjacent to Gly-533. The endoperoxide ring is positioned near the hydrophobic residues, Phe-381, Leu-384, Tyr-385, and Trp-387. Leu-384 and Tyr-385 are rotated away from their normal positions to allow the close approach of the endoperoxide ring. These rotations may be facilitated by the absence of heme in the complex. Modeling indicates that movement of the  $\text{PGG}_2/\text{PGH}_2$  molecule by 1.5 Å to enable its carboxyl to coordinate with Arg-120 would allow Tyr-385 to adopt its normal conformation.<sup>188</sup>

The structures of 20:3 and other fatty acids bound to  $\text{Co}^{3+}$ -ovine COX-1 and  $\text{PGH}_2$  bound to apo murine COX-2 are consistent with expectations for the orientation that the substrate should adopt in the active site to allow oxidation and cyclization to occur with the formation of a trans-dialkyl-substituted endoperoxide ring. The fatty acid substrate is bound in an extended kinked (L-shaped) conformation that



**Figure 51.** Composite of 20:4 and PGG<sub>2</sub> bound in the active site of apo COX-2. The proposed structures of 20:4 (lavender) in an inverted configuration (see Figure 50) and PGG<sub>2</sub> (yellow) in a “normal” orientation (with its carboxyl coordinated to Arg-120) are shown. Figure kindly provided by J. Kiefer.

perfectly complements the protein cavity in the cyclooxygenase active site. In addition, the 13-*pro*-(*S*)-hydrogen is positioned adjacent to the tyrosyl radical oxidizing agent generated following peroxidatic activation. The position of the endoperoxide ring in the PGH<sub>2</sub> structure hints that protein residues actively participate in facilitating cyclization.

## F. Identification of Critical Residues

Extensive site-directed mutagenesis experiments have been performed to evaluate the importance of individual residues in COX–fatty acid interactions. The availability of structures of enzyme–substrate complexes provides a framework for the interpretation of the experimental results. Multiple parameters have been determined in these mutagenesis studies, including  $V_{\max}$  or  $k_{\text{cat}}$  as measures of catalytic activity,  $K_m$  as an approximation for substrate affinity, the regiochemistry of substrate oxygenation [PGH<sub>2</sub>, 11-hydroxy-5,8,12,14-eicosatetraenoic acid (11-HETE), and 15-hydroxy-5,8,11,13-eicosatetraenoic acid (15-HETE)], and the stereochemistry of oxygenation of carbon 15 [15-(*R*)- or 15-(*S*)-HETE]. On the basis of such experiments, Thureson et al. have grouped the active-site residues that contact 20:4 into several classes: (1) residues important for high-affinity 20:4 binding (Arg-120); (2) residues involved in positioning carbon 13 for optimal removal of the 13-*pro*-(*S*)-hydrogen (Tyr-348 and Gly-533); (3) residues directly involved in catalysis (Tyr-385); (4) residues that optimize the conformation leading to PGG<sub>2</sub> (Val-349, Trp-387, and Leu-534); and (5) others.<sup>190</sup> Most site-directed mutations in the cyclooxygenase active site do not significantly alter catalytic activity in the peroxidase active site, suggesting that the effects of the substitutions are restricted to their local environment. The effects of substitutions on oxygenase activity against different fatty acid substrates are comparable, with a few notable exceptions (see below, this section and section VIII.F), and where they have been measured, comparable substitutions made in COX-1 and COX-2 yield similar results (again with a few notable exceptions, see section VIII.E).

Arg-120 provides the sole ionic interaction in the active-site channel, and, as anticipated, mutation of

this residue to Gln or Glu increased the  $K_m$  for 20:4 by ~1000- and ~100-fold, respectively, in COX-1.<sup>191,192</sup> Interestingly, the same mutations in COX-2 had much less significant effects on the  $K_m$  for 20:4, which suggests that ionic interactions are less important for substrate binding in COX-2.<sup>25,26</sup> It is also consistent with the fact that COX-2 can utilize neutral derivatives of 20:4 as substrates (section VIII.F).<sup>28,193</sup> Substitution of Ala, Leu, or Phe for another constriction-site residue, Tyr-355, reduced oxygenase activity 5–10-fold and increased the  $K_m$  2–4-fold, but the magnitude of these changes was much lower than those observed on mutation of Arg-120 in COX-1.<sup>191</sup>

The phenolic hydroxyl of Tyr-385 is located 2.7 Å from carbon 13 of 20:4, consistent with a role for its tyrosyl radical in 20:4 oxygenation. As expected, mutation of Tyr-385 to Phe in COX-1 and COX-2 completely abolished oxygenase activity against all substrates.<sup>185,194</sup> Other active-site residues are involved in the positioning of carbon 13 adjacent to Tyr-385, and mutation of these residues to smaller or larger amino acids dramatically reduces oxygenase activity without changing the products of oxygenation (mainly, PGE<sub>2</sub>, the spontaneous isomerization product of PGH<sub>2</sub>). The two most important residues in this regard appear to be Tyr-348 and Gly-533. Tyr-348 sits across the channel from Tyr-385 and appears to be H-bonded to the latter. This H-bond does not appear to be important to catalytic activity since mutation of Tyr-348- to Phe reduces oxygenase activity by only 50%.<sup>190</sup> However, decreasing or increasing steric bulk at this position (Y348L or Y348W) completely eliminates catalytic activity. Inspection of the crystal structures of protein–substrate complexes suggests that Tyr-348 should restrict fatty acid flexibility in the vicinity of carbon 13 to hold it close to Tyr-385.

Gly-533 is located at the end of the hydrophobic alcove 3.6 Å from the  $\omega$ -carbon of 20:4. Mutation of this residue in COX-1 to Ala completely abolishes oxygenase activity, presumably by a steric clash with carbon 20 of 20:4 that pushes the fatty acid out of register with Tyr-385.<sup>190</sup> Strong support for this hypothesis was provided by analysis of the G533A,

G533V, or G553 L mutants of COX-2.<sup>185</sup> Oxygenase activity was reduced by 85% in the Ala mutant and was absent in the Val and Leu mutants. However, when these mutants were assayed against fatty acids with fewer carbons at the  $\omega$ -end, they exhibited considerable activity. For example, the G533V mutant exhibited wild-type activity against  $\alpha$ -18:3 and 18:4. Interestingly, mutations of other hydrophobic alcove residues in COX-1 (Phe-205, Phe-209, Leu-534) had relatively modest effects on oxygenase activity and product formation, with the exception of a F381A mutation, which reduced oxygenase activity by 96% without changing the  $K_m$  for 20:4 or the products of oxygenation.<sup>186</sup>

COX proteins play an active role in promoting cyclization of the putative carbon 11 peroxy radical to form the endoperoxide. Mutations of Val-349 and Trp-387 in either COX-1 or COX-2 altered the products of oxygenation by decreasing the formation of the bicyclic peroxide, PGG<sub>2</sub>, while increasing the formation of the hydroperoxide (or derived alcohol), 11-hydroperoxy-5,8,12,14-eicosatetraenoic acid (11-HPETE).<sup>188,190</sup> Val-349 is located just above the constriction site and makes close contacts with carbons 3 and 4 of 20:4, which may restrict movement of the carboxyl end of the fatty acid and optimize the conformation for cyclization.<sup>34</sup> Mutation of Val-349 to Ala reduced oxygenase activity toward 20:4 by only ~50% but drastically reduced it toward 20:3 (by a factor of 800).<sup>186</sup> This suggests that the conformation of 20:3 in the carboxyl terminal region is altered compared to 20:4 and that this alteration must play a role in positioning carbon 13 in this fatty acid adjacent to Tyr-385. Trp-387 sits over carbon 11 of the bound fatty acid immediately adjacent to Tyr-385. This positioning should limit the conformational flexibility of the 11-peroxy radical, thereby maximizing the rate of cyclization. As expected, mutation of this residue to Phe or Tyr in either COX-1 or COX-2 reduces the yield of PGG<sub>2</sub> relative to 11-HPETE.<sup>188,190</sup>

Although COX proteins possess side chains that facilitate cyclization of the 11-peroxy radical, it is not clear if the subsequent cyclization of the carbon 8 radical to carbon 12 is enhanced by the protein. Comparison of the structures of fatty acids bound to COX-1 with the structure of PGG<sub>2</sub>/PGH<sub>2</sub> bound to COX-2 suggests that considerable movement of the carbon 8 radical and/or the 12,13-double bond must occur to enable the cyclization to carbon 12 to complete the construction of the endoperoxide ring.<sup>188</sup> This is likely to involve a downward movement of the  $\omega$ -end of the fatty acid out of the hydrophobic alcove. The role of the protein in this step is uncertain. However, it is notable that single-turnover EPR studies of the carbon-centered arachidonyl radical generated at the COX-2 active site indicate that the conformation of this radical places carbon 8 in close proximity to carbon 12.<sup>164</sup>

The stereochemistry of O<sub>2</sub> coupling to the radical intermediates formed at carbons 11 and 15 may be controlled by fatty acid–protein interactions. Inspection of the structures of bound substrate indicates that the top face of the carbon 11–carbon 12 double bond is covered by protein residues, which may limit

attack by O<sub>2</sub> to the opposite face to form the (*R*) peroxy radical. Thus, only 11-(*R*) products are formed (PGG<sub>2</sub>, 11-HPETE) in COX-1, COX-2, and all of the mutants described to date. In contrast, the region around carbon 15 appears more open and flexible; in fact, both 15-(*S*)- and 15-(*R*)-HETE products are detected in oxygenations with wild-type COX-1 and COX-2, although the stereochemistry of PGE<sub>2</sub> formed by wild-type COX-1 and COX-2 is predominantly 15-(*S*).<sup>195–197</sup> A number of studies have explored the role of various residues in determining the stereochemistry at carbon 15. Aspirin acetylation of Ser-530 of COX-1 completely abolished 20:4 oxygenation, but acetylation of COX-2 shifted the product profile to exclusively 15-HPETE and 15-HETE, most of which were the (*R*) stereoisomer.<sup>198,199</sup> Mutation of Ser-530 of ovine COX-1 to Thr reduced the overall enzyme activity and shifted the stereochemistry of 15-HPETE formed to primarily 15-(*R*), whereas the same mutation in human COX-1 abolished all oxygenase activity.<sup>190,196,197</sup> The S530T mutation in human COX-2 converted the stereochemistry of 15-HPETE formation from 86% 15-(*S*) to 87% 15-(*R*) and also completely changed the stereochemistry of PGG<sub>2</sub> formation from 15-(*S*) to 15-(*R*).<sup>196,197</sup> Mutation of Ser-530 of human or mouse COX-2 to Met or Val reversed the stereochemistry of PGG<sub>2</sub> to 15-(*R*) along with the stereochemistry of 15-HPETE formation (mainly (*R*)). The differential effects of aspirin on COX-1 versus COX-2 will be discussed in greater detail in section VIII.A.

A more subtle effect was observed with mutations at Val-349. Mutations of this residue in COX-1 or COX-2 to Ala, Leu, Asn, or Thr did not significantly alter the 15-(*S*) stereochemistry of PGG<sub>2</sub> or 15-HPETE formation.<sup>190,196,197</sup> In contrast, the V349I mutants of COX-1 and COX-2 formed PGG<sub>2</sub> and 15-HPETE with mainly 15-(*R*) stereochemistry.<sup>196,197</sup> The singular effect of the V349I mutation is instructive with respect to the ability of a recently cloned COX enzyme from the coral *Plexaura homomalla* to produce PG's with >95% 15-(*R*) stereochemistry.<sup>200</sup> This enzyme contains Ser at position 530 but Ile at the position corresponding to Val-349.

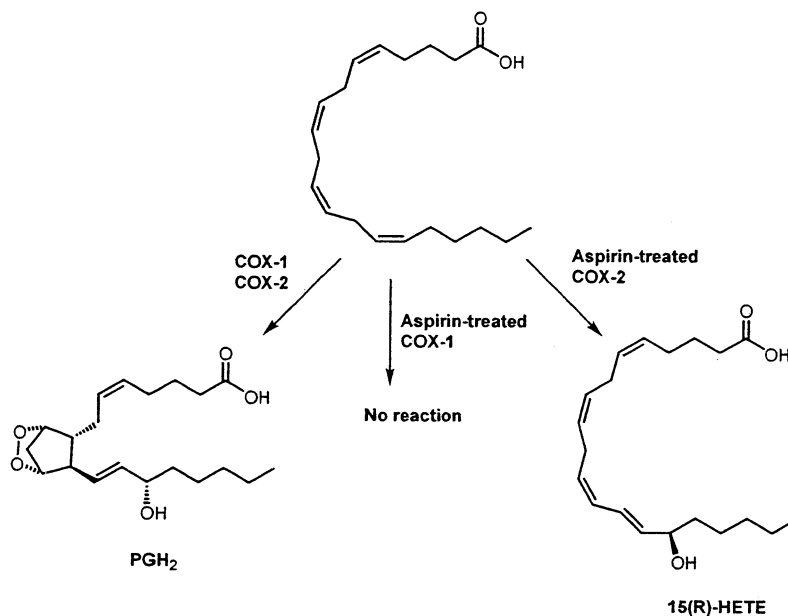
## VIII. Differences between COX-2 and COX-1

### A. Effects of Aspirin

As noted above, most studies of the kinetic mechanism of COX were carried out with the COX-1 isoform. In general, the mechanism of the COX-2 reaction is believed to be essentially the same as that of COX-1. However, some interesting differences have been noted that have shed additional light on the mechanisms of both enzymes. In the following discussion, we will focus on studies that have highlighted structural and functional differences between the two isoforms.

Early evidence that there were differences between COX-1 and COX-2 came from the discovery that the cyclooxygenase activity in ovine tracheal endothelial cells responded differently to aspirin treatment when compared to the cyclooxygenase activity in ovine seminal vesicle microsomes.<sup>198</sup> Incubation of the





**Figure 52.** Both COX-1 and COX-2 produce PGH<sub>2</sub> as the major product of the cyclooxygenase and peroxidase activities. Aspirin treatment eliminates all cyclooxygenase activity of COX-1. In contrast, COX-2 produces 15-(*R*)-HETE.<sup>198,199,201,203</sup>

seminal vesicle enzyme with aspirin resulted in complete inhibition of cyclooxygenase activity, with retention of peroxidase activity. In contrast, treatment of the COX of cultured ovine tracheal endothelial cells resulted in decreased formation of PG's, but with a compensatory increase in the formation of 15-HETE (Figure 52). Evidence that the 15-HETE was formed by an isoform of COX came from the finding that the enzyme activity was inhibited by indomethacin and immunoprecipitated by a polyclonal antiserum against the seminal vesicle enzyme. Evidence that the COX in the endothelial cells was distinct from seminal vesicle COX came from the finding that monoclonal antibodies raised against the seminal vesicle enzyme did not immunoprecipitate the activity in the tracheal endothelial cells.<sup>198</sup>

The difference in response to aspirin treatment between the two isoforms was later verified using enzymes transiently expressed in COS-1 cells. Thus, the cyclooxygenase activity of COX-1 was completely inhibited, whereas aspirin-treated COX-2 converted 20:4 to 15-HETE.<sup>201</sup> Further studies using the COX-2 protein expressed in COS-1 cells indicated that the 15-HETE produced after aspirin treatment was 15-(*R*)-HETE.<sup>199</sup> This indicated that the hydroxyl group was of the opposite configuration from that at the carbon 15 position of PG's.<sup>202</sup> Similar findings were reported by O'Neill et al., who studied COX-1 and COX-2 stably expressed in COS-7 cells using the vaccinia virus expression system.<sup>203</sup>

As in the case of COX-1, aspirin was shown to acetylate the COX-2 protein.<sup>199,204</sup> Mutation of Ser-530 to alanine eliminated aspirin's effects on the cyclooxygenase activity of COX-2 and prevented the acetylation of the enzyme.<sup>199</sup> Peptide analysis confirmed that the acetylated residue in native COX-2 was Ser-530.<sup>204</sup> Since Ser-530 in COX-2 is homologous to the residue that is acetylated by aspirin in COX-1, aspirin appeared to inhibit both isoforms by the same mechanism. Mutation of Ser-530 of COX-2 to methionine resulted in an enzyme that behaved

very much like aspirin-treated COX-2, producing 15-(*R*)-HETE rather than PGH<sub>2</sub>.<sup>199,205</sup> The additional finding that mutation of Ser-530 in COX-1 to asparagine eliminated catalytic activity, whereas the same mutation of Ser-530 in COX-2 resulted in retention of catalytic activity, led to the conclusion that the active site of COX-2 was larger than that of COX-1.<sup>199</sup> This result was also consistent with the formation of 15-HETE rather than PGH<sub>2</sub> by aspirin-treated COX-2. The larger active site in COX-2 allows 20:4 to bind after aspirin treatment, but the presence of the acetyl group alters the conformation of the 20:4 so that the product of oxygenation is 15-HPETE rather than PGG<sub>2</sub>.

As discussed in section VII.D, the X-ray crystal structure of COX-2 demonstrates the presence of a "side pocket" region in the active site, which is not present in COX-1. This side pocket is near the base of the cyclooxygenase active site, below and across the channel from Ser-530. Rowlinson et al. explored the possibility that the side pocket region provides the critical space necessary to allow the binding of 20:4 in aspirin-treated COX-2 so that 15-HETE formation can occur.<sup>206</sup> These investigators generated a murine COX-2 enzyme bearing site-directed mutations at Val-434, Arg-513, and Val-523, converting them to the corresponding residues in COX-1 and eliminating the side pocket. The mutant enzyme possessed cyclooxygenase and peroxidase activities comparable to those of the wild-type enzyme. However, aspirin treatment eliminated the cyclooxygenase activity, and no 15-HETE synthesis was detected. Thus, removal of the side pocket resulted in behavior resembling that of COX-1 with regard to aspirin sensitivity. Interestingly, site-directed mutation of each of the three residues individually reduced but did not completely eliminate 15-HETE synthesis after aspirin treatment. The greatest reduction was seen with mutation of the Val-523 residue, which represents the gatekeeper of the side pocket.

Rowlinson et al. also explored the possibility that synthesis of 15-HETE in aspirin-treated COX-2 resulted from the binding of 20:4 in an altered conformation.<sup>206</sup> Normally, carbons 17–20 bind in the hydrophobic alcove at the top of the active site (section VII.C). It was conceivable that acetylation of Ser-530 resulted in a binding configuration in which these carbons were displaced from the hydrophobic alcove. To test this hypothesis, Rowlinson et al. created a murine COX-2 enzyme bearing a site-directed mutation at Val-228, converting it to Phe. This residue occupies the position at the opening of the alcove, so placing the bulky phenylalanine group there would prevent binding of the tail of 20:4 in this region. This mutant retained cyclooxygenase activity at 20% of the initial rate and 69% of total product formation observed with wild-type enzyme, in the absence of aspirin treatment. However, the aspirin-treated mutant was incapable of forming 15-HETE. The investigators concluded that the altered conformation of binding of 20:4 that leads to 15-HETE formation in aspirin-treated COX-2 still requires access to the hydrophobic alcove by the  $\omega$ -end of the molecule.

The (*R*) configuration of 15-HETE produced by aspirin-treated COX-2 was confirmed by Xiao et al., who also reported that the small amount of 15-HETE formed by native enzyme was in the 15-(*R*) configuration.<sup>158</sup> These authors noted that the 15-(*R*) configuration was inconsistent with abstraction of the 13-*pro*-(*S*) hydrogen of 20:4 followed by the expected antarafacial oxygen addition. To explain this apparent discrepancy, Xiao et al. proposed that formation of 15-(*R*)-HETE resulted from an aberrant binding conformation of 20:4 in the COX-2 active site, which leads to abstraction of the 13-*pro*-(*R*) hydrogen atom. The finding that 15-HETE formation occurred with a higher apparent  $K_m$  than did PGH<sub>2</sub> formation supported the concept of two alternative binding conformations.

The hypothesis proposed by Xiao et al. was tested by Schneider and Brash, who used 20:4 that had been stereospecifically labeled with tritium at either the 13-*pro*-(*R*) or 13-*pro*-(*S*) position.<sup>158,207</sup> They demonstrated that the 15-(*R*)-HETE that was synthesized by aspirin-treated COX-2 had selectively lost the tritium label from the 13-*pro*-(*S*) position, not the 13-*pro*-(*R*) position. Thus, they concluded that acetylation by aspirin had no effect on the stereochemistry of hydrogen abstraction by the enzyme. Instead, Schneider and Brash proposed that the presence of the acetyl group in the active site of COX-2 caused an alteration in the 20:4 binding conformation so that the normal approach of oxygen resulted in addition to C-15 on the opposite side from that seen with the normal orientation of the substrate.

Studying the tyrosyl radical signals produced by recombinant COX-2 in its reaction with EtOOH, Xiao et al. discovered that treatment with aspirin under conditions that led to retention of the ability of the enzyme to synthesize 15-HETE resulted in no change in the wide singlet radical signal generated by the enzyme.<sup>158</sup> These results were confirmed by Tsai et al., who also studied the ability of this tyrosyl radical

to oxidize 20:4.<sup>208</sup> Under anaerobic conditions, Tsai et al. added EtOOH and then octadeuterated 20:4 to aspirin-treated COX-2. They obtained a seven-line EPR spectrum that strongly resembled that of the pentadienyl 20:4 radical generated under the same conditions with native enzyme. However, when 20:4 with no deuterium substitution was used as the substrate, two radical signals were observed. One was characteristic of the pentadienyl radical, but the other, a 26–28-G singlet, was attributed to a strained allyl radical on the basis of computer simulations. Two possible allyl radical conformations were proposed, one of which would be expected to produce 11-HETE and the other 15-HETE upon reaction with oxygen. Interestingly, there was no difference in the kinetic parameters ( $K_m$  and  $V_{max}$ ) between 20:4 and octadeuterated 20:4 that could help to explain the difference in radical signals. It was noted that the octadeuterated substrate is more hydrophilic, as determined by retention time on reverse-phase chromatography. This finding led the authors to suggest that octadeuterated 20:4 would not interact as strongly as 20:4 with hydrophobic residues in the acetylated COX-2 active site. Consequently, interactions leading to the strained allyl radical conformation of the substrate would not occur for the octadeuterated compound. The results of these studies suggest that the synthesis of 15-HETE by aspirin-treated COX-2 is due to the same basic mechanism that results in the formation of PGH<sub>2</sub> in the native enzyme. They also provide evidence for an altered binding conformation in the aspirin-treated enzyme that may be responsible for the formation of 15-HETE in lieu of PGH<sub>2</sub>.

## B. Hydroperoxide Initiator Requirement

Although kinetic and spectroscopic studies had indicated that the mechanism of the cyclooxygenase reaction in COX-2 was basically the same as that in COX-1, Kulmacz and Wang found some interesting differences between the two isoforms regarding their hydroperoxide initiator requirements.<sup>209</sup> These investigators used GSH and GSH peroxidase to study the effects of peroxide scavengers on the activity of purified human and ovine COX-2 as compared to ovine COX-1. They showed that the concentration of peroxide needed to activate and sustain cyclooxygenase activity was approximately 1 order of magnitude lower (2 nM) for COX-2 than for COX-1 (20 nM). Furthermore, by combining the two isoforms in the presence of GSH and GSH peroxidase, Kulmacz and Wang demonstrated that hydroperoxides generated by COX-2 could not efficiently activate COX-1. These results demonstrated that the two isoforms were similar in their requirement for hydroperoxide activation but that they differed significantly in their affinity for the hydroperoxide, a conclusion that was suggested earlier by Capdevila et al.<sup>210</sup> Thus, COX-2 is able to be catalytically active in an environment in which much lower concentrations of hydroperoxide are available, a finding that may have physiological significance.

A kinetic basis for the difference in sensitivity to hydroperoxide activator has been proposed by Lu et

al., who compared the rates of the formation of compound I and intermediate I during the reaction of purified ovine COX-1 and recombinant human COX-2 with various hydroperoxides.<sup>211</sup> They monitored the absorbance of the resting enzyme (410 nm for COX-1 and 408 nm for COX-2) to observe the formation of compound I and the absorbance at 424 nm (the isosbestic point between resting enzyme and compound I) to observe the formation of intermediate I. The results showed that the rate of formation of compound I was nearly identical for the two isoforms ( $k_1 = 2.3 \times 10^7 \text{ M}^{-1} \text{ s}^{-1}$  for COX-1 and  $2.5 \times 10^7 \text{ M}^{-1} \text{ s}^{-1}$  for COX-2 using 15-HPETE). However, the rate of formation of intermediate I was much higher for COX-2 than for COX-1. Thus, for COX-1, the formation of intermediate I was rate-limiting at high hydroperoxide concentrations, and a first-order rate constant of  $10^2$ – $10^3 \text{ s}^{-1}$  was estimated. For COX-2, the formation of intermediate I was faster than the formation of compound I at all hydroperoxide concentrations, so the first-order rate constant for the process could not be measured. Lu et al. postulated that the very rapid formation of intermediate I in COX-2 could explain the much greater sensitivity to hydroperoxide activation of COX-2 as compared to COX-1. Mathematical modeling using numerical integration based on the branched-chain mechanism supported this hypothesis. The results showed that, as the rate constant for intermediate I formation increases, the concentration of hydroperoxide required for activation decreases. According to the branched-chain mechanism (Figure 34), compound I may be converted to intermediate I or reduced to compound II. Therefore, as the rate of conversion to intermediate I increases, the amount of compound I lost to reduction decreases. Thus, less hydroperoxide will be needed to generate compound I in order to obtain a given amount of intermediate I if the rate of conversion to intermediate I is high.

### C. Apparent Cooperativity

The greater sensitivity to hydroperoxide activation of COX-2 has been used to explain an observed kinetic difference between the two isoforms. Swinney et al. reported that COX-1 but not COX-2 demonstrated positive cooperativity with regard to 20:4 concentration (Hill coefficient of 1.29).<sup>212</sup> Their results suggested that the cooperativity was dependent upon a conformational change in the cyclooxygenase active site and that it could be activated by low concentrations of competitive inhibitors. The dimeric structure of COX-1 is consistent with the possible occurrence of an allosteric effect, but there was no obvious explanation why the cooperativity should be limited to the COX-1 isoform. A possible kinetic explanation for the apparent cooperativity was offered by Chen et al.<sup>22</sup> They postulated that the requirement of COX-1 for higher concentrations of peroxide activator leads to unexpectedly low levels of activity at low substrate concentrations. Thus, the apparent cooperativity of COX-1 could be eliminated by the addition of exogenous hydroperoxide activator. Furthermore, substitution of heme with  $\text{Mn}^{3+}$ -PPIX, which results in reduced peroxidase activity, resulted in

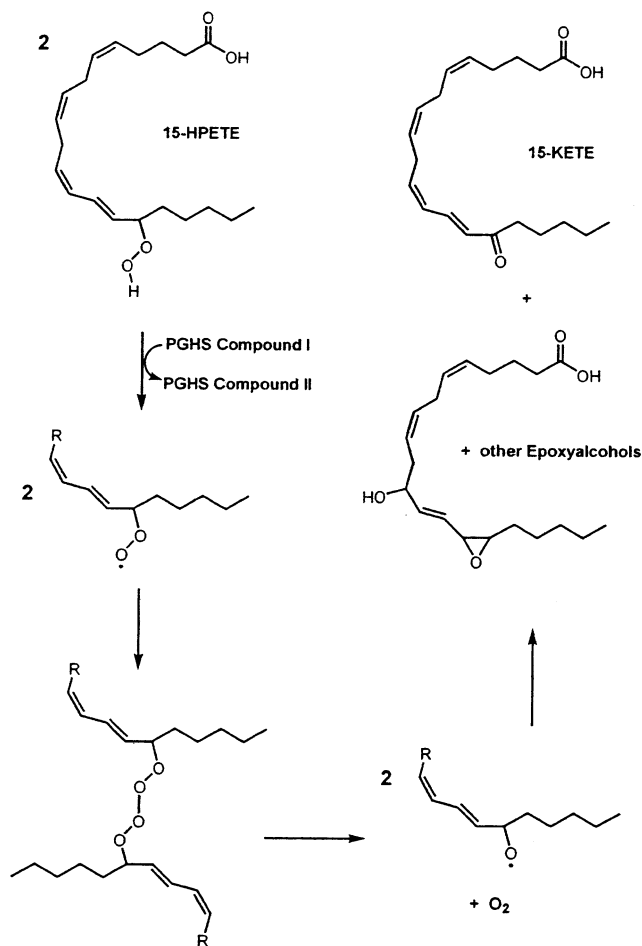
exaggerated apparent cooperativity in COX-1 and the acquisition of apparent cooperativity in COX-2. For both isoforms, addition of exogenous hydroperoxide eliminated the apparent cooperativity in the manganese-substituted enzymes. Finally, mathematical simulations using the branched-chain kinetic model predicted the difference in apparent cooperativity between the two isoforms on the basis of the measured difference in hydroperoxide activator requirement. Thus, it appears likely that the high sensitivity of COX-2 to hydroperoxide activation allows this isoform to be catalytically active at lower levels of substrate than is the case for COX-1 and that the phenomenon reported by Swinney et al. was not true allosteric cooperativity. Furthermore, these results provide additional evidence of the validity of the branched-chain mechanism for predicting COX kinetic behavior.

### D. Hydroperoxide Oxidation by Compound I

Comparative studies of the peroxidase activity of the two COX isoforms have demonstrated some interesting differences between them.<sup>189</sup> When 50  $\mu\text{M}$  15-HPETE was incubated with COX-2 in the presence of 500  $\mu\text{M}$  guaiacol as peroxidase reductant, approximately 60% of the product formed was 15-HETE, which resulted from the expected two-electron reduction of the substrate. The remaining product was 15-ketoeicosatetraenoic acid (15-KETE) and a mixture of epoxyalcohols, products that arise from alkoxy radical intermediates. Under identical conditions, wild-type COX-1 produced 97% 15-HETE. At lower 15-HPETE concentrations (2.5  $\mu\text{M}$ ), COX-2 produced 97% 15-HETE, as did COX-1. The finding that the product profile changes with hydroperoxide concentration for wild-type COX-2 suggests that 15-HPETE competes with reducing substrates for reaction with compound I. Oxidation of 15-HPETE by compound I would form a peroxyl radical. Subsequent dimerization of two peroxyl radicals with loss of oxygen would yield alkoxy radicals, decomposition of which would yield 15-KETE and epoxyalcohols (Figure 53).

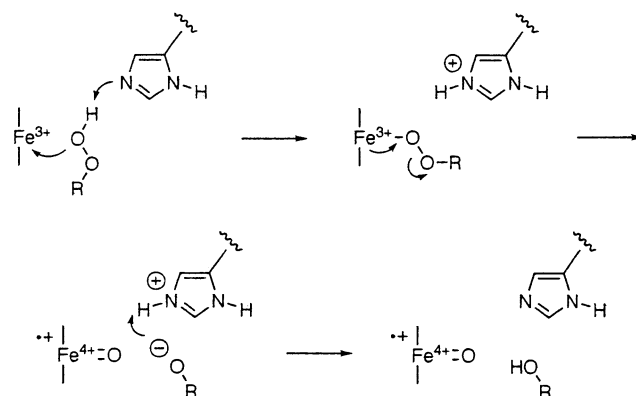
### E. Effects of His Mutations at the Heme-Binding Site

Additional differences between the COX isoforms have been uncovered by site-directed mutation of the histidines either proximal (His-388) or distal (His-207) to the heme. Mutation of either of these residues to alanine in COX-1 completely abolished both cyclooxygenase and peroxidase activities when assayed in microsomal preparations from COS-1 cells expressing the altered proteins.<sup>182</sup> However, mutation of the histidine (His-207) distal to alanine in COX-2 produced an enzyme that exhibited some residual activities.<sup>189</sup> Using the standard guaiacol peroxidase assay, the peroxidase activity of the H207A COX-2 mutant was undetectable, but the use of a highly sensitive assay based on the oxidation of 2,2'-azino-bis(3-ethylbenzthiazoline-6-sulfonic acid) (ABTS) as the reducing substrate revealed significant but low peroxidase activity in this mutant (100 nM H207A



**Figure 53.** Proposed mechanism for the formation of 15-KETE in the reaction of 15-HPETE with COX-2. One-electron reduction of two molecules of 15-HPETE by COX-2 compound I leads to the formation of two peroxy radicals. These dimerize, and then loss of oxygen leads to the formation of two alkoxy radicals. Further oxidation results in the formation of 15-KETE or epoxy alcohols.<sup>189</sup>

COX-2 reconstituted with 50 nM  $\text{Fe}^{3+}$ -PPIX oxidized 78 mol of ABTS per mole of  $\text{Fe}^{3+}$ -PPIX versus 49 mol of ABTS oxidized per mole of  $\text{Fe}^{3+}$ -PPIX for  $\text{Fe}^{3+}$ -PPIX alone, using 15-HPETE as substrate). Incubation of 50  $\mu\text{M}$  15-HPETE with the H207A COX-2 mutant in the presence of 500  $\mu\text{M}$  guaiacol demonstrated that approximately 40% of the product formed was 15-HETE, with the remainder being 15-KETE and epoxyalcohols. Lowering the 15-HPETE concentration to 2.5  $\mu\text{M}$  increased 15-HETE formation to only 61%, indicating that the altered product profiles could not be explained on the basis of competition of 15-HPETE for compound I, as was found for wild-type COX-2 (section VIII.D). This conclusion was further supported by the study of products formed from the reaction of the H207A COX-2 mutant with 10-hydroperoxyoctadeca-8,12-dienoic acid and 13-hydroperoxyoctadeca-9,11,15-trienoic acid (50 or 100  $\mu\text{M}$ ). These substrates yield characteristic products resulting from one- versus two-electron reduction of the hydroperoxide. In both cases, the majority of products formed from the reaction with H207A COX-2 were the result of one-electron reduction (61–84%). This indicates that the distal histidine residue of COX-2 plays a significant role in supporting two-



**Figure 54.** Role of distal histidine in peroxidase catalysis as a general base–acid to facilitate formation of compound I.<sup>261</sup>

electron reduction of the hydroperoxide substrate.

Despite the markedly reduced peroxidase activity of the H207A COX-2 mutant, this enzyme retained considerable cyclooxygenase activity, albeit after a lengthy lag phase.<sup>189</sup> Although the lag phase was increased by 15–20 s, and the maximum velocity of oxygen uptake was reduced to about 30% of that seen with wild-type COX-2, the total extent of oxygen uptake was the same for the mutant and wild-type enzymes. These observations are consistent with the branched-chain mechanism in that reduced peroxidase activity would be expected to result in a slower rate of peroxide activation and longer lag phases but not necessarily reduced fatty acid oxygenation. Interestingly, addition of 2-methylimidazole to reaction mixtures containing the H207A COX-2 mutant resulted in a 2-fold increase in peroxidase turnovers and an increase in the proportion of two-electron reductions from 61 to 70%. Addition of 2-methylimidazole also eliminated the lag phase and increased the rate of product formation of H207A COX-2 without affecting total oxygen uptake. These results demonstrate the importance of the distal histidine residue in COX-2 peroxidase activity and are consistent with the proposed role of the histidine as an acid–base catalyst in the peroxidase reaction (Figure 54).<sup>122</sup> They also provide evidence that compound I, not compound II, is the higher oxidation state of COX-2 that is critical for activation of the cyclooxygenase reaction, since the addition of 2-methylimidazole to the H207A mutant eliminated the cyclooxygenase lag phase while selectively increasing two-electron reductions and the generation of compound I. These findings are completely consistent with, and provide further support for, the branched-chain mechanism.

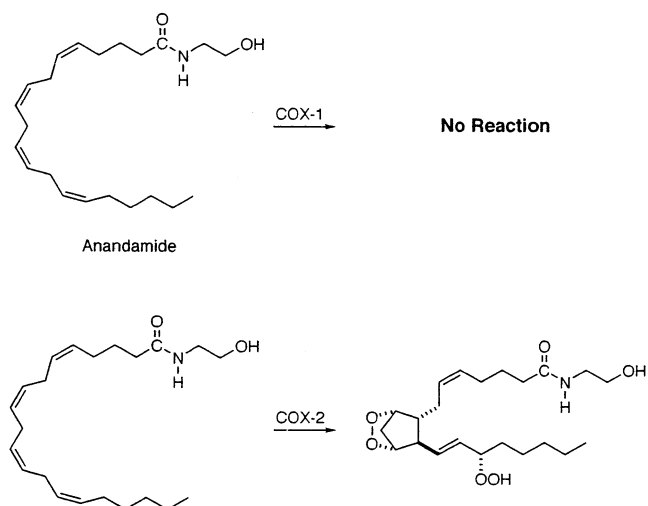
Further insight was gained concerning the link between the peroxidase and cyclooxygenase activities from studies of a COX-2 enzyme bearing a site-directed mutation at the histidine residue ligated to the heme (His-388).<sup>148</sup> Conversion of His-388 to tyrosine, a change expected to lower the reduction potential of the protein, yielded an enzyme with very low peroxidase activity but cyclooxygenase activity similar to that observed with the H207A mutant. Interestingly, the reduction in peroxidase activity was attributable to both an increase in  $K_m$  and a

decrease in apparent  $k_{\text{cat}}$  for all three hydroperoxides tested (*tert*-butyl hydroperoxide, hydrogen peroxide, and 15-HPETE). Thus, the apparent  $k_{\text{cat}}/K_{\text{m}}$  values were  $10^3$ – $10^4$ -fold higher for the wild-type enzyme than for the H388Y mutant, although the relative efficiencies of the three substrates were the same for the mutant and wild-type enzymes. When 20:4 was used as substrate, the rate of oxygen uptake by the H388Y COX-2 mutant was somewhat reduced compared to that of the wild-type, but the total oxygen consumption was the same for the two enzymes. The most striking differences between the wild-type and mutant COX-2 enzymes were the extended lag phase observed with the mutant enzyme and the fact that addition of phenol did not result in conversion of the hydroperoxy-PG products to their corresponding alcohols. The extended lag phase was abolished by addition of hydroperoxides. These results are consistent with the markedly reduced peroxidase activity of the mutant enzyme and provide further support for the importance of the heme-dependent peroxidase activity in the activation of the cyclooxygenase reaction, as predicted in the branched-chain mechanism.

## F. Substrate Specificity

Subtle to substantial differences exist in the substrate specificities of COX-1 and COX-2. 20:4 is the best fatty acid substrate for oxygenation, as judged by the  $k_{\text{cat}}$  and  $K_{\text{m}}$  for  $\text{O}_2$  uptake, and 20:3 is 30–50% as effective as 20:4.<sup>71</sup> Both fatty acids are converted to endoperoxide products. 18:2 and  $\alpha$ -18:3 are rather poor substrates for COX-1 but somewhat better substrates for COX-2. Both substrates are converted to monohydroperoxide products. The inability of either COX enzyme to oxygenate  $\alpha$ -18:3 to an endoperoxide suggests that the 12-peroxyl radical generated by oxidation at carbon 14 is not held in a conformation that enables cyclization to carbon 10 to occur. 20:5 is a poor substrate for COX-1 and COX-2, and, although it is oxygenated to endoperoxide products, it is more likely to be a competitive inhibitor of 20:4 oxygenation than a substrate for the production of bioactive eicosanoids.

As stated earlier (section VII.F), mutation of Arg-120 to Gln dramatically reduces the ability of COX-1 to oxygenate 20:4, consistent with the anticipated importance of ionic interactions in the binding of fatty acid substrates.<sup>191</sup> However, the same mutation in COX-2 is essentially without effect.<sup>26</sup> This suggests that ionic interactions between Arg-120 and fatty acid carboxylates are much less important in this protein and raises the possibility that neutral derivatives of 20:4 are selective substrates for COX-2. Indeed, Yu et al. reported in 1997 that the ethanolamide derivative of 20:4 (AEA or anandamide) is oxygenated to an endoperoxide product by COX-2 but not COX-1 (Figure 55).<sup>193</sup> The  $k_{\text{cat}}/K_{\text{m}}$  for AEA oxygenation was  $\sim 60$ -fold lower than that for 20:4 oxygenation, and the  $K_{\text{m}}$  was several orders of magnitude above the physiological concentrations of AEA. Thus, the physiological significance of this observation is uncertain. Nevertheless, this report is intriguing because AEA is one of the two endogenous ligands for the cannabinoid receptors (CB1 and



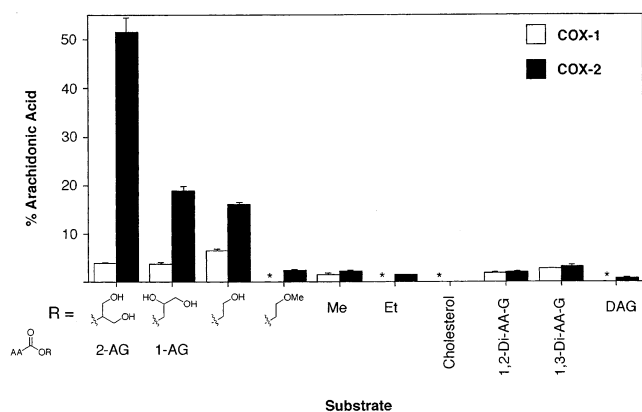
**Figure 55.** Selective oxygenation of anandamide (20:4-ethanolamide) by COX-2.

CB2).<sup>213</sup> The other endocannabinoid is the 2-glycerol ester of 20:4 (2-AG).<sup>214</sup>

Kozak et al. have demonstrated that 2-AG is also a relatively selective substrate for COX-2, but in contrast to AEA, it was found to be kinetically equivalent to 20:4.<sup>28</sup> Furthermore, the  $K_{\text{m}}$  for 2-AG oxygenation was somewhat less than the levels of 2-AG reported to be present in brain and other tissues.<sup>215</sup> This raises the possibility that COX-2-dependent oxygenation of 2-AG occurs under physiological conditions. Indeed, stimulation of LPS-induced macrophages with the calcium ionophore, ionomycin, led to the production and release of glycerol PG's.<sup>28</sup> The role of the calcium ionophore is to trigger the release of 2-AG from phospholipid stores via the intermediacy of diacylglycerol. Since many agonist-dependent signal transduction pathways lead to the release of diacylglycerol, this observation provides a potential link between these signaling pathways and COX-2-selective production of glycerol PG's.

Kozak et al. demonstrated that the products of 2-AG oxygenation by purified, recombinant COX-2 are the glycerol esters of PGG<sub>2</sub>, 11-HPETE, and 15-HPETE.<sup>28</sup> All three products were reduced by the peroxidase to form the corresponding alcohol products. The relative amounts of PGH<sub>2</sub>-G, 11-HETE-G, and 15-HETE-G produced by COX-2 were the same as those of the corresponding products from 20:4. The stereochemistry of all three glycerol esters was identical to the stereochemistry of the 20:4-derived products. PGH<sub>2</sub>-G was converted efficiently by PGH<sub>2</sub>-metabolizing enzymes to PGE<sub>2</sub>-G, PGD<sub>2</sub>-G, PGF<sub>2</sub>-G, and PGI<sub>2</sub>-G; the rates of conversion were comparable to those of PGH<sub>2</sub>.<sup>216</sup> The sole exception was conversion by thromboxane synthase, for which PGH<sub>2</sub>-G was only 3% as active as PGH<sub>2</sub> as a substrate. This suggests that a family of glycerol PG's nearly as diverse as the "primary" PG's may be produced *in vivo*.

Investigation of the susceptibility of various arachidonyl esters to be oxygenated by COX-2 indicated that 2-AG was the most efficient substrate, followed by its isomerization product, 1-AG (Figure 56).<sup>28</sup> The



**Figure 56.** Relative substrate specificity of a series of 20:4 esters for oxygenation by COX-2. Reproduced with permission from ref 28. Copyright 2000 American Society for Biochemistry and Molecular Biology.

ethylene glycol ester of 20:4 was comparable to 1-AG, but simple arachidonyl esters (e.g., methyl- or ethyl-20:4) or more complex esters (cholesteryl esters or phospholipids) were very poor substrates or nonsubstrates, as had been previously reported for COX-1.<sup>217,218</sup> This indicates that the ability of COX-2 to oxygenate arachidonyl esters is maximal with 2-AG. Recently, COX-2 has been shown to oxygenate a series of *N*-arachidonylamino acids (e.g., *N*-arachidonylglycine and *N*-arachidonyl- $\gamma$ -aminobutyric acid).<sup>219</sup> The  $k_{\text{cat}}/K_m$  for oxygenation of these substrates was approximately 10-fold lower than that for the ester, 2-AG, but comparable to that for the amide derivative, AEA. Lipoamino acids such as *N*-arachidonylglycine have been reported to occur naturally in brain tissue and to exhibit analgesic activity. [The existence of 20:4-derived lipoamino acids is the subject of some controversy.]

The structural basis for the ability of COX-2 to oxidize amide and ester derivatives of 20:4 has been explored by site-directed mutagenesis.<sup>220</sup> Amino acids in COX-2 that represent conserved differences between the two isoforms were mutated into their corresponding COX-1 residues, and the ability of the mutant enzyme to oxygenate a series of substrates was determined. These experiments indicated that Arg-513, which sits at the base of the side pocket opposite Arg-120, is the key residue that enables COX-2 to oxygenate the various arachidonyl esters and amides. A slight effect of other side pocket residues was also observed in the triple mutant, V523I/R513H/V434I, which converted all of the COX-2 side pocket residues into the corresponding COX-1 residues. This mutation in COX-2 reduced oxygenation of AEA, 2-AG, and *N*-arachidonylglycine by 80%.<sup>219</sup> A structural model has been proposed in which Arg-120 and Arg-513 simultaneously H-bond with the amide or ester derivative.<sup>220</sup>

The importance of the side pocket of COX-2 in the selective oxygenation of arachidonyl esters and amides is interesting from an evolutionary standpoint in that Arg-513 is conserved in all COX-2 genes sequenced to date, including bony fish. This suggests that the side pocket is conserved in all COX-2 proteins, which implies that there may be a functional reason for this conserved difference between the two COX isoforms.

The side pocket is the molecular target for the diarylheterocycle inhibitors, celecoxib and rofecoxib, but obviously it did not evolve to bind non-natural pharmaceutical agents.<sup>21</sup> Considering that COX-2 selectively oxygenates neutral substrates at rates approaching that of 20:4, that the endoperoxide products are excellent substrates for PGH<sub>2</sub> metabolizing enzymes, and that these transformations can be demonstrated in intact cells stimulated with agonists, it seems reasonable to propose that the side pocket evolved to confer novel substrate selectivity on COX-2. A corollary of this hypothesis is that oxygenation of neutral substrates, and especially 2-AG, represents a physiological function of COX-2.

## IX. Mechanistic Studies of COX Substituted with Manganese Protoporphyrin IX

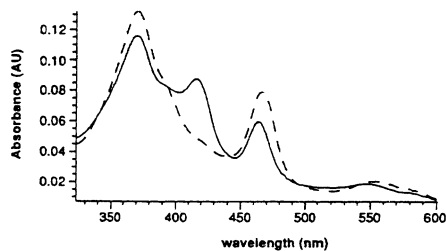
In 1978, Ogino et al. reported that reconstitution of purified COX-1 with Mn<sup>3+</sup>-PPIX resulted in an enzyme (Mn-COX-1) with cyclooxygenase activity equal to that of the native enzyme but which lacked peroxidase activity. The major product of the reaction of 20:4 with this enzyme was PGG<sub>2</sub>.<sup>33</sup> Since that time, Mn-COX-1 has proven to be a useful model system, yielding further insights into the kinetic mechanism of the cyclooxygenase reaction.

### A. Spectral Studies of Higher Oxidation States

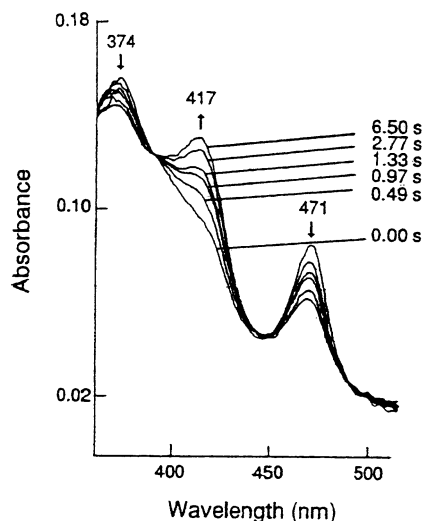
One of the most pronounced effects of Mn<sup>3+</sup>-PPIX substitution on the cyclooxygenase reaction of COX is a marked increase in the lag phase. Hemler et al. noted this phenomenon and used it to study the effects of hydroperoxides on COX-1 activation.<sup>102</sup> They concluded that hydroperoxides were required to activate the cyclooxygenase reaction of Mn-COX-1, but since the enzyme had no detectable peroxidase activity, the mechanism of enzyme activation by the hydroperoxides must be distinct from their role as peroxidase substrates.

This hypothesis made the Mn-COX-1 an interesting target for mechanistic investigations. Odenwaller et al. found that, contrary to previous reports, Mn-COX-1 possessed detectable peroxidase activity, although it was only 0.8% that of native enzyme.<sup>109</sup> Addition of PPHP to Mn-COX-1 resulted in the formation of a new visible absorbing species with a maximum at 418 nm, which was different from that of resting enzyme (Mn<sup>3+</sup>, 468 nm) or reduced enzyme (Mn<sup>2+</sup>, 434 nm). A similar spectral change was observed upon addition of 20:4, but only after a 10-s lag period (Figure 57). Addition of TMPD as peroxidase-reducing substrate resulted in a reduction of the absorbance at 418 nm and an increase in the absorbance at 610 nm, corresponding to oxidized TMPD. These results suggest that the species absorbing at 418 nm is a higher oxidation state of Mn-COX-1, which serves as a peroxidase intermediate. The finding that the formation of this species preceded oxygenation of the fatty acid substrate, 20:2, suggests that this higher oxidation state is required for the cyclooxygenase activity of the enzyme.

Similar findings were reported by Strieder et al., who demonstrated the formation of a species having



**Figure 57.** Electronic absorption spectra obtained from the combination of Mn-COX-1 (1.5  $\mu\text{M}$ ) with 20:4 (100  $\mu\text{M}$ ) in 10 mM Tris-HCl, pH 8. The spectrum of Mn-COX-1 was recorded before the addition of the arachidonic acid (dashed line) and again 95 s after 20:4 addition (solid line). Reproduced with permission from ref 109. Copyright 1992 American Society for Biochemistry and Molecular Biology.



**Figure 58.** Electronic absorption spectra obtained from the combination of Mn-COX-1 (1.5  $\mu\text{M}$ ) with PPHP (16  $\mu\text{M}$ ) in 100 mM Tris-HCl, pH 8.1. The spectra were recorded at the indicated times after addition of the PPHP. Reproduced with permission from ref 108. Copyright 1992 American Society for Biochemistry and Molecular Biology.

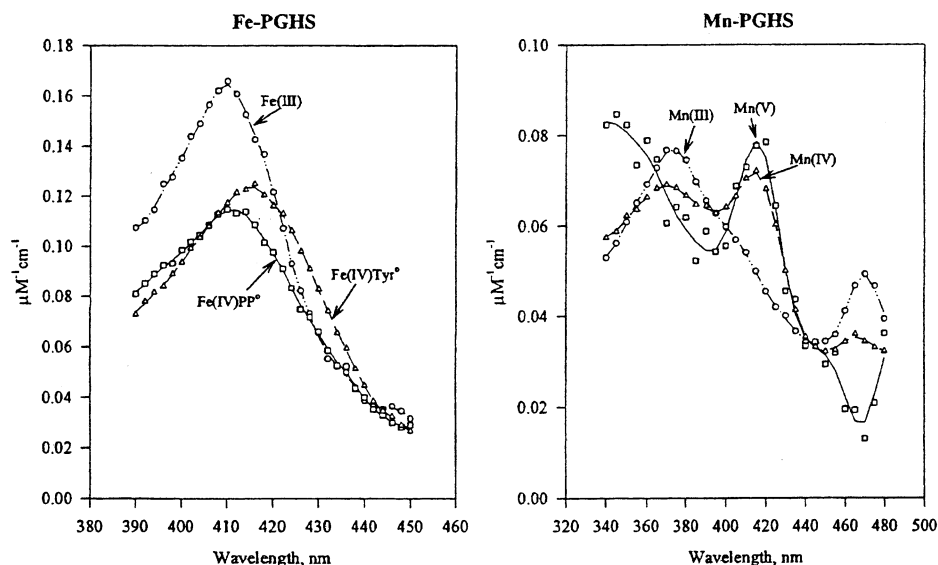
absorbance maxima at 417, 513, and 625 nm after reaction of Mn-COX-1 with hydroperoxides (Figure 58).<sup>108</sup> The 513 and 625 nm absorbances were characteristic of a  $\text{Mn}^{4+}$  complex. In the reaction with  $\text{PGG}_2$ , the rate constant for the formation of the intermediate was estimated to be  $10^4 \text{ M}^{-1} \text{ s}^{-1}$ , indicating that the reaction was 3 orders of magnitude slower than the formation of compound I in the native enzyme. A marked lag phase was noted in the reaction of Mn-COX-1 with 20:4; however, the oxygenation of the substrate clearly occurred after formation of the intermediate. Both Strieder et al. and Odenwaller et al. noted that the cyclooxygenase activity of Mn-COX-1 was much more sensitive to inhibition by GSH and GSH peroxidase than was the activity of the native enzyme, indicating that higher concentrations of hydroperoxide are required to activate and maintain cyclooxygenase activity.<sup>108,109</sup>

These findings are consistent with the hypothesis that hydroperoxide activation is required for the cyclooxygenase reaction and that the slow rate of reaction of Mn-COX-1 with hydroperoxide results in a requirement for higher peroxide concentrations to achieve that activation (previously discussed with regard to COX-2 in section VIII.B). Thus, it appears

that the mechanism of activation of Mn-COX-1 is similar to that of native enzyme and consistent with the branched-chain hypothesis. These conclusions led Strieder et al. to propose a mechanism for the Mn-COX-1 enzyme that is essentially identical to the branched-chain mechanism. The peroxidase cycle begins with a two-electron reduction of the peroxide, yielding a  $\text{Mn}^{5+}$  intermediate. Two subsequent one-electron reductions of the enzyme yield a  $\text{Mn}^{4+}$  species and native enzyme, respectively. Strieder et al. suggested that an intramolecular one-electron transfer from the protein to the porphyrin of the  $\text{Mn}^{5+}$  intermediate would yield a species similar to intermediate I of the native enzyme and that this species would then carry out the cyclooxygenase reaction. They proposed that the relative rates of formation of the various intermediates prevent accumulation of the  $\text{Mn}^{5+}$  species under typical experimental conditions.<sup>108</sup>

More detailed kinetic studies of the rate of formation of the higher oxidation states of Mn-COX-1 were carried out by Tsai et al.<sup>123</sup> They discovered that the apparent rate constant for the formation of the higher oxidation state of Mn-COX-1 increases with increasing peroxide concentration but that the increase is saturable. This observation led Tsai et al. to conclude that another intermediate is being formed prior to the species with an absorbance maximum at 418 nm. They performed stopped-flow kinetic measurements at multiple wavelengths and then applied singular value decomposition to resolve the spectra of the proposed intermediates. This method was verified by a similar analysis of native COX-1, which yielded spectra strongly resembling the known spectra of compound I and intermediate I. For Mn-COX-1, spectra for two intermediates were resolved (Figure 59). One spectrum was very similar to the spectra previously reported by Odenwaller et al. and Strieder et al. and attributed to the  $\text{Mn}^{4+}$  species. The second spectrum was consistent with the  $\text{Mn}^{5+}$  state based on comparison with authentic  $\text{Mn}^{5+}$  model complexes. The existence of a  $\text{Mn}^{5+}$  state, as had previously been proposed by Strieder et al., suggests that a porphyrin cation radical does not form in the two-electron-oxidized form of Mn-COX-1. Both spectra had absorbance maxima at 420 nm; however, the spectrum of the  $\text{Mn}^{4+}$  species also exhibited maxima at 268 and 464 nm. Isosbestic points between resting enzyme and the  $\text{Mn}^{5+}$  species were 352 and 444 nm, whereas those between the  $\text{Mn}^{5+}$  species and the  $\text{Mn}^{4+}$  species were 368, 406, and 433 nm.

Once the spectra of the two intermediates were resolved, it then became possible to obtain estimates of the rate constants for their formation. The second-order rate constant for formation of the  $\text{Mn}^{5+}$  species, using 15-HPETE as substrate at 20  $^\circ\text{C}$ , was  $1.0 \times 10^6 \text{ M}^{-1} \text{ s}^{-1}$ , and the first-order rate constant for the conversion of the  $\text{Mn}^{5+}$  species to the  $\text{Mn}^{4+}$  species was  $400 \pm 100 \text{ s}^{-1}$ . These values were much lower than the corresponding values for native enzyme, obtained under the same conditions ( $k_1 = 1.0 \times 10^8 \text{ M}^{-1} \text{ s}^{-1}$ ,  $k_2 = 950 \text{ s}^{-1}$ ). The lower rate of reaction of Mn-COX-1 with hydroperoxides might be predicted on the basis of studies with horseradish peroxidase.<sup>221</sup>



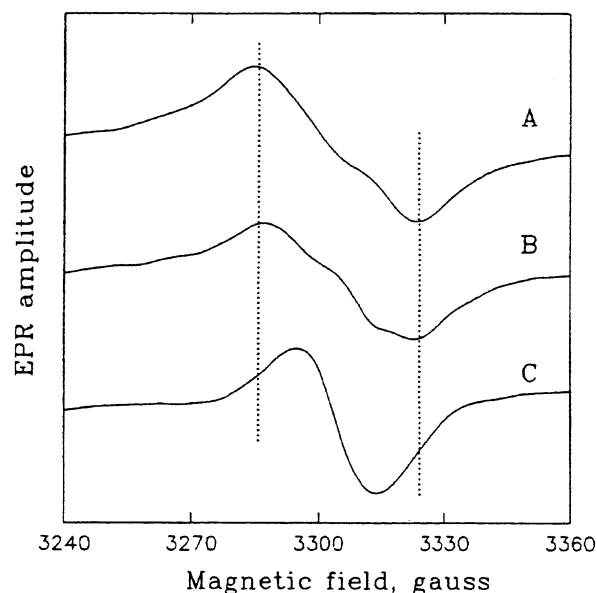
**Figure 59.** Reconstructed spectra of native COX-1 and Mn-COX-1 peroxidase intermediates. Left: Stopped-flow data were obtained from a reaction mixture containing native COX-1 (1  $\mu\text{M}$  heme) and 15-HPETE (15  $\mu\text{M}$ ) at 2  $^{\circ}\text{C}$ . Spectra were taken by kinetic scan at 2-nm increments and analyzed by singular value decomposition. Right: Mn-COX-1 (2.5  $\mu\text{M}$  subunit, 1.25  $\mu\text{M}$  Mn<sup>3+</sup>-PPIX) was combined with 15-HPETE (62.5  $\mu\text{M}$ ) at 20  $^{\circ}\text{C}$ , and kinetic scans were taken at 5-nm intervals for singular value decomposition analysis. Reproduced with permission from ref 123. Copyright 1997 American Society for Biochemistry and Molecular Biology.

For this enzyme, it has been shown that substitution of Fe<sup>3+</sup>-PPIX with Mn<sup>3+</sup>-PPIX results in a marked decrease in the rate of dissociation of the water molecule that serves as the sixth ligand to the metal atom. As a result, the rate of binding of the hydroperoxide substrate is reduced, leading to a much slower rate of reaction. As noted above (section V.A.1), Raman spectroscopic data suggest that water is most likely the sixth ligand in native COX. Therefore, it is reasonable to assume that a similar mechanism might explain the reduced peroxidase reaction rate in Mn-COX-1, although no direct measurements of water dissociation rates for native or Mn-COX-1 have been made.

### B. Tyrosyl Radicals in Mn-COX-1

The electronic spectroscopy studies described above confirmed the formation of two higher oxidation states of Mn-COX-1. Of equal interest was the identification of radical species, in particular a tyrosyl radical, as described for the native enzyme. Lassmann et al. had earlier described the results of EPR studies of the reaction of Mn-COX-1 (75  $\mu\text{M}$ ) with 20:4 (5 mM) at -12  $^{\circ}\text{C}$ .<sup>151</sup> Following a 1-min lag, a weak singlet signal was observed, but then after a 3-min lag a stronger, broad singlet appeared, centered at  $g = 2.0042$ , with a peak-to-trough width of 31 G. No doublet signals were observed at any time during the reaction with 20:4, and addition of PPHP to Mn-COX-1 led to no radical signal at all. Although the singlet observed during the reaction of Mn-COX-1 with 20:4 superficially resembled the broad singlet observed in the reaction of native COX-1, a detailed examination of the hyperfine coupling constants led the investigators to conclude that this signal was not that of a tyrosyl radical.

Using different reaction conditions, Kulmacz et al. observed the rapid formation of a wide doublet signal



**Figure 60.** EPR spectra generated from the reaction of Mn-COX-1 (21  $\mu\text{M}$  subunit) with (A) 2 equiv of 20:4 for 9 s or (B) 2 equiv of 15-HPETE for 7 s. For (C), Mn-COX-1 was pretreated with tetranitromethane, resulting in 95% inactivation of enzyme activity. After purification by gel filtration, the treated enzyme (17  $\mu\text{M}$  subunit) was reacted with 2 equiv of 15-HPETE for 8 s. All reactions were carried out at 0  $^{\circ}\text{C}$ , and spectra were recorded at 93 K. Reproduced with permission from ref 222. Copyright 1994 American Chemical Society.

centered at  $g = 2.005$ , with a peak-to-trough width of 38 G, after reaction of Mn-COX-1 (21  $\mu\text{M}$ ) with 2 equiv of either 20:4 or 15-HPETE at 0  $^{\circ}\text{C}$  (Figure 60).<sup>222</sup> No signal was observed upon reaction with EtOOH. A narrow singlet signal (peak-to-trough width of 19 G) was observed using Mn-COX-1 pretreated with tetranitromethane, and no signal was observed with indomethacin-treated enzyme. The intensity of the signal generated upon reaction



with 20:4 was about one-third as great as that of the signal generated by native enzyme under the same conditions. Power saturation data indicated that the radical generated in Mn-COX-1 was about the same distance from the metalloporphyrin center as the radical generated in native COX-1. Finally, kinetic studies indicated that the radical signal generated by Mn-COX-1 appeared prior to and remained present throughout PG formation by the enzyme. In fact, the radical intensity continued to increase after PGG<sub>2</sub> formation had ceased. Together, these results led the investigators to conclude that the radical signal originates in a tyrosine residue and is involved in cyclooxygenase catalysis. The increase in signal intensity after PGG<sub>2</sub> formation had ceased was attributed to accumulation of the tyrosyl radical that was no longer being used in the cyclooxygenase reaction.

Because the radical signal generated by the reaction of 20:4 or peroxides with Mn-COX-1 was significantly different from that generated by native enzyme, some question remained concerning the catalytic competence of this radical. These doubts were addressed through studies carried out by Tsai et al.<sup>164</sup> These investigators incubated Mn-COX-1 with 15-HPETE to generate the tyrosyl radical and then added 20:4 under anaerobic conditions. The tyrosyl radical signal was replaced by an isotropic signal similar to that of the 20:4-derived radical signal observed in similar experiments performed with native COX-1 and COX-2. Use of octadeuterated 20:4 confirmed the identity of this radical signal. Thus, the chemical competence of the tyrosyl radical of Mn-COX-1 to oxidize 20:4 was confirmed.

### C. One-Electron versus Two-Electron Reductions by Mn-COX-1

The above experiments strongly suggest that the cyclooxygenase mechanism of Mn-COX-1 is identical to that of the native enzyme and that the differences between the two proteins are attributable primarily to the much lower peroxidase activity of the manganese-substituted form. Kinetic studies performed by Kulmacz et al. sought to define the basis for the reduced peroxidase activity of Mn-COX-1.<sup>222</sup> They showed that the  $K_m$  of Mn-COX-1 for 15-HPETE was similar to that of the native enzyme. In contrast, the  $K_m$  of Mn-COX-1 for EtOOH was much higher than that of the native enzyme, indicating that the manganese-substituted enzyme has a much more stringent structural requirement for lipid hydroperoxide substrates. Using 15-HPETE as substrate, the  $V_{max}$  of Mn-COX-1 was about 4% of that of the native enzyme. Interestingly, Mn-COX-1 was found to oxidize  $0.95 \pm 0.05$  mol of TMPD per mole of 15-HPETE, compared to  $2.06 \pm 0.09$  mol of TMPD per mole of 15-HPETE for native enzyme. Reaction of 15-HPETE with Mn-COX-1 resulted in the formation of two products, 15-HETE and 15-KETE, in about equimolar quantities. In contrast, the native enzyme generated only 15-HETE. Kulmacz et al. interpreted this finding to indicate that the oxidized intermediates of Mn-COX-1 can react with 15-HETE, resulting in the two-electron oxidation of 15-

HETE to 15-KETE with concomitant reduction of the metalloporphyrin center of the enzyme to the Mn<sup>3+</sup> state.

Further mechanistic studies by Landino and Marrett confirmed the formation of both 15-HETE and 15-KETE in the reaction of Mn-COX-1 with 15-HPETE.<sup>223</sup> However, when they incubated [<sup>14</sup>C]-15-HETE and unlabeled 15-HPETE with Mn-COX-1, no radioactive 15-KETE was formed. Furthermore, no 15-HETE or 15-KETE was formed when 15-HPETE was reacted with Mn-COX-1 in the absence of a reducing substrate. These results were inconsistent with the proposal by Kulmacz et al. that 15-HETE could serve as a reducing substrate for Mn-COX-1, leading to its oxidation to 15-KETE, unless one assumes that only 15-HETE generated from 15-HPETE in the enzyme active site can be oxidized.<sup>222</sup> As an alternative mechanism for 15-KETE formation during the reaction of 15-HPETE with Mn-COX-1, Landino and Marrett proposed that the enzyme catalyzes a one-electron reduction of 15-HPETE to form an alkoxyl radical, which is then oxidized to 15-KETE. Support for this hypothesis was obtained through the reaction of Mn-COX-1 with 10-hydroperoxyoctadeca-8,12-dienoic acid. Compounds formed from this reaction included the characteristic two-electron reduction product, 10-hydroxyoctadeca-8,12-dienoic acid, as well as the one-electron reduction products, 10-oxooctadeca-8,12-dienoic acid and 10-oxodec-8-enoic acid. Further studies using 13-hydroperoxyoctadeca-8,12-dienoic acid as substrate also led to the formation of one-electron reduction products. Of the three substrates tested, reaction with 15-HPETE led to the greatest total number of enzyme turnovers before inactivation (1010 as compared to <220 for the octadecadienoic acids). The percentage of one-electron reductions was similar for 15-HPETE and 13-hydroperoxyoctadeca-8,12-dienoic acid (approximately 50%), whereas this percentage was only 25% for 10-hydroperoxyoctadeca-8,12-dienoic acid. These results indicated that, unlike the native enzyme, Mn-COX-1 catalyzes a significant percentage of one-electron reduction of hydroperoxides. In addition, the product profiles obtained from the three substrates tested indicate that the protein environment of the enzyme influences the fate of the alkoxyl radicals that result from the one-electron reduction. Finally, the results also indicate that the use of spectrophotometric assays based on the oxidation of a peroxidase reductant can lead to misleading conclusions, since the ratio of peroxidase reductant oxidized to hydroperoxide reduced varies, depending on whether one-electron or two-electron reduction occurs.

### D. Inactivation of Mn-COX

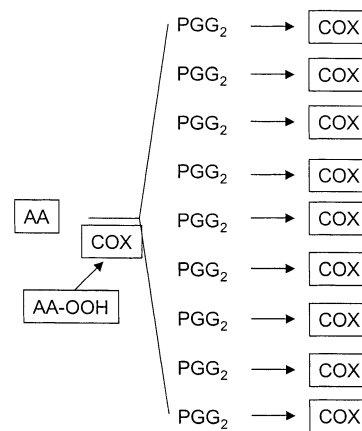
Because the peroxidase activity of Mn-COX is slower, and because enzyme inactivation has been related to peroxidase intermediates, it was of interest to study the inactivation rate and mechanism of Mn-COX-1. Wu et al. showed that the inactivation rate of Mn-COX-1 after exposure to 15-HPETE or PPHP was approximately 1 order of magnitude slower than the inactivation rate of native COX-1 ( $k = 0.03-0.04$

$s^{-1}$ ) and that, even after prolonged incubation, as much as 40% of the activity remained.<sup>115</sup> This accounted for the fact that Mn-COX-1 catalyzed more total turnovers than the native enzyme. However, as in the case of the native enzyme, the rate of inactivation of Mn-COX-1 was a first-order process, independent of peroxide structure or concentration. Spectral studies demonstrated that the reaction of Mn-COX-1 with PPHP led to an increase in absorbance at 420 nm and decreases at 378 and 472 nm during the first 10 s. Singular value decomposition of spectral data over the first 50 s of reaction indicated the presence of three spectral species. The rate constant for the conversion of the first to the second species was  $0.4 s^{-1}$ , whereas the rate constant for the conversion of the second to the third species,  $0.05 s^{-1}$ , was similar to the rate constant for enzyme inactivation. The spectrum of the initial species resembled that of native Mn-COX-1, whereas the spectrum of the enzyme after 10 min of reaction resembled that of the second species, suggesting that the third species was unstable. Analysis of the Mn<sup>3+</sup>-PPIX obtained after inactivation of the enzyme resulted in the detection of no oxidized porphyrin derivatives that would account for the enzyme inactivation process. Evidence was obtained for covalent linkage of porphyrin to protein, but these species were believed to represent too small a fraction of the total porphyrin to account for enzyme inactivation. Wu et al. concluded that the inactivation of Mn-COX-1 resembles that of native enzyme in that it is a multistep process in which loss of activity occurs after the formation of a species resembling intermediate I and is probably not associated with obvious changes in porphyrin structure. The large differences in inactivation rate result from differences in the reactivity of heme versus the Mn<sup>3+</sup>-PPIX prosthetic group.

In conclusion, studies of COX-1 substituted with Mn<sup>3+</sup>-PPIX have provided new insight into the mechanism of the peroxidase and cyclooxygenase reactions. Results have generally been consistent with the branched-chain mechanism and have demonstrated the importance of both the interdependence and the independence of the two COX reactions.

### X. Hydroperoxide Activation under Physiological Conditions

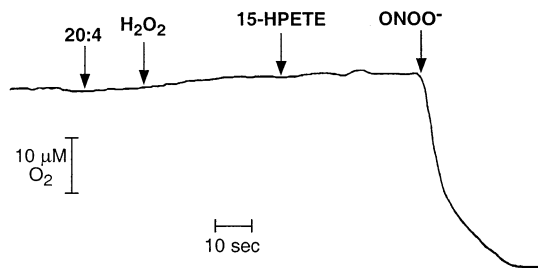
The mechanism of cyclooxygenase activation and catalysis outlined above is strongly supported by experimental evidence. It paints a picture of an inactive enzyme waiting to react with a hydroperoxide activator so that it can oxidize a fatty acid or related derivative. Given the reactivity of the tyrosyl radical and the ferryl-oxo complex, it seems unlikely that the COX protein exists in the active, intermediate I state, poised for oxidation of a substrate. Rather, the catalytic mechanism implies that the COX enzymes are synthesized and exist in cells as mature but inactive proteins that must react with a hydroperoxide activator to initiate cyclooxygenase catalysis. The identity of the hydroperoxide activator is, therefore, of interest. In test tube incubations, this is likely to be an autoxidation product of the poly-



**Figure 61.** Activation of COX proteins by trace quantities of hydroperoxy fatty acids. Hydroperoxide impurities in 20:4 preparations react with the peroxidase activity of a COX molecule to activate the cyclooxygenase activity. This generates multiple molecules of PGG<sub>2</sub>, which activate the remaining COX molecules.

unsaturated fatty acid substrate being assayed. Polyunsaturated fatty acids are extremely sensitive to autoxidation, so most commercially available material contains hydroperoxide impurities on the order of 0.5–1%. Relatively few molecules of fatty acid hydroperoxide are required to activate the first few molecules of COX.<sup>105</sup> These active COX molecules can then oxidize the fatty acid substrates to many molecules of the hydroperoxide products (PGG<sub>2</sub> or HPETE), which can activate the remaining enzyme molecules. This would account for the relatively rapid activation of all the COX molecules in solution (Figure 61).<sup>102</sup>

The situation *in vivo* is complicated by the fact that cells expend considerable energy to limit the generation and reactions of lipid oxidation products (either fatty acid hydroperoxides or phospholipid hydroperoxides). Membrane-soluble and water-soluble antioxidants retard the progress of free radical chain autoxidations, and GSH peroxidases, GSH transferases, and peroxiredoxins reduce lipid hydroperoxides to redox-inactive alcohols.<sup>224,225</sup> An additional complication is that COX enzymes, and specifically the peroxidase active sites, are compartmentalized in the lumen of the endoplasmic reticulum and the nuclear envelope.<sup>35</sup> This may shield the peroxidase active sites from hydroperoxide-generating or hydroperoxide-reducing enzymes. So how are COX enzymes activated in intact cells? This is likely to vary for a given cell type, but a potential hydroperoxide activator in inflammatory cells (monocytes, macrophages, neutrophils, etc.) is peroxynitrous acid (ONOOH).<sup>184</sup> ONOOH is a highly reactive *inorganic* hydroperoxide that is formed in inflammatory cells by the coupling of superoxide anion (O<sub>2</sub><sup>-</sup>) to NO to form peroxynitrite (ONOO<sup>-</sup>), followed by protonation.<sup>226</sup> Both O<sub>2</sub><sup>-</sup> and NO are products of activated inflammatory cells (via NADPH oxidase and NO synthase, respectively), and their coupling occurs at a diffusion-controlled rate. The pK<sub>a</sub> of ONOOH is 6.8, so protonation occurs readily at physiological pH.<sup>227</sup> ONOOH reacts with myeloperoxidase and several other mammalian peroxidases at a rate equal to that



**Figure 62.** Activation of COX molecules by peroxynitrous acid. Purified COX-1 (75 nM) was incubated with 120 units of glutathione peroxidase and 250  $\mu\text{M}$  glutathione, which scavenges available hydroperoxide and inhibits COX activation. Addition of 20:4 to unactivated enzyme results in no  $\text{O}_2$  uptake or  $\text{PGG}_2$  biosynthesis. Addition of 150  $\mu\text{M}$   $\text{H}_2\text{O}_2$  or 15-HPETE does not overcome the inhibition. In contrast, addition of 150  $\mu\text{M}$  peroxynitrite leads to immediate COX activation and oxygenation of 20:4. Reproduced with permission from ref 262. Copyright 1999 Federation of American Societies for Experimental Biology.

**Table 7. Reactivity of COX Peroxidase with Peroxynitrite and Hydroperoxides<sup>184</sup>**

substrate	COX-1			COX-2		
	$K_m$ ( $\mu\text{M}$ )	$V_{\text{max}}^a$	$V_{\text{max}}/K_m$	$K_m$ ( $\mu\text{M}$ )	$V_{\text{max}}^a$	$V_{\text{max}}/K_m$
peroxynitrite	140	759	5.4	100	287	2.9
15-HPETE	24	237	9.7	9	59	6.3
$\text{H}_2\text{O}_2$	287	692	2.4	109	167	1.5

<sup>a</sup> Peroxidase assays were carried out with 100 nM COX, 500  $\mu\text{M}$  guaiacol, and the desired concentration of substrate in 0.1 M sodium phosphate buffer, pH 8.0. Due to the rapid inactivation of the peroxidase that makes rate measurements difficult,  $V_{\text{max}}$  is expressed as the total number of turnovers at saturating concentrations of substrate. The units of  $V_{\text{max}}$  are moles of guaiacol oxidized per mole of COX.

of reaction with  $\text{H}_2\text{O}_2$  to form compound I derivatives.<sup>228</sup>

Landino et al. demonstrated that ONOOH activates cyclooxygenase activity in vitro, even in the presence of a substantial excess of GSH and GSH peroxidase (Figure 62).<sup>184</sup> Activation of cyclooxygenase activity was not exhibited by  $\text{NO}_2^-$ ,  $\text{NO}_3^-$ , NO,  $\text{O}_2^-$ , or *S*-nitrosoglutathione. ONOOH is an excellent substrate for both COX-1 and COX-2 (Table 7), and the rate constant for the reaction of ONOOH with ovine COX-1 to form compound I is  $1.5 \times 10^7 \text{ M}^{-1} \text{ s}^{-1}$  at pH 7 [L. Landino and L. J. Marnett, unpublished observations]. The rate constant for the same reaction is  $1.3 \times 10^6 \text{ M}^{-1} \text{ s}^{-1}$  at pH 8, implying that ONOOH rather than  $\text{ONOO}^-$  is the reactive species. The rate constant for reaction of ONOOH with COX-1 to form compound I is as high as the reported rate constants for reaction of  $\text{PGG}_2$  and 15-HPETE with COX-1 and is some 50-fold greater than the rate constant for reaction with  $\text{H}_2\text{O}_2$ . Thus, ONOOH is a highly efficient peroxidase substrate.

ONOOH-dependent cyclooxygenase activation was inhibited by superoxide dismutase in systems in which ONOOH was generated in situ from NO and  $\text{O}_2^-$ . Superoxide dismutase scavenges  $\text{O}_2^-$  and prevents the formation of  $\text{ONOO}^-/\text{ONOOH}$ . PG synthesis (mainly  $\text{PGD}_2$ ) was inhibited in lipopolysaccharide (LPS)-activated macrophages (RAW264.7 cells) by NO synthase inhibitors or by the membrane-per-

meant superoxide dismutase mimetic agents,  $\text{Cu}^{\text{II}}$ -[diisopropylsalicylate]<sub>2</sub> and  $\text{Mn}^{3+}$ -tetrakis(1-methyl-4-pyridyl)porphyrin. Inhibition was observed regardless of whether 20:4 was added exogenously or released from endogenous stores. If cells treated with Cu-diisopropylsalicylate were washed to remove it prior to activation, no inhibition of PG production was observed. Neither the copper complex nor the manganese complex inhibited the expression of the COX-2 gene following LPS treatment. A role for ONOOH in the activation of COX-2 in inflammatory cells is conceptually attractive because inducible NO synthase and COX-2 are both early response genes that are expressed rapidly and with nearly identical time courses following cell activation with an agonist such as LPS.

Genetic evidence for the importance of NO in regulating PG biosynthesis capacity was acquired with the use of mice bearing targeted deletions in the gene for the inducible form of NO synthase (iNOS).<sup>229</sup> Peritoneal macrophages isolated from these animals were treated with LPS and  $\gamma$ -interferon to induce COX-2 and iNOS. Macrophages from iNOS-deficient animals demonstrated 11- and 19-fold reductions in  $\text{PGE}_2$  production 12 and 24 h after LPS administration compared to wild-type animals. No differences in the levels of COX-2 protein were detected at any time point, indicating that the effect of iNOS deletion was not on gene expression or protein synthesis. The levels of  $\text{PGE}_2$  in urine of iNOS-deficient animals were reduced by 78% compared to those in wild-type animals. Most of the  $\text{PGE}_2$  present in urine is produced in the kidney, so these experiments suggest a role for iNOS in regulating PG biosynthetic capacity in the kidney as well as in macrophages. It is possible that the in vivo reduction in PG production in iNOS-deficient animals is due to the reduced production of the hydroperoxide activator, peroxynitrous acid.

## XI. Structural Changes Associated with Enzyme Inactivation

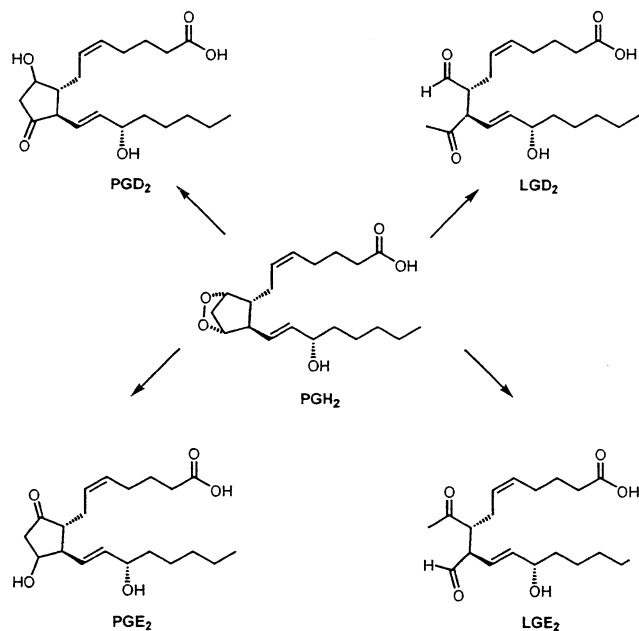
As described above, (sections V.A.2 and IX.D), a number of attempts have been made to describe kinetic models for the self-inactivation of COX. However, of equal interest is the structural change to the enzyme that leads to enzyme inactivation. As described in section VI.B.1, EPR studies indicate that inactivation is associated with a change in the structure or environment of the tyrosyl radical, though the exact nature and significance of this change remain undefined.<sup>142,152,153,155</sup> Similarly, changes in the spectral properties of the heme have been shown to coincide with the inactivation of the peroxidase; however, heme isolated from inactivated enzyme showed no significant chemical modification.<sup>114</sup> An exception was observed in the case of inactivation of the enzyme in the presence of indomethacin, which led to the formation of a chlorin. Furthermore, covalent attachment of the heme to protein was observed both in the case of indomethacin-treated enzyme and in the case of Mn-COX-1.<sup>115</sup>

Although attempts to identify modifications of the heme prosthetic group of COX have met with limited

success, growing evidence indicates that the protein itself is modified during the course of the COX reaction through the covalent binding of a reactive substrate intermediate(s). This possibility was first raised by experiments in which radiolabeled 20:4 was incubated with microsomes from various tissues.<sup>230–233</sup> A portion of the radiolabel (from 3% to 18%, depending on the tissue) became bound to protein and could not be removed by solvent extraction or gel filtration chromatography. This protein binding was inhibited by indomethacin and did not occur when PGE<sub>2</sub>, PGD<sub>2</sub>, PGF<sub>2α</sub>, or other fatty acids were used instead of 20:4. The amount of protein binding was directly correlated with the levels of PGG<sub>2</sub> or PGH<sub>2</sub> generated in the microsomal mixture, and direct incubation of microsomes with radiolabeled PGG<sub>2</sub> and PGH<sub>2</sub> led to similar adduction of radiolabel to protein. These findings led the investigators to propose that a portion of the PGG<sub>2</sub> and/or PGH<sub>2</sub> generated during 20:4 oxygenation reacts covalently with microsomal protein. However, the identity of the modified protein and the nature of the covalent linkage were not explored in these experiments.

Chemical studies of the PG endoperoxide nucleus led Zagorski and Salomon to identify two pathways for the base-catalyzed decomposition of this moiety: fragmentation and disproportionation.<sup>234,235</sup> The disproportionation pathway led to the familiar hydroxycyclopentanone nucleus found in PGE<sub>2</sub> and PGD<sub>2</sub>, whereas fragmentation generated substituted levulinaldehydes. The relative amounts of the various products depended on the reaction conditions, such that the addition of excess acetic acid favored the disproportionation reaction. These studies were extended to include PGH<sub>2</sub>, and Salomon et al. showed that decomposition of PGH<sub>2</sub> in dimethyl sulfoxide led to the formation of levulinaldehyde products in 70–80% yield, and decomposition in aqueous solution (pH 7.9) led to the formation of these products in 22% yield.<sup>236</sup> Two primary levulinaldehyde products (Figure 63) were formed and were named levuglandin E<sub>2</sub> (LGE<sub>2</sub>) and levuglandin D<sub>2</sub> (LGD<sub>2</sub>), based on their relationship to PGE<sub>2</sub> and PGD<sub>2</sub>, respectively, through aldol condensation. The levuglandins were found to be highly reactive to dehydration and to adduction with amines. The latter finding helped to explain why these compounds had not previously been identified as decomposition products of PGG<sub>2</sub> or PGH<sub>2</sub>, since most such studies had been carried out in Tris buffers in which adduct formation with the amine group of Tris would readily occur.<sup>237</sup> Further studies of the levuglandins showed that LGE<sub>2</sub> rapidly became bound to proteins and could effect both protein–protein and protein–DNA cross-links.<sup>238–240</sup>

That a product of 20:4 oxygenation actually became bound to COX was demonstrated by Lecomte et al. through studies in which human platelets (containing predominantly COX-1) were incubated with exogenous radiolabeled 20:4.<sup>241</sup> Subsequent gel electrophoresis identified as many as 12 radiolabeled proteins. However, the most strongly labeled band immunoprecipitated with monoclonal antibodies against COX-1 and demonstrated the correct molecular mass for the COX-1 protein. The labeling also

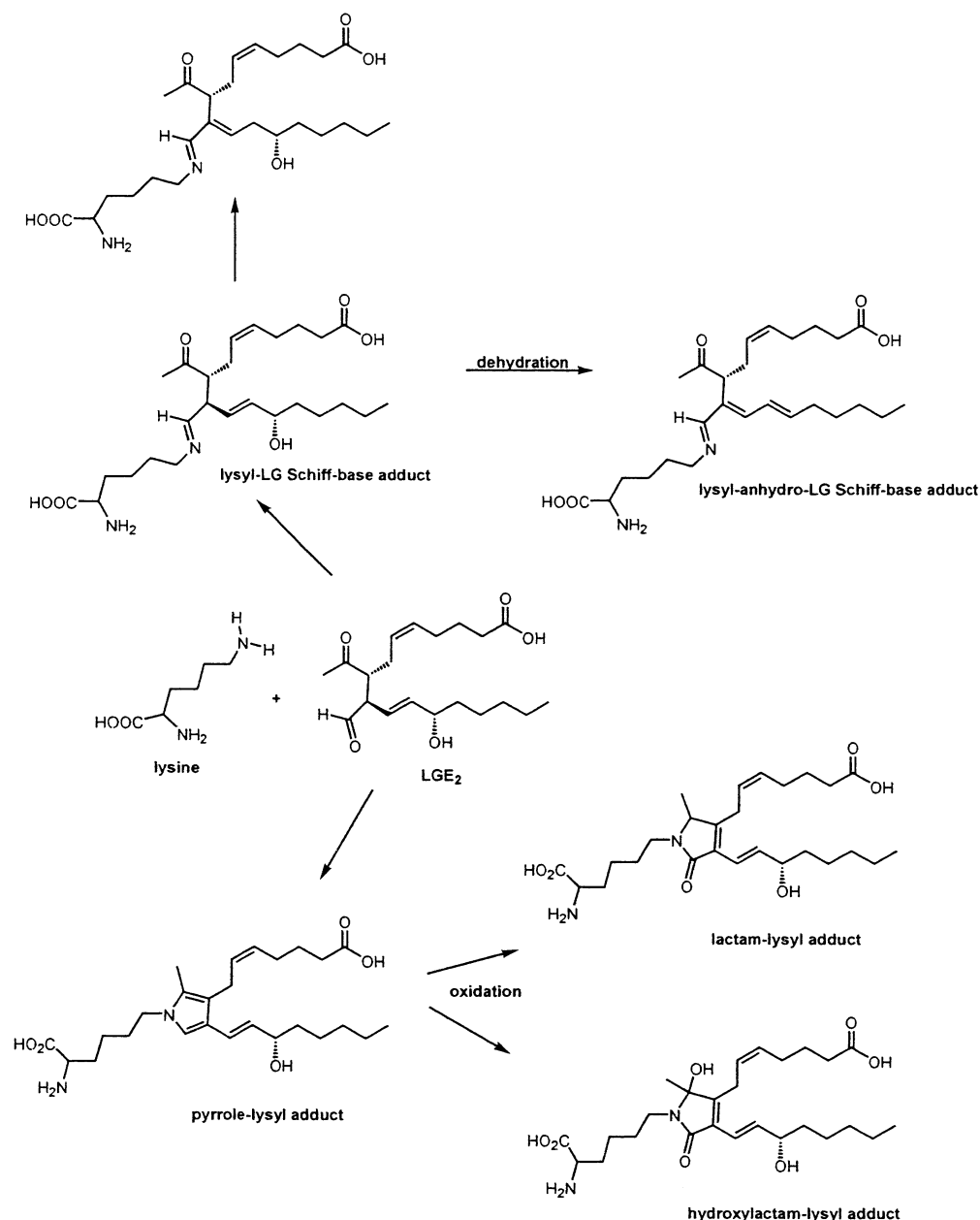


**Figure 63.** Formation of levuglandins. PGH<sub>2</sub> may spontaneously decompose to form PGE<sub>2</sub> or PGD<sub>2</sub>, but it may also form the levulinaldehyde products, LGE<sub>2</sub> and LGD<sub>2</sub>.<sup>234,235</sup>

occurred when platelets were prelabeled with 20:4 and challenged with thrombin to initiate PG synthesis, thus demonstrating the covalent modification of COX-1 with derivatives of endogenously released 20:4. Finally, incubation of purified COX-1 from ram seminal vesicles with 17 μM radiolabeled 20:4 led to covalent binding of radiolabel to 40% of the COX-1 protein.

The work of Lecomte et al. suggested that the major protein covalently modified during the COX reaction was COX itself.<sup>241</sup> However, the exact nature of the covalent modification remained obscure until Boutaud et al. isolated and identified the covalent adducts formed during the reaction of synthetic LGE<sub>2</sub> or PGH<sub>2</sub>-derived levuglandins with lysine.<sup>242</sup> They identified lysyl–levuglandin Schiff base adducts, anhydrolevuglandin Schiff base adducts, and pyrrole-derived lactam and hydroxylactam adducts (Figure 64). Boutaud et al. then went on to demonstrate the formation of lysyl–levuglandin Schiff base adducts in COX-2 protein after its reaction with 20:4.<sup>243</sup> MALDI-TOF mass spectral analysis indicated that, after incubation of 14 μM COX-2 with 944 μM [<sup>14</sup>C]-20:4, an average of 9.3 adducts were bound per molecule of protein and that nearly all of the expected levuglandin products formed had become protein-bound. These results strongly suggest that covalent modification of COX-2 through reaction with levuglandins likely accounts for the earlier observations of covalent adduct formation in microsomal preparations incubated with radiolabeled 20:4 described above.

It is not known at present whether the formation of levuglandin adducts with COX contributes to enzyme inactivation. Kulmacz performed a kinetic study of the covalent modification of COX-1 during its reaction with 20:4 and concluded that adduct formation occurred too slowly to account for enzyme



**Figure 64.** Products of the reaction of LGE<sub>2</sub> with lysine include the lysyl–levuglandin Schiff base adduct, which can undergo both tautomerization and dehydration. Alternatively formation of a pyrrole adduct, followed by oxidation, leads to the lactam and hydroxylactam products.<sup>242</sup>

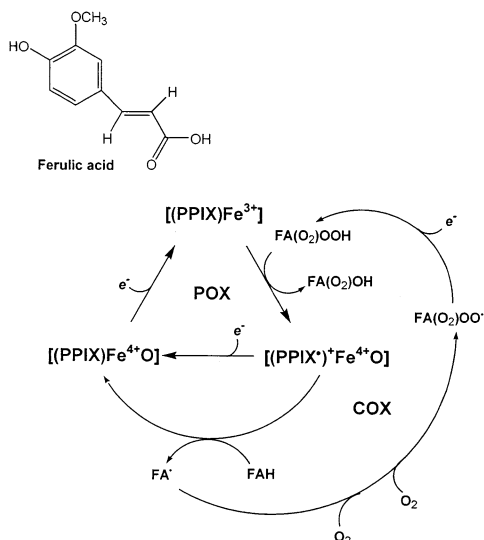
inactivation.<sup>244</sup> However, the reactions were carried out in Tris buffer and did not include reduction to stabilize the Schiff base levuglandin adducts. Therefore, it is likely that the relatively low levels of adduct formation observed in these studies were not due to reaction with levuglandins. In contrast, Boutaud et al. demonstrated high levels of adduct formation occurring within 100 s after the addition of 20:4 to COX-2.<sup>243</sup> Although they did not attempt to correlate the adduction rate to residual enzyme activity, their data suggest that covalent adduction may occur quickly enough to contribute to the self-inactivation of COX-2. An intriguing hypothesis is that covalent adduct formation may account for the fact that the inactivation rate of the cyclooxygenase activity of COX is more rapid than the inactivation rate of the peroxidase activity.<sup>94,95</sup>

## XII. Alternative Cyclooxygenase Mechanisms and Refinements of the Branched-Chain Mechanism

### A. The Tightly Coupled Mechanism

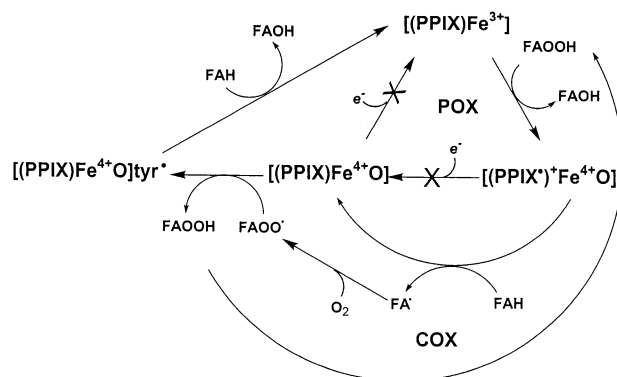
#### 1. Studies of Reaction Stoichiometry

As described above, a large body of evidence has been gathered to confirm the proposal of Deitz et al. that a tyrosyl radical is the oxidant of 20:4 in the cyclooxygenase reaction and that this residue provides the link between the peroxidase and cyclooxygenase activities of the enzyme, as outlined in Figure 34.<sup>39</sup> However, the branched-chain mechanism was called into question through work reported by Bakovic and Dunford. These investigators carried out kinetic studies of the oxygenation of 20:4 by COX-1 using ferulic acid (Figure 65) as reducing substrate.<sup>245</sup>



**Figure 65.** Tightly coupled mechanism for the cyclooxygenase reaction. All steps shown in Figure 18 are included. The enzyme is activated through the reaction with hydroperoxide ( $\text{FA}(\text{O}_2)\text{OOH}$ ) to generate compound I. Compound I abstracts a hydrogen atom from the fatty acid substrate ( $\text{FAH}$ ), yielding the fatty acid radical ( $\text{FA}^\bullet$ ) and compound II. Reaction of the fatty acid radical with two molecules of oxygen yields the peroxy radical of the fatty acid endoperoxide ( $\text{FA}(\text{O}_2)\text{OO}^\bullet$ ). Addition of an electron from the peroxidase reductant converts the peroxy radical of the fatty acid endoperoxide to the hydroperoxide of the fatty acid endoperoxide ( $\text{PGG}_2$  if the substrate is 20:4). A second electron from the peroxidase reductant converts compound II to native enzyme, and the product hydroperoxide is then used to regenerate compound I via the peroxidase reaction so that another cycle can occur. For each enzyme cycle, one molecule of fatty acid substrate is converted to one molecule of the alcohol of the fatty acid endoperoxide ( $\text{PGH}_2$  from 20:4) and two equivalents of peroxidase reductant are consumed. Identification of symbols for all intermediates is given in Table 1.

Enzyme activity was monitored by both the oxygen electrode and the absorbance change resulting from the oxidation of ferulic acid. The results indicated that, regardless of the relative concentration of ferulic acid to 20:4, the two substrates were always consumed in a ratio of 2:1. Bakovic and Dunford argued that the branched-chain mechanism predicts no such tight correlation between 20:4 oxygenation and peroxidase activity, since the cyclooxygenase reaction should be independent of the peroxidase reaction after intermediate I has been formed. They suggested an alternative mechanism in which the cyclooxygenase and peroxidase reactions are tightly coupled, as shown in Figure 65. Note that this mechanism proposes that the oxidant for 20:4 is compound I, leading to its conversion to compound II. Addition of two molecules of oxygen converts the 20:4 radical to the peroxy radical of  $\text{PGG}_2$ . Two equivalents of peroxidase reductant are consumed, one to reduce  $\text{PGG}_2^\bullet$  to  $\text{PGG}_2$  and one to convert compound II to native enzyme. Key to this mechanism is the realization that each cyclooxygenase turnover regenerates native enzyme, which must be activated again through the peroxidase-catalyzed reduction of  $\text{PGG}_2$  to  $\text{PGH}_2$ . This implies a tight coupling between the two enzymatic activities, so each cyclooxygenase turnover would require a turnover of the peroxidase.



**Figure 66.** Tightly coupled mechanism for the oxygenation of 20:2 in the absence of peroxidase reductant. All steps shown in Figure 18 are included; however, in the absence of peroxidase reductant, direct conversion of compound I to compound II and from compound II to native enzyme does not occur. The enzyme is activated through the reaction with hydroperoxide to generate compound I. Compound I abstracts a hydrogen atom from the fatty acid substrate ( $\text{FAH}$ ), yielding the fatty acid radical ( $\text{FA}^\bullet$ ) and compound II. Reaction of the fatty acid radical with one molecule of oxygen yields the peroxy radical ( $\text{FA}(\text{O}_2)\text{OO}^\bullet$ ). Reduction of this radical to the hydroperoxide ( $\text{FA}(\text{O}_2)\text{OOH}$ ) converts compound II to intermediate I. Reaction of intermediate I with a second molecule of fatty acid then regenerates the native enzyme and produces a molecule of the fatty acid alcohol ( $\text{FAOH}$ ). The fatty acid hydroperoxide is then used to regenerate compound I via the peroxidase reaction so that another cycle can occur. For each cycle, two molecules of fatty acid are converted to two molecules of fatty acid alcohol, and one molecule of oxygen is consumed. Identification of symbols for all intermediates is given in Table 1.

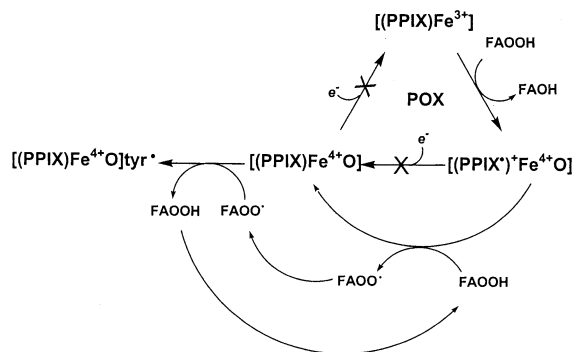
Further evidence for the tightly coupled mechanism came through studies of the conversion of 20:2 to 11-hydroxy-12,14-icosadienoic acid by COX-1 in the absence of peroxidase reductant.<sup>246</sup> In these studies, the rate of formation of the conjugated diene product was monitored by absorbance, and the rate of oxygen consumption was monitored via an oxygen electrode. The results indicated that the ratio of product formation to oxygen consumption was 2:1, a finding inconsistent with the branched-chain mechanism, which would predict a 1:1 ratio. Bakovic and Dunford proposed that compound I is the proximal oxidant for the dienoic acid substrate. The initial reaction forms compound II and the fatty acid radical, which subsequently reacts with oxygen to form the fatty acid peroxy radical, as shown in Figure 66. Compound II then reacts with the fatty acid peroxy radical to form fatty acid hydroperoxide and intermediate I. Finally, intermediate I reacts with a second molecule of fatty acid substrate to form the fatty acid alcohol product and native enzyme, while the hydroperoxide regenerates compound I and a second molecule of fatty acid alcohol product through the peroxidase reaction. Here again, a tight coupling between the cyclooxygenase and peroxidase activities is implied.

## 2. Kinetics of Intermediate I/Compound II Formation

If the mechanism proposed in Figure 66 is correct, one would expect that the conversion of compound I to compound II would be a second-order reaction,

dependent on both compound I and fatty acid concentration. Pre-steady-state kinetic studies of the reaction of COX-1 with 20:2 or 20:4 as substrate in the absence of peroxidase reductant appeared to support this speculation.<sup>247</sup> The isobestic point between native enzyme and compound I (425 nm) can be used to monitor the formation of intermediate I and/or compound II, since the two species have indistinguishable Soret spectra. Bakovic and Dunford monitored the rate of change in absorbance at 425 nm during the reaction of COX-1 with varying concentrations of 20:2 in the presence of a fixed concentration of hydroperoxide. They found that the absorbance change fit a single-exponential equation and that the observed rate constants were a linear function of fatty acid concentration. They concluded from these data that the conversion of compound I to intermediate I/compound II was a bimolecular process involving both enzyme and fatty acid substrate. This result was consistent with the tightly coupled mechanism (Figure 66), which proposes that compound I reacts with fatty acid substrate to form compound II. However, it was not consistent with the branched-chain mechanism (Figure 34), which predicts that intermediate I is formed from compound I via an intramolecular electron transfer and that compound II cannot form from compound I in the absence of peroxidase reductant.

Kinetic studies of the interaction of peroxides with native COX-1 and its compound I provided additional data that apparently contradicted the branched-chain mechanism.<sup>248</sup> The reaction of various hydroperoxides with native COX-1 led to compound I formation in a bimolecular reaction, consistent with earlier findings. Rate constants for a number of peroxides were of the same order of magnitude ( $10^5$ – $10^7$  M<sup>-1</sup> s<sup>-1</sup>) as those reported previously. By monitoring the change in absorbance at 414 nm after the addition of *m*-chloroperoxybenzoic acid (*m*-Cl PBA) to COX, Bakovic and Dunford established conditions (incubation of 0.1 μM COX-1 with 0.13 μM *m*-Cl PBA for 50–60 ms) that they believed resulted in complete conversion of the enzyme to compound I. They then showed that addition of more *m*-Cl PBA (or other hydroperoxides) to the enzyme at this time resulted in an increase in the rate of formation of a second intermediate, as determined by an increase in absorbance of 426 nm. The rate of the absorbance change was directly proportional to the concentration of hydroperoxide added, leading Bakovic and Dunford to conclude that it must result from formation of compound II. They argued that the formation of intermediate I directly from compound I, an intramolecular process, would show no dependence on hydroperoxide concentration. Furthermore, they proposed that compound II was formed from the bimolecular reaction of hydroperoxide with compound I, yielding the peroxy radical, as shown in Figure 67. Since their data suggested that direct conversion from compound I to intermediate I (as proposed in the branched-chain mechanism) did not occur, Bakovic and Dunford explained tyrosyl radical formation during the COX-1 reaction by suggesting that the reaction of compound II with peroxy radical would

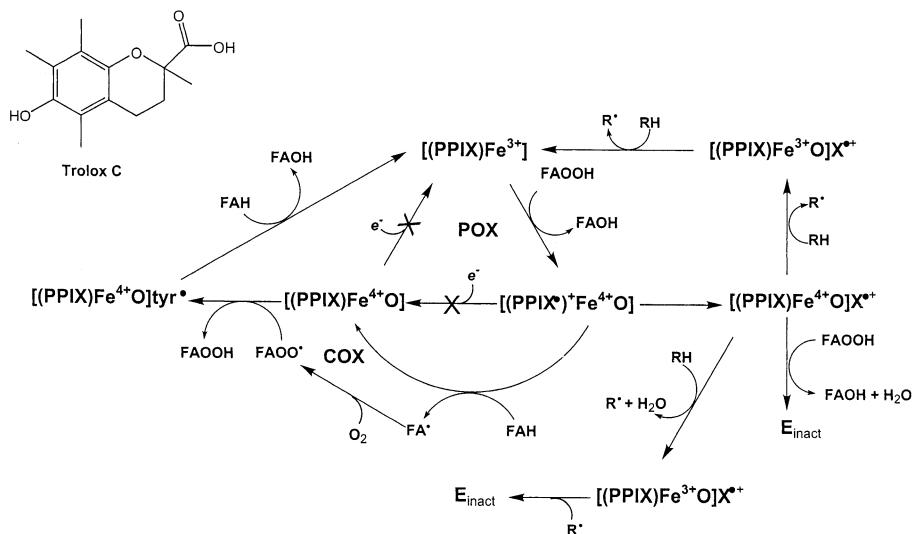


**Figure 67.** Mechanism for the interaction of peroxides with COX in the absence of peroxidase reductant. All steps shown in Figure 18 are included; however, in the absence of peroxidase reductant, direct conversion of compound I to compound II and from compound II to native enzyme does not occur. The enzyme is activated through the reaction with hydroperoxide (FAOOH) to generate compound I. Compound I then reacts with a second molecule of hydroperoxide to yield compound II and peroxy radical (FAOO•). Compound II is converted to intermediate I through reaction with the peroxy radical, regenerating the hydroperoxide (FAOOH). Identification of symbols for all intermediates is given in Table 1.

regenerate the hydroperoxide and intermediate I (Figure 67). Because compound II and intermediate I could not be distinguished spectrophotometrically, the observed second-order rate constants for the conversion of compound I to intermediate I/compound II, as measured by the absorbance change at 426 nm, must reflect the rate-determining step in the series of the two conversions. In any case, these data provided further support for the concept that intermediate I could not be formed in a unimolecular conversion from compound I, as described in the branched-chain mechanism (Figure 34).

### 3. Effects of Peroxidase Reductants

Some refinement of the tightly coupled mechanism resulted from studies of the reaction of 20:2 with COX-1 using Trolox C, a water-soluble analogue of  $\alpha$ -tocopherol, as peroxidase reductant (Figure 68).<sup>249</sup> These studies indicated that low concentrations of Trolox C stimulated the cyclooxygenase reaction rate, whereas high concentrations were inhibitory. However, the ratio of product formation (11-hydroxy-12,14-eicosadienoic acid) to oxygen consumption remained at 2:1, regardless of the concentration of Trolox C. The data indicated that Trolox C did not compete with fatty acid substrate for oxidation by compound I. Rather, it was proposed that compound I could undergo conversion to a species similar to intermediate I (designated [(PPIX)Fe<sup>4+</sup>O]X<sup>+</sup>) and that further oxidation of this species would lead to enzyme inactivation, as shown in Figure 68. The role of peroxidase reductant was to convert the intermediate I-like species (referred to here as intermediate II) back to native enzyme via a series of one-electron reductions (Figure 68). Thus, Trolox C stimulated cyclooxygenase activity by preventing enzyme inactivation. The inhibitory effect of the peroxidase reductant was attributed to a second inactivation step involving Trolox C radical, as shown in Figure 68.



**Figure 68.** Modified tightly coupled mechanism for the oxygenation of 20:2 in the presence of peroxidase reductant (Trolox C). All steps shown in Figure 18 are included. However, Bakovic and Dunford concluded that Trolox C does not compete with fatty acid for reduction of compound I, so it is presumed that the reduction of compound I to compound II and back to native enzyme through the peroxidase cycle does not occur. The enzyme is activated through reaction with hydroperoxide to generate compound I. Compound I abstracts a hydrogen atom from the fatty acid substrate (FAH), yielding the fatty acid radical (FA•) and compound II. Reaction of the fatty acid radical with one molecule of oxygen yields the peroxy radical (FAOO•). Reduction of this radical to the hydroperoxide (FAOOH) converts compound II to intermediate I. Reaction of intermediate I with a second molecule of fatty acid then regenerates the native enzyme and produces a molecule of the fatty acid alcohol. The fatty acid hydroperoxide is used to regenerate compound I via the peroxidase reaction so that another cycle can occur. For each cycle, two molecules of fatty acid are converted to two molecules of fatty acid alcohol, and one molecule of oxygen is consumed. In addition, compound I may undergo an intramolecular electron transfer to form intermediate II, which can then react with hydroperoxide, leading to enzyme inactivation. The proposed role of peroxidase reductant (RH to indicate Trolox C) is to convert intermediate II back to native enzyme via a series of two one-electron reductions, thus preserving enzyme activity. Alternatively, at high concentrations, the reductant may lead directly to enzyme inactivation via a series of two reactions, which reduce the heme moiety first to the Fe<sup>3+</sup> state and then to an unknown species (E<sub>inact</sub>). Identification of symbols for all intermediates is given in Table 1.

## B. Comparison of the Branched-Chain and Tightly Coupled Mechanisms

### 1. Reaction Stoichiometry

The questions raised by the work of Bakovic and Dunford led to a reinvestigation of the branched-chain mechanism. Clearly, the two major arguments for the tightly coupled mechanism derived from studies of the stoichiometry of oxygen and peroxidase reductant consumption relative to the consumption of fatty acid and of the kinetics of the formation of intermediate I/compound II as measured by the absorbance change at 424–428 nm. Wei et al. addressed the issue of reaction stoichiometry in studies that focused on the importance of correcting for oxygen electrode membrane diffusion error.<sup>250</sup> As mentioned in section IV.C, when oxygen consumption rates are high, they may exceed the rate of diffusion of oxygen across the oxygen electrode membrane, resulting in an underestimation of the rate of the enzymatic reaction.<sup>96</sup> When careful corrections for this error were conducted, Wei et al. showed that the ratio of ferulic acid oxidation to 20:4 oxygenation by COX-1 was significantly less than the value of 2:1 reported by Bakovic and Dunford.<sup>245,250</sup> Similarly, Tsai et al. reported that, after correction for the oxygen electrode error, the ratio of oxygen consumption to lipid product formation in the reaction of COX-1, using 20:2 as substrate, was very close to 1:1 (actual value of 1.2:1) rather than the 1:2 ratio observed by Bakovic and Dunford.<sup>195,246</sup> These results

called into question some of the key observations supporting the tightly coupled mechanism.

### 2. Kinetics of Intermediate I/Compound II Formation

Kinetic studies were performed by Tsai et al. to address the dependency of the rate of formation of compound II/intermediate I on hydroperoxide concentration.<sup>195</sup> Rapid-freeze techniques using EPR spectroscopy allowed Tsai et al. to directly monitor the rate of formation of intermediate I (as distinct from compound II) during the interaction of COX-1 with peroxides. The wide doublet tyrosyl radical signal was formed efficiently at a reaction stoichiometry of less than one peroxide per enzyme in only 300 ms of incubation time, indicating that only one molecule of hydroperoxide was required for intermediate I formation. This contradicts the tightly coupled mechanism, which predicts that two molecules of hydroperoxide are required for intermediate I formation (Figure 67). Furthermore, when intermediate I formation was measured directly under the conditions used by Bakovic and Dunford, Tsai et al. showed that addition of *m*-Cl PBA to COX-1 at a molar ratio of 1.3:1 did not lead to complete conversion of the enzyme to compound I.<sup>195,248</sup> Rather, a direct relationship was observed between the quantity of intermediate I formed and the amount of hydroperoxide added for stoichiometric ratios as high as 3.9:1. Finally, under the reaction conditions used by Bakovic and Dunford, Tsai et al. demonstrated that the change in absorbance at 428 nm (used to monitor

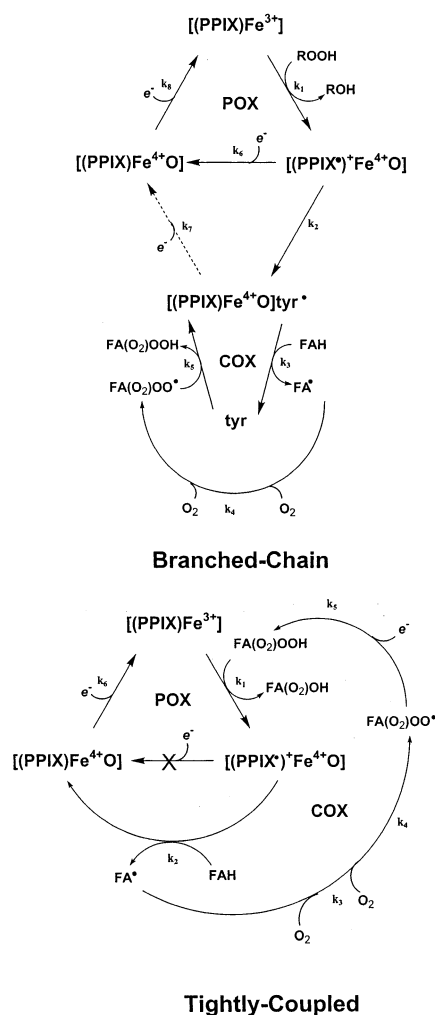


intermediate I/compound II formation) began well before 50 ms. These observations were important, because Bakovic and Dunford's data analysis had depended on their assumption that the formation of compound I from native enzyme was complete and that no formation of compound II or intermediate I had occurred prior to the second addition of hydroperoxide in their experiments. This allowed them to assume that further compound I formation from native enzyme had no effect on the rate of the proposed reaction of compound I with hydroperoxide to form compound II. The findings of Tsai et al. raised serious questions concerning these assumptions. Thus, the dependence of the rate of change in absorbance at 426/428 nm on hydroperoxide concentration could not be analyzed in terms of an isolated bimolecular reaction, as proposed by Bakovic and Dunford. Rather, it was likely due to the combined effects of the kinetics of compound I formation, followed by the conversion of compound I to intermediate I, as originally described by Dietz et al. (discussed in section V.A.1). These results were consistent with the branched-chain mechanism (Figure 34) and called into question the basic kinetic assumptions that supported the tightly coupled mechanism.

### 3. Interaction between the Cyclooxygenase and Peroxidase Activities

A significant difference between the branched-chain and tightly coupled mechanisms is seen in the fact that the tightly coupled mechanism predicts that every molecule of  $\text{PGG}_2$  synthesized must be consumed to regenerate compound I before another reaction cycle may proceed. Thus,  $\text{PGG}_2$  should never accumulate during the COX reaction. In contrast, the branched-chain mechanism proposes that, once a single  $\text{PGG}_2$  molecule is consumed to generate compound I, which goes on to form intermediate I, the synthesis of  $\text{PGG}_2$  then becomes independent of the peroxidase reaction. This mechanism predicts that, in the absence of peroxidase reductant,  $\text{PGG}_2$  should accumulate. Evidence for  $\text{PGG}_2$  accumulation had been noted in early studies of the COX reaction mechanism.<sup>2,3,37,94,251</sup> However, this issue was re-examined by Wei et al., who measured the relative quantities of  $\text{PGG}_2$  and  $\text{PGH}_2$  under varying reaction conditions.<sup>250</sup> They demonstrated that, in the absence of peroxidase reductant,  $\text{PGG}_2$  was the primary product. When phenol was added as peroxidase reductant, the ratio of  $\text{PGH}_2$  to  $\text{PGG}_2$  increased with increasing phenol concentration. These data strongly supported the branched-chain mechanism.

A second significant difference between the branched-chain and tightly coupled mechanisms is observed in their predictions concerning the interaction between the cyclooxygenase and peroxidase activities of COX. Because the tightly coupled mechanism requires a peroxidase turnover for every cyclooxygenase turnover, one would predict that any alteration of peroxidase activity would have a similar effect on cyclooxygenase activity. However, as noted above (sections VIII.E and IX), a number of variant enzymes of both COX-1 and COX-2 exist in which



**Figure 69.** Branched-chain and tightly coupled mechanisms used by Wei for mathematical modeling of COX reaction. The branched-chain mechanism is essentially the same as that shown in Figure 34. The tightly coupled mechanism is essentially the same as that shown in Figure 65, with the exception that the conversion of compound I to compound II by reduction with peroxidase reductant does not occur in order to maintain the tight coupling between the cyclooxygenase and peroxidase activities. Values for kinetic constants used by Wei et al. for numerical integration are given in Table 8. Identification of symbols for all intermediates is given in Table 1.

peroxidase activity is extremely low but cyclooxygenase activity is nearly normal. These include replacement of the native heme with  $\text{Mn}^{3+}$ -PPIX, mutation of His-386 to alanine or glutamine, mutation of His-207 to alanine, or mutation of His-388 to tyrosine.<sup>33,108,109,148,182,189,222</sup> The existence of such enzyme forms is consistent with the branched-chain mechanism but not the tightly coupled mechanism.

### 4. Predictions from Mathematical Models

Because of the high level of complexity of both proposed COX mechanisms, Wei et al. used numerical integration techniques to generate mathematical models for each mechanism.<sup>250</sup> Figure 69 shows the exact mechanism used for each model of the COX reaction. Appropriate rate equations were derived for each step in both mechanisms, and experimental rate constants were applied whenever values were avail-

**Table 8. Rate Constants Used for Mathematical Modeling of Branched-Chain and Tightly Coupled Mechanisms<sup>250</sup>**

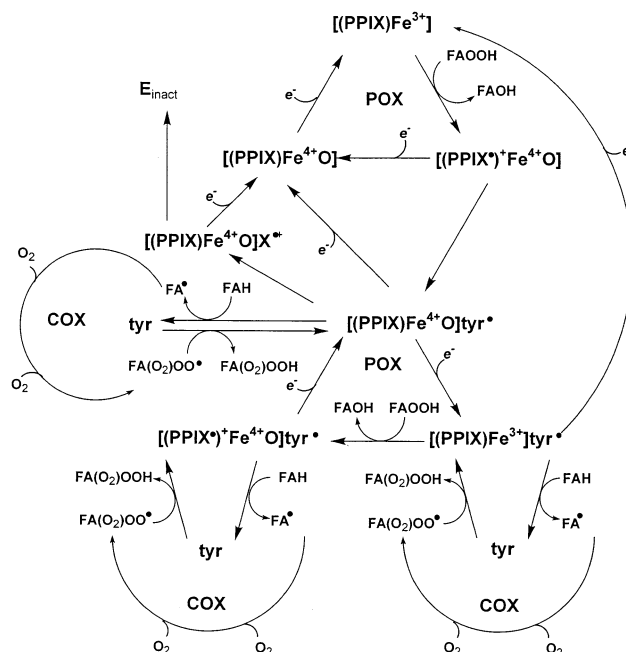
branched-chain mechanism		tightly coupled mechanism	
rate constant	value <sup>a</sup>	rate constant	value <sup>a</sup>
$k_1$	$1 \times 10^8 \text{ M}^{-1} \text{ s}^{-1*}$	$k_1$	$1 \times 10^8 \text{ M}^{-1} \text{ s}^{-1*}$
$k_2$	$350 \text{ s}^{-1*}$	$k_2$	$1 \times 10^6 \text{ M}^{-1} \text{ s}^{-1}$
$k_3$	$1 \times 10^6 \text{ M}^{-1} \text{ s}^{-1*}$	$k_3$	$\geq 5 \times 10^5 \text{ M}^{-1} \text{ s}^{-1}$
$k_4$	$\geq 5 \times 10^6 \text{ M}^{-1} \text{ s}^{-1}$	$k_4$	$\geq 5 \times 10^5 \text{ M}^{-1} \text{ s}^{-1}$
$k_5$	$\geq 5 \times 10^6 \text{ M}^{-1} \text{ s}^{-1}$	$k_5$	$\geq 5 \times 10^5 \text{ M}^{-1} \text{ s}^{-1}$
$k_6$	$\leq 3.5 \times 10^6 \text{ M}^{-1} \text{ s}^{-1}$	$k_6$	$5.5 \times 10^6 \text{ M}^{-1} \text{ s}^{-1*}$
$k_7$	$(0.5-5) \times 10^6 \text{ M}^{-1} \text{ s}^{-1}$		
$k_8$	$5.5 \times 10^6 \text{ M}^{-1} \text{ s}^{-1*}$		

<sup>a</sup> Asterisks indicate values that were experimentally determined. The value of  $k_2$  in the tightly coupled mechanism was assumed to be the same as that for the similar reaction in the branched-chain mechanism ( $k_3$ ). All other values were ranges that were found to predict cyclooxygenase velocities that were within 30% of experimental values.

able (Table 8). Using these techniques, Wei et al. predicted the rates of formation of PGG<sub>2</sub> and PGH<sub>2</sub>, and the rates of disappearance of O<sub>2</sub> and 20:4, for reaction mixtures containing 35 nM COX, 80 μM 20:4, and 100 μM ferulic acid. When the simulated results were compared to experimental values, the branched-chain mechanism proved to be a much better predictor than the tightly coupled mechanism for all parameters. More extensive application of these numerical methods by Kulmacz et al. has shown that the branched-chain mechanism is a good predictor for a number of characteristics of the COX reaction, including inhibition by cyanide and by an exogenous hydroperoxide scavenger (GSH and GSH peroxidase), the effects of peroxidase reductants, and the difference in the rate of reaction using 20:5 as compared to 20:4.<sup>252</sup>

A more subtle weakness in the branched-chain mechanism arose from numerical kinetic modeling studies. Figure 70 shows a composite diagram of the COX reaction mechanism proposed by Bambai and Kulmacz for use in these studies.<sup>126</sup> This mechanism combines concepts included in Figures 25 and 34. Note that the full peroxidase mechanism shown in Figure 25 is included, as is the conversion of compound I to intermediate I. Bambai and Kulmacz proposed that the porphyrin ring of intermediate I could be reduced to the Fe<sup>3+</sup> state and then oxidized through reaction with hydroperoxide to regenerate a species identical to compound I but containing a tyrosyl radical. Reduction of this species would regenerate intermediate I. Together, these reactions form a second peroxidase cycle, which is shown in Figure 70. Bambai and Kulmacz also proposed that all tyrosyl radical-containing species are capable of carrying out the oxygenation of fatty acid substrate, thus generating three potential cyclooxygenase cycles, as shown.

The complex role of reducing substrate in the COX reaction is well-illustrated in Figure 70. Because reducing substrate can reduce compound I, preventing its conversion to intermediate I, and because it can directly reduce intermediate I, one would expect that the addition of reductant to COX reaction mixtures would result in an inhibition of the cy-



**Figure 70.** Expanded branched-chain mechanism proposed by Bambai et al. for mathematical modeling studies. The basic concepts of the branched-chain mechanism have not been altered. However, it is proposed that a second peroxidase cycle may occur in which all species contain a tyrosyl radical. This cycle leads to the formation of three tyrosyl radical-containing species, one of which is intermediate I. All three of these species are proposed to carry out the cyclooxygenase reaction as shown. In addition, conversion of intermediate I to intermediate II, which then results in enzyme inactivation, is shown. Identification of symbols for intermediates is given in Table 1.

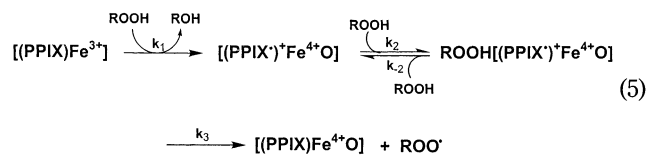
cloxygenase reaction. On the other hand, it has been proposed that reductant can reduce intermediate II to compound II, thus preventing the inactivation of the enzyme via the intermediate II pathway (Figure 70). By preserving enzymatic activity, reducing substrate would be expected to increase cyclooxygenase reaction velocity and the total amount of product formed.

Applying this model, numerical methods predicted that addition of a low concentration of reductant should result in, at most, a 20% increase in reaction velocity and that higher concentrations would be inhibitory.<sup>126</sup> This prediction disagreed with past findings that suggested a much greater increase in reaction velocity in the presence of lower concentrations of reducing substrate.<sup>91,104,106</sup> Bambai and Kulmacz noted that experiments in which reducing substrate had produced large increases in reaction velocity had been carried out using the oxygen electrode to monitor the reaction without correction for electrode diffusion error.<sup>126</sup> They postulated that uncorrected oxygen electrode data would underestimate the reaction velocity in the absence of reducing substrate, since the cyclooxygenase reaction under these conditions was predicted to occur in a very rapid and brief burst. Addition of reductant would slow the initiation but prolong the reaction, leading to a more accurate determination of reaction velocity under these conditions. Thus, the underestimated velocity in the case of the reaction in the absence of reducing substrate would make the stimulatory effect

of reducing substrate appear much greater than it actually was. To test this hypothesis, Bambai and Kulmacz studied the effects of TMPD, phenol, acetaminophen, and Trolox on the cyclooxygenase reaction under conditions of low temperature or elevated pH, which allowed for correction of the oxygen electrode diffusion error. They found that all four reductants increased the reaction velocity at low concentrations, but only by 10–60%, values that were in reasonable agreement with those predicted by the branched-chain model. Bambai and Kulmacz concluded that the primary stimulatory effect of reducing substrates on the cyclooxygenase reaction was through the increase in total number of turnovers, with only a modest effect on reaction velocity. Thus, the branched-chain mechanism had once again correctly predicted COX behavior.

### 5. Remaining Questions

In conclusion, careful comparison of the branched-chain and tightly coupled mechanisms has shown that the branched-chain mechanism is the better model to explain the behavior of COX. An interesting question remains, however, which derives from observations made by Tsai et al. in their studies of the rate of reaction of COX-1 with various hydroperoxides.<sup>123</sup> As noted in section V.A.1, they found that the observed rate constant for the formation of intermediate I/compound II from compound I (as measured by the change in absorbance at 424 nm) was a saturable function of hydroperoxide concentration and also depended on hydroperoxide structure. They tested two kinetic models, using numerical integration, to explain these observations. One model, based on the branched-chain mechanism, was essentially identical to that previously used by Dietz et al. and assumed an initial bimolecular reaction of native enzyme with hydroperoxide to form compound I, followed by a unimolecular conversion of compound I to intermediate I (eq 4A, section V.A.1).<sup>39</sup> The second model, based on the tightly coupled mechanism, assumed a bimolecular reaction between native enzyme and hydroperoxide to form compound I, followed by the formation of a complex between compound I and hydroperoxide, which then is converted to compound II and peroxy radical (eq 5). Both



models explained the dependence of reaction rate on hydroperoxide concentration. However, only the second mechanism explained the dependence of reaction rate on hydroperoxide structure. Tsai et al. argued that, despite these findings, the preponderance of data supported the branched-chain mechanism over the tightly coupled model. They suggested that the differences in rate of intermediate I formation observed in the presence of various hydroperoxides could be due to a conformational change in the enzyme resulting from the binding of the hydroper-

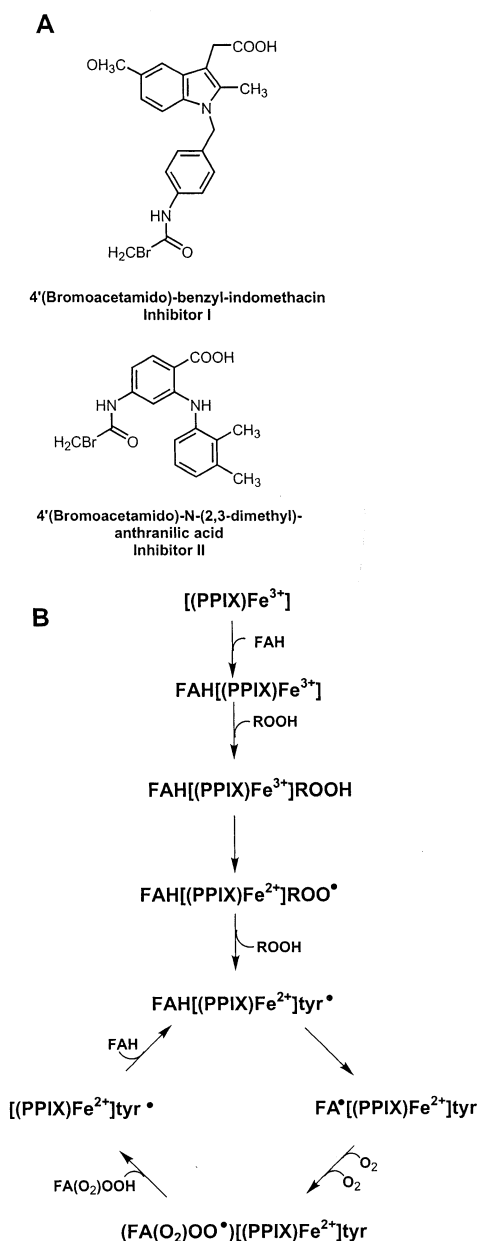
oxide to some site on the enzyme that is unrelated to the actual conversion of compound I to intermediate I. However, there are no additional data to support this hypothesis. Clearly, the unimolecular electron transfer converting compound I to intermediate I should be independent of both hydroperoxide concentration and identity. Thus, this observation remains an unexplained contradiction to the branched-chain mechanism.

### C. The Ferrous Iron Mechanism

Tang et al. have proposed a modification of the branched-chain mechanism, based on the results of their studies of a COX-1 protein, in which the peroxidase activity had been selectively and irreversibly inactivated by covalent modification.<sup>253,254</sup> These researchers synthesized two affinity labeling agents, 1-[4-(bromoacetamido)benzyl]-5-methoxy-2-methylindole-3-acetic acid (inhibitor I) and 4-(bromoacetamido)-*N*-(2,3-dimethylphenyl)anthranilic acid (inhibitor II), through modification of the NSAIDs, indomethacin and mefenamic acid, respectively (Figure 71 A).<sup>253</sup> Each inhibitor caused time-dependent, irreversible inactivation of both the cyclooxygenase and peroxidase activities of COX-1. Thus, these compounds behaved differently from most NSAIDs, which inhibit the cyclooxygenase activity only. The two enzyme activities were inactivated with the same kinetics, suggesting a single binding site; however, both inhibitors were shown to form complexes in which two inhibitor molecules were covalently bound to the COX-1 protein. Furthermore, when either compound was incubated with COX-1 in the presence of saturating concentrations of the reversible inhibitor, mefenamic acid, the cyclooxygenase activity was selectively preserved, and only one molecule of inhibitor I or inhibitor II became protein-bound. These results suggested that each inhibitor binds to both the cyclooxygenase and the peroxidase active sites, resulting in irreversible inactivation of both activities.

COX-1 enzyme (20  $\mu\text{M}$ ) that had been treated for 24 h with inhibitor I (5.3 mM) in the presence of 150  $\mu\text{M}$  mefenamic acid retained 70% of the cyclooxygenase activity, but the peroxidase activity was undetectable. Cyclooxygenase activity was measured by oxygen electrode and was reported in terms of the rate of oxygen consumption. The investigators did not indicate whether they observed unusual lag phases, as has been noted for other COX enzymes with reduced peroxidase activity (sections VIII.E and IX). Their ability to generate an enzyme with intact cyclooxygenase activity that was totally devoid of peroxidase activity led Tang et al. to question the branched-chain mechanism. They argued that, in the absence of any peroxidase activity, it should be impossible to activate the cyclooxygenase via oxidation of the enzyme to form compound I. Therefore, some other mechanism must lead to tyrosyl radical formation.<sup>253</sup>

In their exploration of alternative mechanisms of tyrosyl radical formation, Tang et al. carried out comparative studies of the kinetics of compound I and compound II formation in COX-1 versus COX-2.<sup>254</sup>



**Figure 71.** (A) Structures of the two compounds synthesized by Tang et al. as irreversible covalent inhibitors of COX.<sup>253</sup> (B) Mechanism proposed by Tang et al. for the cyclooxygenase reaction. Native enzyme forms a complex with fatty acid substrate (FAH) and hydroperoxide (ROOH). Oxidation of the hydroperoxide to the peroxy radical (ROO<sup>•</sup>) converts the native enzyme to its ferrous form. The peroxy radical then oxidizes Tyr-385, regenerating the hydroperoxide. The bound fatty acid may now be oxidized to form the fatty acid radical (FA<sup>•</sup>). Addition of two molecules of oxygen yields the peroxy radical of the endoperoxide (FA(O<sub>2</sub>)OO<sup>•</sup>). Subsequent reduction of this peroxy radical to the corresponding hydroperoxide (FA(O<sub>2</sub>)OOH) regenerates the tyrosyl radical.<sup>254</sup>

Using either 20:4 or EtOOH as substrate, they discovered that compound I and compound II formation in COX-1 was very rapid and preceded 20:4 oxygenation, as monitored simultaneously by oxygen electrode. In contrast, when the same experiments were performed with COX-2, they discovered that compound I and compound II were formed very rapidly when 20:4 was used as substrate, but much more slowly when the substrate was EtOOH. Since

the oxygenation of 20:4 occurred much more rapidly than the formation of compound I from EtOOH, Tang et al. concluded that the reaction of COX-2 with hydroperoxide contaminants in the 20:4 substrate could not account for activation of the cyclooxygenase activity. This conclusion was consistent with their hypothesis that compound I formation through the peroxidase reaction is not the mechanism for cyclooxygenase activation.

Tang et al. also explored the spectral changes that occurred when preparations of COX-2 that had been acetylated with aspirin reacted with 20:4 to form 15-HETE (described in section VIII.A). They observed a spectral species that was distinctly different from either compound I or intermediate I/compound II.<sup>254</sup> Comparison of this spectrum to that of COX-2 that had been treated with sodium dithionite under anaerobic conditions led Tang et al. to conclude that the identity of the new species was ferrous COX-2. From these results, they proposed an alternative mechanism for cyclooxygenase activation (Figure 71B). In this mechanism, native COX initially forms a complex with both 20:4 and hydroperoxide. The hydroperoxide reacts with ferric iron to yield ferrous iron and the peroxy radical. The peroxy radical then abstracts a hydrogen atom from Tyr-385 to regenerate the hydroperoxide and form the active tyrosyl radical species. The remaining steps of the cyclooxygenase reaction are very similar to those proposed in the branched-chain mechanism and are shown in Figure 71B. Note that this mechanism does not require a peroxidase cycle, so inactivation of the peroxidase reaction should not lead to loss of cyclooxygenase activity.

The mechanism proposed by Tang et al. was tested by Goodwin et al. in experiments in which the reduction potential of COX-1 and COX-2 were directly measured.<sup>148</sup> The values obtained,  $-167 \pm 2$  and  $-156 \pm 1$  mV, respectively, were too low to account for any of the oxidation reactions that must occur during the cyclooxygenase reaction, including abstraction of a hydrogen atom from 20:4 (reduction potential of 600 mV), oxidation of a hydroperoxide to a peroxy radical (reduction potential of 1020–1100 mV), and oxidation of tyrosine to the tyrosyl radical (reduction potential of 850–930 mV). Goodwin et al. also showed that substitution of the proximal heme histidine ligand (His-388) with tyrosine did not significantly reduce the cyclooxygenase activity of COX-2 (described in section VIII.E). This substitution is expected to destabilize the Fe<sup>2+</sup> state and should lead to a loss of activity if the ferrous enzyme is involved in the cyclooxygenase reaction. The low reduction potential and lack of effect of the H388Y mutation were inconsistent with a role for the ferrous enzyme as proposed in Figure 71. These inconsistencies notwithstanding, the exact nature and function of the new spectral species detected by Tang et al. during the reaction of aspirin-treated COX-2 remains an interesting question.

A critical observation supporting the mechanism shown in Figure 71 was the slow reaction of COX-2 with EtOOH, as described above. In subsequent studies, Lu et al. verified that the rate constant for

the reaction of COX-1 with EtOOH to form compound I ( $3.4 \times 10^6 \text{ M}^{-1} \text{ s}^{-1}$ ) was 7-fold higher than that for the same reaction of COX-2.<sup>211</sup> However, they also discovered that the rate constants for the reaction of the two isoforms with 15-HPETE were almost identical (discussed in section VIII.B) and an order of magnitude higher than the value obtained for EtOOH and COX-1. Since 15-HPETE is more likely to represent the structure of a hydroperoxide that would be present in preparations of 20:4 than EtOOH, these results suggest that the reaction of hydroperoxide with either COX-1 or COX-2 is likely to be rapid enough to account for cyclooxygenase activation.

Tang et al. primarily supported their proposed mechanism on the basis of the intact cyclooxygenase activity of enzymes lacking peroxidase activity.<sup>253</sup> They argued that the existence of such enzymes is inconsistent with the branched-chain hypothesis. A number of COX enzymes have been described in which cyclooxygenase activity remains intact in the presence of markedly reduced peroxidase activity. These include the COX-1 enzyme substituted with  $\text{Mn}^{3+}$ -PPIX, and the COX-2 mutants, H207A and H388Y (discussed in sections VIII.E and IX). In each of these cases, very low levels of peroxidase activity are detectable, and it is possible that, with very sensitive peroxidase assays, residual activity also may be detectable in the enzyme generated by Tang et al.<sup>253</sup> Very early studies by Kulmacz and Lands demonstrated that the concentration of peroxide required for cyclooxygenase activation was much lower than the apparent  $K_m$  for the peroxidase activity.<sup>105</sup> It is notable that the only reaction of the peroxidase cycle required for cyclooxygenase activation, according to the branched-chain hypothesis, is the initial interaction between native enzyme and hydroperoxide to form compound I. Notably, the formation of a compound I-like species has been demonstrated for Mn-COX-1 (section IX.A). Therefore, it is conceivable that a derivative of COX-1 or COX-2 may have very low activity for the overall peroxidase cycle but may retain the ability to form a higher oxidation state that can oxidize Tyr-385.

In conclusion, the preponderance of extant evidence supports the branched-chain hypothesis. The existence of the appropriate enzyme intermediates has been demonstrated, and the kinetics of their formation and decomposition agree with the kinetics of the cyclooxygenase reaction. The tyrosyl radical has been shown to be both kinetically and chemically competent to play the proposed key role in the cyclooxygenase reaction, and the interaction between the cyclooxygenase and peroxidase reactions is well explained by this mechanism.

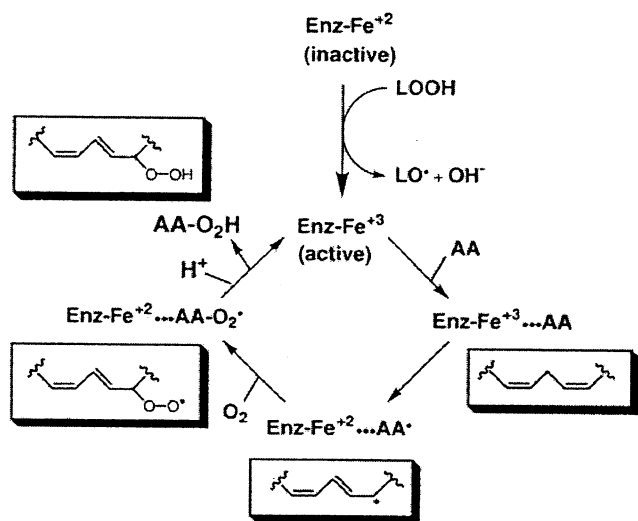
### ***XIII. COX as a Catalyst for Fatty Acid Autoxidation***

In the Introduction, we proposed the concept that cyclooxygenase catalyzes a controlled free radical chain reaction. In light of all the mechanistic information summarized above, it is appropriate to revisit this hypothesis and ask what it means at a practical level. There are, indeed, parallels between the cyclooxygenase-catalyzed oxygenation of polyunsaturated

fatty acids and their free radical autoxidation. A lag phase is evident prior to the onset of the maximal rate of oxygenation and the chemical steps in the enzymatic oxidation, which involve  $\text{O}_2$  coupling to carbon-centered radicals to form peroxy radicals are identical to those in autoxidation. As in autoxidation, the lag phase in cyclooxygenase catalysis corresponds to the time required for attainment of the steady-state rate of oxidation.

The initiator in free radical autoxidations is often poorly characterized and serves only to generate enough peroxy radicals to propagate steady-state oxidation. The initiator in the case of cyclooxygenase catalysis is the peroxidase activity of the enzyme. As in a free radical autoxidation, the peroxidase activates radical chain oxidation, but once it has done so, it serves no further direct role in catalysis. [The only need for continued peroxidase function is to reactivate any enzyme that may have returned to the resting state because a  $\text{PGG}_2$  peroxy radical diffused off the protein before reoxidizing Tyr-385, or because of reduction by peroxidase reductant.] And as in an autoxidation reaction, one initiation event by the peroxidase leads to the consumption of many fatty acid molecules. However, there is a major difference between the nonenzymatic and enzymatic oxygenation of fatty acids, which has to do with the involvement of protein tyrosyl radicals in the initiation and propagation of fatty acid oxidation. In an autoxidation, the initiator directly oxidizes a fatty acid, whereas in cyclooxygenase catalysis, the initiator oxidizes the protein to a tyrosyl radical, which oxidizes the fatty acid. The protein tyrosyl radical is regenerated at the end of every catalytic cycle and propagates the radical chain by oxidizing the next molecule of fatty acid. Since the tyrosyl radical is present in the active site of a COX protein, its continual regeneration allows the protein to control substrate specificity, rate, and stereochemistry of oxygenation. The intermediacy of protein radicals is the device that cyclooxygenase has used to adopt a facile chemical process for polyunsaturated fatty acid oxygenation. It is notable, however, that the propagation of the reaction by cyclooxygenase requires the continued presence of active enzyme. Therefore, COX auto-inactivation may be considered a chain-terminating event. Furthermore, as the peroxidase activity serves to prevent the accumulation of peroxides, which mediate enzyme inactivation, the peroxidase indirectly facilitates the cyclooxygenase reaction by preserving enzyme activity.

A different strategy was used to generate lipoxigenase enzymes, which also catalyze what appears to be a controlled free radical autoxidation of polyunsaturated fatty acids. Lipoxigenases catalyze the oxygenation of 20:4 to monohydroperoxide products but, in contrast to cyclooxygenase, do not generate protein radicals as intermediates in catalysis. Lipoxigenases use a high-potential non-heme iron as the fatty acid oxidizing agent, and this oxidant is regenerated in the final step of each catalytic cycle (Figure 72). The redox potential of the  $\text{Fe}^{3+}$  enzyme is quite high compared to that of cyclooxygenase (+700 vs -150 mV), which enables it to directly oxidize the substrate without generating a higher



**Figure 72.** Catalytic cycle of fatty acid oxygenation by lipoxygenases.

oxidation state.<sup>255,256</sup> In fact, the redox potential of the  $\text{Fe}^{3+}$  enzyme is sufficiently high that the resting enzyme occurs as the  $\text{Fe}^{2+}$  form, which is catalytically inactive. A lag phase is evident in lipoxygenase catalysis, which corresponds to the requirement for oxidation of the  $\text{Fe}^{2+}$  enzyme to the  $\text{Fe}^{3+}$  enzyme by a molecule of fatty acid hydroperoxide or some other hydroperoxide.<sup>257</sup> Thus, although catalysis by cyclooxygenase and that by lipoxygenase appear qualitatively similar, the mechanisms employed by the two enzymes are very different.

#### XIV. Conclusion

COX proteins hold a special fascination for biomedical scientists because of the interesting chemistry they catalyze, the role of their PG products as mediators of signaling pathways, and the importance of the cyclooxygenase active sites as targets for a large and growing class of drugs that alleviate human suffering. COX enzymes have adapted the facile chemical process of fatty acid autoxidation to provide a highly efficient synthetic route to PG endoperoxides. The introduction of a protein radical-based mechanism for fatty acid oxidation has conferred kinetic, regiochemical, and stereochemical control over a series of reactions that normally generate hundreds of compounds in an uncontrolled fashion.

Intensive studies over the past 15 years have provided strong support for the basic tenets of the branched-chain mechanism linking peroxidase catalysis to cyclooxygenase activation via the formation of a protein tyrosyl radical.<sup>39,144</sup> The rates of many of the electron-transfer reactions have been measured, the tyrosyl radical at position 385 has been trapped, and its ability to oxidize fatty acid substrates has been documented. The structural elements of the COX proteins responsible for substrate binding and oxidation have been identified, and the ability of individual residues to direct the chemistry of peroxy radical intermediates has been elucidated. It is fair to say that the cyclooxygenase mechanism is one of the most well-understood of all those in "radical enzymology."

The synergy between the peroxidase and cyclooxygenase activities is a thing of beauty. The use of an intermediate in the peroxidase catalytic cycle to oxidize the critical Tyr-385 solves the problem of generating a thermodynamically reasonable cascade of reactions to effect fatty acid oxidation. The juxtaposition of the peroxidase and cyclooxygenase active sites on opposite faces of the heme enables COX proteins to utilize a single prosthetic group to service two active sites while maximizing the efficiency of intramolecular electron transfer between them. And the requirement that the peroxidase must only *activate* the cyclooxygenase but not support its continuing turnover ensures that some PG endoperoxides can be made, regardless of the mix of reducing agents in a particular cellular environment. Considering the importance of the peroxidase activity to the cyclooxygenase reaction, it is not surprising that COX proteins evolved from a peroxidase superfamily.

Although there is strong evidence for the branched-chain mechanism, it should be clear from the foregoing treatment that there are still points of debate and experimental uncertainties that should not be swept under the rug. The reason for the dependence of the rate of intermediate I formation on hydroperoxide structure, and the possible role of a ferrous enzyme in aspirin-modified COX, are two cases in point. Also, attention is beginning to focus on alternate substrates for COX-2 as a possible justification for its existence. This may be fertile ground for plowing. So, there remain plenty of interesting things to do, and the experiments will build on the substantial base of structural and functional information summarized above.

#### XV. Abbreviations

COX	cyclooxygenase or prostaglandin H synthase or 5,8,11,14-eicosatetraenoate:oxygen oxidoreductase (EC 1.14.99.1)
PG	prostaglandin
TX	thromboxane
20:4	5,8,11,14-eicosatetraenoic acid or arachidonic acid
20:3	8,11,14-eicosatrienoic acid
20:2	11,14-eicosadienoic acid
18:2	9,12-octadecadienoic acid or linoleic acid
$\alpha$ -18:3	9,12,15-octadecatrienoic acid or $\alpha$ -linolenic acid
18:4	6,9,12,15-octadecatetraenoic acid or stearidonic acid
11-HPETE	11-hydroperoxy-5,8,12,14-eicosatetraenoic acid
11-HETE	11-hydroxy-5,8,12,14-eicosatetraenoic acid
15-HPETE	15-hydroperoxy-5,8,11,13-eicosatetraenoic acid
15-HETE	15-hydroxy-5,8,11,13-eicosatetraenoic acid
15-KETE	15-keto-5,8,11,13-eicosatetraenoic acid
NSAID	non-steroidal anti-inflammatory drug
PPIX	protoporphyrin IX
DDC	diethyldithiocarbamate
PPHP	5-phenyl-4-pentenyl hydroperoxide
TMPD	<i>N,N,N,N</i> -tetramethylphenylenediamine
ABTS	2,2'-azino-bis(3-ethylbenzthiazoline-6-sulfonic acid)
EtOOH	ethyl hydroperoxide
<i>m</i> -Cl PBA	<i>m</i> -chloroperoxybenzoic acid

EPR	electronic paramagnetic resonance spectroscopy
GSH	glutathione
Mn-COX	COX substituted with Mn <sup>3+</sup> -protoporphyrin IX
AEA	anandamide, arachidonic acid ethanolamide

## XVI. Acknowledgments

Research on COX structure and function in the authors' laboratory is supported by research grants from the National Institutes of Health (CA89450 and GM15431). The authors are grateful to Jeffery Prusakiewicz for assistance with molecular graphics.

## XVII. Note Added in Proof

Recent sequence analysis of human COX-1 cDNA's indicates that intron 1, which is retained in COX-3, is 94 nucleotides in length compared to 93 nucleotides in length in the mouse and dog. This would appear to shift the reading frame of the coding sequence for the rest of the protein out-of-frame, generating a catalytically inactive protein. Dinchuk, J. E.; Liu, R. Q.; Trzaskos, J. M. *Immunol. Lett.* **2003**, *86*, 12.

## XVIII. References

- Hamberg, M.; Samuelsson, B. *Proc. Natl. Acad. Sci. U.S.A.* **1973**, *70*, 899.
- Nugteren, D. H.; Hazelhof, E. *Biochim. Biophys. Acta* **1973**, *326*, 448.
- Hamberg, M.; Svensson, J.; Wakabayashi, T.; Samuelsson, B. *Proc. Natl. Acad. Sci. U.S.A.* **1974**, *71*, 345.
- Smith, W. *Adv. Exp. Med. Biol.* **1997**, *400B*, 989.
- Funk, C. D. *Science* **2001**, *294*, 1871.
- Vane, J. R. *Nature New Biol.* **1971**, *231*, 232.
- Vane, J. R.; Botting, R. M. *Scand. J. Rheumatol.* **1996**, *25* (Suppl. 102), 9.
- Smith, W. L.; DeWitt, D. L.; Garavito, R. M. *Annu. Rev. Biochem.* **2000**, *69*, 145.
- Xie, W.; Chipman, J. G.; Robertson, D. L.; Erikson, R. L.; Simmons, D. L. *Proc. Natl. Acad. Sci. U.S.A.* **1991**, *88*, 2692.
- Kujubu, D. A.; Fletcher, B. S.; Varnum, B. C.; Lim, R. W.; Herschman, H. R. *J. Biol. Chem.* **1991**, *266*, 12866.
- O'Banion, M. K.; Winn, V. D.; Young, D. A. *Proc. Natl. Acad. Sci. U.S.A.* **1992**, *89*, 4888.
- Hla, T.; Neilson, K. *Proc. Natl. Acad. Sci. U.S.A.* **1992**, *89*, 7384.
- Herschman, H. R. *Biochim. Biophys. Acta Lipids Lipid Metab.* **1996**, *1299*, 125.
- Vane, J. R.; Bakhle, Y. S.; Botting, R. M. *Annu. Rev. Pharmacol. Toxicol.* **1998**, *38*, 97.
- Masferrer, J. L.; Zweifel, B. S.; Manning, P. T.; Hauser, S. D.; Leahy, K. M.; Smith, W. G.; Isakson, P. C.; Seibert, K. *Proc. Natl. Acad. Sci. U.S.A.* **1994**, *91*, 3228.
- DeWitt, D. L. *Mol. Pharmacol.* **1999**, *55*, 625.
- Silverstein, F. E.; Faich, G.; Goldstein, J. L.; Simon, L. S.; Pincus, T.; Whelton, A.; Makuch, R.; Eisen, G.; Agrawal, N. M.; Stenson, W. F.; Burr, A. M.; Zhao, W. W.; Kent, J. D.; Lefkowitz, J. B.; Verburg, K. M.; Geis, G. S. *JAMA, J. Am. Med. Assoc.* **2000**, *284*, 1247.
- Smith, W. L.; Garavito, R. M.; DeWitt, D. L. *J. Biol. Chem.* **1996**, *271*, 33157.
- Picot, D.; Loll, P. J.; Garavito, R. M. *Nature* **1994**, *367*, 243.
- Luong, C.; Miller, A.; Barnett, J.; Chow, J.; Ramesha, C.; Browner, M. F. *Nature Struct. Biol.* **1996**, *3*, 927.
- Kurumbail, R. G.; Stevens, A. M.; Gierse, J. K.; McDonald, J. J.; Stegeman, R. A.; Pak, J. Y.; Gildehaus, D.; Miyashiro, J. M.; Penning, T. D.; Seibert, K.; Isakson, P. C.; Stallings, W. C. *Nature* **1996**, *384*, 644.
- Chen, W.; Pawelek, T. R.; Kulmacz, R. J. *J. Biol. Chem.* **1999**, *274*, 20301.
- Guo, Q.; Wang, L.-H.; Ruan, K.-H.; Kulmacz, R. J. *J. Biol. Chem.* **1996**, *271*, 19134.
- Wong, E.; Bayly, C.; Waterman, H. L.; Riendeau, D.; Mancini, J. A. *J. Biol. Chem.* **1997**, *272*, 9280.
- Greig, G. M.; Francis, D. A.; Falgueyret, J. P.; Ouellet, M.; Percival, M. D.; Roy, P.; Bayly, C.; Mancini, J. A.; O'Neill, G. P. *Mol. Pharmacol.* **1997**, *52*, 829.
- Rieke, C. J.; Mulichak, A. M.; Garavito, R. M.; Smith, W. L. *J. Biol. Chem.* **1999**, *274*, 17109.
- Kalgutkar, A. S.; Crews, B. C.; Rowlinson, S. W.; Marnett, A. B.; Kozak, K. R.; Remmel, R. P.; Marnett, L. J. *Proc. Natl. Acad. Sci. U.S.A.* **2000**, *97*, 925.
- Kozak, K. R.; Rowlinson, S. W.; Marnett, L. J. *J. Biol. Chem.* **2000**, *275*, 33744.
- Chandrasekharan, N. V.; Dai, H.; Roos, K. L.; Evanson, N. K.; Tomsik, J.; Elton, T. S.; Simmons, D. L. *Proc. Natl. Acad. Sci. U.S.A.* **2002**, *99*, 13926.
- Van Der Ouderaa, F. J.; Buytenhek, M.; Nugteren, D. H.; Van Dorp, D. A. *Biochim. Biophys. Acta* **1977**, *487*, 315.
- Van Der Ouderaa, F. J.; Buytenhek, M.; Slikkerveer, F. J.; Van Dorp, D. A. *Biochim. Biophys. Acta* **1979**, *572*, 29.
- Miyamoto, T.; Ogino, N.; Yamamoto, S.; Hayaishi, O. *J. Biol. Chem.* **1976**, *251*, 2629.
- Ogino, N.; Ohki, S.; Yamamoto, S.; Hayaishi, O. *J. Biol. Chem.* **1978**, *253*, 5061.
- Malkowski, M. G.; Ginell, S. L.; Smith, W. L.; Garavito, R. M. *Science* **2000**, *289*, 1933.
- Spencer, A. G.; Woods, J. W.; Arakawa, T.; Singer, I. I.; Smith, W. L. *J. Biol. Chem.* **1998**, *273*, 9886.
- Xiao, G.; Chen, W.; Kulmacz, R. J. *J. Biol. Chem.* **1998**, *273*, 6801.
- Ohki, S.; Ogino, N.; Yamamoto, S.; Hayaishi, O. *J. Biol. Chem.* **1979**, *254*, 829.
- Kulmacz, R. J.; Lands, W. E. M. *J. Biol. Chem.* **1984**, *259*, 6358.
- Dietz, R.; Nastainczyk, W.; Ruf, H. H. *Eur. J. Biochem.* **1988**, *171*, 321.
- Daiyasu, H.; Toh, H. *J. Mol. Evol.* **2000**, *51*, 433.
- Stubbe, J. S.; van der Donk, W. A. *Chem. Rev.* **1998**, *98*, 705.
- Lundberg, W. O. *Autoxidation and Antioxidants*, John Wiley and Sons: New York, 1961.
- Kohn, H. I.; Liversedge, N. *J. Pharmacol. Exp. Ther.* **1944**, *82*, 292.
- Bernheim, F.; Bernheim, M. L. C.; Wilbur, K. M. *J. Biol. Chem.* **1948**, *174*, 257.
- Gardner, H. W. *Free Radical Biol. Med.* **1989**, *7*, 65.
- Nugteren, D. H.; Vonkemann, H.; Van Dorp, D. A. *Recl. Trav. Chim.* **1967**, *86*, 1237.
- Pryor, W. A.; Stanley, J. P. *J. Org. Chem.* **1975**, *40*, 3615.
- Porter, N. A.; Nixon, J.; Isaac, R. *Biochim. Biophys. Acta* **1976**, *441*, 506.
- Porter, N. A. *Acc. Chem. Res.* **1986**, *19*, 262.
- Porter, N. A.; Lehman, L. S.; Weber, B. A.; Smith, K. A. *J. Am. Chem. Soc.* **1981**, *103*, 6447.
- Brash, A. R. *Lipids* **2000**, *35*, 947.
- Mills, K. A.; Caldwell, S. E.; Dubay, G. R.; Porter, N. A. *J. Am. Chem. Soc.* **1992**, *114*, 9689.
- Tallman, K. A.; Pratt, D. A.; Porter, N. A. *J. Am. Chem. Soc.* **2001**, *123*, 11827.
- Porter, N. A.; Caldwell, S. E.; Mills, K. A. *Lipids* **1995**, *30*, 277.
- Morrow, J. D.; Roberts, L. J., II. *Methods Enzymol.* **1999**, *300*, 3.
- Mayo, F. R. *Acc. Chem. Res.* **1968**, *1*, 193.
- Howard, J. A. *Free Radicals Volume II*; Wiley-Interscience: New York, 1973; p 3.
- Burton, G. W.; Foster, D. O.; Perly, B.; Slater, T. F.; Smith, I. C.; Ingold, K. U. *Philos. Trans. R. Soc. London B: Biol. Sci.* **1985**, *311*, 565.
- Ingold, K. *Acc. Chem. Res.* **1969**, *2*, 1.
- Kurzrok, R.; Lieb, C. *Proc. Soc. Exp. Biol.* **1930**, *28*, 268.
- Bergstrom, S.; Sjoval, J. *Acta Chem. Scand.* **1960**, *14*, 1693.
- Bergstrom, S.; Sjoval, J. *Acta Chem. Scand.* **1960**, *14*, 1701.
- Bergstrom, S.; Ryhage, R.; Samuelsson, B.; Sjoval, J. *Acta Chem. Scand.* **1962**, *16*, 501.
- Hamberg, M.; Svensson, J.; Samuelsson, B. *Proc. Natl. Acad. Sci. U.S.A.* **1975**, *72*, 2994.
- Bunting, S.; Gryglewski, R.; Moncada, S.; Vane, J. R. *Prostaglandins* **1976**, *12*, 897.
- Porter, N. A.; Funk, M. O. *J. Org. Chem.* **1975**, *40*, 3614.
- Lands, W. E. M.; LeTellier, P. R.; Rome, L. H.; Vanderhoek, J. Y. *Advances in the Biosciences*; Pergamon Vieweg: Oxford, 1973; p 15.
- Theorell, H.; Holman, R. T.; Åkeson, Å. *Acta Chem. Scand.* **1946**, *1*, 571.
- Van Dorp, D. A.; Berthuis, R. K.; Nugteren, D. H.; Vonkeman, H. *Biochim. Biophys. Acta* **1964**, *90*, 204.
- Bergstrom, S.; Danielsson, H.; Samuelsson, B. *Biochim. Biophys. Acta* **1964**, *90*.
- Laneville, O.; Breuer, D. K.; Xu, N.; Huang, Z. H.; Gage, D. A.; Watson, J. T.; Lagarde, M.; DeWitt, D. L.; Smith, W. L. *J. Biol. Chem.* **1995**, *270*, 19330.
- Klenberg, D.; Samuelsson, B. *Acta Chem. Scand.* **1965**, *19*, 16.
- Hamberg, M.; Samuelsson, B. *J. Biol. Chem.* **1967**, *242*, 5336.
- Ryhage, R.; Samuelsson, B. *Biochem. Biophys. Res. Commun.* **1965**, *19*, 279.
- Nugteren, D. H.; Van Dorp, D. A. *Biochim. Biophys. Acta* **1965**, *98*, 652.

- (76) Samuelsson, B. *J. Am. Chem. Soc.* **1965**, *87*, 3011.
- (77) Nugteren, D. H.; Beerthuis, R. K.; Van Dorp, D. A. *Recl. Trav. Chim.* **1966**, *85*, 405.
- (78) Foss, P.; Takeguchi, C.; Tai, H.; Sih, C. *Ann. N.Y. Acad. Sci.* **1971**, *180*, 126.
- (79) Samuelsson, B.; Granstrom, E.; Green, K.; Hamberg, M. *Ann. N.Y. Acad. Sci.* **1971**, *180*, 138.
- (80) Anggård, E.; Samuelsson, B. *J. Biol. Chem.* **1965**, *240*, 3518.
- (81) Wlodawer, P.; Samuelsson, B. *J. Biol. Chem.* **1973**, *248*, 5673.
- (82) Hamberg, M.; Samuelsson, B. *J. Biol. Chem.* **1967**, *242*, 5344.
- (83) Marnett, L. J.; Maddipati, K. R. *Peroxidases in chemistry and biology*, Vol. 1; CRC Press: Boca Raton, FL, 1991; p 293.
- (84) Hemler, M. E.; Crawford, C. G.; Lands, W. E. M. *Biochemistry* **1978**, *17*, 1772.
- (85) Hecker, M.; Ullrich, V.; Fischer, C.; Meese, C. O. *Eur. J. Biochem.* **1987**, *169*, 113.
- (86) Samuelsson, B. *Prog. Biochem. Pharmacol.* **1967**, *3*, 59.
- (87) Yoshimoto, A.; Ito, H.; Tomita, K. *J. Biochem.* **1970**, *68*, 487.
- (88) Marnett, L. J.; Wlodawer, P.; Samuelsson, B. *J. Biol. Chem.* **1975**, *250*, 8510.
- (89) O'Brien, P. J.; Rahimtula, A. *Biochem. Biophys. Res. Commun.* **1976**, *70*, 832.
- (90) Pagels, W. R.; Sachs, R. J.; Marnett, L. J.; DeWitt, D. L.; Day, J. S.; Smith, W. L. *J. Biol. Chem.* **1983**, *258*, 6517.
- (91) Hsuanyu, Y.; Dunford, H. B. *J. Biol. Chem.* **1992**, *267*, 17649.
- (92) Kulmacz, R. J.; Miller, J. F., Jr.; Lands, W. E. M. *Biochem. Biophys. Res. Commun.* **1985**, *130*, 918.
- (93) Marshall, P. J.; Kulmacz, R. J. *Arch. Biochem. Biophys.* **1988**, *266*, 162.
- (94) Kulmacz, R. J. *Prostaglandins* **1987**, *34*, 225.
- (95) Raz, A.; Needleman, P. *Biochem. J.* **1990**, *269*, 603.
- (96) Cook, H. W.; Ford, G.; Lands, W. E. *Anal. Biochem.* **1979**, *96*, 341.
- (97) Bailey, J. M.; Bryant, R. W.; Whiting, J.; Salata, K. *J. Lipid Res.* **1983**, *24*, 1419.
- (98) Setty, B. N.; Stuart, M. J.; Walenga, R. W. *Biochim. Biophys. Acta* **1985**, *833*, 484.
- (99) Weller, P. E.; Markey, C. M.; Marnett, L. J. *Arch. Biochem. Biophys.* **1985**, *243*, 633.
- (100) Lands, W. E. M.; Lee, R.; Smith, W. L. *Ann. N.Y. Acad. Sci.* **1971**, *180*, 107.
- (101) Cook, H. W.; Lands, W. E. *Biochem. Biophys. Res. Commun.* **1975**, *65*, 464.
- (102) Hemler, M. E.; Graff, G.; Lands, W. E. M. *Biochem. Biophys. Res. Commun.* **1978**, *85*, 1325.
- (103) Hemler, M. E.; Cook, H. W.; Lands, W. E. M. *Arch. Biochem. Biophys.* **1979**, *193*, 340.
- (104) Hemler, M. E.; Lands, W. E. M. *J. Biol. Chem.* **1980**, *255*, 6253.
- (105) Kulmacz, R. J.; Lands, W. E. M. *Prostaglandins* **1983**, *25*, 531.
- (106) Kulmacz, R. J.; Lands, W. E. M. *Prostaglandins* **1985**, *29*, 175.
- (107) Lands, W. E.; Cook, H. W.; Rome, L. H. *Adv. Prostaglandin Thromboxane Res.* **1976**, *1*, 7.
- (108) Strieder, S.; Schaible, K.; Scherer, H.-J.; Dietz, R.; Ruf, H. H. *J. Biol. Chem.* **1992**, *267*, 13870.
- (109) Odenwaller, R.; Maddipati, K. R.; Marnett, L. J. *J. Biol. Chem.* **1992**, *267*, 13863.
- (110) Smith, W. L.; Lands, W. E. M. *Biochemistry* **1972**, *11*, 3276.
- (111) Egan, R. W.; Paxton, J.; Kuehl, F. A. *J. Biol. Chem.* **1976**, *251*, 7329.
- (112) Markey, C. M.; Alward, A.; Weller, P. E.; Marnett, L. J. *J. Biol. Chem.* **1987**, *262*, 6266.
- (113) Kulmacz, R. J. *Arch. Biochem. Biophys.* **1986**, *249*, 273.
- (114) Wu, G.; Wei, C. H.; Kulmacz, R. J.; Osawa, Y.; Tsai, A. L. *J. Biol. Chem.* **1999**, *274*, 9231.
- (115) Wu, G.; Vuletich, J. L.; Kulmacz, R. J.; Osawa, Y.; Tsai, A. L. *J. Biol. Chem.* **2001**, *276*, 19879.
- (116) Gaspard, S.; Chottard, G.; Mahy, J. P.; Mansuy, D. *Eur. J. Biochem.* **1996**, *238*, 529.
- (117) Lou, B. S.; Snyder, J. K.; Marshall, P.; Wang, J. S.; Wu, G.; Kulmacz, R. J.; Tsai, A. L.; Wang, J. *Biochemistry* **2000**, *39*, 12424.
- (118) Kulmacz, R. J.; Tsai, A.-L.; Palmer, G. *J. Biol. Chem.* **1987**, *262*, 10524.
- (119) O'Brien, P. J. *Prog. Lipid Res.* **1981**, *20*, 295.
- (120) Nastainczyk, W.; Schuhn, D.; Ullrich, V. *Eur. J. Biochem.* **1984**, *144*, 381.
- (121) Lambeir, A. M.; Markey, C. M.; Dunford, H. B.; Marnett, L. J. *J. Biol. Chem.* **1985**, *260*, 14894.
- (122) Poulos, T. L.; Kraut, J. *J. Biol. Chem.* **1980**, *255*, 10322.
- (123) Tsai, A.; Wei, C.; Baek, H. K.; Kulmacz, R. J.; Van Wart, H. E. *J. Biol. Chem.* **1997**, *272*, 8885.
- (124) Hsuanyu, Y.; Dunford, H. B. *Arch. Biochem. Biophys.* **1992**, *292*, 213.
- (125) Dunford, H. B.; Stillman, J. S. *Coord. Chem. Rev.* **1976**, *19*, 187.
- (126) Bambai, B.; Kulmacz, R. J. *J. Biol. Chem.* **2000**, *275*, 27608.
- (127) Takeguchi, C.; Kono, E.; Sih, C. *J. Biochemistry* **1971**, *10*, 2372.
- (128) Sih, C. J.; Takeguchi, C.; Foss, P. *J. Am. Chem. Soc.* **1970**, *92*, 6670.
- (129) Vanderhoek, J. Y.; Lands, W. E. *Biochim. Biophys. Acta* **1973**, *296*, 382.
- (130) Egan, R. W.; Gale, P. H.; Kuehl, F. A., Jr. *J. Biol. Chem.* **1979**, *254*, 3295.
- (131) Egan, R. W.; Gale, P. H.; Vandenheuvel, W. J.; Baptista, E. M.; Kuehl, F. A. *J. Biol. Chem.* **1980**, *255*, 323.
- (132) Egan, R. W.; Gale, P. H.; Baptista, E. M.; Kennicott, K. L.; Vandenheuvel, W. J. A.; Walker, R. W.; Fagerness, P. E.; Kuehl, F. A., Jr. *J. Biol. Chem.* **1981**, *256*, 7352.
- (133) Marnett, L. J.; Bienkowski, M. J.; Pagels, W. R. *J. Biol. Chem.* **1979**, *254*, 5077.
- (134) Marnett, L. J.; Bienkowski, M. J.; Pagels, W. R.; Reed, G. A. *Advances in Prostaglandin and Thromboxane Research*, Vol. 6; Raven Press: New York, 1980; p 149.
- (135) Reed, G. A.; Brooks, E. A.; Eling, T. E. *J. Biol. Chem.* **1984**, *259*, 5591.
- (136) Sivarajah, K.; Lasker, J. M.; Eling, T. E.; Abou-Donia, M. B. *Mol. Pharmacol.* **1982**, *21*, 133.
- (137) Lasker, J. M.; Sivarajah, K.; Mason, R. P.; Kalyanaraman, B.; Abou-Donia, M. B.; Eling, T. E. *J. Biol. Chem.* **1981**, *256*, 7764.
- (138) Hsuanyu, Y.; Dunford, H. B. *J. Biol. Chem.* **1992**, *267*, 17649.
- (139) Ple, P.; Marnett, L. J. *J. Biol. Chem.* **1989**, *264*, 13983.
- (140) Mason, R. P.; Kalyanaraman, B.; Tainer, B. E.; Eling, T. E. *J. Biol. Chem.* **1980**, *255*, 5019.
- (141) Schreiber, J.; Eling, T. E.; Mason, R. P. *Arch. Biochem. Biophys.* **1986**, *249*, 126.
- (142) Kalyanaraman, B.; Mason, R. P.; Tainer, B.; Eling, T. E. *J. Biol. Chem.* **1982**, *257*, 4764.
- (143) Ruf, H. H.; Schuhn, D.; Nastainczyk, W. *FEBS Lett.* **1984**, *165*, 293.
- (144) Karthein, R.; Dietz, R.; Nastainczyk, W.; Ruf, H. H. *Eur. J. Biochem.* **1988**, *171*, 313.
- (145) Chance, B.; Powers, L.; Ching, Y.; Poulos, T.; Schonbaum, G. R.; Yamazaki, I.; Paul, K. G. *Arch. Biochem. Biophys.* **1984**, *235*, 596.
- (146) DeFilippis, M. R.; Murthy, C. P.; Brotiman, F.; Weinraub, D.; Faraggi, M.; Klapper, M. H. *J. Phys. Chem.* **1991**, *93*, 3416.
- (147) Koppol, W. H. *FEBS Lett.* **1990**, *264*, 165.
- (148) Goodwin, D. C.; Rowlinson, S. W.; Marnett, L. J. *Biochemistry* **2000**, *39*, 5422.
- (149) Tsai, A.-L.; Kulmacz, R. J.; Wang, J.-S.; Wang, Y.; Van Wart, H. E.; Palmer, G. *J. Biol. Chem.* **1993**, *268*, 8554.
- (150) Kulmacz, R. J.; Ren, Y.; Tsai, A.-L.; Palmer, G. *Biochemistry* **1990**, *29*, 8760.
- (151) Lassmann, G.; Odenwaller, R.; Curtis, J. F.; DeGray, J. A.; Mason, R. P.; Marnett, L. J.; Eling, T. E. *J. Biol. Chem.* **1991**, *266*, 20045.
- (152) DeGray, J. A.; Lassmann, G.; Curtis, J. F.; Kennedy, T. A.; Marnett, L. J.; Eling, T. E.; Mason, R. P. *J. Biol. Chem.* **1992**, *267*, 23583.
- (153) Shi, W.; Hoganson, C. W.; Espe, M.; Bender, C. J.; Babcock, G. T.; Palmer, G.; Kulmacz, R. J.; Tsai, A. L. *Biochemistry* **2000**, *39*, 4112.
- (154) Dorlet, P.; Seibold, S. A.; Babcock, G. T.; Gerfen, G. J.; Smith, W. L.; Tsai, A. L.; Un, S. *Biochemistry* **2002**, *41*, 6107.
- (155) Tsai, A.-L.; Palmer, G.; Kulmacz, R. J. *J. Biol. Chem.* **1992**, *267*, 17753.
- (156) Tsai, A. L.; Wu, G.; Palmer, G.; Bambai, B.; Koehn, J. A.; Marshall, P. J.; Kulmacz, R. J. *J. Biol. Chem.* **1999**, *274*, 21695.
- (157) Hsi, L. C.; Hoganson, C. W.; Babcock, G. T.; Smith, W. L. *Biochem. Biophys. Res. Commun.* **1994**, *202*, 1592.
- (158) Xiao, G.; Tsai, A. L.; Palmer, G.; Boyar, W. C.; Marshall, P. J.; Kulmacz, R. J. *Biochemistry* **1997**, *36*, 1836.
- (159) Shimokawa, T.; Kulmacz, R. J.; DeWitt, D. L.; Smith, W. L. *J. Biol. Chem.* **1990**, *265*, 20073.
- (160) Tsai, A.-L.; Hsi, L. C.; Kulmacz, R. J.; Palmer, G.; Smith, W. L. *J. Biol. Chem.* **1994**, *269*, 5085.
- (161) Hsi, L. C.; Hoganson, C. W.; Babcock, G. T.; Garavito, R. M.; Smith, W. L. *Biochem. Biophys. Res. Commun.* **1995**, *207*, 652.
- (162) Goodwin, D. C.; Gunther, M. H.; Hsi, L. H.; Crews, B. C.; Eling, T. E.; Mason, R. P.; Marnett, L. J. *J. Biol. Chem.* **1998**, *273*, 8903.
- (163) Tsai, A.-L.; Kulmacz, R. J.; Palmer, G. *J. Biol. Chem.* **1995**, *270*, 10503.
- (164) Tsai, A.-L.; Palmer, G.; Xiao, G.; Swinney, D. C.; Kulmacz, R. J. *J. Biol. Chem.* **1998**, *273*, 3888.
- (165) Peng, S.; Okeley, N. M.; Tsai, A. L.; Wu, G.; Kulmacz, R. J.; van der Donk, W. A. *J. Am. Chem. Soc.* **2001**, *123*, 3609.
- (166) Peng, S.; Okeley, N. M.; Tsai, A. L.; Wu, G.; Kulmacz, R. J.; van der Donk, W. A. *J. Am. Chem. Soc.* **2002**, *124*, 10785.
- (167) Yokoyama, C.; Tanabe, T. *Biochem. Biophys. Res. Commun.* **1989**, *165*, 888.
- (168) Otto, J. C.; DeWitt, D. L.; Smith, W. L. *J. Biol. Chem.* **1993**, *268*, 18234.
- (169) Nemeth, J. F.; Hochgesang, G. P., Jr; Marnett, L. J.; Caprioli, R. M.; Hochensang, G. P., Jr. *Biochemistry* **2001**, *40*, 3109.
- (170) Li, S.; Wang, Y.; Matsumura, K.; Ballou, L. R.; Morham, S. G.; Blatteis, C. M. *Brain Res.* **1999**, *825*, 86.



- (171) Riendeau, D.; Percival, M. D.; Boyce, S.; Brideau, C.; Charleson, S.; Cromlish, W.; Ethier, D.; Evans, J.; Falguyret, J. P.; Ford-Hutchinson, A. W.; Gordon, R.; Greig, G.; Gresser, M.; Guay, J.; Kargman, S.; Léger, S.; Mancini, J. A.; O'Neill, G.; Ouellet, M.; Rodger, I. W.; Thérien, M.; Wang, Z.; Webb, J. K.; Wong, E.; Xu, L.; Young, R. N.; Zamboni, R.; Prasit, P.; Chan, C.-C. *Br. J. Pharmacol.* **1997**, *121*, 105.
- (172) Riendeau, D.; Percival, M. D.; Brideau, C.; Charleson, S.; Dube, D.; Ethier, D.; Falguyret, J. P.; Friesen, R. W.; Gordon, R.; Greig, G.; Guay, J.; Mancini, J.; Ouellet, M.; Wong, E.; Xu, L.; Boyce, S.; Visco, D.; Girard, Y.; Prasit, P.; Zamboni, R.; Rodger, I. W.; Gresser, M.; Ford-Hutchinson, A. W.; Young, R. N.; Chan, C. C. *J. Pharmacol. Exp. Ther.* **2001**, *296*, 558.
- (173) Dougados, M.; Behier, J. M.; Jolchine, I.; Calin, A.; van der Heijde, D.; Olivieri, I.; Zeidler, H.; Herman, H. *Arthritis Rheum.* **2001**, *44*, 180.
- (174) Chang, D. J.; Desjardins, P. J.; Chen, E.; Polis, A. B.; McAvoy, M.; Mockoviak, S. H.; Geba, G. P. *Clin. Ther.* **2002**, *24*, 490.
- (175) Camu, F.; Beecher, T.; Recker, D. P.; Verburg, K. M. *Am. J. Ther.* **2002**, *9*, 43.
- (176) Kennedy, T. A.; Smith, C. J.; Marnett, L. J. *J. Biol. Chem.* **1994**, *269*, 27357.
- (177) Kamp, F.; Zakim, D.; Zhang, F.; Noy, N.; Hamilton, J. A. *Biochemistry* **1995**, *34*, 11928.
- (178) Zeng, J.; Fenna, R. E. *J. Mol. Biol.* **1992**, *226*, 185.
- (179) Varvas, K.; Järving, I.; Koljak, R.; Valmsen, K.; Brash, A. R.; Samel, N. *J. Biol. Chem.* **1999**, *274*, 9923.
- (180) DeWitt, D. L.; El-Harith, E. A.; Kraemer, S. A.; Andrews, M. J.; Yao, E. F.; Armstrong, R. L.; Smith, W. L. *J. Biol. Chem.* **1990**, *265*, 5192.
- (181) Smith, C. J.; Marnett, L. J. *Arch. Biochem. Biophys.* **1996**, *355*, 342.
- (182) Shimokawa, T.; Smith, W. L. *J. Biol. Chem.* **1991**, *266*, 6168.
- (183) Reed, G. A.; Marnett, L. J. *J. Biol. Chem.* **1982**, *257*, 11368.
- (184) Landino, L. M.; Crews, B. C.; Timmons, M. D.; Morrow, J. D.; Marnett, L. J. *Proc. Natl. Acad. Sci. U.S.A.* **1996**, *93*, 15069.
- (185) Rowlinson, S. W.; Crews, B. C.; Lanzo, C. A.; Marnett, L. J. *J. Biol. Chem.* **1999**, *274*, 23305.
- (186) Thuresson, E. D.; Malkowski, M. G.; Lakkides, K. M.; Rieke, C. J.; Mulichak, A. M.; Ginell, S. L.; Garavito, R. M.; Smith, W. L. *J. Biol. Chem.* **2001**, *276*, 10358.
- (187) Malkowski, M. G.; Thuresson, E. D.; Lakkides, K. M.; Rieke, C. J.; Micielli, R.; Smith, W. L.; Garavito, R. M. *J. Biol. Chem.* **2001**, *276*, 37547.
- (188) Kiefer, J. R.; Pawlitz, J. L.; Moreland, K. T.; Stegeman, R. A.; Hood, W. F.; Gierse, J. K.; Stevens, A. M.; Goodwin, D. C.; Rowlinson, S. W.; Marnett, L. J.; Stallings, W. C.; Kurumbail, R. G. *Nature* **2000**, *405*, 97.
- (189) Landino, L. M.; Crews, B. C.; Gierse, J. K.; Hauser, S. D.; Marnett, L. J. *J. Biol. Chem.* **1997**, *272*, 21565.
- (190) Thuresson, E. D.; Lakkides, K. M.; Rieke, C. J.; Sun, Y.; Wingerd, B. A.; Micielli, R.; Mulichak, A. M.; Malkowski, M. G.; Garavito, R. M.; Smith, W. L. *J. Biol. Chem.* **2001**, *276*, 10347.
- (191) Bhattacharyya, D. K.; Lecomte, M.; Rieke, C. J.; Garavito, R. M.; Smith, W. L. *J. Biol. Chem.* **1996**, *271*, 2179.
- (192) Mancini, J. A.; Riendeau, D.; Falguyret, J.-P.; Vickers, P. J.; O'Neill, G. P. *J. Biol. Chem.* **1995**, *270*, 29372.
- (193) Yu, M.; Ives, D.; Ramesha, C. S. *J. Biol. Chem.* **1997**, *272*, 21181.
- (194) Shimokawa, T.; Kulmacz, R. J.; DeWitt, D. L.; Smith, W. L. *J. Biol. Chem.* **1990**, *265*, 20073.
- (195) Tsai, A.-L.; Wu, G.; Kulmacz, R. J. *Biochemistry* **1997**, *36*, 13085.
- (196) Schneider, C.; Boeglin, W. E.; Prusakiewicz, J. J.; Rowlinson, S. W.; Marnett, L. J.; Samel, N.; Brash, A. R. *J. Biol. Chem.* **2002**, *277*, 478.
- (197) Schneider, C.; Boeglin, W. E.; Prusakiewicz, J. J.; Rowlinson, S. W.; Marnett, L. J.; Samel, N.; Brash, A. R. *J. Biol. Chem.* **2002**, *277*, 478.
- (198) Holtzman, M. J.; Turk, J.; Shornick, L. P. *J. Biol. Chem.* **1992**, *267*, 21438.
- (199) Lecomte, M.; Laneuville, O.; Ji, C.; DeWitt, D. L.; Smith, W. L. *J. Biol. Chem.* **1994**, *269*, 13207.
- (200) Valmsen, K.; Järving, I.; Boeglin, W. E.; Varvas, K.; Koljak, R.; Pehk, T.; Brash, A. R.; Samel, N. *Proc. Natl. Acad. Sci. U.S.A.* **2001**, *98*, 7700.
- (201) Meade, E. A.; Smith, W. L.; DeWitt, D. L. *J. Biol. Chem.* **1993**, *268*, 6610.
- (202) Abrahamsson, S. *Acta Crystallogr.* **1965**, *16*, 409.
- (203) O'Neill, G. P.; Mancini, J. A.; Kargman, S.; Yergey, J.; Kwan, M. Y.; Falguyret, J. P.; Abramovitz, M.; Kennedy, B. P.; Ouellet, M.; Cromlish, W.; et al. *Mol. Pharmacol.* **1994**, *45*, 245.
- (204) Wennogle, L. P.; Liang, H.; Quintavalla, J. C.; Bowen, B. R.; Wasvary, J.; Miller, D. B.; Allentoff, A.; Boyer, W.; Kelly, M.; Marshall, P. *FEBS Lett.* **1995**, *371*, 315.
- (205) Mancini, J. A.; O'Neill, G. P.; Bayly, C.; Vickers, P. J. *FEBS Lett.* **1994**, *342*, 33.
- (206) Rowlinson, S. W.; Crews, B. C.; Goodwin, D. C.; Schneider, C.; Gierse, J. K.; Marnett, L. J. *J. Biol. Chem.* **2000**, *274*, 6586.
- (207) Schneider, C.; Brash, A. R. *J. Biol. Chem.* **2000**, *275*, 4743.
- (208) Tsai, A. L.; Palmer, G.; Wu, G.; Peng, S.; Okeley, N. M.; van der Donk, W. A.; Kulmacz, R. J. *J. Biol. Chem.* **2002**, *277*, 38311.
- (209) Kulmacz, R. J.; Wang, L. H. *J. Biol. Chem.* **1995**, *270*, 24019.
- (210) Capdevila, J. H.; Morrow, J. D.; Belosludtey, Y. Y.; Beauchamp, D. R.; DuBois, R. N.; Falck, J. R. *Biochemistry* **1995**, *34*, 3325.
- (211) Lu, G. Q.; Tsai, A. L.; Van Wart, H. E.; Kulmacz, R. J. *J. Biol. Chem.* **1999**, *274*, 16162.
- (212) Swinney, D. C.; Mak, A. Y.; Barnett, J.; Ramesha, C. S. *J. Biol. Chem.* **1997**, *272*, 12393.
- (213) Devane, W. A.; Hanus, L.; Breuer, A.; Pertwee, R. G.; Stevenson, L. A.; Griffin, G.; Gibson, D.; Mandelbaum, A.; Etinger, A.; Mechoulam, R. *Science* **1992**, *258*, 1946.
- (214) Mechoulam, R.; Ben-Shabat, S.; Hanus, L.; Ligumsky, M.; Kaminski, N. E.; Schatz, A. R.; Gopher, A.; Almog, S.; Martin, B. R.; Compton, D. R. *Biochem. Pharmacol.* **1995**, *50*, 83.
- (215) Kondo, S.; Kondo, H.; Nakane, S.; Kodaka, T.; Tokumura, A.; Waku, K.; Sugiura, T. *FEBS Lett.* **1998**, *429*, 152.
- (216) Kozak, K. R.; Crews, B. C.; Morrow, J. D.; Wang, L. H.; Ma, Y. H.; Weinander, R.; Jakobsson, P. J.; Marnett, L. J. *J. Biol. Chem.* **2002**.
- (217) Lands, W. E. M.; Samuelsson, B. *Biochim. Biophys. Acta* **1968**, *164*, 426.
- (218) Vonkeman, H.; Van Dorp, D. A. *Biochim. Biophys. Acta* **1968**, *164*, 430.
- (219) Prusakiewicz, J. J.; Kingsley, P. J.; Kozak, K. R.; Marnett, L. J. *Biochem. Biophys. Res. Commun.* **2002**, *296*, 612.
- (220) Kozak, K. R.; Prusakiewicz, J. J.; Rowlinson, S. W.; Schneider, C.; Marnett, L. J. *J. Biol. Chem.* **2001**, *276*, 30072.
- (221) Gupta, R. K.; Mildvan, A. S.; Schonbaum, G. R. *Arch. Biochem. Biophys.* **1980**, *202*, 1.
- (222) Kulmacz, R. J.; Palmer, G.; Wei, C.; Tsai, A. L. *Biochemistry* **1994**, *33*, 5428.
- (223) Landino, L. M.; Marnett, L. J. *Biochemistry* **1996**, *35*, 2637.
- (224) Cook, H. W.; Lands, W. E. M. *Nature* **1976**, *260*, 630.
- (225) Marshall, P. J.; Kulmacz, R. J.; Lands, W. E. M. *J. Biol. Chem.* **1987**, *262*, 3510.
- (226) Koppenol, W. H.; Moreno, J. J.; Pryor, W. A.; Ischiropoulos, H.; Beckman, J. S. *Chem. Res. Toxicol.* **1992**, *5*, 834.
- (227) Koppenol, W. H.; Kissner, R. *Chem. Res. Toxicol.* **1998**, *11*, 87.
- (228) Floris, R.; Piersma, S. R.; Yang, G.; Jones, P.; Wever, R. *Eur. J. Biochem.* **1993**, *215*, 767.
- (229) Marnett, L. J.; Wright, T. L.; Crews, B. C.; Tannenbaum, S. R.; Morrow, J. D. *J. Biol. Chem.* **2000**, *275*, 13427.
- (230) Eling, T. E.; Wilson, A. G.; Chaudhari, A.; Anderson, M. W. *Life Sci.* **1977**, *21*, 245.
- (231) Wilson, A. G.; Kung, H. C.; Anderson, M. W.; Eling, T. E. *Prostaglandins* **1979**, *18*, 409.
- (232) Crutchley, D. J.; Hawkins, H. J.; Eling, T. E.; Anderson, M. W. *Biochem. Pharmacol.* **1979**, *28*, 1519.
- (233) Anderson, M. W.; Crutchley, D. J.; Chaudhari, A.; Wilson, A. G.; Eling, T. E. *Biochim. Biophys. Acta* **1979**, *573*, 40.
- (234) Zagorski, M. G.; Salomon, R. G. *J. Am. Chem. Soc.* **1982**, *104*, 3498.
- (235) Zagorski, M. G.; Salomon, R. G. *J. Am. Chem. Soc.* **1984**, *106*, 1750.
- (236) Salomon, R. G.; Miller, D. B.; Zagorski, M. G.; Coughlin, D. J. *J. Am. Chem. Soc.* **1984**, *106*, 6049.
- (237) Salomon, R. G.; Miller, D. B. *Adv. Prostaglandin Thromboxane Leukot. Res.* **1985**, *15*, 323.
- (238) Salomon, R. G.; Jirousek, M. R.; Ghosh, S.; Sharma, R. B. *Prostaglandins* **1987**, *34*, 643.
- (239) Iyer, R. S.; Ghosh, S.; Salomon, R. G. *Prostaglandins* **1989**, *37*, 471.
- (240) Murthi, K. K.; Friedman, L. R.; Oleinick, N. L.; Salomon, R. G. *Biochemistry* **1993**, *32*, 4090.
- (241) Lecomte, M.; Lecocq, R.; Dumont, J. E.; Boeynaems, J.-M. *J. Biol. Chem.* **1990**, *265*, 5178.
- (242) Boutaud, O.; Brame, C. J.; Salomon, R. G.; Roberts, L. J., II; Oates, J. A. *Biochemistry* **1999**, *38*, 9389.
- (243) Boutaud, O.; Brame, C. J.; Chaurand, P.; Li, J.; Rowlinson, S. W.; Crews, B. C.; Ji, C.; Marnett, L. J.; Caprioli, R. M.; Roberts, L. J., II; Oates, J. A. *Biochemistry* **2001**, *40*, 6948.
- (244) Kulmacz, R. J. *Biochem. Biophys. Res. Commun.* **1987**, *148*, 539.
- (245) Bakovic, M.; Dunford, H. B. *Biochemistry* **1994**, *33*, 6475.
- (246) Bakovic, M.; Dunford, H. B. *Prostaglandins Leukot. Essent. Fatty Acids* **1995**, *53*, 423.
- (247) Bakovic, M.; Dunford, H. B. *Biophys. Chem.* **1995**, *54*, 237.
- (248) Bakovic, M.; Dunford, H. B. *J. Biol. Chem.* **1996**, *271*, 2048.
- (249) Bakovic, M.; Dunford, H. B. *Prostaglandins Leukot. Essent. Fatty Acids* **1996**, *54*, 341.
- (250) Wei, C.; Kulmacz, R. J.; Tsai, A.-L. *Biochemistry* **1995**, *34*, 8499.
- (251) Eling, T. E.; Glasgow, W. C.; Curtis, J. F.; Hubbard, W. C.; Handler, J. A. *J. Biol. Chem.* **1991**, *266*, 12348.
- (252) Kulmacz, R. J.; Pendleton, R. B.; Lands, W. E. J. *J. Biol. Chem.* **1994**, *269*, 5527.
- (253) Tang, M. S.; Askonas, L. J.; Penning, T. M. *Biochemistry* **1995**, *34*, 808.

- (254) Tang, M. S.; Copeland, R. A.; Penning, T. M. *Biochemistry* **1997**, *36*, 7527.
- (255) Nelson, M. J. *Biochemistry* **1988**, *27*, 4273.
- (256) Jonas, R. T.; Stack, T. D. P. *J. Am. Chem. Soc.* **1997**, *119*, 8566.
- (257) Funk, M. O., Jr.; Carroll, R. T.; Thompson, J. F.; Sands, R. H.; Dunham, W. R. *J. Am. Chem. Soc.* **1990**, *112*, 5375.
- (258) MacDonald, I. D.; Graff, G.; Anderson, L. A.; Dunford, H. B. *Arch. Biochem. Biophys.* **1989**, *272*, 194.
- (259) Hamberg, M.; Samuelsson, B. *J. Biol. Chem.* **1967**, *242*, 5329.
- (260) Marnett, L. J.; Reed, G. A.; Johnson, J. T. *Biochem. Biophys. Res. Commun.* **1977**, *79*, 569.
- (261) Poulos, T. J.; Kraut, J. *J. Biol. Chem.* **1980**, *255*, 8199.
- (262) Goodwin, D. C.; Landino, L. M.; Marnett, L. J. *FASEB J.* **1999**, *13*, 1121.
- (263) Reed, G. A.; Brooks, E. A.; Eling, T. E. *J. Biol. Chem.* **1984**, *259*, 5591.

CR000068X